THE UNIVERSITY *of* EDINBURGH

SYNAPTIC VESICLE PROTEIN 2A-DEPENDENT FUNCTION AND DYSFUNCTION AT THE PRESYNAPSE

Darryl Weijun Low

Thesis Submitted for the Degree of

Doctor of Philosophy in Biomedical Sciences

The University of Edinburgh

August 2017

Contents

Acknowledgements

First and foremost, I would like to thank Prof. Mike A. Cousin at the Centre of Integrative Physiology, Edinburgh for giving me the opportunity to work in his lab and for all his help and supervision during my time as a PhD student. This would not have been possible without you. Huge thanks also to the Cousin Lab: Sarah Gordon, Karen Smillie, Jamie Marland, Callista Harper, Robyn McAdam, Jessica Nicholson-Fish, Alex Kokotos, Katherine Bonnycastle and Rona Wilson for all the help and support throughout this time. Many thanks also to the Wishart Group at the Roslin Institute for helping me with mass spectrometry data.

Secondly, I would like to thank my mum and stepdad, Shirley and Alex Smith, for their unwavering support through the years. There have been many joys and challenges in the last few years and you were both there with me through it all. I cannot express how much I love and appreciate you both.

Last, but not least, I would also like to thank all of my wonderful friends in Edinburgh and abroad who have made life so joyful: Jilly Hope, Keir Shaffick-Richardson, Alex Kokotos, Rodrigo Bacigalupe and Jemi Malkemus. You all never failed to bring a smile to my face whenever I felt down.

Declaration

I, Darryl W. Low, have composed this thesis myself. The work and the results reported herein are my own except where indicated, and have not been submitted for any other degree or professional qualification.

Abstract

Neurotransmission is essential for neuronal communication. At the presynapse, synaptic vesicles (SVs) undergo exocytosis to release neurotransmitter in response to incoming action potentials, and endocytosis to maintain the supply of SVs needed for further rounds of exocytosis. A key event during SV endocytosis is the efficient sorting and localisation of SV proteins at the plasma membrane. This ensures that nascent SVs that are formed have the correct molecular composition to participate in subsequent exocytic events. The sorting of SV proteins at the plasma membrane is usually facilitated by adaptor proteins (e.g. AP-2) which recognise binding motifs present on key SV proteins and facilitate their internalisation during endocytosis. In addition to this, certain SV proteins possess the ability to chaperone each other as part of an endocytic transport complex throughout the SV recycling process. In conjunction with AP-2-facilitated sorting, the transport of complexed SV proteins during endocytosis provides further mechanistic insight into how SVs are generated with consistent high fidelity for functional viability.

Using pHluorins as a tool to visualise SV protein trafficking in hippocampal cultures, the relationship between two key SV proteins, synaptic vesicle protein 2A (SV2A) and synaptotagmin I (SYT1), was investigated. SYT1 predominantly acts as the Ca^{2+} sensor for fast synchronous release at the presynapse, whilst the exact function of SV2A remains unknown to this day. In this study, the ablation of the AP-2 binding site in SV2A (Y46A) resulted in increased SYT1 surface expression and accelerated SYT1 retrieval compared to WT SV2A. No additive defects were observed when a second point mutation (T84A) was introduced to SV2A that disrupts the phosphorylation-dependent interaction between SV2A and SYT1, thus confirming

that SYT1 localisation and retrieval is dependent on normal SV2A retrieval by AP-2. The hypothesis that disruption of the SV2A-SYT1 interaction may provide an underlying mechanism for motor onset seizures in epilepsy was also investigated. An epilepsy-related mutation (R383Q) in SV2A also resulted in increased SYT1 surface expression and accelerated SYT1 retrieval mirroring the defects caused by the Y46A mutation. Introduction of Y46A or T84A mutation into SV2A R383Q resulted in no additive defects compared to the single mutant, suggesting that the observed defects in SYT1 localisation and retrieval kinetics in the epilepsy-related mutant may be caused by the ablation of normal SV2A internalisation. GST pulldown assays, mass spectrometry and western blotting data indicate that presence of the mutation disrupts normal binding of the SV2A cytosolic loop with actin, tubulin and certain subunits of V-ATPase. Finally, a link between SV2A-dependent presynaptic dysfunction and epilepsy was examined through studies utilising the anti-epileptic drug, levetiracetam (LEV). SV2A contains a binding site for LEV, suggesting that it may act as a carrier for the drug into the presynapse. Hippocampal neuronal cultures were treated with LEV at various concentrations in the presence of specific patterns of neuronal activity. No observed effects of the drug on synaptophysin, vesicular glutamate transporter 1 (VGLUT1) and SYT1 recycling were observed, suggesting that LEV is unlikely to function as a modulator of excitatory presynaptic activity or by influencing SV2A function.

In conclusion, this work demonstrates that SV2A is essential for accurate SYT1 trafficking and a link has been established between defective SV2A internalisation and subsequent downstream effects on SYT1 localisation and retrieval during SV recycling.

Lay Summary

Neurotransmission is the process by which chemicals are released by one nerve cell and accepted by another nerve cell to allow nerve impulses to travel through the body. Neurotransmission is required for different nerve cells in the body to communicate with each other. Inside the chemical-releasing cell, known as the presynaptic cell, the chemicals are packed into small fatty packages known as synaptic vesicles. When a neural impulse arrives at the presynaptic cell, it triggers a response that causes these vesicles to fuse to the cell membrane and release the chemicals. When all vesicles are used up in fusion, it results in a shortage of available vesicles for fusion when the next neural impulse arrives. In order to address this, the vesicles, as well as its related biological proteins, are recycled within the nerve cell. This recycling of vesicles and its proteins is crucial for maintaining neural activity. A key event during the recycling process is the efficient sorting of vesicle-associated proteins at the cell membrane by biological machinery. This ensures that newly formed vesicles contain the correct number of different proteins to participate in the next cycle of fusion. The sorting process at the cell membrane is usually done by a specific family of adaptor proteins; however, this is not always the case. Certain vesicle-associated proteins possess the ability to sort and chaperone each other, as part of a unit, during the recycling process. This mutual aid between proteins during the sorting process helps to ensure that SVs will have the right composition to maintain neurotransmission. Therefore, when one of the proteins fails to sort accurately, it may lead to resulting defects in the sorting of the partner protein.

The aim of this thesis is to characterise such a relationship between two specific vesicle proteins, synaptic vesicle protein 2A (SV2A) and synaptotagmin 1 (SYT1),

during synaptic vesicle recycling and establish a link to the onset of epilepsy which may arise from disruption to this relationship. A failure of normal SV2A function is thought to result in defects in the sorting and recycling of SYT1 from the cell membrane. In order to investigate this, the proteins were visualised in live mice nerve cells by genetically fusing them to a fluorescent protein.

In this study, normal SV2A protein was subjected to a single change (amino acid tyrosine to alanine at position 46, Y46A) in the protein sequence that results in disruption of its recycling at nerve terminals. It is reported here that this change resulted in an increased amount of SYT1 located at the cell membrane and acceleration in the rate of SYT1 retrieval during vesicle recycling. This suggests that defects in SYT1 sorting and recycling defects could be attributed to the initial disruption in SV2A recycling. Previous studies have identified another key protein sequence change (arginine to glutamine at position 383, R383Q) which results in the onset of epilepsy and developmental difficulties. However, the molecular pathways underlying the onset of epilepsy are yet to be determined. It is hypothesised that the disruption of the previously described SV2A-SYT1 relationship during vesicle recycling may provide an underlying cause for the onset of epilepsy that was initially found in a human patient. In this study, the presence of the R383Q change in SV2A also resulted in an increased amount of SYT1 located at the cell membrane and acceleration in the rate of SYT1 retrieval during SV recycling. These results mirror the observations previously described with the Y46A change, and presents a strong indication that this particular form of epilepsy may be caused by dysfunction of SV2A recycling. Therefore, it is proposed that the disruption of normal SV2A function represents a major cause for the observed dysfunction in SYT1 recycling. In

order to determine further the mechanistic causes of these recycling defects, biochemical experiments were designed to investigate if interactions between SV2A and other unknown vesicle proteins were altered when the R383Q change was present. It is reported that SV2A interactions with other proteins such actin, tubulin and V-ATPase was altered when the R383Q change was present.

Finally, the link between normal function of SV2A at the presynapse and epilepsy was investigated through use of the anti-epileptic drug levetiracetam (LEV). LEV has been a popular drug of choice for the treatment of partial onset epilepsy for many years, but the way in which it works has never been fully understood. Previous studies have indicated that SV2A is a carrier for the drug into the nervous system, however direct evidence of a therapeutic function mediated by SV2A has yet to be presented. In this study, the effects of various concentrations of LEV on general SV recycling at the presynapse were investigated. These results show that there was no obvious LEV-mediated effect at the presynaptic nervous system, indicating that the drug is unlikely to function by regulating the relationship between SV2A and SYT1 during SV recycling.

In conclusion, this work has established a link between abnormal SV2A retrieval and its resulting effects on the localisation of SYT1 at the cell surface and its retrieval during SV recycling.

List of Abbreviations

4-AP	4-aminopyridine
ADBE	activity dependent bulk endocytosis
AED	anti-epileptic drug
AMPA	α-amino-3-hydroxy-5-methyl-4-isoxazolepropionic acid
AP	action potential
AP-180	adaptor protein 180
AP-1/2/3	adaptor protein 1/2/3
ARF	ADP ribosylation factor
A(T/D/M)P	adenosine tri/di/mono-phosphate
BAR	Bin/amphiphysin/RVS
BDNF	brain derived neurotrophic factor
CALM	clathrin assembly lymphoid myeloid leukaemia protein
CDK5	cyclin dependent kinase 5
CME	clathrin-mediated endocytosis
DYN	dynamin
EA1	episodic ataxia type 1
EGTA	ethyleneglycol tetraacetic acid
ENTH	epsin N-terminal homology
EPS15	epidermal growth factor pathway substrate 15

FCHO	FCH domain only protein
GEF	guanine nucleotide exchange factor
Grb2	growth factor receptor-bound protein 2
GSK3	glycogen synthase kinase 3
HRP	horseradish peroxidase
Hsc70	70-kDa heat shock protein
KO	knockout
LEV	levetiracetam
nAChR	nicotinic acetylcholine receptors
NMDA	*N*-methyl-D-aspartate
NMJ	neuromuscular junction
NPF	asparagines/proline/phenylalanine
NSF	N-ethylmalemide sensitive factor
N-WASP	neuronal Wiskott-aldrich syndrome protein
PACSIN	Protein kinase C and casein kinase substrate in neurons protein (also known as Syndapin)
PALM	photoactivated localisation microscopy
$PI(4,5)P_2$	phosphatidylinositol-4,5-bisphosphate
RP	reserve pool
RRP	readily releasable pool

RtP	resting pool
SNAP	soluble NSF attachment protein
SNARE	SNAP and NSF attachment receptors
STED	stimulated emission and depletion (microscopy)
SV	synaptic vesicle
SV2A	synaptic vesicle protein 2a
SVE	synaptic vesicle endocytosis
SYB	synaptobrevin
SYJ	synaptojanin
SYP	synaptophysin
SYT	synaptotagmin
TIRF	total internal reflection fluorescence
TRP	total recycling pool
t-SNARE	target SNARE
TTBK	tau tubulin kinase
UFE	ultrafast endocytosis
VAMP	vesicle associated membrane protein
VGLUT	vesicular glutamate transporter
v-SNARE	vesicular SNARE
WT	wild type

1.0 – General Introduction

1.1 – General Introduction to Neurotransmission

The human brain is a highly flexible neural machine that is able to discriminate a large variety of information and stimuli from the environment. The continuous stream of information is organised by the brain into perceptions and memory, and these perceptions trigger appropriate behavioural responses in living things for survival and function. Different parts of the brain are responsible for the different physiological functions: 1) the cerebral cortex is the largest part of the brain and is responsible for higher functions like interpreting touch, vision and hearing, speech, reasoning, emotions, learning, and fine control of movement; 2) the cerebellum coordinates muscle movements and plays a role in maintaining posture and balance; 3) the brainstem is responsible for the maintenance of homeostasis functions such as breathing, body temperature, heart rate sleep cycles and digestion. Deeper structures such as hypothalamus, thalamus and hippocampus play important roles in behaviour control, hormonal secretion, pain sensation and long/short-term memory (Kandel and Hudspeth, 2012).

The brain is a large network of interconnected nerve cells (or neurones) which share the same basic architecture. Neurones in the network communicate with each other through an intricate process known as *synaptic transmission*. There are two basic forms of synaptic transmission: electrical synaptic transmission and chemical synaptic transmission. Electrical synaptic transmission is rapid and is used primarily to send simple depolarising signals. Electrical synaptic transmission tends not to produce inhibitory action or make long-lasting changes in the electrical properties of postsynaptic cells. In contrast, chemical synapses are capable of more variable signalling and can therefore produce complex neuronal behaviours. Chemical

synapses can mediate either excitatory or inhibitory actions in postsynaptic cells and produce electrical changes in the postsynaptic cell that last from milliseconds to many minutes.

At electrical synapses, electrical currents flow between pre- and postsynaptic neurones through gap junction channels, which are specialised protein structures that provide a low-resistance pathway for conducting the flow of ionic current from the presynaptic to the postsynaptic neurone. Electrical current flowing from a presynaptic neurone into a postsynaptic neurone deposits a positive charge on the inside of the membrane of the postsynaptic neurone and depolarizes the membrane. Excess current then flows out through resting voltage-gated ion channels in the postsynaptic neuronal membrane. If the depolarization exceeds threshold, voltage-gated ion channels in the postsynaptic neurone opens and generates an action potential (see chapter 1.1). Thus, these voltage-gated ion channels not only have to depolarise the presynaptic cell above the threshold for an action potential, they must also generate sufficient ionic current to produce a change in potential in the postsynaptic cell.

At chemical synapses, there is no direct low-resistance pathway between the pre- and postsynaptic neurones. Instead, the arrival of an action potential in the presynaptic neurone initiates the release of chemical neurotransmitter molecules, which diffuse across the synaptic cleft to interact with receptors on the membrane of the postsynaptic neurone. Receptor activation causes either depolarisation of hyperpolarisation of the cell membrane in the postsynaptic neurone, which acts to propagate further the action potential though the body or stop the propagation entirely (Siegelbaum and Kandel, 2012).

This thesis will specifically examine the process of synaptic transmission at chemical synapses. It will aim to provide a background on the morphology and function of neurones and its presynaptic features, as well as how these features play a key role in maintaining viable, long-term neurotransmission.

1.2 – Structure and Morphology of a Neurone

A typical neurone generally has four morphologically defined regions, namely the cell body, dendrites, axons and the synaptic terminals (Figure 1.2). Each of these regions plays a distinct role in the generation and reception of nerve signals by the neurone, and thus has an overarching influence on neuronal communication.

The cell body (also known as soma) is the metabolic centre of the cell and contains the nucleus and endoplasmic reticulum. The nucleus stores the genes of the cell and the endoplasmic reticulum is the primary location of cellular protein synthesis. Newly synthesised proteins are transported throughout the cell by anterograde transport systems such as motor proteins. The cell body gives rise to two kinds of neuronal structures: dendrites and axons. Dendrites branch out from the cell body in a tree-like fashion and are responsible for receiving incoming electrical signals from other neurones. In contrast, axons extend away from the cell body in a tubular fashion along distances that may range from 0.1 mm to > 2 m (Kandel et al., 2012). Axons are responsible for conducting outgoing electrical and chemical signals to other neurones.

The electrical signals that form the basis of neuronal communication are termed *action potentials*. Action potentials constitute the signals by which the brain receives,

analyses, and conveys information about the environment. These signals are highly regulated throughout the nervous system, even though they may be initiated by a great variety of stimuli such as light, mechanical contact, odours and tastes. The information conveyed by an action potential is determined not by the form of the signal but by the pathway in which the signal travels in the brain. The brain analyses and interprets the patterns of incoming action potentials to create our everyday sensations of sight, touch, taste, smell, and sound. In order to increase the speed by which action potentials are conducted, neuronal axons are typically wrapped in a fatty, insulating sheath of myelin. This myelin sheath is interrupted by regions of unprotected axon, known as the nodes of Ranvier, to allow regeneration of the action potential along the cell.

At the terminus of the axon, the neurone splits into fine branches that form sites of connection with other neurones. The presynaptic neurone transmits signals from the presynaptic nerve terminals in the form of chemical molecules termed as *neurotransmitters*. Neurotransmitter molecules diffuse across the space between the presynaptic neurone and the postsynaptic neurone known as the *synaptic cleft*, and bind onto specific neurotransmitter receptors on the postsynaptic nerve terminal. This initiates a biochemical process to propagate the neuronal signal.

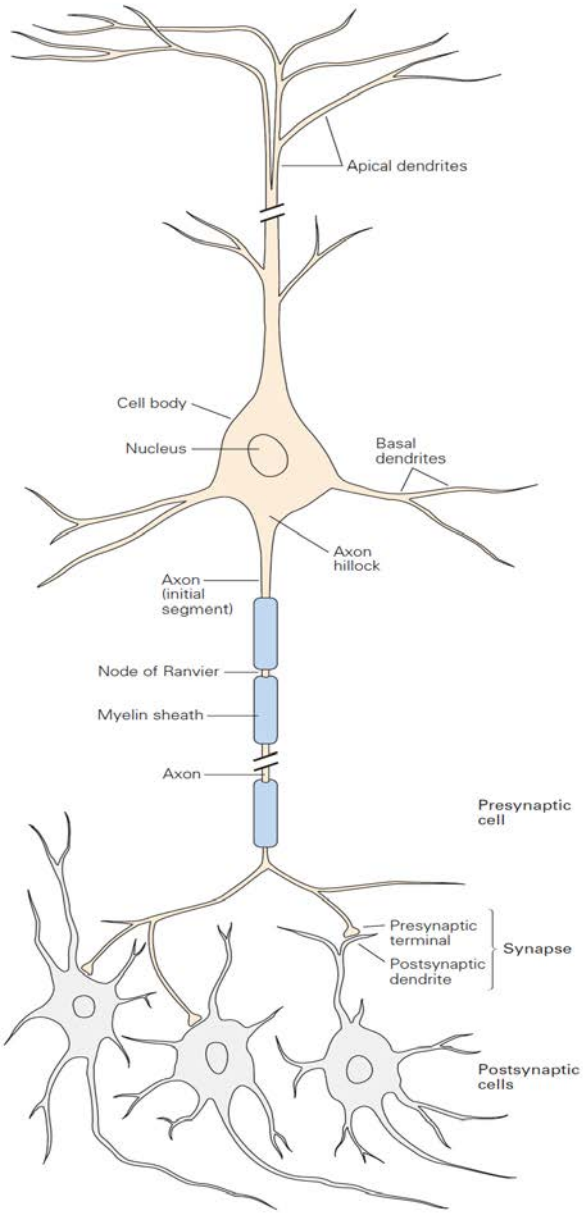

Figure 1.2: Morphology of a Typical Neurone (Kandel et al., 2012). Most neurons in the vertebrate nervous system have several main features in common. The cell body (soma) contains the nucleus and endoplasmic reticulum and gives rise to two types of cell processes, axons and dendrites. Dendrites, both apical and basal, are responsible for receiving incoming electrical signals from other neurones. Axons can vary greatly in length (from 0.1 mm to > 2 m) and are responsible for conducting electrical signals to other neurones. Most axons in the central nervous system are very thin (between 0.2 and 20 µm in diameter) compared with the diameter of the cell body (50 µm or more). Branches of the axon of one neurone (the presynaptic neurone) transmit signals to another neuron (the postsynaptic neurone) at a site called the synapse. The branches of a single axon may form synapses with thousands of other neurones.

1.2.1 – Structure and Function of a Neuronal Pre/Postsynaptic Terminal

A presynaptic terminal consists of around 200 - 300 synaptic vesicles (SVs), which form different vesicle pools within the synapse (See chapter 1.2). Some synaptic vesicles are clustered at specialised regions of the presynaptic membrane called active zones, and these are the primary sites of neurotransmitter release (Figure 1.2.1). The plasma membrane of a presynaptic terminal consists of SV-related proteins as well voltage-gated Ca^{2+} channels, which open to allow Ca^{2+} to enter the presynaptic terminal resulting from an incoming action potential. The rise in intracellular Ca^{2+} concentration triggers a biochemical reaction that leads to fusion of SVs with the presynaptic membrane and release of neurotransmitter into the synaptic cleft. This process is termed SV *exocytosis*. Membrane is then retrieved and reformed back into SVs in a process termed SV *endocytosis*. The processes of exocytosis and endocytosis will be discussed in more detail in later chapters. SVs contain thousands of neurotransmitter molecules, and the identity of the neurotransmitter depends on the type of neurone and its role in neural network. A number of small molecules can act as a neurotransmitter in central synapses. Acetylcholine is present at all neuromuscular junction synapses, whilst classical amino acid derivatives such as glutamate (>50% of synapses) γ-aminobutyric acid (25-40% of synapses) and glycine. Apart from classical amino acid derivatives, a small percentage of synapses also use monoamine derivatives (e.g. dopamine, norepinephrine, epinephrine, serotonin, histamine and melatonin) as neurotransmitters.

At the postsynaptic terminal, receptor proteins specific to the neurotransmitter released are embedded into surface of the plasma membrane. Activation of these

receptors leads to the opening of gated ion channels, which changes the membrane conductance and membrane potential of the postsynaptic neurone and either allows or inhibits action potential propagation depending on whether the neurone is excitatory or inhibitory. Post-synaptic receptors can gate ligand channels either directly or indirectly. Receptors that undergo a conformation change and open the corresponding ion channels directly are known as *ionotropic* receptors e.g. acetylcholine receptors at the neuromuscular junction. Receptors that gate ion channels indirectly usually function by producing a second chemical messenger such as cyclic AMP or diacylglycerol upon activation and are known as *metabotropic* receptors. These second messenger molecules usually activate protein kinases that will phosphorylate ion channels, leading to their opening or closing (Siegelbaum and Kandel, 2012).

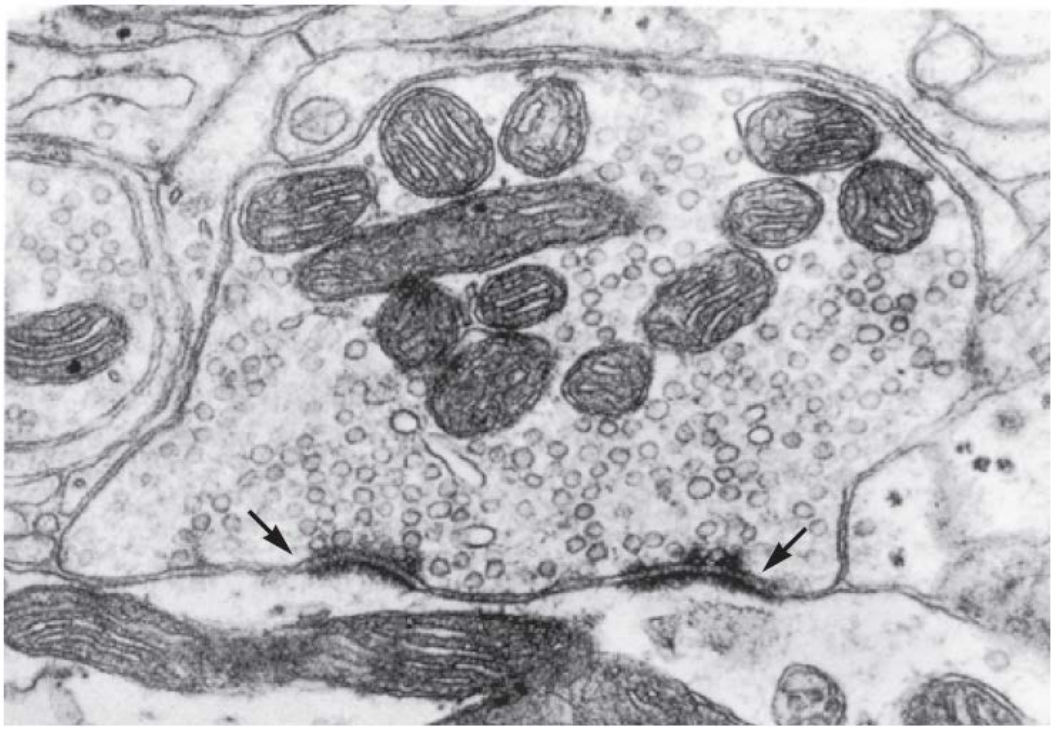

Figure 1.2.1: Fine Structural Morphology of a Synaptic Terminal (Heuser and Reese, 1973). This electron micrograph of a frog neuromuscular junction synapse shows the presence of synaptic vesicles (SVs) as small round bodies and mitochondria as the larger, darker bodies. Clustering of SVs at the active zones along the presynaptic membrane can also be observed (black arrows). Active zones are specialised region that are thought to be sites for the docking and fusion of SVs. Beyond the presynaptic terminal, the synaptic cleft separating the pre- and postsynaptic cell membranes can be observed as a white extracellular space.

1.2.2 – Synaptic Vesicle Pools in Central Synapses

SVs at the presynaptic terminal morphologically exist as a cluster surrounding the plasma membrane, but have functional differences that allow them to be framed into different pools based on their relevance to difference aspects of neurotransmitter release. The current opinion in the field is that SVs exist in three different canonical pools that are differentiated by the kinetics and probability of SV release: 1) the readily releasable pool (RRP); 2) the reserve pool (RP) and 3) the resting pool (RtP). The RRP and the RP together make up the total recycling pool (TRP) of vesicles that are mobilised upon an action potential stimulus. The mean size of the TRP directly correlates to synaptic release probability, and therefore many studies have tried to provide an accurate estimate of its size in central synapses. Differences in measuring approaches, sample preparation and stimulation parameters, however, have led to discrepancies between studies. Estimates of the TRP size may range from 15-20% (Marra et al., 2012) to about 50-60% (Ikeda and Bekkers, 2009) of the total vesicle pool at a synapse.

The RRP consists of 5-10% of total SVs on average at a synapse (Dobrunz and Stevens, 1997). SVs in the RRP are docked to the active zone and are primed for release even at low-frequency stimulation. Depletion of the RRP can be achieved by 1-2 s of electrical stimulation at 10-40 Hz or application of a hypertonic solution for 1 s (Stevens and Williams, 2007). Replenishment of the RRP may be mediated by transitioning SVs from the RP, or by both clathrin-dependent (Cheung et al., 2010) and clathrin-independent modes of SV endocytosis (Watanabe et al., 2014) (see chapter 1.5 for detailed treatment of various endocytosis modes). Electrophysiological experiments in rat calyx of Held synapses have demonstrated

that replenishment of the RRP is regulated by Ca^{2+} and calmodulin, and takes place on a timescale of around 5-10 s (Stevens and Tsujimoto, 1995, Sakaba and Neher, 2001).

The RP (reserve pool) is a small body of SVs that are primed to replenish the RRP upon its depletion during high intensity stimulation. This means that there are extra transitions for the SVs to take to become fusion ready, and thus RP to RRP transitions often limit the rate of neurotransmitter release during persistent activity (Alabi and Tsien, 2012). The mean size of the RP is harder to estimate accurately, however it is typically approximately three times the size of the RRP in central synapses (Murthy and Stevens, 1999). Replenishment of the RP is Ca^{2+}-dependent and takes places on a timescale of about 10 s, however in the presence of high-frequency stimulation, the refilling rate doubles with 1-2 sec of the onset of the stimulus (Stevens and Wesseling, 1998). FM labelling studies in central synapses have demonstrated that activity-dependent bulk endocytosis, which is a specific mode of clathrin-independent endocytosis, selectively replenishes the reserve pool of SVs as compared to other modes that replenishes the RRP (Cheung et al., 2010).

Finally, the RtP (resting pool) of SVs is defined as the subset of SVs that remain unreleased in even during saturation of SV turnover under extended stimulation (Harata et al., 2001, Li et al., 2005). Both pHluorin imaging (Fernandez-Alfonso and Ryan, 2008) and fluorescence dye photoconversion (Harata et al., 2001)assays have indicated that the mean RtP size is around 50% of total SVs at central synapses. Given that there are only around 200-300 SVs present at a nerve terminal, the idea around half of these SVs do not participate in neurotransmitter release remains difficult to explain. Fluorescence labelling experiments in mammalian central

synapses have provided evidence that SVs in the RtP participate in spontaneous neurotransmitter release (Sara et al., 2005, Fredj and Burrone, 2009) (see 1.2.1), however similar studies in various NMJ model systems have disputed this (Wilhelm et al., 2010). RtP SVs have also been suggested to act as a buffer for soluble accessory proteins involved in SV recycling, preventing loss of protein into the axon by acting as a depository for non-functioning SVs prior to degradation (Denker et al., 2011).

More recently, a novel pool classification has emerged which is functionally and organisationally distinct from the previous three canonical fields. The idea that each presynaptic terminal has its own supply and pools of SVs has now been challenged as increasing evidence emerges of a SV 'superpool' that is dynamically shared between multiple presynaptic terminals from fluorescence and electron microscopy studies (Darcy et al., 2006, Staras et al., 2010, Herzog et al., 2011). It has been postulated that the superpool may be responsible for preserving presynaptic identity by acting as extrasynaptic resource to support changes to the properties of a host terminal (Staras and Branco, 2010). Several key synaptic proteins such as synapsin (Orenbuch et al., 2012), and α-synuclein (Scott and Roy, 2012) have been identified as regulators for the superpool, indicating that there may be possible connections between inter-synapse SV trafficking and disease-related synaptic dysfunction.

1.2.3 – Morphology of a Typical Synaptic Vesicle

The typical synaptic vesicle has a diameter of about 40 nm, and they can be considered the basic units of membrane traffic. SV membrane is predominantly composed of cholesterol (40 mol %), along with a mixture of phospholipids such as phosphatidylcholine, phosphatidylethanolamine, phosphatidylserine, phosphatidylinositol (Takamori et al., 2006). Transport of the SV, recognition of active site, docking and fusion process each involve the sequential and ordered recruitment of specific protein complexes from the cytoplasm. The proteins constituents embedded in the SV membrane must therefore play a key role in the association of these complexes, allowing the complex to fulfil its task and then facilitate disassembly of the protein complex upon task completion. There have been a couple of elegant studies directed at identifying and quantifying the range of proteins on an SV. A proteomics study led by Takamori et. al. using enhanced mass spectrometry has identified around 80 different integral membrane proteins including trafficking proteins, transporter and channel proteins, cytoskeletal proteins, cell-surface and signalling proteins (Figure 1.2.3) (Takamori et al., 2006). A combinatorial approach using quantitative immunoblotting, mass spectrometry and super-resolution microscopy has also shed light on SV protein copy numbers and protein localisation in synaptosomes (Wilhelm et al., 2014). For the sake of brevity, this introduction will cover a just a selection of key SV proteins integral to SV function.

1.2.3.1 – Soluble NSF Attachment Protein Receptor (SNARE) Proteins

The SNARE proteins are a group of proteins consisting of synaptobrevin/vesicle-associated membrane protein II (SYB2/VAMP2), syntaxin-1 and synaptosomal-associated protein-25 kDa (SNAP-25) (Südhof and Rothman, 2009). SNARE proteins are the key molecular machinery responsible for the docking, priming and fusion of SVs during exocytosis. SYB2 is a vesicle-associated SNARE (v-SNARE) with approximately 70 copies per SV (Takamori et al., 2006, Wilhelm et al., 2014). Syntaxin-1 and SNAP-25 are target membrane-associated SNAREs (t-SNAREs) with approximately 6 and 2 copies per SV respectively. This is an unusually low number since they are plasma membrane proteins, which suggests that the sorting of these proteins must be efficiently regulated to maintain SV fidelity for neurotransmission. SNARE proteins contain a stretch of amino acids called a SNARE motif. SYB2 and syntaxin-1 each contain one SNARE motif preceding the C-terminal transmembrane region, whereas SNAP-25 contains two SNARE motifs. Prior to exocytosis, the four SNARE motifs assemble into a tight SNARE complex that bridges both the vesicle and target cell membranes (Söllner et al., 1993). A more detailed treatment of the mechanisms underlying exocytosis is given in chapter 1.3.

1.2.3.2 – Synaptophysin (SYP)

Synaptophysin (SYP) is a 38-kDa glycoprotein containing four transmembrane domains and two intra-vesicular loops. It is the most abundant integral membrane protein in SVs by molecular weight, with approximately 30 copies per SV (Takamori et al., 2006, Wilhelm et al., 2014). The exact role of SYP in the SV cycle remains to be elucidated. Protein cross-linking experiments have shown that isolated pure SYP

has a tendency to form homo-oligomers with physophilin that contain unstable intramolecular disulphide bonds (Thomas and Betz, 1990). As a result, SYP was suggested to play a role in the formation of a putative fusion pore during SV exocytosis. More recently, SYP has been elegantly shown to play a key role in the trafficking of SYB2 in the SV cycle. Protein cross-linking experiments have shown that SYP and SYB2 forms a complex with each other, mediated by the transmembrane regions of both proteins (Calakos and Scheller, 1994, Edelmann et al., 1995, Washbourne et al., 1995). Immunofluorescence studies in primary neuronal cultures have shown that the overexpression of SYB2 resulted in increased expression along the axon of a neurone and mislocalisation of SYB2 at a terminal (Pennuto et al., 2003). This expression defect could be rescued by the co-expression of SYP in neurones. In agreement with this finding, genetic ablation of SYP in mouse hippocampal cultures demonstrate reduced expression of endogenous SYB2 in nerve terminals as well as stranding of the genetic reporter SYB2-pHluorin on their plasma membrane (Gordon et al., 2011). Critically, the retrieval of SYB2-pHluorin from the plasma membrane was greatly retarded during SV endocytosis in the same knockout cultures. This defect was again fully rescued by the co-expression of wild-type SYP (Gordon et al., 2011). Photoactivated localisation microscopy (PALM) studies have also shown that SYP plays a role in the release site clearance of SYB2 at the active zone (Rajappa et al., 2016). The intricacies between the interaction between SYP and SYB2 in SV trafficking will be further explored in chapter 3.

1.2.3.3 – Synaptic Vesicle Protein 2 (SV2)

Synaptic vesicle protein 2 (SV2) is a glycoprotein which is present in the secretory vesicles of neural and endocrine cells, with approximately 2-12 copies per SV (Takamori et al., 2006, Wilhelm et al., 2014). SV2 consists of 12 transmembrane domains and cytoplasmic N- and C- terminus regions. The exact role of SV2A in SV recycling and neurotransmission remains unclear to this day, and there have been many possible roles for SV2A discussed in the literature. A detailed review of these possible roles is covered in chapter 3.

1.2.3.4 – Synaptotagmin I (SYT1)

Synaptotagmin I (SYT1) is a member of a family of proteins that are defined by a single transmembrane domain that is joined onto two Ca^{2+}-binding domains (C2A and C2B) through a linker region. It is present on an SV with approximately 15-20 copies per SV (Takamori et al., 2006, Wilhelm et al., 2014). SYT1 has a primary role in facilitating Ca^{2+}-dependent interactions at the presynapse, in particular as the Ca^{2+} sensor in the triggering of SV fusion during exocytosis. A detailed review of these possible roles is covered in chapter 3.

1.2.3.5 – Vesicular Glutamate Transporter 1 (VGLUT1)

Vesicle glutamate transporter 1 (VGLUT1) is a twelve-transmembrane domain protein with intracellular N- and C-terminal domain regions, and is present on an SV with approximately 10 copies per excitatory SV (Wilhelm et al., 2014, Takamori et al., 2006). Biochemical studies on *Xenopus* oocytes and human pancreatic tumour

cells have shown that VGLUT1 is exclusively present on SVs and function as the vesicular glutamate transporter for excitatory synapses (Bellocchio et al., 2000, Takamori et al., 2000). In the mammalian brain, VGLUT1 is expressed predominant in the neocortex, striatum, hippocampus, thalamus and cerebellum (Liguz-Lecznar and Skangiel-Kramska, 2007).

1.2.3.6 – Vesicular ATPase (VTP-ase)

Vacuolar-type H^+-ATPase (V-ATPase) is a highly conserved enzyme that enables proton transport across the cellular plasma membrane to produce a proton gradient. The energy required to produce this gradient derives from the hydrolysis of adenosine triphosphate (ATP) (Nelson and Harvey, 1999). V-ATPases are located on a SV with approximately 2 copies per SV (Takamori et al., 2006, Wilhelm et al., 2014), and their primary role is the re-acidification of a SV to maintain the luminal pH of 5.5 for a functional SV. In experiments using hippocampal neurones transfected with pHluorin reporters, it was shown that V-ATPase activity allows SVs to re-acidify with first-order kinetics with a tau of approximately 5-15 s after compensatory endocytosis (Atluri and Ryan, 2006, Egashira et al., 2015).

1.2.3.7 – RAB

RAB proteins are a superfamily of small GTP-binding proteins that have been suggested to mediate the recognition of interacting components of the membrane prior to membrane fusion (Bourne, 1988). Proteomic analysis has identified more than 30 distinct RAB proteins to be present in highly purified SVs, however RAB3A

in particular was found to be present in up to 10 copies per SV (Takamori et al., 2006, Wilhelm et al., 2014). The exact function for RAB3A at a nerve terminal has not been defined; however, it has been suggested to play a role in the targeting, docking and fusion of SVs at the active zone of the plasma membrane. Recent functional studies with RAB3A have revealed a binding interaction with the C2A domain of SYT1 during immunoprecipitation, giving credence to the argument of RAB3A's role in targeting and fusion of SVs at the membrane surface (Tang et al., 2017). Lysosomal studies in HeLa cells have shown that silencing of RAB3A expression changes the intracellular localisation of lysosomes and blocks repair of the plasma membrane (Encarnação et al., 2016), suggesting that RAB3A may play an important role in maintaining the fidelity of SV membranes after various cycles of exocytosis and endocytosis. A summary of key synaptic proteins and their features is given in a table below (Table 1.2.3).

SV Protein	Copy Number (per SV)	Key Function
SNAP-25	2	t-SNARE protein
Syntaxin-1	6	t-SNARE protein
Synaptophysin	30	SYB2 iTRAP
Synaptobrevin 2	70	v-SNARE protein
SV2A	2-12	SYT1 iTRAP
Synaptotagmin 1	20	Ca^{2+} sensor for synchronous release
V-GLUT1	10	Transporter for glutamate loading into SVs
V-ATPase	2	Vesicular proton pump to maintain intravesicular pH
RAB(s)	10	Targeting of SVs to active zone

Table 1.2.3: Summary of key SV proteins and their functions. The table above summarises a selection of key SV proteins, their copy numbers (per SV) and their key features at the presynaptic terminal.

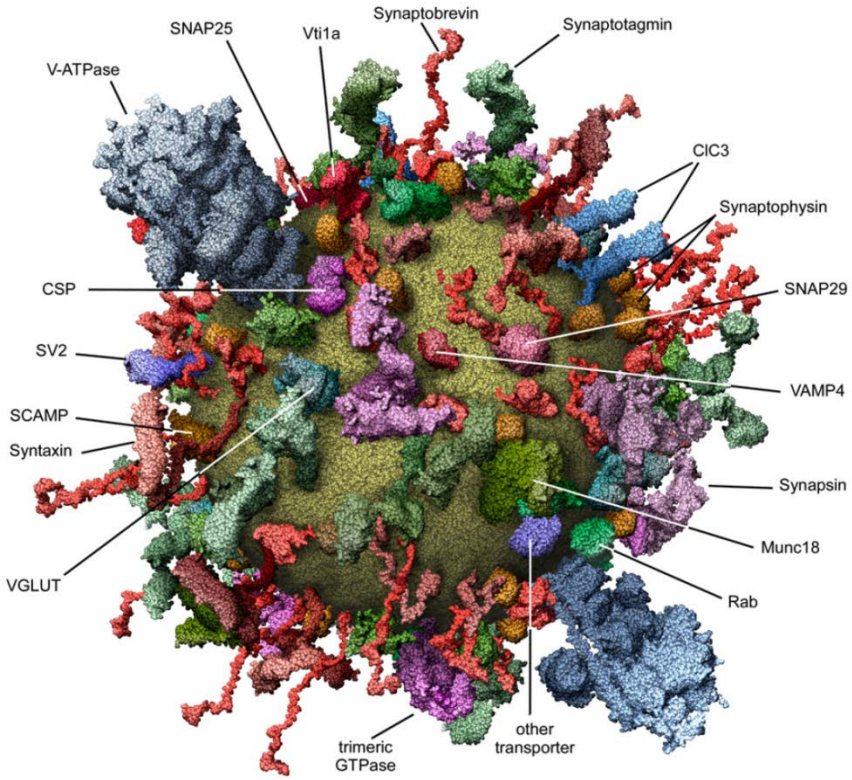

Figure 1.2.3: Molecular Model of a Typical Synaptic Vesicle(Takamori et al., 2006). The figure shows the morphology of a typical synaptic vesicle (SV) and its various key SV proteins. The most abundant protein is synaptobrevin II (SYB2), with approximately 70 copies per SV. SYB2 plays an integral role in SV exocytosis as one of the SNARE proteins alongside syntaxin and SNAP-25. The next most abundant protein is synaptophysin (SYP), with approximately 30 copies per SV. SYP plays a key role in the localisation of SYB2 to nerve terminals as well as the retrieval of SYB2 during SV endocytosis. Synaptotagmin I (SYT1) is the Ca^{2+} sensor for activity-induced SV exocytosis and is present on the SV with approximately 15 copies per SV. Vesicle glutamate transporter protein 1 (VGLUT1) and RAB3A are present with approximately 10 copies per SV, and have roles in loading of neurotransmitter and targeting of SVs to the active zone respectively.

1.3 – Synaptic Vesicle Exocytosis: Fusion of Vesicles and Release of Neurotransmitter

On average, around 20-50% of SVs are stored in the TRP of the nerve terminal under resting conditions. When there is intense synaptic activity occurring in the neurone, SVs in the TRP are translocated to the active zone (see chapter 1.1). At the active zone, the recruitment and assembly of SNARE proteins into a complex is crucial for the docking and priming of SVs (Figure 1.3). Docked SVs at the plasma membrane collectively form the RRP. These SVs subsequently fuse and release neurotransmitter (a process termed exocytosis) upon activity-dependent calcium influx. Neurotransmitter release mediated by Ca^{2+} -induced action potentials occurs at a fast speed and vesicle fusion is synchronised to the activity at the synapse. This type of release is also known as *synchronous* release.

The synaptic proteins synaptobrevin 2 (SYB2), syntaxin-1 and SNAP-25 make up the SNARE family proteins (Südhof and Rothman, 2009). SYB2 is localised on the SV, whilst syntaxin-1 and SNAP-25 are located at the presynaptic plasma membrane (Sudhof, 2004). Syntaxin-1 is first kept in a 'closed conformation' by the protein Munc18 prior to SV arrival at the active zone (Dulubova et al., 1999). Syntaxin-1 cannot form SNARE complexes in this conformation, presumably as a preventative mechanism to inhibit premature SNARE complex assembly. Arrival of a SV at the active zone triggers a conformational change in Munc18 that alters its interaction with syntaxin-1 at two spatially separated sites (Burkhardt et al., 2008). Another protein, Munc13, is then presumed to adopt a role in unlocking syntaxin-1 from Munc18 and allows syntaxin-1 to adopt an 'open conformation' and promote SNARE complex assembly (Ma et al., 2011). Munc13 is also shown to play a role in

priming the attachment site of the vesicle at the active zone (Augustin et al., 1999), as it has been shown to form a tripartite complex with the proteins RAB3A and RIM (RAB3 interacting molecule, an organiser of the active zone) (Lu et al., 2006). Upon contact of the SV and membrane SNAREs, the proteins associate with each other in a trans-conformation at the N-terminal ends. A tight bundle consisting of four parallel α-helical domains (one each from SYB2 and syntaxin-1, two from SNAP-25) is progressively formed and proceeds in an amino to carboxy-terminal direction (Hanson et al., 1997). This pulls the membrane tightly together in a zippering action to initiate priming. The zippering process is proposed to be controlled by a small cytoplasmic protein, complexin, which occurs via two possible mechanisms: 1) binding to the surface of the SNARE complex to start the zippering process (Xue et al., 2010); 2) acting as a clamp to prevent full progression of the SNARE zippering (Yang et al., 2010). Once primed, the SV readily fuses when the SNARE machinery is triggered into action by influx of calcium into the nerve terminal.

The role as molecular sensors for calcium influx at the presynaptic nerve terminal is generally mediated by the synaptotagmins, which are a family of membrane trafficking proteins. There has been many studies performed which investigate the role of the various isoforms of synaptotagmin at the presynapse. However, synaptotagmin I (SYT1) is the dominant isoform for evoked synchronous neurotransmitter release. SYT1 is a SV protein consisting of a single transmembrane region connected to two C2 domains (termed C2A and C2B) via flexible linker regions (see chapter 3 for a more detailed review on SYT1). Ablation of SYT1 in mice resulted in a selective loss of fast Ca^{2+}-triggered exocytosis both in hippocampal synapses without impairment of other parameters of synaptic function

(Geppert et al., 1994). In the presence of Ca^{2+}, the C2 domains of SYT1 can chelate the Ca^{2+} ions and bind them with acidic phospholipid residues at the presynaptic membrane (Chapman, 2008). The chelation process moves the SV into close proximity with the membrane and potentially destabilises the membrane bilayers in order to facilitate the fusion process. The merger of the vesicle bilayer and the membrane bilayer at the contact site develops into the opening of an aqueous channel (termed as the fusion pore) whereby neurotransmitter is released from the luminal domain of the vesicle into the synaptic cleft (Qian and Huang, 2012).

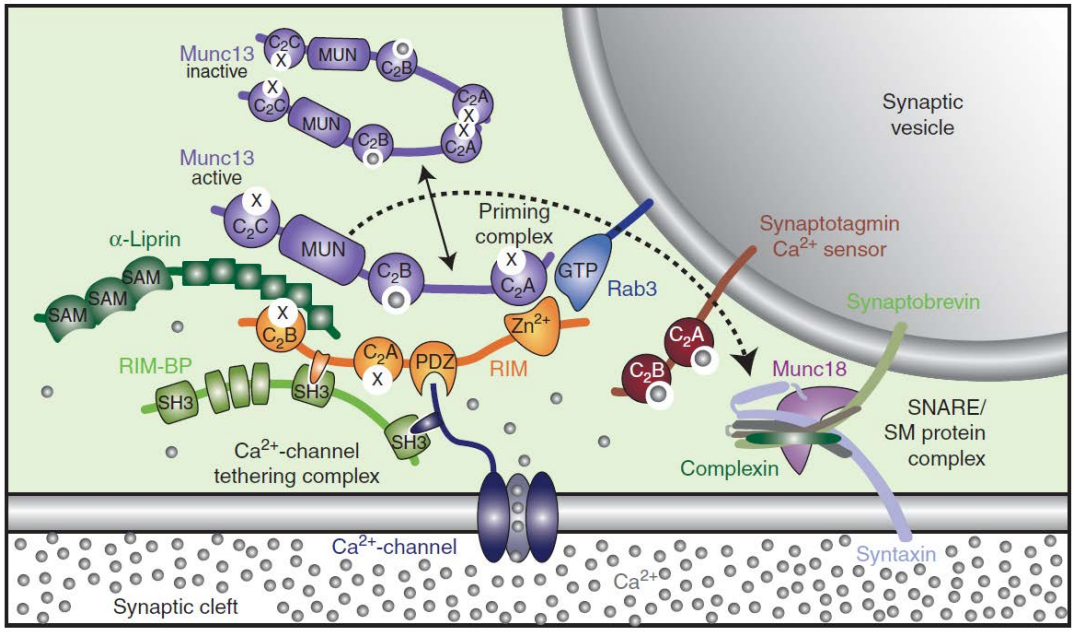

Figure 1.3: Docking and priming of a SV at the active zone (Südhof and Rizo, 2011). The modular protein Munc13 forms a priming complex with the active zone organiser RIM and Rab3. Calcium influx triggers two reactions which facilitate exocytosis: 1) The liberation of Munc13 from the priming complex which unlocks syntaxin-1 from Munc18 and allows SNARE assembly to complete zippering; 2) The coordination of the C2 domains of synaptotagmin I and the acidic phospholipid residues in the plasma membrane to Ca^{2+} ions, bringing the vesicle into close proximity whilst destabilising the membrane bilayer, allowing for fusion with the plasma membrane.

1.3.1 – Asynchronous and Spontaneous Release

Fast synaptic transmission (or synchronous release) in the brain requires coordinated vesicle fusion that is evoked by action potentials induced by Ca^{2+} influx. However, nerve terminals are also able to release neurotransmitters in the absence of an action potential. There are two main types of neurotransmitter release in the absence of an action potential: 1) *Asynchronous* release, which is a persistent release of neurotransmitter immediately after action potential-dependent synchronous release and 2) *Spontaneous* release, which occurs in the absence of presynaptic membrane depolarisation and occurs stochastically throughout the lifetime of a neurone.

Although synchronous release accounts for almost all (greater than 90%) neurotransmitter release at synapses under low-frequency stimulation, asynchronous release is also prominent in certain networks in the brain, in particular the synapses from the deep cerebellar nuclei to the inferior olive (Best and Regehr, 2009). Asynchronous release is usually evoked by sustained moderate to high-frequency stimulation, and the magnitude of asynchronous release is usually linked to a steep frequency dependence that are aligned to the range of firing frequencies experienced by the synapse (Kaeser and Regehr, 2014). Numerous roles have been suggested for asynchronous release in mammalian physiology. One of the key roles is the prolonged release of GABA in inhibitory synapses to provide a smooth and gradual inhibition that is unreliant on the precise timing of individual action potentials (Lu and Trussell, 2000). High-frequency activation of fast-spiking cortical interneurones results in the asynchronous release of GABA which lasts several seconds (Manseau et al., 2010), suggesting that asynchronous release may play a role in the suppression of epileptiform activity caused by widespread synchronous activity.

Asynchronous release is triggered by Ca^{2+} influx in a manner similar to synchronous release. The introduction of the slow Ca^{2+} chelator, ethyleneglycol tetraacetic acid (EGTA), into the presynaptic terminal eliminated the presence of asynchronous release whilst having very little effect on synchronous release (Atluri and Regehr, 1998), suggesting that a different Ca^{2+} sensor is responsible for asynchronous release that responds to general bulk cytosolic Ca^{2+} levels rather than high local Ca^{2+} caused by influx. Several Ca^{2+}-sensing proteins, such as SYT7 (Maximov et al., 2008) and DOC2 (Yao et al., 2011), have been proposed to be mediators for asynchronous release. Other SV proteins such as VAMP4 have been proposed to play a mediating role in SV movement in asynchronous release by binding to t-SNAREs in order to drive asynchronous SV fusion. Overexpression of VAMP4 in SYB2-knockout mice showed limited rescue of synchronous release and a prolonged postsynaptic current late in a train of stimuli that could be eliminated in the presence of EGTA (Raingo et al., 2012). There have been many research studies on the diverse mechanisms that mediate asynchronous release in a variety of neuronal sub-types. These mechanisms will not be covered in the scope of this review.

Spontaneous release is the release of neurotransmitter that is independent of action potential-induced presynaptic membrane depolarisation. Spontaneous release was first described in experiments by Bernard Katz and colleagues in the 1950s, where they observed neurotransmitter release occurring in discrete ‘quantal’ events in cholinergic neuromuscular junction preparations (FATT and KATZ, 1950, FATT and KATZ, 1952). Spontaneous release occurs at a rate of around 10^{-3} SVs per second, which is far reduced from the rate of synchronous release (10^{3} SVs per second) (Kaeser and Regehr, 2014). Unlike evoked release, which is mediated by the

total recycling pool of SVs, spontaneous release in central synapses is mediated by the resting pool of SVs (Sara et al., 2005, Fredj and Burrone, 2009). Effectively, this limits action potential-independent activity at the synapse. Spontaneous release has been implicated in synaptic stabilisation as well as long-term synaptic plasticity. Cell spine density and length in hippocampal slice cultures decreased after application of AMPA receptor antagonists to block spontaneous glutamate release (McKinney et al., 1999), suggesting that spontaneous release exerts a trophic effect on dendritic spines to maintain their fidelity. In cultured hippocampal pyramidal cells, spontaneous glutamate release activates NMDA receptors and suppresses local protein synthesis in dendrites (Sutton et al., 2006). Pharmacological blockade of NMDA receptors resulted in a regulatory increase of AMPA receptors after a few hours, an effect which required a much longer timeframe if only evoked activity was eliminated. This suggests that spontaneous release plays a key role in regulating homeostatic plasticity at the synaptic terminal through regulation of local dendritic protein synthesis.

1.4 – Synaptic Vesicle Endocytosis: Retrieval of Vesicular Cargo and Membrane

SV endocytosis involves both: 1) retrieval of SV proto-vesicle components from the plasma membrane and 2) the regeneration of functional SVs with the proper molecular composition. Neuronal synapses differ greatly with respect to typical firing pattern, thus different neuronal subtypes may require specific adaptations to meet the needs of membrane retrieval and reformation of functional synaptic vesicles to replenish the reserve pool. For example, high firing synapses such as the Calyx of Held (firing at many hundreds of Hz) require a more efficient and faster mode of SV cargo retrieval in order to release vesicle docking sites compared to synapses in the hippocampus (firing at tens to low hundreds of Hz) (Neher, 2010). As different neurones are exposed to different range of stimulus frequencies, several endocytic pathways exist in neurones that differ in their capabilities to retrieve SV cargo with respect to speed of retrieval, maintenance of SV identity and molecular composition. There are currently three distinct endocytosis pathways shown to occur in neurones: 1) Clathrin-mediated endocytosis; 2) Bulk endocytosis and 3) Ultrafast endocytosis. The study of SV recycling is complex, and many tools and assay techniques have been generated by various academic groups to study different presynaptic phenomena. A selection of these tools and techniques are discussed in the sub-sections below and a summary table is provided (Table 1.4.1).

1.4.1 – Methods to Visualise and Monitor SV Cargo Retrieval in Neurones

There are several methods and tools available for conducting investigations of SV exocytosis and endocytosis at the presynaptic nerve terminal. The most common

protocols are based on fluorescence imaging techniques such as styryl FM dye assays, pHluorin retrieval assays as well as internalisation of bulk fluorescent molecules such as dextran. Electron microscopy may also be utilised for resolution of fine structural morphology at the synaptic terminal.

1.4.1.1 – Styryl (FM) Dyes

Styryl (FM) dyes are chemical molecules that have a hydrophilic head group and a hydrophobic tail, which gives the dye molecules similar chemical properties to phospholipid molecules in the plasma membrane. The dye molecules can partition themselves reversibly into the plasma membrane without fully permeating the membrane. Fluorescence only occurs when the molecules are partitioned in the membrane and not in solution. These properties makes styryl dyes a useful tool for tracking the kinetics of SV recycling in living cells. The length of the lipophilic tail in the dye determines the intensity of fluorescence output as well as how permanently the dye is partitioned into the membrane. Dyes with short tails are less lipophilic, so bind less tightly to the membrane and fluoresce less brightly (e.g. FM2-10, which contains two carbon atoms in its tail). Dyes with longer tails are more lipophilic so bind strongly to the membrane and fluoresce more brightly (e.g. FM1-43, which has four carbon atoms in its tail) (Betz et al., 1996). Neuronal cultures incubated in the presence of FM dyes will have selected vesicle pools labelled when stimulated by either an elevated K^+ solution or a train of action potentials. The FM dye molecules partition themselves into the neuronal plasma membrane and the membrane is retrieved by various mechanisms of SV endocytosis. This labels all SVs that are turned over because of the stimulus. The remaining unpartitioned dye

molecules can be washed away with extracellular media, leaving the FM-labelled synapse. Since these FM dyes can be departitioned from the plasma membrane, a subsequent stimulus can release the SV-partitioned dyes during exocytosis. The decrease in the level of fluorescence due to this stimulus can be quantified to provide information about the turnover of SVs at the synapse (Cousin and Robinson, 1999). FM dyes may also be photo-converted into an electron dense marker for SVs at a presynapse so that it may be imaged using electron microscopy (Harata et al., 2001). This allows FM-labelling investigations of SV turnover at the individual synapse level, allowing clarification of the endocytosis pathway that is in use by the specific synapse in question.

1.4.1.2 – PH Sensitive GFP-Fused Protein Reporters (pHluorins)

The advent of pHluorins have enabled the study of the kinetics of vesicle re-acidification and other aspects of SV trafficking. pHluorins are green fluorescent proteins (GFP) which have been genetically engineered to be highly sensitive to pH changes and can be fused to a target SV-related protein of choice to be investigated. The pH-sensitive GFP in pHluorins is located in the intraluminal domain of the vesicle (as it is specifically fused to the luminal domain of an exogeneous SV protein) and fluorescence is quenched under the pH conditions in this domain (pH ~ 5.6). During SV exocytosis, the vesicle fuses to the plasma membrane and the pH-sensitive GFP fluoresces when exposed to the high pH of the extracellular environment (pH ~ 7.4). Fluorescence is quenched again following SV endocytosis and re-acidification and the GFP molecule is returned to the environment of the intraluminal domain (Miesenböck et al., 1998, Sankaranarayanan and Ryan, 2000).

In cultures of hippocampal neuronal synapses, SV re-acidification was thought to occur on a timescale of around 4-5 s after internalisation (Granseth and Lagnado, 2008, Atluri and Ryan, 2006), however more recent experiments using the probe mOrange have indicated it to be around 15 s (Egashira et al., 2015). The rate-limiting step is therefore the rate of pHluorin internalisation during SV endocytosis, thus the rate of pHluorin quenching can be directly linked as a measure of SV endocytosis at the synaptic terminal. As SV endocytosis and re-acidification takes place at the same time as SV exocytosis during evoked stimulation, delinearisation of the two processes is required to provide accurate information of rates of SV exocytosis. Prevention of SV re-acidification can be achieved by pharmacological inhibition of the vesicle proton pump V-ATPase using the drug bafilomycin, allowing rates of SV exocytosis to be directly related to rates of pHluorin fluorescence (Ryan, 2001). Different SV protein-pHluorin constructs have been reported in the literature. These include, but are not limited to: 1) SynaptopHluorin, which is a conjugate of synaptobrevin II and pHluorin (SYB2-pHluorin) (Sankaranarayanan and Ryan, 2000); 2) SypHy, which is a conjugate of synaptophysin and pHluorin (SYP-pHluorin) (Granseth et al., 2006); 3) SYT1-pHluorin (Wienisch and Klingauf, 2006); 4) VGLUT1-pHluorin (Voglmaier et al., 2006); SV2A-pHlourin (Kwon and Chapman, 2012) and 5) VAMP4-pHluorin (Raingo et al., 2012).

Elegant use of pHluorins in various experiments may provide specific information on SV protein expression and retrieval mechanisms at the synaptic terminal. The surface fraction of SV protein expression and the variations in fluorescence along the neurite can be revealed using acidic (pH ~ 5.5) and basic (pH 7.4) imaging media to reveal the total expressed pHluorin in the neurone(Gordon et al., 2011). Recent work has

shown that most SV pHluorins report protein retrieval via the CME mechanism, with the exception of VAMP4-pHluorin, which reports retrieval of VAMP4 via ADBE (Nicholson-Fish et al., 2015). Therefore, future investigations to determine pathways of endocytic retrieval in novel cell types may use SYP-pHluorin and VAMP4-pHluorin as reporters for CME and ADBE respectively.

1.4.1.3 – Dextran Conjugates

Dextrans are large, inert polysaccharide molecules that are conjugated to fluorescent dyes such as rhodamine. Fluorescent conjugates of dextran are impermeable to the plasma membrane and are generally excluded from uptake by single recycling SVs due to their large molecular size. As a result, dextran conjugates can be used as selective markers for fluid phase ADBE events at the synapse without being affected by CME. Large fluorescent dextrans have been used in snake motor neurone terminals (Teng et al., 2007), retinal bipolar cells in goldfish (Holt et al., 2003) and rat cerebellar granule neurones (Clayton et al., 2008).

1.4.1.4 – Horseradish Peroxidase (HRP)/Electron Microscopy (EM)

The uptake of horseradish peroxidase (HRP) has been frequently used as a method to visualise the fine structural morphology of neurones as well as to distinguish between the various mechanisms of endocytosis in neurones. As a fluid phase marker, neurones are able to uptake HRP during SV endocytosis, which provides non-selective labelling of different endocytosis pathways. During preparation, the membrane is stained using osmium or uranium and HRP is converted into an electron

dense product by oxidation with 3-diaminobenzidine and hydrogen peroxide. This increases scattering of electrons to give high contrast 'dark spots' in the electron micrograph. This method can be used to visualise synaptic vesicle pools, bulk endosome vacuoles, plasma membrane deformities and other morphological changes at individual synapses (Marxen et al., 1999, Leenders et al., 2002, de Lange et al., 2003, Evans and Cousin, 2007).

1.4.1.5 – Membrane Capacitance Measurements

The fusion and retrieval of SV cargo and membrane leads to change in the total volume of membrane at the cell surface. As biological membranes have an electrical potential across them, accurate measurements of the change in the electrical capacitance of the membrane can be directly related to the insertion and removal of membrane volume at a nerve terminal (Neher and Marty, 1982). This method is best used to observe bulk trafficking of membrane and cargo in large synapses such as retinal bipolar cells or the Calyx of Held. Although membrane capacitance measurements are a useful tool, they lack specificity in the identities of the cargo being trafficked and their use is limited to large synapses as central nerve terminals are generally too small to patch and produce accurate readings.

Method of Visualisation	**Measured Parameter**	**Advantages**	**Disadvantages**
Styryl (FM) Dyes	• Changes in fluorescent dye binding to membranes	• Live monitoring of fluorescent probe recycling • No need for genetic manipulation or transfection	• Poor temporal resolution • Low signal to noise ratio
pHluorins	• pH dependence of intravesicular fluorescence	• Recycling can be monitored in live cell preparations • Good temporal resolution	• Requires genetic manipulation/transfection • Dependency on SV re-acidification kinetics to give indirect measure of SV recycling
Fluid phase markers (e.g. dextran or HRP)	• Morphology of plasma membrane or membrane-derived intermediates	• Very high spatial resolution	• Poor temporal resolution • Requires careful tissue preservation • Time consuming
Membrane Capacitance	• Membrane surface area	• Very high temporal resolution	• Limited to large presynaptic terminals (e.g. calyx of Held) • Limited detail in the nature of internalisation and its contents

Table 1.4.1: A summary table comparing the advantages/disadvantages of the different methods of visualising SV cargo retrieval.

1.4.2 – Clathrin-mediated Endocytosis

The internalisation of SV membrane into the cell from the membrane surface by SVs coated with the structural protein clathrin is known as *clathrin-mediated endocytosis* (CME). CME is remains to this date as the best-characterised and understood model of endocytosis. Clathrin was initially discovered to form a lattice-like coat structure around SVs in 1976 (Pearse, 1976). Clathrin-coated SVs isolated later from nerve terminals exhibited strong association with SV proteins, giving the first indication that clathrin plays a key role in the recycling of SV proteins at the synapse (Maycox et al., 1992). The formation of clathrin-coated SVs develops through six stages: nucleation, cargo sorting, coat assembly, membrane deformation, scission and uncoating.

1.4.2.1 – Initiation of Endocytosis and Cargo Sorting

The budding of a vesicle from the plasma membrane starts from the formation of a membrane invagination called a 'pit'. Initiation of a clathrin-coated pit is triggered by the recruitment of the assembly protein complex 2 (AP-2), mediated by the binding of endocytic motifs in the cytoplasmic tail of AP-2 (α and μ subunits) to the plasma-membrane specific lipid phosphatidylinositol-4,5‑bisphosphate [$PI(4,5)P_2$] (Höning et al., 2005). Recent work has suggested that formation of a putative nucleation module on the plasma membranes defines the sites of clathrin recruitment. FCH domain only protein (FCHO), intersectins (Henne et al., 2010) and epidermal growth factor pathway substrate 15 (EPS15) (Suzuki et al., 2012) have been suggested to be essential for the function of the nucleation module, as mutation or

depletion of these proteins result in the inhibition of clathrin coat recruitment. Clathrin coats are formed from the cytosolic recruitment and assembly of three clathrin heavy chain units and three clathrin light chain units into a polyhedral lattice (Brodsky et al., 2001). The nucleation module is responsible for the recruitment the AP-2 which in turn binds clathrin and other cargo specific adaptor proteins (e.g. stonin-2, AP-180, CALM) to mediate cargo selection (Koo et al., 2011, Kononenko et al., 2013). AP-2 also targets transmembrane proteins with tyrosine (Yxxϕ, where ϕ is a bulky hydrophobic residue) and di-leucine ([DE]XXXL[LI]-based motifs for internalisation. The specific mechanisms behind endocytic sorting signals and adaptors will be described in more detail in chapter 3.

1.4.2.2 – Membrane Deformation and Scission

After the sorting of SV cargo and clathrin around the membrane, it is necessary to deform the membrane in order to initiate budding of the SV from the cell surface. It is currently accepted that mechanisms that initiate invaginations of early clathrin coated pits involves membrane-deforming proteins. The most important class of these membrane-deforming proteins is the Bin-Amphyphysin-RVS (BAR) domain-containing superfamily of proteins. BAR-domain-containing proteins include examples such as amphiphysin, endophilin, syndapin and sorting nexin 9 (SNX9) (Qualmann et al., 2011). BAR-domain proteins were initially discovered as conserved domains in BIN1, amphiphysin and the yeast proteins RVS161p and RVS167p (David et al., 1994). Crystallographic studies later revealed that the BAR-domain proteins are dimers consisting of three long helices of each monomer. BAR-domain proteins are known effectors of membrane curvature, and the scaffolding

mechanism is generally mediated by the binding of positively charged membrane-interacting residues with negatively charged lipids such as phosphoinositide and phosphatidylserine (Peter et al., 2004). BAR-domain proteins are intrinsically curved, thus forces the membrane surface to adopt a similar shape. Within the superfamily of BAR-domain proteins, different proteins effect different levels of curvature on the membrane. N-BAR proteins such as amphiphysin and endophilin have strong curvatures where the angle of the dimer interception point is approximately 30º (Casal et al., 2006), whereas in F-BAR proteins such as syndapin the angle of interception is much less at approximately 10º (Wang et al., 2009). This suggests that F-BAR proteins may act at the early stages of membrane deformation, whilst the N-BAR proteins act as late-stage co-ordinators of SV scission and uncoating (Frost et al., 2009).

Another class of membrane-deforming proteins include epsin and its auxiliary interacting partner EPS15. Epsin contains the epsin N-terminal homology (ENTH) which binds directly to the membrane lipid $PI(4,5)P_2$, in conjunction with clathrin, and induces membrane curvature. Binding of epsin to $PI(4,5)P_2$ results in the formation of an amphipathic α-helix in epsin, which is inserted into one leaflet of the lipid bilayer and induces membrane curvature (Ford et al., 2002). Disruption of epsin interactions by use of presynaptic microinjections of antibodies to either the ENTH domain or the clathrin/AP-2 binding region resulted in accumulation of distorted coated structures and the presence of a bias towards early endocytic intermediates such as shallow coated pits (Jakobsson et al., 2008). This suggests that epsin not only has a role in curvature generation, but also in the generation of uniform SVs.

BAR domain proteins also harbour Src Homology 3 (SH3) domains that bind to the proline-rich domain of the GTP-ase protein dynamin I (DYN1) (Anggono et al., 2006, Sundborger et al., 2011). DYN1 plays a key role in the membrane scission of the fully formed clathrin coated pits, suggesting an extremely close physical and functional link that exists between membrane deformation and SV scission. Oligomeric polymerisation of dynamin around the neck of the clathrin-coated pit facilitates GTP-mediated hydrolysis of the protein and subsequent membrane scission (Sweitzer and Hinshaw, 1998). The exact mechanism of dynamin action at the SV neck remains debated to this day, but several proposals have been made: 1) DYN1 acts like a spring which 'pops' the coated pit from the plasma membrane upon hyperextension of the protein helix (Stowell et al., 1999); 2) DYN1 constricts around the neck of the coated pit, thereby 'pinching' it free from the plasma membrane (McNiven et al., 2000); 3) DYN1 induces a 'twisting' action on the neck of the coated pit upon GTP hydrolysis, inducing a high tension which is only released when the tubule breaks and the SV is free (Roux et al., 2006) and 4) DYN1 constriction acts like a 'corkscrew', based on X-ray crystallography and cryo-electron microscopy studies (Mears et al., 2007). The functional role of DYN1 in scission cannot be disputed, since various electron microscopy studies on central synapses from several mammalian DYN1 knockout systems have demonstrated defective fission of clathrin-coated pits from the plasma membrane (Ferguson et al., 2007, Raimondi et al., 2011).

1.4.2.3 – Uncoating of Clathrin from the SV

Shortly after vesicle scission, the released nascent vesicles shed their coat as the clathrin lattice assemblies disassemble back to their triskelia forms. SV uncoating is mediated by the ATPase heat shock protein – 70 kDa (HSC70) and its cofactor, auxilin (Rothnie et al., 2011). Since HSC70 is an ATPase, the uncoating process is ATP-dependent. This is evidenced by the observation that presence of ATP significantly increases the rate of HSC70/auxilin complex formation, whilst presence of ADP inhibits this complex formation (Prasad et al., 1994). The cofactor, auxilin, was identified early on as a member of the DnaJ protein family due to the presence of the J-domain at its C-terminus. DnaJ proteins have roles in protein folding, transmembrane protein transport as well as selective disruption of protein-protein interactions. Deletion of the J-domain in auxilin resulted in the loss of cofactor activity (Ungewickell et al., 1995). The interactions between clathrin, auxilin and HSC70 are highly specific. Biochemical studies have revealed that auxilin first binds to clathrin triskelion baskets on the SV, followed by binding of HSC70-ATP to the auxilin-clathrin complex. After initiation of the uncoating process, auxilin can then migrate to another clathrin triskelion (Barouch et al., 1997). Cryo-electron microscopy studies on the HSC70/auxilin/clathrin interaction showed that binding of auxilin induced a local change in the contacts of clathrin heavy chains, creating a distortion of the clathrin coat. This destabilisation of the clathrin lattice facilitates general SV uncoating (Fotin et al., 2004). Electron microscopy studies have further demonstrated that knockout of auxilin in mice central synapses results in the inhibition of SV uncoating at the synapse (Yim et al., 2010).

Another key protein associated with the SV uncoating process is synaptojanin I (SYJ1). SYJ1 is a phosphatidylinositol-5-phosphate (PI(5)P) phosphatase, which is directly responsible for the dephosphorylation of $PI(4,5)P_2$. The BAR proteins endophilin and amphiphysin bind SYJ1 via their SH3 domains (Cestra et al., 1999). Total internal reflection fluorescence microscopy studies have shown that endophilin and SYJ1 are recruited together at a late stage of clathrin-coated pit formation, suggesting that endophilin may play a role as a recruiter of SYJ1 to the plasma membrane (Perera et al., 2006). However, recent electron microscopy studies have shown that endophilin may play a more active role in the timing of SV uncoating. Genetic ablation of all three isoforms of endophilin in mice resulted in the accumulation of clathrin-coated SVs, but not clathrin-coated pits, at the synapse (Milosevic et al., 2011). This suggests that presence of SYJ1 at the SV is required for uncoating, but a precise trigger mediated by endophilin is required for activation of the uncoating process. SYJ1 knockout neurones have shown that dual action of both phosphatase domains in SYJ1 is necessary for SV cycling. Rescue with SYJ1 containing point mutations in either phosphatase domain resulted in a failure to restore the normal phenotype as observed when rescued using wild type SYJ1 (Mani et al., 2007). If we consider all evidence, it is highly likely that SV uncoating requires the coordinated action of several mechanisms involving SYJ1, HSC70 and auxilin.

1.4.2.4 – Kinetics of CME

The kinetics of CME has been a widely debated topic in presynaptic neuronal cell biology over the last decade. Several optical imaging and membrane capacitance studies in different model systems have shown that it occurs on a timecourse of around 10-20 s at room temperature using lower intensity stimulation paradigms (Granseth et al., 2006, Jockusch et al., 2005, Balaji and Ryan, 2007). Increasing the intensity of stimulation in central synapses appears to increase the timecourse of which CME operates to about 30-60 s (Sankaranarayanan and Ryan, 2000, Wu et al., 2014). There is evidence which indicates that CME generally accelerates to a timecourse of around 5-6 s under physiological temperatures (37ºC) (Nicholson-Fish et al., 2015), however the role of CME as the dominant mode of SV endocytosis at physiological temperatures has been debated (Watanabe et al., 2014).

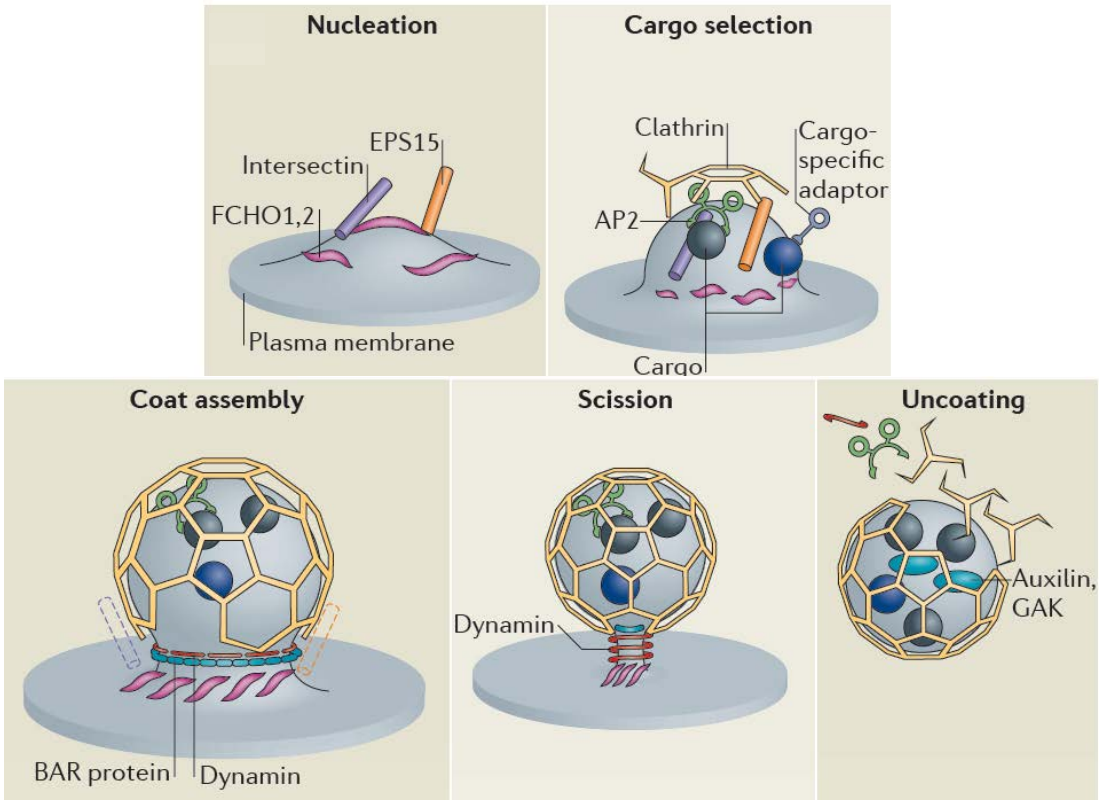

Figure 1.4.2: The clathrin-mediated endocytosis (CME) pathway (McMahon and Boucrot, 2011). Formation of a putative nucleation module is mediated by the proteins FCHO, EPS15 and intersectin. The nucleation module is responsible for the recruitment of AP-2 and other cargo specific adaptors (e.g. stonin-2, AP-180, CALM) to ensure the correct SV molecular composition. AP-2 is also responsible for the recruitment of clathrin triskelia, which assembles into a polyhedral lattice. Association of clathrin with BAR proteins, which effect membrane curvature, allows the formation of an early stage clathrin coated pit. BAR proteins are also responsible for the recruitment of the GTPase dynamin to the neck of the pit. GTP-hydrolysis mediated conformational changes in dynamin initiate membrane scission and fission of the nascent vesicle. The clathrin coat then disassembles back into triskelia by through the co-ordinated action of HSC70, auxilin, and the PI(4,5)P2 phosphatase synaptojanin I.

1.4.3 – Activity Dependent Bulk Endocytosis

Although CME alone is capable of regenerating SVs from the plasma membrane, the timescale of which it occurs (15-20 s) is too slow for maintaining neurotransmission under periods of intense neuronal activity. The recruitment of clathrin triskelia itself requires seconds (Cocucci et al., 2012), therefore CME cannot be solely responsible for the retrieval of SVs during intense activity. Previously discussed pHluorin-imaging experiments in hippocampal neurones have also showed that CME has a maximal rate that does not scale with increasing stimulation intensity (Granseth et al., 2006, Balaji and Ryan, 2007). Therefore, under prolonged periods of high-frequency stimulation (up to hundreds of Hz), CME becomes saturated with activity and an additional mechanism for fast membrane retrieval is required to maintain neurotransmission. Electron microscopy studies have shown that under periods of high-frequency stimulation (40-80 Hz), large endosomal vacuoles of plasma membrane are internalised via a clathrin-independent retrieval pathway in rat cerebellar granule neurones (Clayton et al., 2008). This specific clathrin-independent pathway of membrane retrieval is known as *activity-dependent bulk endocytosis* (ADBE). Since ADBE is triggered only by high-frequency stimulation and has the capacity to rapidly reverse the increase in plasma membrane surface area of a nerve terminal due to excess SV exocytosis, it is the dominant mode of membrane retrieval during intense neuronal activity.

The mechanism by which ADBE operates is driven by the dephosphorylation of the GTPase protein dynamin I (DYN1) by the calcium-dependent phosphatase calcineurin triggered by calcium influx during intense stimulation (Clayton et al., 2009). Mutagenesis studies have identified two key phosphorylation sites on DYN1

which are crucial to mediating the interaction between DYN1 and the BAR protein syndapin I (PACSIN1) (Anggono et al., 2006). The recruitment of PACSIN1 is essential for the maintenance of ADBE, as methods that inhibit or ablate expression of the protein resulted in arrest of the retrieval process (Koch et al., 2011). PACSIN1 is a BAR protein containing an F-BAR domain, which is responsible for in the initiation of membrane curvature to produce a bulk invagination in ADBE. F-BAR domain proteins such as PACSIN1 have been demonstrated to have low-curvature (around 10º), and thus they are suggested to fit the profile of large diameter organelles (such as bulk endosomes) better in comparison to high-curvature N-BAR domain proteins such as endophilin and amphiphysin (Henne et al., 2007, Shimada et al., 2007). Deeper probing of the mechanisms behind ADBE has revealed a role for the enzymes glycogen synthase kinase 3 (GSK3) and cyclin-dependent kinase 5 (CDK5) in the phosphorylation-dependent activation of DYN1 in ADBE. Protein mutagenesis studies in rat cerebellar granule neurones have shown that CDK5 primes DYN1 by phosphorylating at residue S778, allowing GSK3 to phosphorylate DYN1 at residue S774 to prime DYN1 for ADBE (Clayton et al., 2010). The specific requirement for DYN1 for ADBE has been contested. ADBE was still observed in DYN1/DYN3 knockout mice, possibly due to very low but functional levels of DYN2 present (Raimondi et al., 2011). Photo-inactivation of dynamin in drosophila mutants has shown that bulk membrane cisternae are still present at the nerve terminal despite the apparent lack of dynamin (Kasprowicz et al., 2014). More recently, pHluorin imaging and biochemical studies have indicated that vesicle associated membrane protein 4 (VAMP4) is another essential protein for the

maintenance of ADBE, though its exact role is yet to be elucidated (Nicholson-Fish et al., 2015).

After the DYN1/PACSIN1-mediated formation and internalisation of the bulk endosome vacuole is complete, SVs begin to bud from the endosome to replenish the depleted SV pools. The exact mechanisms underlying the SV budding process are currently still unclear. The process is clathrin-dependent, as photo-inactivation of clathrin heavy chain in drosophila neurones resulted in the arrest of the SV cycle even though bulk endosomes were still observed to be present by electron microscopy (Heerssen et al., 2008, Kasprowicz et al., 2008). Calcium and calcineurin activity has also been demonstrated to a key process in SV budding. Chelation of both calcium and calcineurin by pharmacological methods resulted in the arrestment of SV generation from bulk endosomes (Cheung and Cousin, 2013). Interestingly, the inhibition of SV re-acidification using bafilomycin also arrested SV generation, suggesting that calcium release upon endosome re-acidification plays a major role in SV budding.

1.4.3.1 – Cargo Sorting at the Bulk Endosome

In order to ensure that viable SVs are formed from the bulk endosome, an efficient SV cargo sorting process must take place on the endosome itself, in a similar manner to SV cargo sorting at the plasma membrane. There are lines of evidence that implicates the requirement of adaptor proteins in generating viable SVs from the bulk endosome. Early studies show that brefeldin A-mediated inhibition of the GTPase ADP-ribosylation factor 1 (ARF1) resulted in the arrests SV generation from synthetic endosomes (Drake et al., 2000). ARF1 was previously shown to be

essential for the recruitment of the adaptor proteins AP-1 and AP-3 to the plasma membrane (Faúndez et al., 1998). Taken together, the data suggests that AP-1 and AP-3 plays a crucial role in facilitating SV generation at bulk endosomes. In agreement with this, later FM-dye labelling studies showed that genetic ablation of AP-1 and AP-3 in rat cerebellar granule neurones resulted in inhibition of reserve pool replenishment from bulk endosomes (Cheung and Cousin, 2012). There is also evidence for a key role for AP-2 in SV generation from endosomes. Electron microscopy studies in hippocampal neurones from conditional AP-2(μ) knockout mice revealed an accumulation of endosome-like vacuoles in the structure as well as reduced SV density (Kononenko et al., 2014).

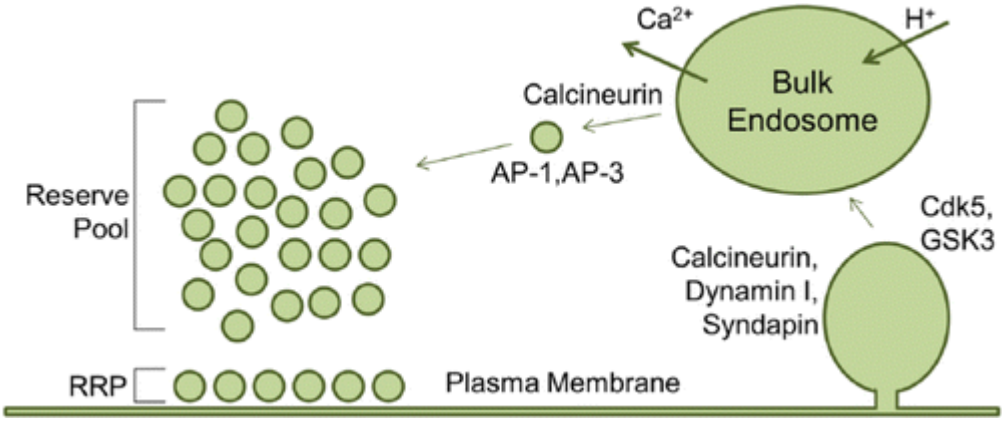

Figure 1.4.3: Molecular mechanisms for activity-dependent bulk endocytosis (ADBE) (Cousin, 2015). ADBE is the dominant mode for membrane retrieval during high-frequency stimulation. Phophorylation of S778 of Dynamin I (DYN1) by cyclin-dependent kinase 5 (CDK5) primes another residue, S774, for phosphorylation by glycogen synthase kinase 3 (GSK3). Subsequent dephosphorylation of both residues in DYN1 by the calcineurin results in the triggering of a DYN1/syndapin 1 (PACSIN1) interaction, which is key to formation and internalisation of the bulk endosome. On the bulk endosome, the generation of viable SVs is mediated by the proteins AP-1, AP-2, AP-3 and calcineurin. Calcineurin is thought to play in role in calcium release during endosome re-acidification, whilst the adaptor proteins AP-1/2/3 play a role in SV cargo sorting to reform viable SVs.

1.4.4 – Ultrafast Endocytosis

Recent experiments using high pressured, flash freezing of neuronal cells in worms and mouse hippocampal neurones (Watanabe et al., 2013a, Watanabe et al., 2013b)have detailed a novel mode of ultrafast endocytosis (UFE) observed at physiological temperatures which is fundamentally different from CME and ADBE. In UFE, bulk membrane invaginations of ~80 nm in diameter appear within 50-100 ms of a single action potential between the active and the peri-active zone of the plasma membrane(Watanabe et al., 2013b).

UFE is clathrin-independent at the membrane retrieval stage, but subsequently requires clathrin to form fully functional SVs from the internalised endosomes (Watanabe et al., 2014). This has led to the theory that ultrafast endocytosis may be required as a specialised mechanism to rapidly restore the surface area on the plasma membrane. More recently, direct patch clamp recordings of membrane capacitance from small central synapses in real time have corroborated earlier results using flash-freezing (Delvendahl et al., 2016). The mechanism behind this novel mode of endocytosis remains to be elucidated in full. UFE appears to share the same molecular mechanisms as ADBE but have two key differences: 1) the timeframe of completion of UFE is within 100 ms, whereas ADBE operates on a timeframe of seconds to minutes and 2) the amount of membrane internalised by UFE is much more consistent than ADBE (~60-80 nm in diameter). Nevertheless, these experiments have demonstrated that UFE is dependent upon the activity of dynamin I/III and actin polymerisation. GTPase-dependent activity and actin polymerisation are both known to be temperature sensitive and therefore may explain the diminishing influence of UFE at lower temperatures. There is an argument against

the importance of CME at physiological temperatures and that UFE is the dominant mode of endocytosis in these conditions. In support of this theory, SV endocytosis in hippocampal neurones has been shown to occur on multiple timescales from less than a second to several seconds at physiological temperature and is largely independent of clathrin and AP-2 (Soykan et al., 2017). However, there is recent evidence that suggest that CME does still occur at physiological temperatures (with a tau of around 5-6 s) (Nicholson-Fish et al., 2015).

1.5 – Overall Hypothesis and Aims of Research

This thesis will focus on the core interaction between two key SV proteins SV2A and SYT1. SV2A is retrieved by the adaptor protein AP-2, whilst SYT1 is retrieved by its monomeric adaptor protein, stonin-2. Recent evidence has indicated that the trafficking of SYT1 is intrinsically linked to SV2A function (Kaempf et al., 2015, Zhang et al., 2015)during SV recycling. The overall hypothesis of this work is that disruption of SV2A retrieval by AP-2 will lead to downstream defects in the recycling of SYT1, a key SV protein involved in SV docking and fusion at the plasma membrane. Malfunctions in the intrinsic trafficking partnership between SV2A and SYT1 may represent a novel underlying mechanism by which epileptogenesis may occur, as well as a novel presynaptic target by which certain anti-epileptic drugs (such as levetiracetam) may have a mode of action in the treatment of epilepsy.

The aims of the research are:

1) To establish and characterise the phenotype of SYT1 and general SV recycling when SV2A recycling is perturbed in mouse hippocampal neurones.

2) To establish and characterise the phenotype of SYT1 and general SV recycling when known human mutation of SV2A implicated in epilepsy (R383Q) replaces normal SV2A in mouse hippocampal neurones.

3) To determine if the anti-epileptic drug, levetiracetam, has a mode of action on SYT1 or general SV recycling at the presynaptic terminal.

2.0 – Materials and Methods

2.1 – Materials

Synaptophysin (SYP) -pHluorin was obtained from Dr. Leon Lagnado (Sussex, UK). Vesicular glutamate transporter 1 (VGLUT1) -pHluorin was a gift from Dr. Rob Edwards, MD (San Francisco, USA). Synaptotagmin (SYT1) -pHluorin was a gift from Prof. Volker Haucke (Berlin, Germany). SV2A knockdown was achieved using the published oligonucleotide sequence (GAATTGGCTCAGCAGTATGTTCAAGAGACATACTGCTGAGCCAATTC) which forms a short hairpin against the rat sequence of SV2A that is identical to the mouse sequence (shRNA) (Zhang et al., 2015). SV2AshRNA, SV2AshRNA-SYT1-pHluorin, wild type (WT) SV2A-mCer and T84A SV2A-mCer plasmids were obtained courtesy of Prof. Dario Alessi (Dundee, UK). All other SV2A-mCer plasmids were synthesised in-house. Full details are provided in the tables below (Tables 2.2.11, 2.2.14).

FastDigest and Rapid Ligation enzymes and buffers were obtained from ThermoFisher Scientific™ (Paisley, UK). p-GEM T-Easy Vector system was obtained from Promega™ (Southampton, UK). P-GEX 4T-1 GST Gene Fusion System was obtained from GE Healthcare™ (Amersham, UK). Primary antibodies against SV2A, V-ATPase, Tubulin and eGFP were obtained from Abcam (Cambridge, UK). Primary antibody against Actin was obtained from Sigma-Aldrich™ (Poole, UK). Fluorescent secondary antibodies were obtained from Life Technologies™ (Paisley, UK). Minimal Essential Media (MEM) and Lipofectamine 2000 used in cultures and transfections were obtained from Invitrogen™ (Paisley, UK). XL10 *E.Coli* DNA Expression and BL21 *E.Coli* Protein Expression systems were obtained from Invitrogen™ (Paisley, UK) and bacteria were continually

replicated in-house from commercial stocks. All other chemicals and reagents used were obtained from Sigma-Aldrich™ (Poole, UK). Materials and media used in cell culture of mouse primary hippocampal neurones are listed in the table below (Table 2.2).

Reagent	**Supplier**	**Catalogue**
Foetal bovine serum	Biosera (Sussex, UK)	S1810-500
B27 supplement	Life Technologies (Paisley, UK)	17504-044
DMEM/F-12 medium	Life Technologies	21331-020
Dulbecco's phosphate buffered saline	Life Technologies	14190-094
L-Glutamine solution	Life Technologies	25030-024
Neurobasal medium	Life Technologies	21103-049
Penicillin-Streptomycin solution	Life Technologies	15140-122
Boric acid	Sigma-Aldrich (Poole, UK)	B6768
Cytosine β-D-arabinofuranoside	Sigma-Aldrich	C1768-100MG
Laminin	Sigma-Aldrich	L2020
Phosphate buffered saline	Sigma-Aldrich	P4417
Poly-D-lysine hydrobromide	Sigma-Aldrich	P7886-50MG
25mm glass coverslips	VWR (Leicestershire, UK)	631-1584
Papain	Worthington Biochemicals (New Jersey, USA)	PAP2

Table 2.1: Materials and media required for cell culture of mouse hippocampal neurones.

2.2 – Methods

2.2.1 – Preparation of Hippocampal Neuronal Cultures

Wild type mice were maintained from a C56BL/6J background line. Primary hippocampal dissociated cultures were prepared from embryonic day 17.5 mice. Pregnant mice were culled by neck dislocation by a technician, in accordance with Schedule 1 Section F2 of the Animals (Scientific Procedures) Act 1986. Embryonic mice were extracted from the parent and culled by decapitation, in accordance with Schedule 1 Section F6B of the Animals (Scientific Procedures) Act 1986.

Prior to animal collection, pre-autoclaved microscope coverslips were soaked in a solution of poly-D-lysine [PDL, 50 µg/mL final concentration] in sterile boric acid (100 mM, pH 8.5) and placed on a tube roller overnight. The boric acid was removed and the coverslips washed with water (x 4), separated and left to air-dry on a piece of sterilised lab paper for 30 min. Coverslips were placed into each well of the required number of 6-well plates. Laminin was thawed on ice and added to Neurobasal media (supplemented with B-27 supplement (2% v/v), L-glutamine (0.5 mM) and penicillin/streptomycin solution (1% v/v)] to a final concentration of 0.1 µg/mL and mixed by gentle inversion. The laminin-enriched Neurobasal was pipetted as 50 µL spots onto the centre of each coverslip in 6-well plates and placed in a 37°C / 5% CO_2 incubator.

Hippocampi were dissected from the brains and digested in papain (10 units/mL) for 20 min at 37ºC. Excess papain was removed using a pipette, the cells were resuspended in DMEM/F12 [2 mL, supplemented with penicillin/streptomycin solution (1% v/v) and foetal bovine serum (FBS, 10% w/v), and carefully titurated

until a homogeneous suspension was obtained. Excess DMEM/F12 (3 mL) was added, the cells were pelleted (340 g, 5 min, RT) and the supernatant was removed. Supplemented Neurobasal media (100 µL per head dissected) was added to the cell pellet and the cells were titurated carefully until a homogeneous suspension was obtained. The cells were counted using a haemocytometer and the final cell count was multiplied by 10^4 to give a concentration (in cells/mL) then further diluted to a final concentration of 0.5 x 10^7 cells per mL. The diluted cell suspension (10 µL, 50000 cells) was injected into the 50 µL Laminin-enriched Neurobasal spots in the pre-prepared 6-well plates and incubated for 45 min in a 37°C / 5% CO_2 incubator. Supplemented Neurobasal media (2 mL) was added to each well and the cells maintained in a 37°C / 5% CO_2 incubator for 2-3 days in culture. Cytosine β-D-arabinofuranoside (Ara-C) was added to a final concentration of 1 µM per well to prevent glia proliferation.

2.2.2 – Transfections

Transfections using two or less DNA constructs were performed after 7 days in culture. Conditioned Neurobasal media was removed from each well (containing cell cultures to be transfected), replaced with Minimum Essential Media (MEM, ThermoFisher Scientific) (2 mL) and incubated at 5 % CO_2 at 37°C. The required DNA constructs (1 µg/well) and Lipofectamine 2000 (2 µL/well) were mixed and preincubated in MEM (0.5 mL/well) for 20 min. The DNA/Lipofectamine mixture was then added to the cells (0.5 mL/well) and incubated for 2 h. After transfection, the cells were washed with MEM (1 mL per well) prior to replacement of conditioned Neurobasal media.

Transfections using three DNA constructs were performed after 7 days in culture. Conditioned Neurobasal media was removed from each well (containing cell cultures to be transfected), replaced with Opti-MEM (2 mL, ThermoFisher Scientific) and incubated at 5% CO_2 at 37°C. The required DNA constructs (0.7 µg/well) and Lipofectamine 2000 (2 µL/well) were mixed and preincubated in Opti-MEM (0.5 mL/well) for 20 mins. The DNA/Lipofectamine mixture was then added to the cells (0.5 mL/well) and incubated for 2 h. After transfection, the cells were washed with Opti-MEM (1 mL per well) prior to replacement of conditioned Neurobasal media.

2.2.3 – Imaging of pHluorin-mediated Fluorescence Responses

PHluorins were used to report the trafficking of a target SV protein as well as general SV recycling. The pH-sensitive GFP in pHluorins is located in the intraluminal domain of the vesicle (as it is specifically fused to the luminal domain of an exogeneous SV protein) and fluorescence is quenched under the pH conditions in this domain (pH ~ 5.6). During SV exocytosis, the vesicle fuses to the plasma membrane and the pH-sensitive GFP fluoresces when exposed to the high pH of the extracellular environment (pH ~ 7.4). Fluorescence is quenched again following SV endocytosis and re-acidification and the GFP molecule is returned to the environment of the intraluminal domain (Miesenböck et al., 1998).

Hippocampal cell cultures were mounted in a Warner RC-21BRFS imaging chamber with embedded parallel platinum wires and placed on the stage of a Zeiss Axio Observer A1 epifluorescence microscope. Neurones were visualized with a Zeiss Plan Apochromat x40, 1.3 numerical aperture (NA 1.3) oil-immersion objective lens.

The transfected neurones were visualised at either 430 nm (mCerulean – a cyan fluorescent protein used as a marker for transfected cells) or 500 nm (pHluorin reporters) excitation using a dichroic > 525 nm and a long-pass emission filter > 535 nm. Fluorescent images were captured at 4 s intervals. For imaging certain pHluorins with low photon emission, individual pixels were 'binned' together as a group in order to increase the signal to noise ratio (no binning for SYP-pHluorin and VGLUT1-pHluorin imaging; 2:2 binning for SYT1-pHluorin imaging). Images were captured using a Zeiss AxioCam MRm Rev.3 digital camera and a workstation installed with Zeiss Zen2012 Blue software. Cultures were subjected to continuous perfusion with cell imaging buffer [NaCl (119 mM), KCl (2.5 mM), $CaCl_2$ (2.0 mM), $MgCl_2$ (2.0 mM), glucose (30 mM), HEPES (2.5 mM), pH 7.4] for 60 s (15 image frames) to capture baseline fluorescence then stimulated with a train of 300 action potentials delivered at 10 Hz (100 mA, 1 ms pulse width). In these experiments, there were no independent measures of action potentials taken and the term 'action potential' is used to describe the number of electrical pulses given. All results given in this thesis are described and explained based on the assumption that the full number of pulses given is successfully converted into action potentials by the observed neurone. A caveat of this assumption is that any observed phenotype (or lack thereof) may be a result of a failure of the neurone to convert all electrical pulses into action potentials. The subsequent neuronal response and fluorescence recovery was recorded for 220 s (55 image frames) after which perfusion was changed to an alkaline cell imaging buffer [NaCl (69 mM), NH_4Cl (50 mM), KCl (2.5 mM), $CaCl_2$ (2.0 mM), $MgCl_2$ (2.0 mM), glucose (30 mM), HEPES (2.5 mM),

pH 7.4] for a period of 120 s (30 image frames) to reveal the total SV pool in the synapses.

2.2.4 – Imaging Surface Fraction Expression of pHluorin Reporters

Quantification of the surface fraction expression of various pHluorin reporters was achieved by perfusion of acidic imaging buffer to quench the surface expressed pHluorin after imaging of its resting fluorescence. The average fluorescence difference between both conditions the reveals the surface expressed fraction of the cell (Gordon et al., 2011).

Hippocampal cell cultures were perfused with standard cell imaging buffer for 90 s and switched to an acidic cell imaging buffer [NaCl (119 mM), KCl (2.5 mM), $CaCl_2$ (2.0 mM), $MgCl_2$ (2.0 mM), glucose (30 mM), MES hydrate (2.5 mM), pH 5.5] for 90 s and 5 image frames (4 s interval) were captured. The cells were perfused with standard cell imaging buffer for another 90 s to allow pHluorin fluorescence recovery, after which alkaline cell imaging buffer was perfused for further 90 s to reveal the total SV pool. Fluorescent images were captured for 20 s (4 s intervals) after the end of each perfusion period. Neurones were visualized on a Zeiss Axio Observer A1 epifluorescence microscope using a Zeiss Plan Apochromat x40 (NA 1.3) oil-immersion objective and fluorescence was visualised at either 430 nm (mCerulean) or 500 nm (pHluorin reporters) excitation using a dichroic > 525 nm and a long-pass emission filter > 535 nm. Images were captured using a Zeiss AxioCam MRm Rev.3 digital camera and Zeiss Zen2012 Blue software.

2.2.5 – Analysis of Surface Fraction Expression of pHluorin Reporters

Regions of Interest (ROIs) were selected as described previously. The surface fraction of pHluorin (as a percentage of total pHluorin) expressed within each ROI was estimated using the following equation: [(average resting baseline fluorescence – minimum acidic fluorescence) / (maximum alkaline fluorescence – minimum acidic fluorescence) x 100]. The values obtained from each ROI were then averaged to give a representative value of surface expression for each coverslip (Gordon et al., 2011). Experimental results were averaged over several replicates and analysed for statistical significance. All statistical analyses were performed using Microsoft Excel 2013 and GraphPad Prism 6.0 software.

2.2.6 – Analysis of Coefficient of Variation for Surface Fraction

The coefficient of variation (CV) is a calculation for the diffuseness of the fluorescence for the total pHluorin pool along a fixed length of neurite (Lyles et al., 2006). Captured images of hippocampal cell cultures subjected to alkaline imaging buffer (see chapter 2.2) were used for these analyses. Lines of interest (LOI) of at least 50-µm long were drawn over selected neurones using FIJI's freehand line drawing tool and the fluorescence was quantified along the profile. CV of pHluorin fluorescence along axons was determined by the following equation:

[(standard deviation of the fluorescence signal / the mean value of the fluorescence signal) x 100].

Five LOIs were taken for each coverslip and examined to obtain an average CV value for the coverslip. Experimental results were averaged over several replicates

and analysed for statistical significance. All statistical analyses were performed using Microsoft Excel 2013 and GraphPad Prism 6.0 software.

2.2.7 – Imaging of Intracellular Free Calcium Responses using Fluo-3 AM

Fluo-3 was used to monitor evoked changes in intracellular free calcium in response to action potential stimulation. It reports this by exhibiting a large fluorescence increased upon co-ordination of the molecule to free Ca^{2+} ions (Minta et al., 1989).

Hippocampal cell cultures were incubated with the fluorescent Ca^{2+} indicator Fluo-3 AM (10 µM in cell imaging buffer, ThermoFisher Scientific) for 30 min. Excess Fluo-3 AM was washed off by perfusion with normal cell imaging buffer prior to stimulation. In experiments using elevated KCl to clamp membrane potential at an excited state, a solution of elevated KCl cell imaging buffer [NaCl (71.5 mM), KCl (50 mM), $CaCl_2$ (2.0 mM), $MgCl_2$ (2.0 mM), glucose (30 mM), HEPES (2.5 mM), pH 7.4] was perfused over the cells for a period of 30 s and subsequently washed away with a second perfusion of imaging buffer. After a recovery period of 60 s, the cells were stimulated with a train of 300 action potentials at 10 Hz (100 mA, 1 ms pulse width) and visualised using a Zeiss Axio Observer A1 epifluorescence microscope using a Zeiss Plan Apochromat x40 (NA 1.3) oil-immersion objective and fluorescence was visualised at 500 nm excitation using a dichroic > 525 nm and a long-pass emission filter > 535 nm. Images were captured with a Zeiss AxioCam MRm Rev.3 digital camera and Zeiss Zen2012 Blue software.

In order to increase the neuronal network activity of the cultures, a solution of 4-aminopyridine (4-AP, 50 µM in cell imaging buffer) was perfused over the cells for a

period of 120 s and subsequently washed away with a second perfusion of imaging buffer. After a recovery period of 90 s, the cells were stimulated with a train of 300 action potentials at 10 Hz (100 mA, 1 ms pulse width) and visualised using the same system described above.

2.2.8 – Analysis of pHluorin/Fluo-3 AM Imaging

The series of raw images captured from the microscope workstation were aligned and analysed using Fiji is Just ImageJ (FIJI) software (National Institute of Health, Maryland, USA) together with the following plugins Time Series Analyser v3.0 (Balaji J., UCLA California, USA) and MBGReg (Donal Stewart, Edinburgh, UK). In order to correct for slight occurences of image drift, raw images were first aligned using the MBGReg plugin to the frame with maximal pHluorin fluorescence (Frame 90). Responsive nerve terminals were selected by toggling between the image frames and visually identifying boutons that displayed a clear increase in fluorescence when perfused with alkaline image buffer (Frames 90-120) when compared to baseline fluorescence under standard imaging buffer (Frames 1-20). Between 75 to 100 regions of interest (ROIs) of identical size (5x5 pixels for 1:1 binning; 3x3 pixels for 2:2 binning) were placed over the selected nerve terminal boutons (Figure 2.2.8 **A**) and the total fluorescence intensity of each ROI was monitored over time and plotted as a graph of fluorescence vs time. The data of each individual ROI was input into ROITraceSelector v11.0 software (Donal Stewart, Edinburgh) in order to remove unsuitable ROIs from the data pool. Selection of usable ROIs were based on three criteria: 1) an increase in fluorescence upon stimulation; 2) a mono-exponential decay of fluorescence back down to baseline or close to baseline; 3) A sharp, visible increase of fluorescence after perfusion with alkaline imaging buffer to reveal to total SV pool (Figure 2.2.8 **B**). After ROI selection, the data was transferred to Microsoft Excel 2013 where the pHlourin fluorescence change was expressed as a ratio of the raw fluorescence of each ROI (ΔF) over the average baseline fluorescence prior to stimulation (F_0) as represented by the following formula:

PHlourin fluorescence change ($\Delta F/F_0$) = [ROI fluorescence during selected frame / ROI average fluorescence during last 5 frames of acquisition prior to stimulation (frames 11-15)]

The time constant of the fluorescence decay (tau) of each ROI after stimulation is indicative of the time it takes for pHluorin fluorescence to fall to 37% of its initial maximum fluorescence (which can be associated with the time taken to retrieve 63% of pHluorin molecules from the plasma membrane). In order to obtain this value, data was taken from the time point immediately after stimulation to a cut-off point at 180 s after the start of the experiment (image frames 16 - 45). A mono-exponential decay curve function was fitted to the data using GraphPad Prism 6.0 software, as described below:

$$[F = (F0 - F_{min})\exp(-Kt) + F_{min}]$$

where F = normalised fluorescence, F0 = maximum fluorescence after stimulation, F_{min} = minimum fluorescence after decay, K = rate constant and t = time after stimulation.

Tau values were then obtained from calculating 1/K. It is noted that pHlourin experiments produce, on occasion, a mono-exponential decay with a non-zero asymptote. This phenomenon has been previously observed in similar experiments from other research groups (Fernández-Alfonso et al., 2006, Kaempf et al., 2015) and its underlying cause remains unexplained to date. As a result, no constraints have been placed on the value of the asymptote during fitting of the mono-exponential decay function in this thesis. The fitting of a mono-exponential decay function to non-equal, non-zero asymptotes may produce small systematic errors due to

comparison differences; however, these differences are considered very small and are assumed not to affect the overall statistical significance of any observed phenotype in the experiments. Traces that did not produce tau values or produced tau values of infinity were discarded and removed from analysis. Individual ROI traces were then averaged to produce a single representative trace for all responding boutons with the coverslip field of view.

Any traces that displayed mono-exponential decay prior to stimulation (due to photobleaching) were corrected using GraphPad Prism 6.0 software by fitting the above described mono-exponential decay function to the first 15 frames of image acquisition. The decay function was then mathematically subtracted from the raw trace in order to produce the decay corrected trace.

The resulting values were normalised in two different manners for further analysis: ***1)*** Normalisation to the peak of stimulation (maximum fluorescence value obtained during the 300 AP, 10 Hz stimulation period) to reveal differences in the rates of pHluorin retrieval during SV endocytosis; ***2)*** Normalisation to the peak of the alkaline buffer pulse (maximum fluorescent value obtained during the alkaline NH4 buffer pulse period = 1) to reveal differences in the amount of externalised pHluorin at the plasma membrane during stimulation during SV exocytosis. All ‘n’ values expressed in this thesis refer to the number of coverslips examined. Experimental results were averaged over several replicates and analysed for statistical significance. All statistical analyses were performed using Microsoft Excel 2013 and GraphPad Prism 6.0 software.

A

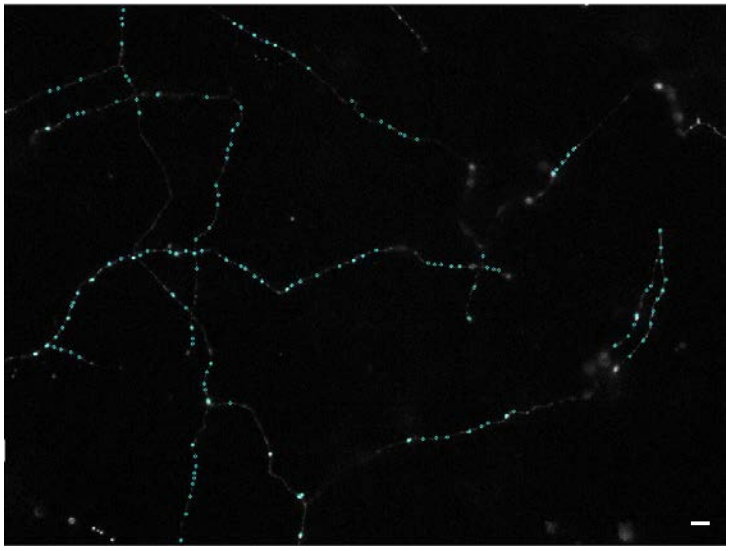

B

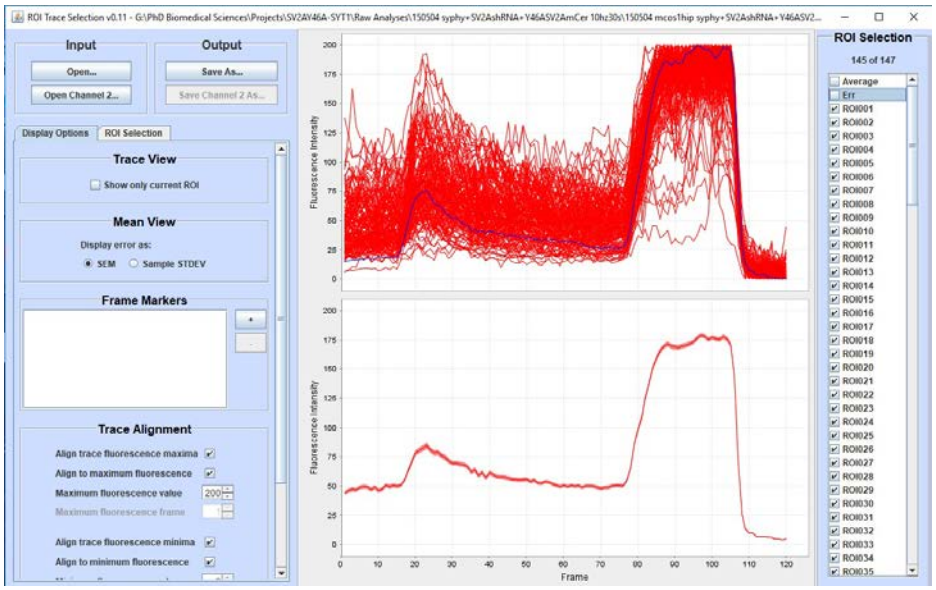

Figure 2.2.8: Analysis of pHluorin imaging. A) Regions of interest (ROIS, blue circles) were selected on the neuronal field of view using the FIJI plugin Times Series Analyser v3.0. The change in fluorescence after baseline correction ($\Delta F/F_0$) vs. time was calculated for each individual ROI and averaged to give the average trace for the experiment. Scale bar = 10 µM. **B)** Screening of ROIs using ROI Trace Selector v0.11. Selection of usable ROIs were based on three criteria: 1) an increase in fluorescence upon stimulation; 2) a mono-exponential decay of fluorescence back down to baseline or close to baseline; 3) A sharp, visible increase of fluorescence after perfusion with alkaline imaging buffer to reveal to total SV pool. ROIS deemed unsuitable were unchecked from the list to the right.

2.2.9 – Immunocytochemistry of SV2A Expression

Culture media was aspirated from each coverslip and the transfected cells washed with phosphate buffered saline [PBS, NaCl (140 mM), Na_2PO_4 (10 mM), KCl (2.7 mM), KH_2PO_4 (1.8 mM)]. Paraformaldehyde (PFA, 4 % in PBS) was added to each coverslip and incubated at room temperature for 20 min to fix the cells. The PFA was aspirated, a solution of NH_4Cl (50 mM in PBS) was added to quench the excess PFA and the cells incubated at room temperature for 10 min. The NH_4Cl solution was aspirated, cells were washed with PBS (x 3), a solution of Triton-X 100 (0.1% in 1 % BSA/PBS) was added to permeabilise the cell membrane and the cells incubated for 5 min. The Triton-X solution was aspirated, cells washed with PBS (x 1), and a solution of BSA (1 % in PBS) was added as a blocking reagent and the cells incubated for a further 30 min. Coverslips were then removed and incubated in rabbit anti-SV2A (1:200, 1 % BSA in PBS, Abcam) and chicken anti-GFP (1:5000, 1% BSA in PBS, ThermoFisher Scientific) primary antibodies at room temperature for 1 hr. The coverslips were washed with PBS (x 3) and incubated in the corresponding secondary antibodies [goat anti-rabbit AlexaFluor 568 (A21069, ThermoFisher Scientific), goat anti-chicken AlexaFluor 488 (A11039, ThermoFisher Scientific), 1% BSA in PBS] in the dark at room temperature for 1 hr. The coverslips were then rinsed with ddH_2O, dried in the dark and mounted onto glass microscope slides with FluorSafe™ mounting medium. Immunostained neurones were visualised using a Zeiss Axio Observer A1 epifluorescence microscope using a Zeiss Plan Apochromat x40 (NA 1.3) oil-immersion objective and fluorescence was visualised at either 500 nm excitation / 525 nm emission (GFP, AlexaFluor 488) or 550 nm excitation / 603 nm emission (SV2A, AlexaFluor 568) using a dichroic > 525 nm and a long-pass

emission filter > 535 nm. Images were captured with a Zeiss AxioCam MRm Rev.3 digital camera and Zeiss Zen2012 Blue software.

2.2.10 – Analysis of SV2A Immunocytochemistry

Images obtained from fluorescence imaging were analysed and aligned using the Align RGB planes plugin (G.Landini, Birmingham, UK) in FIJI software (National Institute of Health, Maryland, USA). Still images of GFP and SV2A expression were exactly aligned and between 75-100 counts of regions of interest (ROIs) of identical size (5x5 pixels) were placed over nerve terminal boutons where both proteins were co-expressed to represent transfected boutons. ROIs (75-100 count) of untransfected boutons in the same field of view (not overlaying with GFP) were visually selected separately from the whole field. Excessively bright or dim boutons were not included in the data. ROIs (75-100 count) were also randomly chosen from dark regions of the field of view where there was absence of neurites to quantify the background auto-fluorescence. Immunofluorescence was quantified and normalised to the average fluorescence of non-transfected nerve terminal boutons using the following equation:

[(Raw transfected ROI average fluorescence – raw background ROI average fluorescence) / (Raw non-transfected ROI average fluorescence – raw background ROI average fluorescence)].

Experimental results were averaged over several replicates and analysed for statistical significance. All ‘n’ values refer to the number of neurones examined for immunocytochemistry experiments only. All statistical analyses were performed using Microsoft Excel 2013 and GraphPad Prism 6.0 software.

2.2.11 – Site Directed Mutagenesis of SV2A-mCer Mutants

Template DNA (1 ug/mL) and the appropriate sense primer and anti-sense primers (0.5 nM, see Table 2.2.11 below) were dissolved in PCR master mix buffer (50 µL) [dNTP mixture (20 µM), Tris-HCl (20 mM), KCl (10 mM), $(NH_4)_2SO_4$ (10 mM), $MgSO_4$ (2 mM), Triton® X-100 (0.1% v/v) and nuclease-free BSA (0.1 mg/mL), pH 8.8]. Pfu DNA polymerase enzyme (0.5 µL, 1 unit, Promega) was added and the reaction subjected to PCR mediated site directed mutagenesis (1 Cycle – 96ºC for 2 min; 20 Cycles – 96 ºC for 30 s, 52 ºC for 10 s, 72 ºC for 8 minutes (1 minute/kb plasmid); 1 Cycle – 72 ºC for 10 min; Hold at 4 ºC). DPN1 enzyme (1 µL, 5 units, Promega) was added to the PCR product to digest template DNA and the reaction mixture incubated at 37°C for 1 hr and immediately transformed (see 2.2.12) into competent XL10 *E. Coli* bacterial cells for expression. Transformed bacteria were plated onto agar plates containing either ampicillin (100 µg/mL) or kanamycin (50 µg/mL) overnight and single colonies were selected. Bacterial cultures were grown overnight at 37°C from the colonies in LB media (10 g/L tryptone, 5 g/L yeast extract, 0.086 M NaCl) (5 mL) and DNA was extracted by use of a GENEJet Plasmid Miniprep Kit (ThermoScientific™) as per manufacturer's instructions.

Primer	Sequence
Y46A SV2A Sense	TATTCCCGAAGGTCCGCCTCCCGCTTTGAGGAG
Y46A SV2A Anti-Sense	CTCCTCAAAGCGGGAGGCGGACCTTCGGGAATA
R383Q SV2A Sense	CACGACACCAACATGCAAGCCAAGGGCCACCCT
R383Q SV2A Anti-Sense	AGGGTGGCCCTTGGCTTGCATGTTGGTGTCGTG

Table 2.2.11: List of SV2A primers used for site-directed mutagenesis studies. All primers were commercially purchased from Eurogentec Ltd.

2.2.12 – Preparation of Chemically Competent *E.Coli* Cells

A sample of commercially available Top 10/XL10/BL21 *E.coli* bacteria (Sigma Aldrich) were obtained from commercially available sources and inoculated in a 5 mL culture overnight at 37ºC with shaking. A sample of the overnight culture (1 mL) was added to LB media (100 mL) and sterile $MgSO_4$ (20 mM) was added to the mixture. The new culture was incubated at 37ºC until an optical density of 0.4-0.6 was reached to allow bacteria to reach maximum growth rate. Cells were centrifuged (5000 g, 5 min, 4°C), the supernatant was discarded and the remaining pellet re-suspended in a solution of TFB1 (40 mL) [Potassium acetate (30 mM), $CaCl_2$ (10 mM), $MnCl_2$ (50 mM), RbCl (100 mM), Glycerol (15% final conc)] for 5 min. After incubation, the cells were centrifuged again (5000 g, 5 min, 4°C), the supernatant was discarded and the cells re-suspended in a solution of TFB2 (5 mL) [MOPS (10 mM), $CaCl_2$ (75 mM), RbCl (10 mM), Glycerol (15% final conc.)] for 30 min. After incubation, the cells were aliquoted, snap frozen and stored at -80ºC for future use.

2.2.13 – Transformation of DNA into Competent *E.Coli* Cells

An aliquot of competent *E.Coli* cells was defrosted on ice and the desired DNA (5 ng) was added. The mixture was then incubated on ice for 30 min to allow DNA attachment to the cells. The *E.Coli* cells were then heat shocked at 42ºC for 45 s and allowed to incubate on ice for a further 2 min. LB medium (200 µL) was added to the cells and allowed to recover for 30 min at 37ºC. A sample of the mixture (100 µL) was plated of agar plates containing either ampicillin (100 µg/mL) or kanamycin (50 µg/mL).

2.2.14 – Fusion Protein Expression of Glutathione S-Transferase (GST) – SV2A Mutants

Template DNA (1 ug/mL), dNTPs (20 µM) and the appropriate sense primer and anti-sense primers (0.5 nM, see table 2.2.14) were dissolved in 1 x Expand High Fidelity PCR buffer (Sigma-Aldrich™, w/ 1.5 mM $MgCl_2$). GoTaq Expand DNA polymerase enzyme (1 µL, 5 units, Promega) was added and the reaction subjected to PCR mediated DNA amplification (1 Cycle – 95ºC for 2 min; 30 Cycles – 95 ºC for 30 s, 55 ºC for 1 min, 72 ºC for 1 minute (0.5 minute/kb plasmid); 1 Cycle – 72 ºC for 10 min; Hold at 4 ºC). The PCR product was ligated into a p-GEM T-Easy Vector System for easy formation of a circular vector to aid accuracy of digestion. The ligation was performed by adding T4 DNA Ligase (1 µL, 5 units) to a mixture of PCR product (1 µL), vector (3 µL) and 1 x Rapid Ligation Buffer (up to 10 uL). The p-GEM PCR product was digested using BamHI and XhoI FastDigest™ restriction enzymes (1 µL each, 1 unit) and ligated into a p-GEX 4-T1 GST Gene Fusion System for expression of the GST-fused DNA, using the same protocol as described above. The pGEX-ligated DNA was then transformed (as previously described in 2.2.13) into competent XL10 *E. Coli* bacteria for complete plasmid expression. Transformed bacteria were plated onto agar plates w/ ampicillin (100 µg/mL) overnight and single colonies were selected. Bacterial cultures were grown overnight at 37°C from the colonies in LB media (5 mL) [10 g/L tryptone, 5 g/L yeast extract, 0.086 M NaCl] and DNA was extracted by use of a GENEJet Plasmid Miniprep Kit (ThermoScientific™) and test-digested using BamHI and XhoI FastDigest™ enzymes (1 µL each, 1 unit, ThermoFisher Scientific) for the presence of the vector insert. Samples containing the correct plasmid DNA were then re-transformed in

BL21 *E.Coli* bacteria for high level IPTG-induced protein expression of target genes in T7 expression vectors and 40% glycerol stocks were made and stored at -80ºC. Mutations in the SV2A cytosolic loop (R383Q + R383E) were created using the same primers and methods as previously described in 2.2.11.

Primer	**Sequence**
GST SV2A loop Sense (BamHI)	GGATCCGAGAGTCCCCGCTTCTTCCTAGAGA
GST SV2A loop Sense (XhoI)	CAGTCCAGAGTATCGGCGCATCACGTGACTCGAG
Y46A SV2A Sense	TATTCCCGAAGGTCCGCCTCCCGCTTTGAGGAG
Y46A SV2A Anti-Sense	CTCCTCAAAGCGGGAGGCGGACCTTCGGGAATA
R383Q SV2A Sense	CACGACACCAACATGCAAGCCAAGGGCCACCCT
R383Q SV2A Anti-Sense	AGGGTGGCCCTTGGCTTGCATGTTGGTGTCGTG
R383E SV2A Sense	CACGACACCAACATGGAAGCCAAGGGCCACCCT
R383E SV2A Anti-Sense	AGGGTGGCCCTTGGCTTCCATGTTGGTGTCGTG

Table 2.2.14: List of primers used for engineered GST-SV2A loop constructs and its mutants. All primers were commercially purchased from Eurogentec Ltd.

2.2.15 – Preparation of GST-SV2A Tagged Glutathione Beads for Pulldown Assay

GST pulldown assays were used to identify any interactions between the SV2A cytosolic loop and proteins in the brain lysate. The strong interaction between glutathione and glutathione transferase acts as the anchor for the fusion protein, allowing all interacting proteins to be isolated (Smith and Johnson, 1988).

The Glutathione Sepharose 4B (GS4B) resin (1 mL, 50% slurry, GE Healthcare) was prepared by washing with PBS (x 1), then with PBS-Triton X [0.1 % v/v] (x 1) to remove hydrophobic impurities and again with PBS (x 1). The beads were then pelleted (23 g, 5 min, 4°C) and kept at 4°C until later use. A sample of GST-SV2A DNA variants in BL21 *E.Coli* bacteria, taken from previously made glycerol stocks, were cultured overnight at 37°C in ampicillin (100mg/mL) enriched LB media (5 mL) [10 g/L tryptone, 5 g/L yeast extract, 0.086 M NaCl]. The overnight culture (3 mL) was further diluted in LB media (250 mL) to allow the bacteria to reach their maximum growth phase and the new culture was incubated at 37°C until the culture reached an optical density of 0.6 as the bacteria enters this phase. Isopropyl β-D-1-thiogalactopyranoside (IPTG, 1 mM) was added to induce protein expression and the culture was allowed to incubate for a further 4 hrs. The culture was then pelleted in a centrifuge (1137 g, 15 min, 4°C), supernatant discarded, and the pellet resuspended in STE buffer (40 mL) [Tris buffer (10 mM), NaCl (150 mM), EDTA (1 mM), phenylmethylsulfonyl fluoride (1 mM), protease inhibitor cocktail (150 µL of a DMSO solution, P8849, Sigma Aldrich), pH 8]. Lysosyme (13.3 µg/mL final concentration) was added to lyse the bacterial cells and the suspension was incubated on ice for 30 min. Dithiothreitol (DTT, 5 mM) and Triton-X 100 (1% v/v) was added as further measure to prevent protease action and the lysate was sonicated on ice (30

s x 6) and pelleted (12000 rpm, 5 min, 4°C). The lysate supernatant was incubated with previously prepared GS4B beads for 1 hr at 4°C. Protein bound beads were pelleted (23 g, 5 min, 4°C), washed with PBS (x 5), washed with NaCl (1.2 M, x 1) to remove any non-specific bound proteins, and then washed again with PBS (x 2). The resulting beads were then made up to a 50% slurry in PBS ready for use in GST pulldown assays.

2.2.16 – Preparation of Crude P2 Synaptosomes

One adult rat was killed by cervical dislocation and the brain removed. The cerebellum and visible white matter was then removed and the remaining cortex rinsed in an ice-cold sucrose/EDTA solution (20-50 mL) [Sucrose (0.32 M), ethylenediamine tetraacetic acid (EDTA, 1 mM), Tris buffer (5 mM), pH 7.4]. The cortices were transferred to a tube containing ice-cold sucrose/EDTA (10 mL/rat, ~10% suspension), minced with a pair of scissors and homogenised immediately using a Thomas "AA" 5 mL teflon/glass homogeniser. The homogenised mixture was then pelleted (403 g, 10 min, 4°C), re-suspended in ice-cold sucrose/EDTA solution (15 mL) and pelleted again (403 g, 10 min, 4°C). The supernatants from both spins were combined and re-pelleted (8691 g, 10 min, 4°C). The crude synaptosome P2 pellet was re-suspended in ice cold HEPES-Buffered-Krebs (20 mL) [NaCl (118.5 mM), KCl (4.7 mM), Na_2HPO_4 (1 mM), $MgSO_4$ (1.2 mM), glucose (10 mM), HEPES (20 mM), pH 7.4], pelleted (8691 g, 10 min, 4°C) and the supernatant removed. Ice-cold lysis buffer (8 mL) [Tris-HCl (25 mM), NaCl (150 mM), ethyleneglycol tetraacetic acid (EGTA, 1 mM), EDTA (1 mM), PMSF (1 mM), Protease Inhibitors (150 µL of DMSO solution, P8849, Sigma Aldrich)] was added

and the mixture pelleted once more (8691 g, 10 min, 4°C). The supernatant lysate was then aliquoted (200 µL each) and stored at -80°C.

2.2.17 – Pulldown Assay for GST-SV2A Mutants

A suspension of GST coupled beads in PBS (150 µL) was added to a MobiSpin mini spin filter column (Boca Scientific), washed with lysis buffer (0.5 mL) and the buffer extracted by centrifugation (728 g, 10 s , 4°C). Crude P2 synaptosome lysate (200 µL) was then added to the beads in the column and incubated at 4°C for 2 hrs with rotation using a sample tube rotator. The synaptosome lysate was then extracted by centrifugation (728 g, 10 s, 4°C) and the beads washed sequentially with ice cold lysis buffer (x 3), high salt lysis buffer (x 1) [Tris-HCl (25 mM), NaCl (150 mM), ethyleneglycol tetraacetic acid (EGTA, 1 mM), EDTA (1 mM), PMSF (1 mM), Protease Inhibitors (75 µL of DMSO solution, P8849, Sigma Aldrich)], lysis buffer (x 3) and Tris buffer (20 mM, pH 7.4). The bound proteins were extracted with 1 x SDS sample buffer [Tris buffer (67 mM) EDTA (2 mM), sodium dodecyl sulfate (SDS) (67 mM), Glycerol (3%), Bromophenol blue (0.0002%), β-mercaptoethanol (0.04%)], boiled at 90°C and separated by SDS gel electrophoresis (SDS-PAGE) using a mini-PROTEAN Tetracell electrophoresis chamber (Bio-Rad) at 120 V with a 10% acrylamide gel [ddH_2O (3.2 mL), acrylamide/bis (2.67 mL, 30%, 37.5:1), Tris-HCl (2 mL, 1.5 M, pH 8.8), N,N,N′,N′-tetramethylethylene-diamine (TEMED, 8 µL), SDS (80 µL, 10%), ammonium persulfate (APS, 80 µL, 10%)] in gel running buffer [Tris (25mM), Glycine (190 mM), SDS (0.1% w/v), pH 8.3]. The gel was stained with Coomassie Blue for mass spectrometry and scanned with an Epson scanner. Identified bands of interest were excised using a scalpel, with appropriate

care to avoid contamination, and placed in autoclave tubes. Samples were sent to the Wishart Group (Roslin Institute, Edinburgh) for analysis by ESI-QUAD TOF mass spectrometry.

2.2.18 – Western Blotting of GST Isolated Proteins

Western blotting was used to characterise all interacting proteins identified from the GST pull down and mass spectrometry experiments (Burnette, 1981).

Eluted proteins from the pulldown assays (in 1 x SDS sample buffer) were separated by SDS-PAGE using a mini-PROTEAN Tetracell electrophoresis chamber (Bio-Rad) at 120 V with a 10% acrylamide gel [ddH_2O (3.2 mL), acrylamide/bis (2.67 mL, 30%, 37.5:1), Tris-HCl (2 mL, 1.5 M, pH 8.8), N,N,N′,N′-tetramethylethylene-diamine (TEMED, 8 µL), SDS (80 µL, 10%), ammonium persulfate (APS, 80 µL, 10%)] in running buffer. The separated proteins were transferred to a nitrocellulose membrane using a mini Trans-Blot electrophoretic transfer cell for 15 hours (20 V, Bio-Rad) [Transfer buffer recipe: Tris buffer (25 mM), glycine (190 mM), methanol (20% v/v)]. The nitrocellulose membrane was stained with Ponceau S after transfer to check the viability of the transfer. The membrane was destained with water and blocked with LICOR™ blocking buffer (LBB) /PBS (1:1) for 1 hr. The membrane was incubated with the desired primary antibodies [see table 2.2.18; dissolved in 1:1 LBB/PBS-Tween (0.1% v/v)] for 1 hr. The membrane was then washed with PBS-Tween (0.1% v/v) for 5 min (x 4). The membrane was incubated with the desired LICOR™ secondary antibodies [see table 2.2.18, dissolved in 1:1 LBB/PBS-Tween (0.1% v/v)] for 1 hr and washed with PBS-Tween (0.1%) (x 4). The membrane was

allowed to dry and was imaged with a LICOR™ Odyssey scanner at 700 and 800 nm wavelengths.

Primary Antibody	**Company (Product No.)**	**Species**	**Dilution**	**Dye**
Anti-GST	Abcam (ab19256)	Rabbit	1:10000	
Anti-actin	Sigma Aldrich (A2228)	Mouse	1:100000	-
Anti-β3-tubulin	Sigma Aldrich (SAB4300623)	Rabbit	1:10000	-
Anti-V-ATPase V1B2	Abcam (ab183887)	Rabbit	1:5000	-
Anti-V-ATPase V1E1	Abcam (ab111733)	Rabbit	1:5000	-
Anti-SV2A	Abcam (ab32942)	Rabbit	1:1000	-
Anti-SYT1	Abcam (ab13259)	Mouse	1:1500	-
Anti-SYP	Synaptic Systems (SS101002)	Rabbit	1:8000	-
Secondary Antibody	**Company**	**Species**	**Dilution**	**Dye**
Anti-Rabbit	Li-Cor (P/N 925-32210)	Goat	1:10000	IRDye 680
Anti-Mouse	Li-Cor (P/N 925-68071)	Goat	1:10000	IRDye 800

Table 2.2.18: List of antibodies used for western blotting analysis. The antibodies are listed along with the company which they are obtained from, the animal species in which they were raised in, the dilution used in the experiments and the dye wavelength in which they emit.

2.2.19 – Analysis of Western Blots

Western blot images taken with the LICOR Odyssey scanner was analysed using ImageStudio Lite software (LICOR Biotechnology, UK). Rectangular ROIs were placed over the blots using the in-built analysis toolbar in the software, providing raw quantification of the fluorescence as an integer. Background correction was automatically accounted for by the software and the background region was defined as the area surrounding the perimeter of the blot. In order to account for slight differences in protein loading, the GST fusion protein loading for each experiment was analysed and normalised to the lowest amount to obtain a ratio. Raw data from each experiment was then normalised to this ratio to obtain the final data used for analysis.

Normalised blot data = [Raw blot fluorescence/ Normalised GST fluorescence]

In order to provide an improved analysis of the pulldown assay results of each condition (GST, WT SV2A, R383Q SV2A and R383E SV2A), the collated normalised blot data was expressed as a ratio of amount of WT SV2A present (WT SV2A set to a value of 1.0). All normalisations were performed on Microsoft Excel 2013 software and statistical analysis was performed using GraphPad Prism 6.0 software.

2.2.20 – Statistical Analysis

All datasets with n = or > 7 used in this thesis were tested for a normal distribution using the Shapiro-Wilk normality test. All of these datasets were found to be normally distributed ($p > 0.05$). Datasets with $n < 7$ were assumed to fit a normal distribution, as the small sample size did not allow for good curve fitting.

For normally distributed datasets with three or more independent groups (surface fraction, CV, pHluorin taus, fraction of externalisation), a one-way analysis of variance (ANOVA) with Bonferroni's post-hoc test (to account for multiple tests) was used to determine statistically significant differences (P and F values). For experiments where there are two or more independent variables interacting with a dependent variable (pHluorin $\Delta F/F_0$ vs time), a two-way ANOVA with Bonferroni's post-hoc test was used to determine any statistically significant differences. Where there is a comparison of only two independent variables, a student's t-test was used to determine any statistically significant differences. Values of $p < 0.05$ were deemed statistically significant. One star represents statistical significance of $p \leq 0.05$; two stars $p \leq 0.01$; three stars $p \leq 0.001$; and four stars $p \leq 0.0001$. All experiments were expressed as mean +/- standard error measurement (SEM). All statistical analyses were performed using Microsoft Excel 2013 and GraphPad Prism 6.0. Unless otherwise specified, all 'n' values refer to the number of independent experiments (coverslips) analysed.

3.0 – The Effects of Ablating the SV2A/AP-2 Interaction on SYT1 Trafficking at the Presynapse

3.1 – Introduction to SV Cargo Retrieval

The maintenance of neurotransmission is dependent upon the reformation of synaptic vesicles (SVs) with the correct molecular composition during the endocytic process. The selection, sorting and incorporation of SV cargo into nascent SVs needs to be a tightly regulated process in order to ensure that the cargo is present in the correct stoichiometries for SV function. Under normal physiological conditions, cargo is incorporated into SVs during clathrin-mediated endocytosis (CME, see chapter 1.3). Under CME conditions, clathrin adaptor proteins (AP) act as the primary medium that facilitates cargo selection as well as the recruitment of necessary accessory molecules associated with endocytosis (Kelly and Owen, 2011). Despite this clear importance of APs in CME, it was demonstrated that both expression silencing and genomic ablation of the classical adaptor protein AP-2 resulted in only minor observable effects on SV endocytosis (Kim and Ryan, 2009, Kononenko et al., 2014). This suggests that AP-2 is not the only molecule responsible for the sorting and clustering of SV cargo and that other molecules are required for this process. Many monomeric, cargo-specific adaptor proteins (e.g. stonin-2, AP-180/CALM) have been identified which have been shown to be essential for ensuring efficient SV cargo retrieval during endocytosis (Rao et al., 2012). Most interestingly, several lines of evidence have recently been documented which suggests that SV cargos have the ability to interact between themselves to ensure accurate sorting and retrieval(Gordon et al., 2011, Kononenko et al., 2013, Zhang et al., 2015). This introduction will explore the roles and interactions of two crucial SV cargoes in particular, synaptic vesicle protein 2A (SV2A) and synaptotagmin I (SYT1), and the

mechanisms by which these interactions assist the accurate sorting and retrieval of both proteins during SV endocytosis.

3.1.1 – Role of Synaptic Vesicle Protein 2 (SV2) at the Presynapse

Synaptic vesicle protein 2 (SV2) is a synaptic vesicle glycoprotein which is present in the secretory vesicles of neural and endocrine cells. SV2 consists of 12 transmembrane domains and cytoplasmic N- and C- terminus regions (Figure 3.1.1). Three isoforms of SV2 are currently known to exist: SV2A, SV2B and SV2C. SV2A is the most widely expressed throughout the body and is most widely abundant in subcortical areas such as the thalamus and basal ganglia (Bajjalieh et al., 1993). SV2B (which has a 57% identity match with SV2A) is enriched and has an overlapping expression with SV2A in the cortex and hippocampus but is absent in other areas such as the pallidum, hippocampal dentate gyrus, reticular substantia nigra and reticular thalamic nucleus (Bajjalieh et al., 1994). The third isoform, SV2C (62% identity match with SV2A), is expressed in high levels in phylogenetically old regions of the brain such as the pallium, substantia nigra, midbrain, brain stem and olfactory bulb. No SV2C expression was detected in the cerebral cortex or hippocampus (Janz and Südhof, 1999). SV2A has a large, 169 amino acid-long N-terminus which consists of a phosphorylation-dependent binding region for the calcium sensor protein synaptotagmin I (SYT1) (Pyle et al., 2000, Schivell et al., 2005). The role of SYT1 will be further described in the next section. SV2A also contains a conserved, 91 amino acid-long cytoplasmic loop between the sixth and seventh transmembrane domains, as well as a highly glycosylated, 130 amino acid-long extracellular loop between the seventh and eighth transmembrane domains.

The exact role of SV2A in SV recycling and neurotransmission remains unclear. SV2A was initially proposed to be a transporter, due to its high degree of sequence homology with the major facilitator superfamily (MFS) transporters and its localisation on SVs. Visualisations of SV2A conformations *in situ* by use of protein tomography revealed a compact, funnel shaped structure that is indicative of a pore opening (Lynch et al., 2008). This conformation is highly similar in configuration to another MFS transporter, the *E.Coli* lactose permease sugar transporter (Holyoake and Sansom, 2007), giving evidence of a role in transport. In agreement with this hypothesis, human SV2A has recently been demonstrated to function as a galactose transporter in yeast cells (Madeo et al., 2014).

SV2A has been found in nerve terminals that utilise different neurotransmitters, therefore a role as a specific neurotransmitter carrier has been ruled out. In agreement with this, the absence of SV2A does not affect mEPSC amplitudes at synapses. This suggests that the amount of glutamate molecules being packaged into SVs remains unaffected by the loss of SV2A (Custer et al., 2006). The role of SV2A as a Cl^- transporter has also been discussed. The widespread expression of SV2A throughout the brain is consistent with the fact that Cl^- transport is required by all SVs (Bajjalieh et al., 1994). Interactions of SV2A with presynaptic Cl^- channels may also affect the ability of GABAergic neurones to produce or sustain action potentials (Crowder et al., 1999). In disagreement with these lines of evidence, it has been shown that vesicular glutamate transporter 1 (VGLUT1), rather than SV2A, represents the major Cl^- permeation pathway in SV recycling (Schenck et al., 2009). SV2A is also hypothesised to be a Ca^{2+} transporter, as there is existing evidence to suggest that the conserved presence of negatively charged residues in the first

transmembrane region of SV2A plays a role in facilitating Ca^{2+}-dependent regulation of neurotransmitter release during repetitive stimulation (Janz et al., 1999). In contrast to this evidence, it was later demonstrated that neither overexpression nor the isoform-specific silencing of SV2A affected depolarisation-triggered Ca^{2+} influx, arguing against a Ca^{2+} transport role for SV2A (Iezzi et al., 2005).

Though SV2A may not be directly responsible for Ca^{2+} transport, there have been several lines of evidence presented to suggest that they could play in a role in the maintenance of neurotransmission. SV2A knockout mice demonstrate limited growth and are excessively prone to seizures that lead to death approximately 3 weeks after birth (Crowder et al., 1999). Loss of SV2 results in a reduction of both excitatory and inhibitory action potential-dependent neurotransmission, whereas action potential-independent neurotransmission remained unaffected. The altered neurotransmission in SV2A KO mice did not arise from changes in the number of synapses or the morphology of the synapses, and was not required for SV biogenesis (Crowder et al., 1999, Custer et al., 2006). Analyses of soluble NSF attachment protein receptor (SNARE) complexes in brain tissue have shown that a loss of SV2A results in the association of fewer complexes, indicating that SV2A may play a role in the modulating the formation of key protein complexes integral for fusion and therefore the progression of SVs to a fusion competent state (Xu and Bajjalieh, 2001). Several studies have suggested that SV2 may play a role in modulating Ca^{2+} mediated exocytosis. Firstly, deletion of SV2 resulted in diminished synaptic transmission which could be reversed by application of the Ca^{2+} -chelating agent EGTA, indicating that SV2 has an effect downstream of SV priming but upstream of the Ca^{2+} triggering of release (Chang and Suedhof, 2009). A plausible explanation for

this phenomenon is that SV2 enhances the responsiveness of primed SVs to Ca^{2+} influx. Secondly, SV2 (primarily SV2B) regulates the concentration of resting and evoked presynaptic Ca^{2+} levels indicating a role in the regulation of exocytosis (Wan et al., 2010).

Another function that SV2A may play is in the immobilisation and subsequent liberation of neurotransmitter. The glycosylated region of SV2A in the intraluminal region of the SV forms a proteoglycan matrix that controls the adsorption of acetylcholine and ATP in *Torpedo* SVs. SV2A is suggested to modulate neurotransmitter release by regulating the availability of freely diffusible acetylcholine and ATP (Reigada et al., 2003).

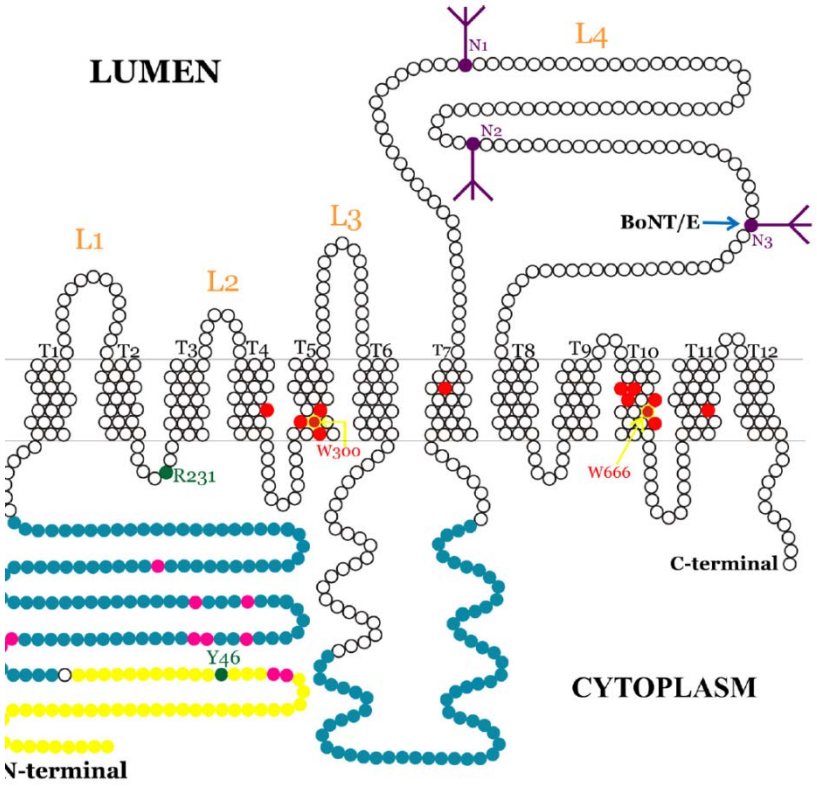

Figure 3.1.1: Schematic Representation of Synaptic Vesicle Protein 2A (SV2A) (Mendoza-Torreblanca et al., 2013). SV2A is 12-transmembrane domain protein with a large, 169 amino acid-long N-terminus which consists of a phosphorylation-dependent binding region for the calcium sensor protein synaptotagmin I (SYT1). SV2A also contains a conserved, 91 amino acid-long cytoplasmic loop between the sixth and seventh transmembrane domains, as well as a highly glycosylated, 130 amino acid-long extracellular loop between the seventh and eighth transmembrane domains. Y46 (green) is required for trafficking of SV2A to SVs via AP-2 binding. Ten putative protein phosphorylation sites in the N-terminus are shown in pink. Fourteen amino acids implicated in racetam binding (red) are also highlighted. R231 is a canonical MFS transporter motif, and W300 and W666 are essential for SV2 action in synaptic transmission.

3.1.2 – Roles of Synaptotagmin I (SYT1) at the Presynapse

Synaptotagmin I (SYT1) is a member of a family of proteins that are defined by a single transmembrane domain that is joined to two Ca^{2+} binding domains (C2A and C2B) through a linker region. Initial efforts to characterise the function of SYT1 revealed that loss of the protein resulted in defects in neurotransmission in several animal models (Littleton et al., 1994, Nonet et al., 1993, Borden et al., 2005). The presence of these calcium binding C2 domains on SYT1 strongly indicates a primary role for SYT1 in facilitating Ca^{2+}-dependent interactions. At the presynapse, neurotransmitter release can be classified into two forms: 1) a fast, synchronous form which is Ca^{2+}-dependent and takes place on a timescale of around 5-10 ms; and 2) a slower, asynchronous form which is predominantly Ca^{2+}-independent and takes place on a time scale of 100-200 ms (Goda and Stevens, 1994). This dual phase nature of neurotransmitter release supports the hypothesis that two separate Ca^{2+} sensors are involved in each form. In order for a protein to function as a viable Ca^{2+} sensor to facilitate neurotransmission, it needs to have two major properties: 1) an ability to bind quickly and reversibly to Ca^{2+} and 2) an ability to form an integral relationship with other SNARE proteins to facilitate their interactions with membrane phospholipids. The ablation of the C2B domain of SYT1 in mice resulted in a reduction of the fast synchronous release without affecting the slower asynchronous release in electrophysiological studies (Geppert et al., 1994). In support of this, similar results were obtained in Drosophila SYT1 null mutants where the fast component of release was absent and synaptic communication was limited to the slower release component (Yoshihara and Littleton, 2002). These lines of evidence strongly indicates that SYT1 acts as a Ca^{2+} sensor for fast synchronous release, but

does not do so for the slower asynchronous release. Apart from sensing Ca^{2+}, a second postulated function for SYT1 at the presynapse is a role in the regulation of SNARE complex machinery. SNARE complex machinery is involved in SV docking and fusion to the plasma membrane during exocytosis (see chapter 1). Binding of SYT1 to SNARE machinery to trigger membrane fusion takes place in a Ca^{2+}-dependent manner on a millisecond timescale (Chapman et al., 1995, Bai et al., 2004). The way in which SYT1 drives membrane fusion under Ca^{2+} influx remains controversial, however recent studies have shed further light on three possible mechanisms: 1) Formation of specific interfaces that promote interactions between SYT1 and the plasma membrane to re-model areas of the membrane in order to drive fusion (Zhou et al., 2015); 2) Regulating the binding of SYT1 to $PI(4,5)P_2$ in membrane patches (Park et al., 2015); 3) Facilitation of dynamic interactions between SYT1 and SNARE complexes in driving membrane fusion (Brewer et al., 2015). A third major protein interaction mediated by SYT1 C2 domains is the Ca^{2+}-induced oligomerisation of SYT1 on SVs. Overexpression of SYT1 in PC12 cells extends the transition between fusion pore opening and dilation, indicating that SYT1 oligomerisation may play a stabilising role in maintaining the fusion pore prior to full fusion(Wang et al., 2001).

Although it is clear for both mammals and flies that the function of SYT1 is required for the fast component of release, the biochemical properties that provide the molecular basis for Ca^{2+} sensing remain in debate. The C2 domains of SYT1 are homologous to the C2 domains of protein kinase C (PKC), and therefore SYT1 was believed to facilitate the localisation of PKC onto the plasma membrane by binding to membrane phospholipids in a Ca^{2+}-dependent manner (Nishizuka, 1988). Initial

biochemical studies on SYT1 revealed that it binds to both Ca^{2+} and phospholipids on a millisecond timescale (Brose et al., 1992, Davis et al., 1999), which satisfies the requirements for it to function as a Ca^{2+} sensor. Early work on the Ca^{2+} cooperativity of neurotransmitter release has shown a minimum of four Ca^{2+} ions are required to bind onto a single neurotransmitter molecule in order to trigger transmission (Dodge and Rahamimoff, 1967). After the discovery of SYT1 as the primary Ca^{2+} sensor, functional analysis using genetic deletions or mutations in alleles coding for specific regions of SYT1 revealed the identity of the domains which were integral for Ca^{2+} binding and modulation (Littleton et al., 1994). The different mutant versions of SYT1 investigated were: AD1, which contained a deletion of the entire C2B domain and resulted in the loss of oligomerisation and SNARE-binding activity of the protein; AD3, which contained a point mutation (Y364N) and ablated oligomerisation activity only; AD4, which consisted of an early stop codon that deleted the entire cytoplasmic region of SYT1 and represented a complete loss-of-function model. The AD4 mutant (both C2 domains deleted) exhibited a complete loss of synchronous release but interestingly, also showed an increase in the amount of asynchronous release. Compared to AD4, the AD1 mutant (C2B domain deleted) only partially restored synchronous release and resulted in the slight increase of asynchronous release. Furthermore, the C2B domain deletion reduced the Ca^{2+} cooperativity of neurotransmission from 4 to 0.77. The AD3 mutant (both C2 domains present), which restored the ability of SYT1 to bind to the SNARE complex via the C2B domain, allowed near-full synchronised release to take place (Ca^{2+} cooperativity ~ 3.5) but had no significant effect on asynchronous release (Yoshihara and Littleton, 2002). Because the AD1 mutant protein lacks the C2B domain, this

indicates that the C2B domain is required for Ca^{2+} cooperativity. Therefore, the reductions in Ca^{2+} cooperativity values associated with certain mutations of SYT1 indicate the Ca^{2+} sensing domain of SYT1 can be primarily attributed to the C2B domain. These results also support the idea that both the C2A and the C2B domains of SYT1 are involved in the suppression of asynchronous release. However, the primary Ca^{2+} sensing function for SV fusion is provided mainly by the C2B domain (Gaffaney et al., 2008), thereby distinguishing the molecular determinants of synchronicity of release. Recent work on the linker region between the C2A and C2B domain indicated that the region plays a role in mediating the ability of SYT1 to insert into the plasma membrane as well facilitate interactions between the C2A and C2B domain that allows control of both synchronous and asynchronous release (Lu et al., 2014).

In addition to roles as a Ca^{2+} sensor and a SNARE fusion complex effector, SYT1 has also been proposed to play other key roles at the presynaptic terminal. Discrete Ca^{2+} co-ordinating residues in both the C2A and C2B domain of SYT1 have an effect on the SV endocytosis kinetics as well as SV size (Poskanzer et al., 2006). More recently, the juxtamembrane region of SYT1 has been shown to interact with the pleckstrin homology (PH) domain of dynamin I, leading to a prolonging of the fission pore lifetime that affects the overall dynamics of vesicle retrieval (McAdam et al., 2015).

3.1.3 – Classical Mechanisms of SV2A and SYT1 Retrieval during Endocytosis

Newly formed SVs need to be consistently generated with consistent high fidelity for functional viability to participate in subsequent exocytic events. A large proportion of transmembrane proteins use a number of unrelated sorting signals to allow regulation of protein numbers during membrane uptake. The sorting of SV proteins at the plasma membrane is usually facilitated by adaptor proteins (e.g. AP-2) which recognise binding motifs present on key SV proteins and facilitate their internalisation during endocytosis. Two major classes of frequently used endocytic sorting signals have been identified for AP-2 binding: 1) tyrosine-based [YxxØ] motifs, and 2) acidic cluster di-leucine ([DE]xxLL) motifs (where x = any amino acid and Ø = a bulky hydrophobic amino acid). Both of these signals directly bind to distinct sites on the AP-2 complex (Royle et al., 2005). SV2A contains two such distinct tyrosine motifs: 1) YSRF at amino acids 46-49 in the cytoplasmic N-terminus, and 2) YRRI at amino acids 443-446 in the cytoplasmic loop preceding transmembrane domain 7. This suggests the existence of two possible sites where SV2A may bind to AP-2 in order to facilitate its sorting into SVs. In studies on SYT1 endocytic binding motifs, an AP-2-binding site has been located in the C2B domain of SYT1 although the site appears to lack the classical tyrosine or di-leucine based endocytic motifs. This was supported by evidence showing that a basic C2B domain-derived peptide was able to disrupt interactions between native SYT1 and the µ2 subunit of AP-2 (Grass et al., 2004). In addition to AP-2, SYT1 retrieval is further facilitated during endocytosis by a second adaptor protein, stonin-2. Systematic deletion and site-directed mutagenesis approaches paired with modelling studies have been identified the interaction sites involved in complex formation between

SYT1 and stonin-2 (Jung et al., 2007). These studies have revealed that the μ-homology domain of stonin-2 recognises basic motifs present within both C2 domains of SYT1, with C2A forming the major interaction surface. Expression of stonin-2 also is sufficient to drive clathrin/AP-2-dependent internalisation of SYT1 in non-neuronal cells, while leaving transferrin or EGF endocytosis unaffected (Diril et al., 2006). Knockout of stonin-2 in neurones result in the accumulation of SYT1 at the plasma membrane and an acceleration of SYT1 retrieval during SV endocytosis, similar to the phenotype seen in the total absence of SV2A (Kononenko et al., 2013). These data establish stonin-2 as a SYT1-specific endocytic sorting adaptor for SV recycling.

3.1.4. – Trafficking Partnerships of SV Cargo during Endocytosis

Although the classical adaptor proteins are central to the process for SV cargo selection and recruitment to nascent SVs, they do not seem to be essential to the maintenance and regulation of SV endocytosis. When the expression of AP-2 is reduced using siRNA or ablated using genomic knockout strategies, relatively minor effects on SV endocytosis at the plasma membrane are observed (Willox and Royle, 2012, Jung et al., 2015), suggesting that other key molecules are required to ensure efficient cargo retrieval and SV endocytosis in general. Intriguingly, certain SV cargos interact with each other during recruitment and thus facilitate each other's retrieval during SV endocytosis as part of a transport complex. These co-interacting SV cargos have been termed 'intrinsic trafficking partners'(Gordon and Cousin, 2016). This unusual relationship has been documented in two sets of integral

membrane proteins: 1) synaptobrevin II (SYB2; also called vesicle associated membrane protein 2, VAMP2) and synaptophysin (SYP), and 2) SV2A and SYT1.

3.1.4.1. – Intrinsic Trafficking Partners: SYB2 and SYP

Synaptobrevin II (SYB2) is a vesicular SNARE protein that associates with the membrane SNARE proteins syntaxin and SNAP-25 for priming and driving SV fusion during exocytosis (see chapter 1). SYB2 is an essential component of the molecular machinery of the SV, and thus its correct targeting and localisation is essential for maintaining neurotransmission. SYB2 has no canonical motifs for AP-2, therefore the recruitment of SYB2 to SVs must be a result of the function of other trafficking partner molecules. Early work identified the monomeric clathrin adaptor protein AP-180 and the related protein clathrin assembly lymphoid myeloid leukaemia (CALM) as regulators of SYB2 targeting in *C.elegans* (Nonet et al., 1999). Subsequently, AP-180 and CALM were demonstrated to regulate SYB2 targeting in other model systems such as lap (drosophila analogue for AP-180) mutant flies (Bao et al., 2005) and mice (Koo et al., 2011). In the latter studies, immunoprecipitation experiments revealed a direct interaction between the ANTH domains of AP-180 and CALM and the SNARE motif of SYB2. Knockout of AP-180 results in the stranding of SYB2 to the surface of the plasma membrane and its inefficient retrieval during endocytosis. This effect is exacerbated in AP-180 knockout mammalian neuronal systems (Koo et al., 2015).

It has been shown recently that synaptophysin (SYP), a four-transmembrane domain protein that contains cytoplasmic N- and C-termini, also plays a role as an intrinsic

trafficking partner for SYB2 to facilitate targeting of SYB2 to SVs in parallel with AP-180 and CALM. Recent studies of SYB2 trafficking in SYP-knockout mice have shed some light on the intricacies of the SYB2-SYP relationship. In the absence of SYP, SYB2 was mislocalised from synaptic terminals and accumulated at the plasma membrane. This mistargeting of protein was shown to be a result of a specific deficit in the activity-dependent retrieval of SYB2 from the plasma membrane during compensatory endocytosis. SYB2 retrieval was severely slowed in SYP-knockout neurones. The re-addition of exogenous SYP to the SYP-knockout neurones resulted in the full rescue of SYB2 retrieval to wild type levels (Gordon et al., 2011). Further evidence for a key role for SYP in SYB2 retrieval came from the analysis of various SYP mutants identified in X-linked intellectual disability. SYP mutants identified to be implicated in intellectual disability all failed to rescue wild type SYB2 retrieval in the knockout model system (Gordon and Cousin, 2013). Interestingly, all except one of the mutations were predicted to interfere with the transmembrane SYB2-SYP interaction (Calakos and Scheller, 1994, Adams et al., 2015). This data establishes that SYP is essential for the accurate retrieval of SYB2 during compensatory endocytosis.

3.1.4.2. – Intrinsic Trafficking Partners: SV2A and SYT1

The interaction between SV2A and SYT1 has been mapped, showing that the cytoplasmic N-terminus of SV2A binds to the C2B domain of SYT1 (Schivell et al., 1996). This binding interaction is enhanced by casein kinase 1 family (CK1) dependent phosphorylation of SV2A *in vitro*(Pyle et al., 2000). It was recently established that the CK1 kinases are responsible for promoting and modulating the

phosphorylation of SV2A, and this occurs at a highly conserved cluster of amino acids in SV2A (S80, S81 and T84) (Zhang et al., 2015). Within the C2B domain of SYT1, the SV2A binding site resides within a specific, surface-exposed pocket of three lysine residues (K314, K326, K328). This lysine pocket resides in close proximity to various other molecules such as phosphoinositides (Schiavo et al., 1996), calcium channels (Leveque et al., 1992), t-SNARE dimers (Bhalla et al., 2006) as well as other isoforms of synaptotagmin (Chapman et al., 1996), indicating that modulation of SYT1 at this specific pocket may affect its function in other presynaptic processes.

SV2A functions to direct SYT1 targeting to SVs alongside stonin-2. In neurones that have SV2A depleted or removed, SYT1 fails to target correctly to synaptic terminals and accumulates at the plasma membrane. This effect was shown to be SV2A-dependent, since restoration of wild type SV2A in the neurones restored normal plasma membrane levels of SYT1 (Yao et al., 2010, Kaempf et al., 2015). SV2A-deficient neurones which were rescued with mutant forms of SV2A which did not bind AP-2 (Yao et al., 2010) or SYT1 (Kaempf et al., 2015) also resulted in the same stranding of SYT1 at the plasma membrane, providing strong evidence that the SV2A-SYT1 interaction is required for efficient targeting of SYT1 to synaptic terminals. In addition to the synaptic targeting, deficiencies in SV2A expression also resulted in accelerated SYT1-specific retrieval during SV endocytosis (Kaempf et al., 2015, Zhang et al., 2015). This was an unexpected observation, as the stranding of SV cargo at the plasma membrane has been historically linked to a perturbation of SV endocytosis (Willox and Royle, 2012, Kononenko et al., 2014). Interestingly, silencing of SV2A expression in stonin-2 knockout neurones revealed an

exacerbation of SYT1 accumulation and a further re-acceleration of its retrieval (Kaempf et al., 2015). This work provided strong evidence that both stonin-2 and SV2A are required for efficient SYT1 trafficking. These additive effects on SYT1 suggest that SV2A and stonin-2 function via discrete parallel mechanisms, or perform synergistic roles in SYT retrieval.

3.1.4.3 – Further Evidence for Intrinsic Trafficking Partnerships

In addition to specific SYB2-SYP and SV2A-SYT1 interactions as documented above, vesicular glutamate transporter 1 (VGLUT1) has recently been shown to have a central role in co-ordinating SV cargo retrieval during compensatory endocytosis. The siRNA-mediated silencing of VGLUT1 in rat hippocampal cultures resulted in defective retrieval of the key SV cargos SV2A, SYB2 and SYP. SYT1, however, was shown to be unaffected by VGLUT1 perturbations (Pan et al., 2015). The demonstration that different cargos may be retrieved with different kinetics at the same synaptic terminals provides evidence that SV cargos are not equally sorted at the plasma membrane and that SV cargo sorting is likely to be function of multiple parallel mechanisms. It was proposed that SYT1 and VGLUT1 could be acting in parallel upstream in the endocytic sorting mechanisms; however, this proposal is in disagreement the previously described works that directly link the trafficking of SV2A and SYT1. Nevertheless, a role for VGLUT1 in SV cargo sorting cannot be ruled out.

3.1.5 – Aims and Objectives

Mutation of the Y46 residue from tyrosine to alanine (Y46A) was previously shown to ablate SV2A binding to AP-2, resulting in the stranding of SYT1 at the plasma membrane (Yao et al., 2010). However, there is currently no published literature that investigates the effect of the Y46A SV2A mutation on the internalisation of SYT1 during compensatory endocytosis. I hypothesise that as SV2A and SYT1 are intrinsic trafficking partners, the disruption of SV2A trafficking by ablation of AP-2 binding will also result in downstream disruption of SYT1 trafficking and thus its internalisation from the plasma membrane during endocytosis. Previously published literature has demonstrated that mutation of residue 84 in SV2A from threonine to alanine (T84A) results in the disruption of the phosphorylation dependent binding of SV2A to SYT1, leading to defects in SYT1 trafficking during SV recycling(Zhang et al., 2015). In this investigation, I also aim to compare and contrast the mechanisms by which mutation of the SV2A/AP-2 binding motif and SV2A/SYT1 binding motif operates.

The primary objectives of the research in this chapter are:

1) To validate the knockdown of wild type SV2A by use of a small hairpin RNA (shRNA) sequence and subsequent rescue of SV2A expression with wild type (WT) or Y46A SV2A

2) To characterise the effect of Y46A SV2A on the surface expression of SYT1 at the plasma membrane and its localisation to presynaptic terminals

3) To characterise the effect of Y46A SV2A on the rate of SYT1 retrieval from the plasma membrane during compensatory endocytosis

4) To establish the SYT1 specificity of defects in SV recycling which are caused by Y46A SV2A

5) To distinguish the different mechanistic pathways which alter the SV2A-SYT1 interaction and result in defective SYT1 retrieval from the plasma membrane

3.2. – Results of Studies Using Y46A SV2A

Prior studies have evidenced a role for the Y46 residue in SV2A in binding to the adaptor protein, AP-2 during SV recycling. Disruption of this tyrosine-based binding motif by mutation of the tyrosine residue to alanine (Y46A) ablates the binding of SV2A to AP-2 at the N-terminus, resulting in the stranding of SYT1 at the plasma membrane surface and a failure of SYT1 to localise to synaptic terminals (Yao et al., 2010). This phenotype may cause defects in the efficiency of SYT1 internalisation during SV compensatory endocytosis. In support of this hypothesis, it has been reported that ablation of the phosphorylation-dependent interaction of SV2A with SYT1 by mutation of residue 84 from threonine to alanine (T84A) results in the increased SYT1 plasma membrane expression and accelerated SYT1 retrieval during compensatory endocytosis (Zhang et al., 2015). Although the partnership between SV2A and SYT1 during endocytosis has been widely documented, there is currently no published literature on the effects of disruption of SV2A retrieval on the activity-dependent retrieval of SYT1. In this chapter, I aimed to characterise the effect of SV2A Y46A mutation on: 1) surface fraction and localisation of SYT1 and 2) rate of retrieval of SYT1 during SV endocytosis. I then proceeded to distinguish the mechanism of Y46A SV2A action of SYT1 and other known mechanisms by which SYT1 trafficking dysfunction may be caused (T84A SV2A).

Key research findings of this chapter:

- Y46A SV2A leads to the acceleration of SYT1 retrieval kinetics, increased surface expression and mislocalisation of SYT1 on the plasma membrane.
- The Y46A and T84A SV2A mutations perturb the same mechanistic pathway at the presynapse, suggesting SV2A modulates retrieval of SYT1 by AP-2.

3.2.1 – Expression of Y46A SV2A-mCer Successfully Rescues Defects in SV2A Expression Levels Caused By shRNA-mediated Knockdown

The first experiments aimed to validate and quantify the effectiveness of the efficiency of the exogeneously expressed wild-type SV2A-mCer (WT SV2A) and Y46A SV2A-mCer (Y46A SV2A) plasmids in rescuing the depletion of SV2A expression levels caused by shRNA-mediated knockdown. Primary cultures of mice hippocampal cells were co-transfected with: 1) a SYT1-pHluorin plasmid also containing a shRNA sequence for SV2A (SV2A shRNA/SYT1-pHluorin) to simultaneously deplete SV2A levels and express SYT1-pHluorin in neurones; 2) plasmids containing either WT SV2A-mCer or Y46A SV2A-mCer to rescue SV2A expression after shRNA-mediated knockdown. Final SV2A expression levels in the cultures after transfection were detected by immunofluorescence experiments (Figure 3.2 **A**).

The co-transfection of the SV2A shRNA/SYT1-pHluorin with an mCerulean N1 (mCer) empty plasmid into neurones resulted in up to 48% knockdown of SV2A expression. The levels of SV2A observed in non-transfected neurones in the same field of view was used as an internal control for each experiment [Ratio of SV2A expression in transfected neurones/untransfected neurones = 0.521 ± 0.039 (mCer); $p < 0.0001$ (mCer vs WT), one-way ANOVA, Bonferroni's post-hoc]. The co-transfection of the SV2A shRNA/SYT1 pHluorin with either wild-type (WT) SV2A or Y46A SV2A plasmids into neurones resulted in a complete rescue of SV2A expression [Ratio of SV2A expression in transfected neurones/untransfected neurones = 1.062 ± 0.077 (WT SV2A), 1.138 ± 0.050 (Y46A SV2A); $p < 0.0001$

(WT vs mCer, Y46A vs mCer); one-way ANOVA, $P < 0.0001$, $F = 33.9$, Bonferroni's post-hoc] (Figure 3.2 **B**).

These experiments therefore show that neuronal SV2A levels were successfully depleted by transfection of a previously described combined SV2A shRNA/SYT1-pHluorin plasmid. Normal SV2A expression was successfully rescued when neurones were co-transfected with plasmids expressing either exogeneous WT SV2A or Y46A SV2A, indicating that the neuronal culture system was able to withstand acute genetic depletion of SV2A and expression of exogeneously mutant SV2A.

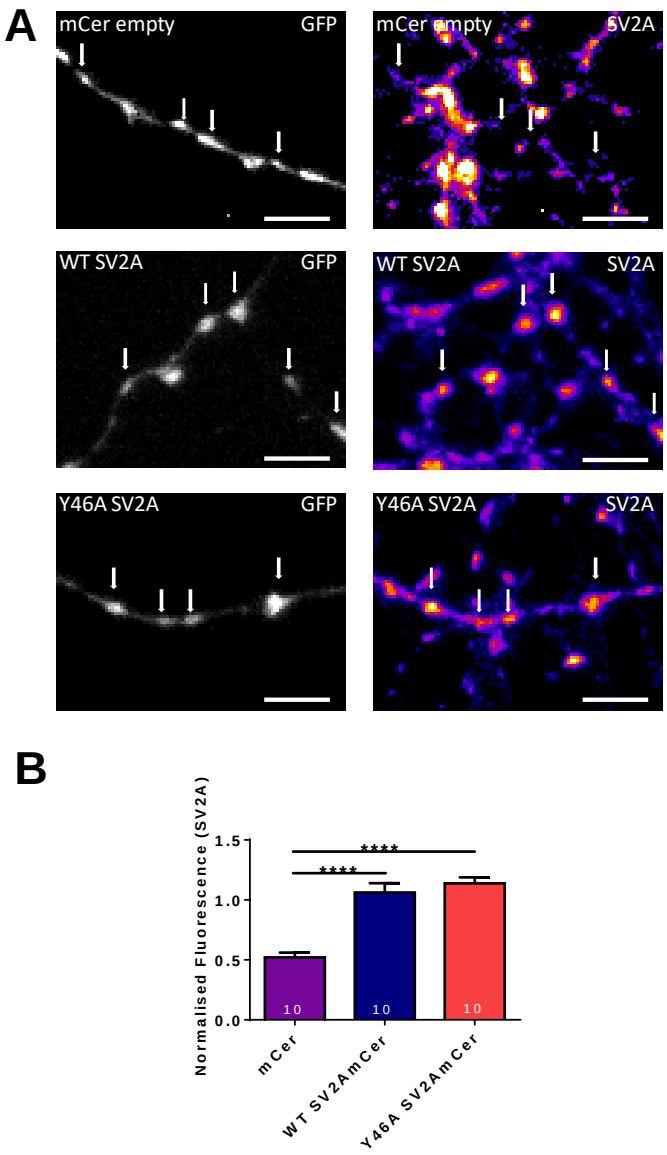

Figure 3.2: Expression of Y46A SV2A-mCer rescues deficits in SV2A expression caused by shRNA-mediated knockdown: A) Images of cultures co-transfected with SV2A shRNA/SYT1–pHluorin vector and either empty rescue (mCer), wild-type (WT) SV2A-mCer or Y46A SV2A-mCer. Grayscale panels highlight transfected neurones (GFP), whereas false colour panels display exogenous SV2A revealed by immunofluorescence staining. Arrows highlight nerve terminals. Scale bar = 10 µM. **B)** Bar graph shows levels of rescue of SV2A expression. The background-corrected SV2A immunofluorescence obtained from transfected neurones was normalised to the SV2A immunofluorescence obtained from non-transfected neurones within the same field of view [n=10 mCer empty, purple; n=10 WT SV2A-mCer, blue; n=10 Y46A SV2A-mCer, red; ****p<0.0001 (mCer vs WT, mCer vs Y46A); one-way ANOVA, Bonferroni's post-hoc, $P < 0.0001$, $F = 33.9$].

3.2.2 – Y46A SV2A Results in Increased but Delocalised Surface Expression of SYT1

Previous studies have shown that the Y46A mutation in SV2A results in the stranding of SYT1 at the plasma membrane surface and a failure for SYT1 to localise to synaptic terminals (Yao et al., 2010). In order to corroborate this previous observation in my model system, I proceeded to investigate the effect of mutating the AP-2 binding motif in SV2A on the surface expression and localisation of SYT1 to presynaptic terminals. As in the above experiments, SV2A shRNA/SYT1-pHluorin was transfected into primary cultures to knockdown SV2A expression and co-express the SYT1-pHluorin reporter. Neuronal SV2A expression was rescued by co-transfection of either WT or Y46A SV2A-mCer plasmid (Figure 3.3 **A**).

In order to investigate surface expression of SYT1 after perturbation of SV2A levels, the fraction of surface-expressed SYT1-pHluorin in transfected neurones was compared to the total SYT1-pHluorin pool in the neurone (see chapter 2.2). Surface fraction experiments revealed that knockdown of SV2A in neurones and rescue using an empty plasmid resulted in a significant increase of surface-expressed SYT1-pHluorin compared to control rescue experiments using WT SV2A. Knockdown of SV2A in neurones and rescue with Y46A SV2A plasmid also resulted in a significant increase in the percentage of surface-expressed SYT1-pHluorin when compared to control rescue experiments using WT SV2A [Surface expression of SYT1-pHluorin (% of total SYT1-pHluorin pool) = 18.5 ± 2.3 (WT SV2A), 38.8 ± 1.9 (mCer), 49.8 ± 4.0 (Y46A SV2A); $p < 0.0001$ (Y46A vs WT), $p < 0.001$ (mCer vs WT); one-way ANOVA, Bonferroni's post-hoc, $P < 0.0001$, $F = 27.6$] (Figure 3.3 **B**). These results demonstrate that depletion of SV2A in neurones leads to increased expression of SYT1 at the plasma membrane surface. Rescue of SV2A expression with the Y46A

SV2A fails to rescue this defect in the proportion of surface-expressed SYT1. These observations suggest that the Y46A mutation in SV2A plays a crucial role in disrupting the internalisation of SYT1.

In order to investigate the effect of Y46A SV2A on the localisation of SYT1 to synaptic terminals, an analysis of the coefficient of variation (CV) for SYT1-pHluorin fluorescence was performed. The CV is a calculation for the diffuseness of the fluorescence for the total pHluorin pool along a fixed length of neurite (see chapter 2.2). CV analysis of the expression of the total SYT1-pHluorin pool in a 50-µm length of neurite in SV2A knockdown cultures co-expressing a mCer empty plasmid revealed a significantly decreased coefficient of variation compared to control rescue experiments using WT SV2A. In SV2A knockdown cultures co-expressing the Y46A SV2A plasmid, CV analysis of SYT1-expression in a 50-µm length of neurite revealed similarly decreased CVs compared to control rescue experiments using WT SV2A [Mean CV = 33.6 ± 6.2 (WT SV2A), 13.2 ± 2.7 (mCer), 14.8 ± 0.9 (Y46A SV2A); $p < 0.01$ (mCer vs WT), $p < 0.05$ (Y46A vs WT); one-way ANOVA, Bonferroni's post-hoc, $P = 0.0053$, $F = 8.37$] (Figure 3.3 **C**).

These experiments demonstrate that depletion of SV2A leads to increased diffuseness of SYT1 expression across the neurite, suggesting a defect in the targeting SYT1 to presynaptic terminals during SV recycling. A similar phenotype is observed when the AP-2 binding motif in SV2A is mutated, suggesting that the binding site in SV2A plays a significant role in regulating the mechanism for SYT1 targeting to presynaptic terminals.

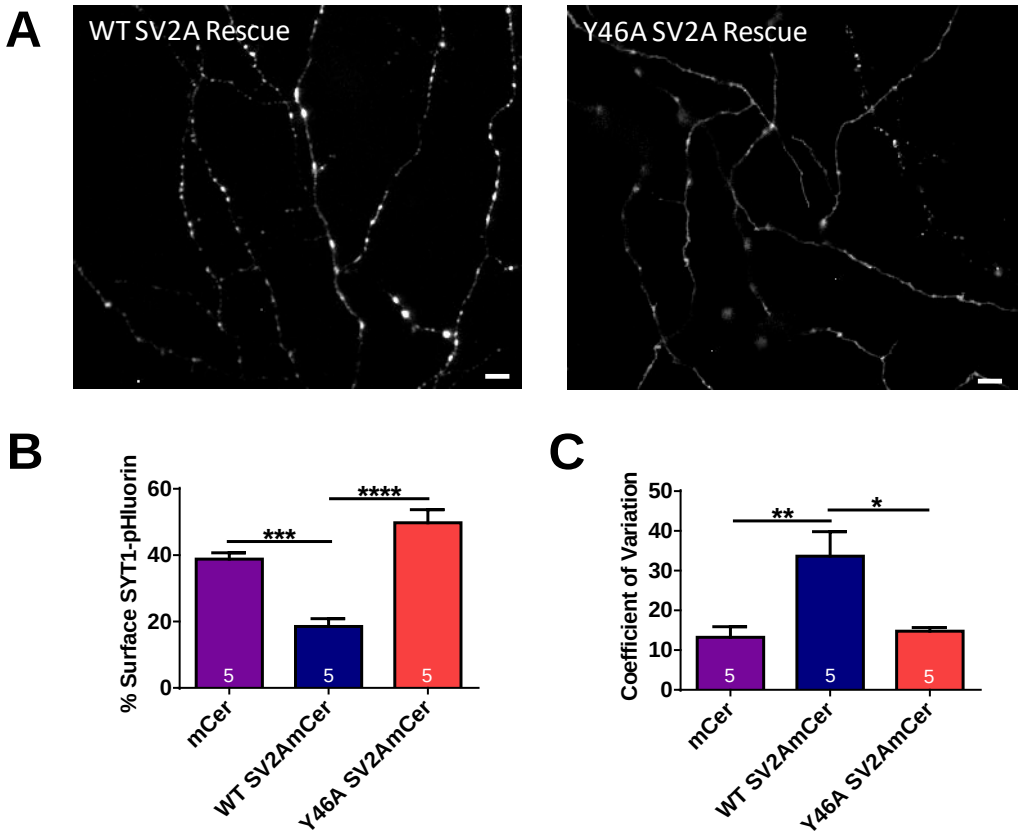

Figure 3.3: Y46A SV2A results in increased but delocalised surface expression of SYT1. A) Hippocampal neurones were co-transfected with an SV2A shRNA/SYT1-pHluorin plasmid and either wild-type (WT) or Y46A SV2A-mCer. Representative greyscale images show that rescue with Y46A SV2A-mCer resulted in less localisation to nerve terminals compared to WT SV2A-mCer rescue. Scale bar = 10 µM. **B)** Surface expression of SYT1–pHluorin after rescue with SV2A-mCer variants displayed as a percentage of total SYT1-pHluorin pool ± SEM [n=5 mCerN1 empty, purple; n=5 WT SV2A-mCer, blue; n=5 Y46A SV2A-mCer, red; ****p<0.0001 (Y46A vs WT); ***p<0.001 (mCer vs WT); one-way ANOVA, Bonferroni's post-hoc, P<0.0001, F=27.6]. **C)** Bar graph displays the mean coefficient of variation of SYT1-pHluorin fluorescence along axons of neurones in alkaline buffer. Data are presented as ± SEM (n=5 mCerN1 empty, purple; n=5 WT SV2A-mCer, blue; n=5 Y46A SV2A-mCer, red; **p<0.01 (mCer vs WT); *p<0.05 (Y46A vs WT); one-way ANOVA, Bonferroni's post-hoc, P=0.0053, F=8.37).

3.2.3 – Y46A SV2A Fails to Rescue the Acceleration of SYT1 Retrieval caused by Knockdown of SV2A

In order to determine the effect of mutating the AP-2 binding motif in SV2A on SYT1 trafficking, I proceeded to investigate SYT1 trafficking during SV recycling in the presence of Y46A SV2A. As in previous experiments, SV2A shRNA/SYT1-pHlourin was used as a reporter for SYT1 recycling at the synaptic terminal and for knockdown of SV2A expression after transfection into neurones. Neuronal SV2A expression was rescued by the co-transfection either WT or Y46A SV2A-mCer.

ShRNA-mediated knockdown of SV2A in neurones and rescue with an empty plasmid resulted in a slowing of SYT1 retrieval compared with control rescue experiments using WT SV2A [$p < 0.05$ (mCer vs WT), two-way ANOVA of traces normalised to peak at evoked transmission]. Knockdown of SV2A and rescue with mutant Y46A SV2A in neurones resulted in a failure to rescue SYT1 retrieval to WT levels, mimicking the SYT1-pHlourin recycling phenotype seen in SV2A-deficient neurones [$p < 0.05$ (Y46A vs WT), two-way ANOVA of traces normalised to the peak at evoked stimulation] (Figure 3.4 **A**). Knockdown of SV2A and rescue with the Y46A mutant resulted in a non-significant, slightly increased proportion of SYT1 externalisation during stimulation [Max $\Delta F/F_0$ (as a fraction of the total pHluorin pool) = 0.463 ± 0.086 (WT SV2A), 0.565 ± 0.068 (mCer), 0.630 ± 0.035 (Y46A SV2A); ns, one-way ANOVA, P = 0.197, F = 1.74] (Figure 3.4 **B**), suggesting that presence of Y46A SV2A exerts no significant effect on SYT1 trafficking during exocytosis. The quantification of the average time constant for retrieval (tau) of the evoked SYT1-pHluorin response allows for a direct comparison of retrieval time constants between the different experimental conditions. This provides an extra line

of evidence to demonstrate that the rate of SYT1 retrieval during compensatory endocytosis accelerated when SV2A levels are depleted in neurones. In agreement with the analysis of the average time traces, the knockdown of SV2A in neurones and rescue using either mCer or Y46A SV2A significantly decreased the tau of SYT1-pHluorin retrieval compared to control rescue experiments using WT SV2A. [Tau (s) = 75.0 ± 9.2 (WT SV2A), 47.3 ± 5.2 (mCer), 38.8 ± 3.8 (Y46A SV2A); $p < 0.01$ (Y46A vs WT), $p < 0.05$ (mCer vs WT); one-way ANOVA, Bonferroni's post-hoc, $P = 0.0018$, $F = 8.33$] (Figure 3.4 **C**). Therefore, the phenotype observed with the Y46A SV2A rescue experiments was similar to that seen with the mCerN1 empty vector rescue in all cases.

These experiments indicate that depletion of SV2A/mutation of the SV2A AP-2 binding region in neurones results in faster retrieval of SYT1 during endocytosis without affecting its trafficking during exocytosis. The possible reasons for these observations will be evaluated in the later discussion chapters.

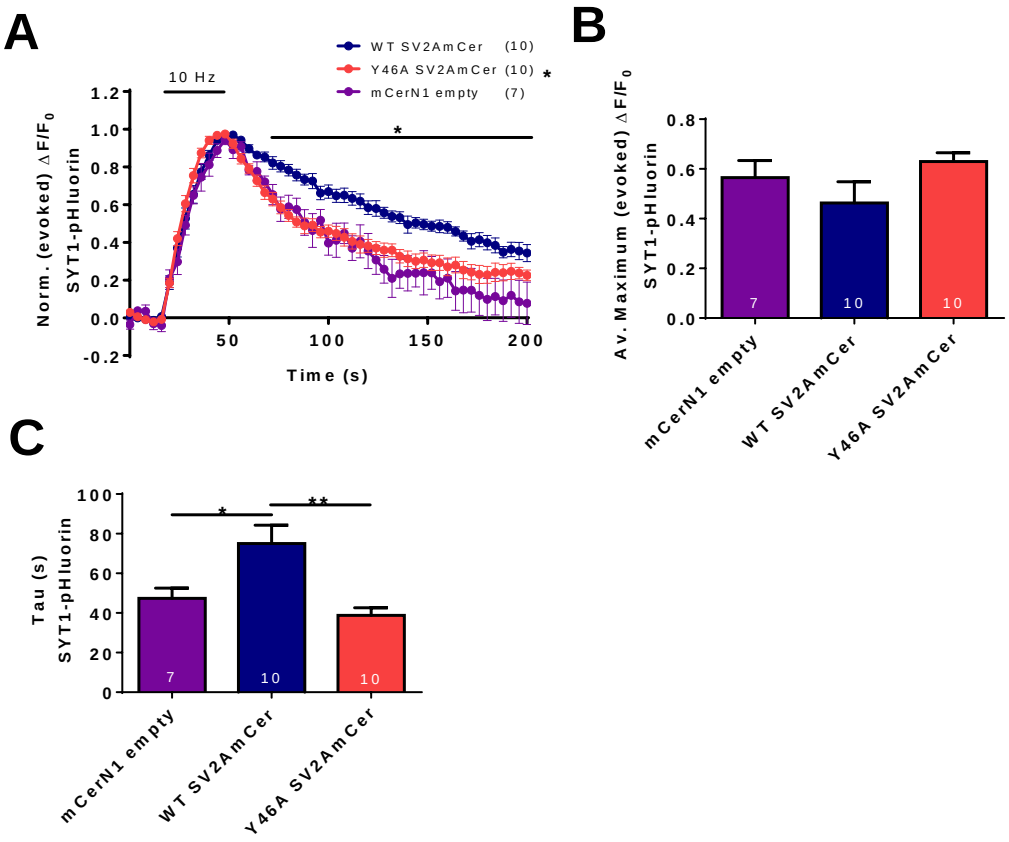

Figure 3.4: Y46A SV2A fails to rescue the acceleration of SYT1 retrieval caused by knockdown of SV2A. A) Hippocampal neurones were co-transfected with an SV2A shRNA/SYT1-pHluorin vector and either mCerulean (mCer) empty vector or SV2A-mCer variants. Cultures were stimulated using a train of 300 action potentials (APs, 10 Hz, indicated by bar). After 200 seconds of recovery, the total recycling synaptic vesicle (SV) pool was revealed with a NH_4Cl pulse. Graph displays the mean $\Delta F/F_0$ time course for SYT1–pHluorin ± SEM normalized to the peak of stimulation [n=7 mCer empty, purple; n=10 wild-type (WT) SV2A-mCer, blue; n=10 Y46A SV2A-mCer, red; *p<0.05 (Y46A vs WT); two-way ANOVA, Bonferroni's post-hoc (over times indicated by solid lines)]. **B)** Mean maximum evoked SYT1-pHluorin response ($\Delta F/F_0$) expressed as a fraction of the total SV pool (ns, one-way ANOVA, P=0.197, F=1.74). **C)** Graph shows quantification of the average time constant (Tau) ± SEM of the evoked SYT1-pH response [**p<0.01 (Y46A vs WT), *p<0.05 (mCerN1 vs WT); one-way ANOVA, Bonferroni's post-hoc, P=0.0018, F=8.33].

3.2.4 – Y46A SV2A Does Not Affect Synaptophysin Retrieval or Surface Expression

Previous results have shown that mutation of the AP-2 binding motif in SV2A leads to a defect in the localisation and the retrieval of SYT1 at the presynaptic terminal. However, it is unknown of this defect was specific to SYT1 or a general dysfunction of SV cargo sorting which may affect several key SV proteins. In order to discount the possibility of Y46A SV2A having a global effect on SV recycling, I investigated the effect of Y46A SV2A on the localisation of synaptophysin (SYP) and the rate of SYP retrieval from the plasma membrane. In these experiments, neuronal cultures were transfected with three constructs: 1) SV2A shRNA to knockdown SV2A expression in neurones; 2) synaptophysin-pHluorin (SYP-pHluorin) as a reporter for SYP expression and retrieval in neurones during compensatory endocytosis; 3) either WT or Y46A SV2A-mCer for the purposes of rescuing SV2A expression after knockdown.

ShRNA-mediated knockdown of SV2A in neurones and rescue using an empty vector resulted in no observable effect on SYP-pHluorin retrieval during endocytosis compared to control rescue experiments using WT SV2A. Similarly, shRNA-mediated knockdown of SV2A and rescue using Y46A SV2A did not affect the rate of SYP-pHluorin retrieval compared to control rescue experiments using WT SV2A (ns, two-way ANOVA of traces normalised to peak at evoked transmission) (Figure 3.5 **A**). Knockdown of SV2A and rescue using either an empty vector or Y46A SV2A also did not have an effect on the amount of SYP-pHluorin externalisation during stimulation when compared to control rescue experiments with WT SV2A [Max $\Delta F/F_0$ (as a fraction of the total pHluorin pool) = 0.372 ± 0.027 (WT SV2A), 0.378 ± 0.019 (mCer), 0.375 ± 0.025 (Y46A SV2A); ns, one-way ANOVA, P =

0.988, F = 0.0121] (Figure 3.5 **B**). In agreement with the analysis of the average time traces, the quantification of the retrieval time constants for SYP-pHluorin in SV2A knockdown neurones rescued with Y46A SV2A revealed no significant effect compared to control rescue experiments using WT SV2A [Tau (s) = 38.1 ± 4.6 (WT SV2A), 40.9 ± 8.9 (mCer), 32.5 ± 2.7 (Y46A SV2A); ns, one-way ANOVA, P = 0.486, F = 0.752] (Figure 3.5 **C**). Surface fraction experiments revealed that knockdown of SV2A in neurones and rescue using an empty plasmid did not affect the expression of SYP-pHluorin compared to control rescue experiments using WT SV2A. Likewise, the rescue of SV2A expression using Y46A SV2A did not affect the surface expression of SYP-pHluorin [Surface expression of SYP-pHluorin (% of total SYP-pHluorin pool) = 20.0 ± 2.4 (WT SV2A), 23.8 ± 4.8 (mCer), 23.4 ± 3.0 (Y46A SV2A); ns, one-way ANOVA, P = 0.718, F = 0.344] (Figure 3.5 **D**).

This set of results provides evidence to support the hypothesis suggesting that mutation of the AP-2 binding motif in SV2A does not have an effect on the rate of SV retrieval, amount of externalisation during compensatory endocytosis and the surface expression of synaptophysin. Therefore, the findings from previous observations made using SYT1-pHluorin as a reporter can be attributed to a specific effect on the trafficking of SYT1 at the synaptic terminal and not a global effect on SV recycling.

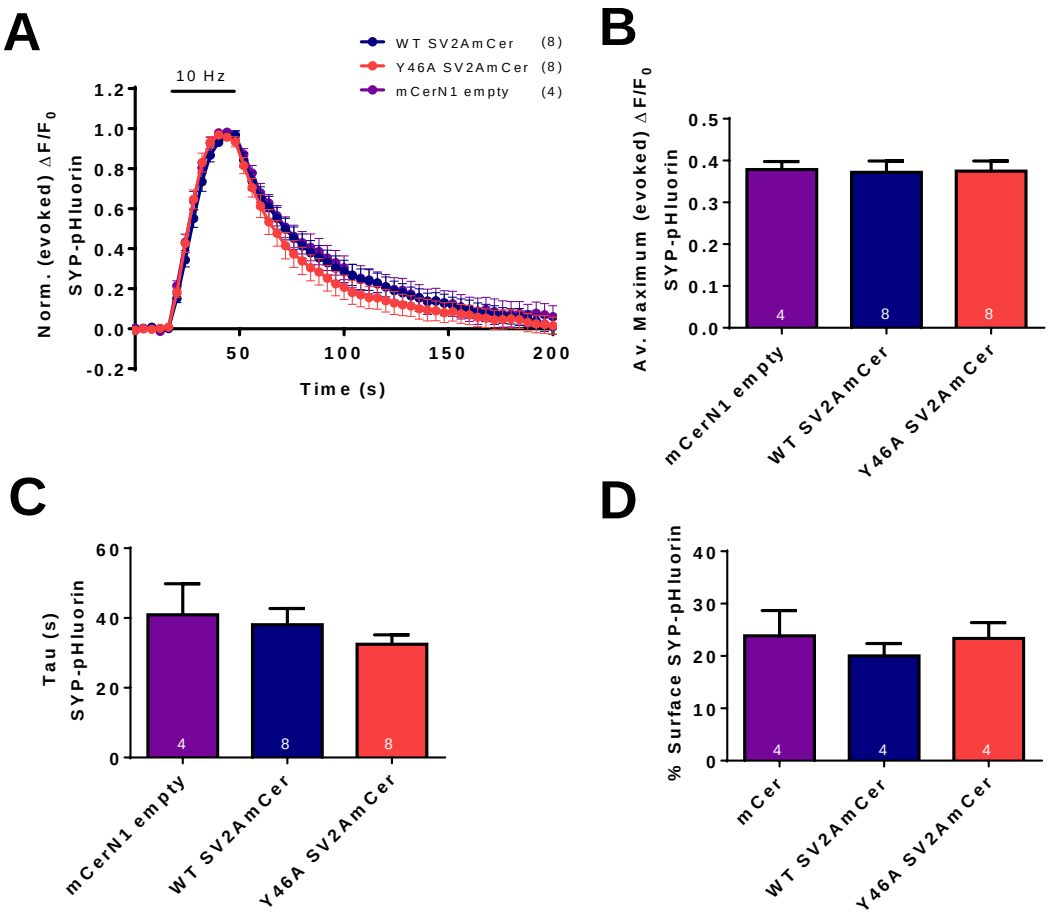

Figure 3.5: Y46A SV2A does not affect SYP retrieval or surface expression. A) Hippocampal neurones were co-transfected with SV2AshRNA, SYP-pHluorin and mCer or SV2A-mCer variants. Cultures were stimulated using a train of 300 APs (10 Hz, indicated by bar) and the total recycling synaptic vesicle (SV) pool was revealed with a NH_4Cl pulse at the end of the experiment. Graph displays the mean $\Delta F/F_0$ time course for SYP–pHluorin ± SEM normalized to the peak of stimulation (n=4 mCerN1 empty, purple; n=8 wild type (WT) SV2A-mCer, blue; n=8 Y46A SV2A-mCer, red; ns, two-way ANOVA). **B)** Mean maximum evoked response ($\Delta F/F_0$) of SYP-pHluorin during stimulation expressed as a fraction of the total SV pool (ns, one-way ANOVA, P=0.988, F=0.0121). **C)** Graph shows quantification of the average time constant (Tau) ± SEM of the evoked SYP-pHluorin response (ns, one-way ANOVA, P=0.486, F=0.752). **D)** Surface expression of SYP–pHluorin after rescue with SV2AmCer variants displayed as a percentage of total releasable pHluorin pool ± SEM (n=4 mCerN1 empty, purple; n=4 WT SV2A-mCer, blue; n=4 Y46A SV2A-mCer, red; ns, one-way ANOVA, P=0.718, F=0.344).

3.2.5 – T84A/Y46A SV2A Does Not Exacerbate Defects in SYT1 Retrieval

The findings from previous experiments have given evidence to support a role for the tyrosine-based AP-2 binding motif in SV2A in the surface expression, localisation and retrieval kinetics of SYT1 in cultured neurones. These effects are dependent on the phosphorylation-mediated binding of SV2A to SYT1 at T84A. As a result, the combination of both T84A and Y46A SV2A mutations should not exacerbate the observed defects to SYT1 trafficking and any exacerbation observed may be a direct indication of a separate SYT1 retrieval mechanism in action during endocytosis.

In order to shed further light on the SYT1-binding dependency of Y46A SV2A-induced defects in SYT1 trafficking, the T84A/Y46A SV2A double mutant was genetically engineered and used to rescue SV2A expression in SV2A knockdown neurones and the rate of SYT1 retrieval during endocytosis was compared with the individual single mutants to reveal any additive defects in SYT1 trafficking that may be present. The shRNA-mediated knockdown of SV2A and rescue using the T84A/Y46A SV2A double mutant resulted in a failure to rescue normal SYT1 recycling behaviour compared to control rescue experiments using WT SV2A. The observed phenotype was consistent with the findings obtained from rescue experiments using the single mutants only. Comparison of the average SYT1-pHluorin traces obtained from experiments using the T84A/Y46A SV2A double mutant to experiments using the corresponding single mutants did not reveal any additive defects in SYT1 recycling ($p < 0.05$ (T84A/Y46A vs WT), ns (T84/Y46A vs T84A or Y46A), two-way ANOVA of traces normalised to the peak at evoked stimulation) (Figure 3.6 **A**). Knockdown of SV2A in neurones and rescue using the T84A/Y46A SV2A double mutant did not affect the proportion of SYT1

externalisation during evoked transmission when compared to control rescue experiments using WT SV2A. Comparison of the proportion of SYT1 externalisation in experiments using the T84A/Y46A SV2A double mutant and the T84A SV2A single mutant revealed no significant defects. This observation is in contrast with experiments using the Y46A single mutant, which indicated an increased level of SYT1 externalisation during evoked transmission [Max $\Delta F/F_0$ (as a fraction of the total pHluorin pool) = 0.339 ± 0.029 (WT SV2A), 0.377 ± 0.022 (T84 SV2A), 0.473 ± 0.040 (Y46A SV2A), 0.340 ± 0.008 (T84A/Y46A SV2A); $p < 0.05$ (Y46A vs WT), one-way ANOVA, Bonferroni's post-hoc, P = 0.0101, F = 5.17] (Figure 3.6 **B**). The quantification of retrieval time constants for SYT1-pHluorin in SV2A knockdown neurones rescued with T84A/Y46A SV2A revealed a significant decrease in retrieval time compared to control rescue experiments using WT SV2A. No additive disruption to SYT1 retrieval was observed when analysis of the T84A/Y46A double mutant time constants was compared to T84A and Y46A SV2A single mutants [Tau (s) = 70.8 ± 5.1 (WT SV2A), 45.0 ± 3.4 (T84A SV2A), 47.2 ± 4.9 (Y46A SV2A), 44.8 ± 7.1 (T84A/Y46A SV2A); $p < 0.05$ (T84A/Y46A vs WT), ns (T84A/Y46A vs T84A or Y46A), one-way ANOVA, Bonferroni's post-hoc, P = 0.0082, F = 5.46] (Figure 3.6 **C**).

These experiments indicate that mutation of both the AP-2 binding motif and the SYT1 binding motif in SV2A result in a failure to rescue normal SV2A function. The presence of T84A/Y46A SV2A resulted in faster retrieval of SYT1 during endocytosis and no significant effect on its trafficking during exocytosis. The results suggest that Y46A-induced defects in SYT1 trafficking are dependent upon binding of SV2A to SYT1.

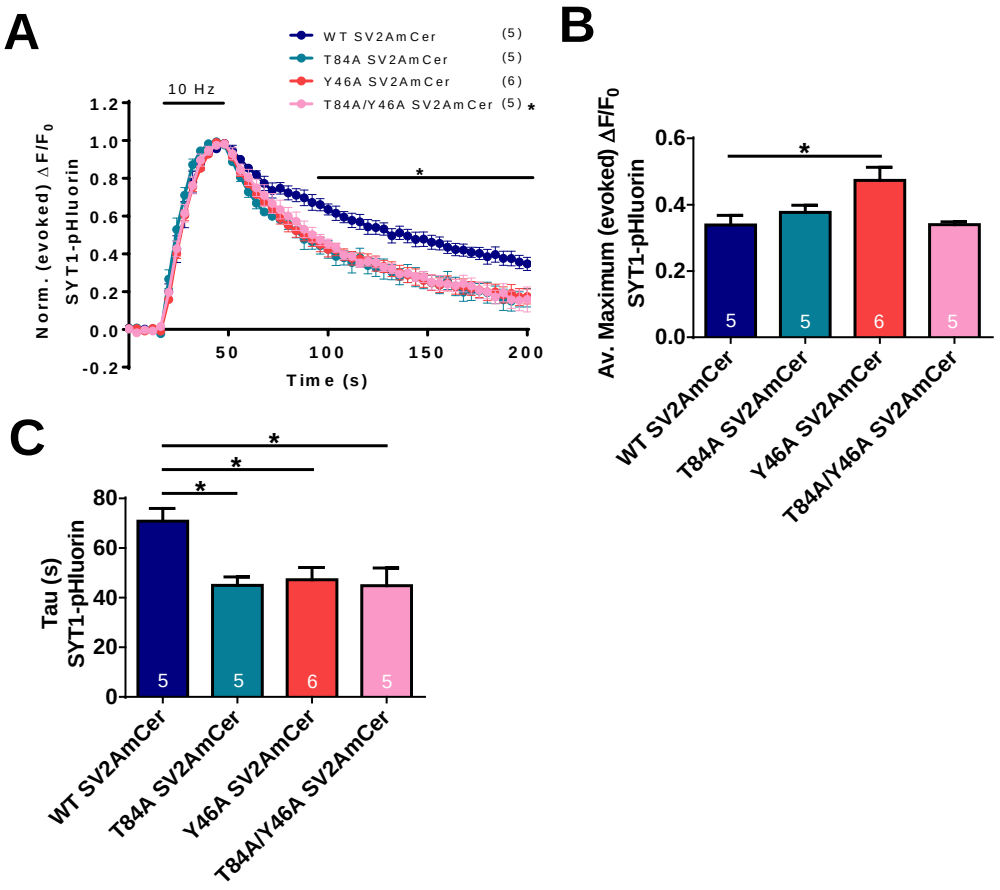

Figure 3.6: T84A/Y46A SV2A does not exacerbate defects in SYT1 recycling. A) Hippocampal neurones were co-transfected with SV2AshRNA-SYT1-pHluorin and mCer or SV2A-mCer variants. Cultures were stimulated using a train of 300 APs (10 Hz, indicated by bar) and the total releasable vesicle pool was revealed with a NH_4Cl pulse at the end of the experiment. Graph displays the mean $\Delta F/F_0$ time course for SYT1–pHluorin ± SEM normalized to the peak of stimulation [n=5 wild type (WT) SV2A-mCer, blue; n=5 T84A SV2A-mCer, cyan; n=6 Y46A SV2A-mCer, red; n=5 T84A/Y46A SV2A-mCer, pink; *p<0.05 (T84A/Y46A vs WT), two-way ANOVA, Bonferroni's post-hoc (over times indicated by solid lines)]. **B)** Mean maximum evoked response ($\Delta F/F_0$) of SYT1-pHluorin during stimulation expressed as a fraction of the total releasable vesicle pool [*p<0.05 (Y46A vs WT); one-way ANOVA, Bonferroni's post-hoc, P=0.0101, F=5.17]. **C)** Graph shows quantification of the average time constant (Tau) ± SEM of the evoked SYT1-pH response [*p<0.05 (T84A/Y46A vs WT, T84A vs WT, Y46A vs WT); one-way ANOVA, Bonferroni's post-hoc, P=0.0082, F=5.46].

3.2.6 – T84A/Y46A SV2A Does not Exacerbate Defects in SYT1 Surface Expression and Localisation

After ascertaining that the double mutation of the SV2A/AP-2 and SV2A/SYT1 binding motifs had no significant additive effect on the time constant of SYT1 retrieval and its externalised proportion during stimulation, I proceeded to investigate if the same SV2A double mutation could potentially affect the surface expression of SYT1 and its localisation to presynaptic terminals in neurones. As in previous experiments, SV2A shRNA/SYT1-pHluorin was transfected into primary cultures to knockdown SV2A expression and co-express the SYT1-pHluorin reporter. Neuronal SV2A expression was rescued by co-transfection of WT, T84A, Y46A and T84A/Y46A SV2A-mCer plasmids (Figure 3.7 **A**).

An investigation of the fraction of surface-expressed SYT1-pHluorin in SV2A knockdown neurones rescued with T84A/Y46A SV2A double mutant revealed a significant increase of surface fraction when compared to control rescue experiments using WT SV2A, consistent with previous results obtained from the single SV2A mutants. Comparison of results obtained from experiments rescued with the T84A/Y46A double mutant to experiments rescued with the corresponding single mutants revealed no additive effects to the surface expression of SYT1 [Surface expression of SYT1-pHluorin (% of total SYT1-pHluorin pool) = 16.0 ± 0.9 (WT SV2A), 36.0 ± 3.5 (mCer), 32.1 ± 3.0 (T84A SV2A), 44.5 ± 3.3 (Y46A SV2A), 34.6 ± 4.4 (T84A/Y46A SV2A); $p < 0.01$ (T84A/Y46A SV2A vs WT), ns (T84A/Y46A SV2A vs T84A or Y46A SV2A), one-way ANOVA, Bonferroni's post-hoc, $P = 0.0001$, $F = 10.3$] (Figure 3.7 **B**). CV analysis of the expression of the total SYT1-pHluorin pool in a 50-µm length of neurite in SV2A knockdown cultures co-

expressing the T84A/Y46A SV2A double mutant revealed a significantly decreased coefficient compared to control rescue experiments using WT SV2A. Comparison of rescue experiments using the T84A/Y46A double mutant to rescue experiments using the corresponding single mutants revealed no additive effects to the CV [Mean CV = 29.3 ± 3.0 (WT SV2A), 11.7 ± 0.9 (mCer), 16.2 ± 1.9 (T84A SV2A), 14.8 ± 0.9 (Y46A SV2A), 18.9 ± 1.4 (T84A/Y46A SV2A); $p < 0.01$ (T84A/Y46A SV2A vs WT), ns (T84A/Y46A SV2A vs T84A or Y46A SV2A), one-way ANOVA, Bonferroni's post-hoc, $P < 0.0001$, $F = 14.1$] (Figure 3.7 **C**).

These experiments demonstrate that mutation of both the SV2A/AP-2 and SV2A/SYT1 binding motifs in SV2A leads to increased surfaced expression and increased diffuseness of SYT1 expression across the neurite, but with no additive effects compared to those observed in experiments with just a single SV2A mutation. This suggests that mutation of both binding sites in SV2A serve to disrupt targeting of SYT1 to presynaptic terminals via a similar mechanistic pathway to be discussed in later chapters.

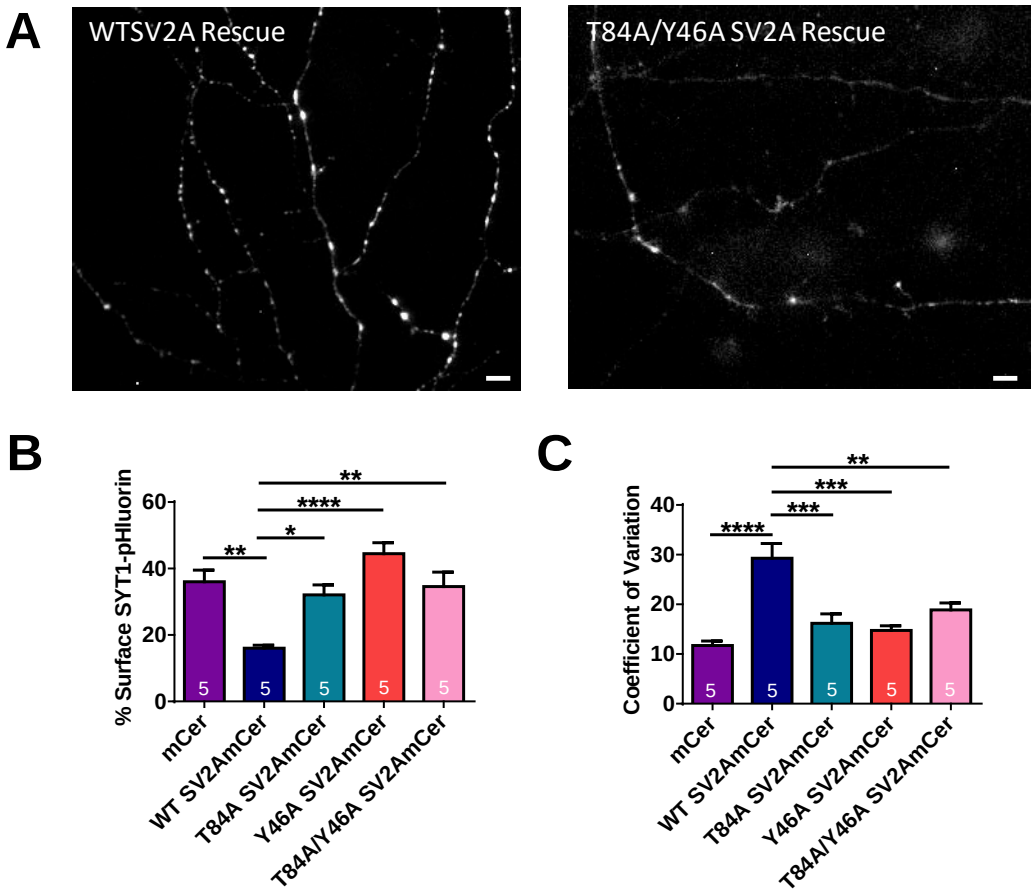

Figure 3.7: T84A/Y46A SV2A does not exacerbate defects to SYT1 surface expression and localisation. A) Hippocampal neurones were co-transfected with an SV2A shRNA-SYT1-pHluorin plasmid and either wild-type (WT) or SV2A-mCer variants. Representative greyscale images show that rescue with T84A/Y46A SV2A-mCer resulted in less localisation to nerve terminals compared to WT SV2A-mCer rescue. Scale bar = 10 µM. **B)** Surface expression of SYT1–pHluorin after rescue with SV2AmCer variants displayed as a percentage of total SYT1-pHluorin pool ± SEM [n=5 mCerN1 empty, purple; n=5 WT SV2A-mCer, blue; n=5 T84A SV2A-mCer, cyan; n=5 Y46A SV2A-mCer, red; n=5 T84A/Y46A SV2A-mCer, pink; ****p<0.0001 (Y46A vs WT); **p<0.01 (mCer vs WT, T84A/Y46A vs WT); *p<0.05 (T84A vs WT); one-way ANOVA, Bonferroni's post-hoc, P=0.0001, F=10.3]. **C)** Bar graph displays the mean coefficient of variation of SYT1-pHluorin fluorescence along axons of neurones in alkaline buffer. Data are presented as ± SEM (n=5 mCerN1 empty, purple; n=5 WT SV2A-mCer, blue; n=5 T84A SV2A-mCer, cyan; n=5 Y46A SV2A-mCer, red; n=5 T84A/Y46A SV2A-mCer, pink; ****p<0.0001 (mCer vs WT); ***p<0.001 (T84A vs WT, Y46A vs WT); **p<0.01 (T84A/Y46A vs WT); one-way ANOVA, Bonferroni's post-hoc, P<0.0001, F=14.1).

3.3. –Discussion on the Presynaptic Effects of Y46A SV2A

SV2A and SYT1 are hypothesised to be intrinsic trafficking partners, therefore the disruption of SV2A trafficking by ablation of AP-2 binding should also result in downstream disruption of SYT1 trafficking and thus its internalisation from the plasma membrane during endocytosis. Mutation of the Y46 residue from tyrosine to alanine (Y46A) was previously shown to ablate SV2A binding to AP-2, resulting in the stranding of SYT1 at the plasma membrane (Yao et al., 2010). Recent studies have confirmed that Y46A SV2A displays retarded retrieval during endocytosis (Dr. C. Harper, Cousin Lab, data not shown), confirming a role for the AP-2 binding motif in clustering SV2A during SV compensatory endocytosis. However, the effect of Y46A SV2A on SYT1 trafficking, and by extension SV recycling has never been documented in previously published literature.

3.3.1 – ShRNA-mediated Knockdown of SV2A Expression in Neurones Can Be Successfully Rescued by Use of Exogeneously Transfected Y46A SV2A

Knockdown of endogeneous SV2A was achieved using a small hairpin DNA sequence and successfully reduced expression of SV2A to about 50% of its original level. This observation was noted to be slightly lower than in previously reported data (>75%) (Zhang et al., 2015) and discrepancies may have arisen from the method of immuno-quantification used. In this approach, averaged fluorescence from SV2A-depleted nerve terminals was expressed as a percentage of averaged fluorescence from normal, non-SV2A-depleted nerve terminals within the same field of view. Selection of nerve terminals for analysis is highly subjective between persons and

may inevitably lead to differences when reporting data. In comparison with internal controls, there was still significant reduction in average SV2A levels. SV2A is known to have a relatively low copy number on SVs at the nerve terminal (around 2-12 per SV) compared to other intergral SV proteins such as SYT1 (20 per SV), SYP (30 per SV) and SYB (70 per SV) (Takamori et al., 2006, Wilhelm et al., 2014), therefore a 50% reduction in expression levels would still be expected to greatly affect the sorting of SV2A and its related cargo.

SV2A expression in these knockdown cells was then rescued by the transfection of exogenous DNA that codes for either full length WT SV2A or full length Y46A SV2A. The Y46A SV2A mutant was shown to rescue SV2A expression to similar levels to that seen when WT SV2A is used. Therefore, any observable phenotype due to the use of these constructs is attributed to an effect resulting from the presence of the Y46A mutation and not due to an experimental failure to rescue SV2A expression in the cell.

3.3.2 – Y46A SV2A Leads to Acceleration of SYT1 Retrieval Kinetics and Increased Surface Expression and Mislocalisation of SYT1

The presence of Y46A SV2A in hippocampal neurones resulted in an acceleration of SYT1 retrieval during compensatory endocytosis, mimicking the phenotype observed when there is a deficiency of SV2A at the synaptic terminal. This was not a general acceleration of endocytosis, as other SV cargos such as synaptophysin were not affected in a similar manner by the presence of the Y46A mutation. The Y46A SV2A mutation also leads to an increased fraction of SYT1 surface expression and

defective localisation of SYT1 to synaptic terminals. These observations are in agreement with previously published work describing specific defects in SYT1 trafficking upon perturbation of SV2A (Yao et al., 2010, Zhang et al., 2015).

The acceleration of SYT1 retrieval caused by Y46A SV2A is unusual, since the disruption of endocytic sorting mechanisms either by depletion of monomeric adaptors or adaptor protein complexes (Willox and Royle, 2012, Kononenko et al., 2014) or by mutagenesis of key endocytosis motifs (Foss et al., 2013) usually result in the retardation of SV cargo retrieval during compensatory endocytosis. When considering other SV cargo complexes at the presynapse such as the synaptophysin-synaptobrevin 2 (SYP-SYB2) complex, evidence has shown that the trafficking of SYB2 is retarded in neurones derived from mice lacking in either SYP (Gordon et al., 2011) or the classical SYB2-specific adaptor, AP-180 (Koo et al., 2015). In contrast, increased SYT1 surface expression and an acceleration of SYT1 retrieval during endocytosis has also been previously observed in neurones derived from stonin-2 knockout mice (Kononenko et al., 2013). Stonin-2 is a specific endocytic adaptor for SYT1, providing further evidence that perturbation of the trafficking partners of SYT1 leads to very specific defects in SYT1 trafficking which do not fall in line with the trafficking behaviour of other SV cargo complexes.

There are several potential explanations for this interesting phenotype. The most likely explanation is that SYT1 is retrieved by a parallel endocytic mode with faster retrieval kinetics than classical clathrin-mediated endocytosis (CME). Examples of fast modes of retrieval are ADBE (Clayton et al., 2008) and ultrafast endocytosis (Watanabe et al., 2013b). It is possible that the accumulation of SYT1 at the plasma membrane acts as a trigger for these modes. Thus, although the Y46A SV2A

mutation may lead to underlying defects in post-exocytic SYT1 retrieval via CME (which is evidenced from the increased stranding of SYT1 at the surface plasma membrane), the retrieval of newly deposited SYT1 could be mediated by an alternate endocytosis mode. In order to test this hypothesis, labelling of SYT1 during immunoelectron microscopy of cultured neurones after stimulation may shed light on the possible increased accumulation of SYT1 on bulk endosomal structures in Y46A SV2A or defective SYT1-binding stonin-2 neurones compared to WT neurones, thus providing evidence of ADBE as an alternative retrieval mechanism for SYT1 when CME is perturbed by ablation of AP-2 binding. In addition, immunolabelling of SYT1 during 'flash-and-freeze' cryo-electron microscopy studies (Watanabe et al., 2013b) on hippocampal tissue from Y46A SV2A or stonin-2 knockout mice models may provide evidence of a role for ultrafast endocytosis in the retrieval of SYT1 when CME is perturbed.

Another possible explanation for this phenotype is that there is a reduction in SYT1 retrieval during spontaneous SV endocytosis, but an increase in the retrieval of SYT1 during activity dependent SV endocytosis. However, in argument against this theory, it was previously observed that plasma membrane SYT1 levels remained normal and that there was no gradual accumulation of SYT1 at the plasma membrane when neuronal activity was silenced in neurones depleted in SV2A (Kaempf et al., 2015). Spontaneous/Active SV recycling assays using single-label marking of SVs with biotinylated antibodies recognising the luminal domain of SYT1 (Wilhelm et al., 2010) applied to cultured tissue from Y46A or stonin-2 knockout mice may shed further light on this theory.

3.3.3 – How Might SV2A Control SYT1 Retrieval?

In conjunction with the classical monomeric adaptors AP-2 and stonin-2, SV2A is reported here to be a chaperone for the efficient post-exocytosis trafficking of SYT1. Specific interactions between SV2A, SYT1, stonin-2 and AP-2 at the synaptic terminal may aid the presentation of these SV cargos in the correct conformation needed for binding and clustering. It is possible that these conformations are not wholly achieved or maintained in the absence of one or more members of the complex. SV2A interacts with SYT1 at the C2B domain in a phosphorylation dependent manner (Zhang et al., 2015), whereas stonin-2 primarily interacts with the C2A domain of SYT1 (Jung et al., 2007). This means that it is possible that SV2A and stonin-2 could interact simultaneously with SYT1 via different C2 domains. In addition, both SV2A and stonin-2 interact with AP-2 via canonical internalisation motifs (Diril et al., 2006, Yao et al., 2010), however SV2A and stonin-2 do not appear to interact directly with each other. This provides further evidence that SV2A may have the ability to control SYT1 endocytosis through regulation of the binding affinity between stonin-2 and SYT1. In support of this concept, the region within the μ2 subunit of AP-2 where SV2A interacts is distinct from the region that interacts with the SYT1 C2B domain, explaining its ability to increase affinity (Haucke et al., 2000). Co-immunoprecipitation studies have also shown the presence of a tripartite complex of SV2A, AP-2 and SYT1, suggesting they come together to form an internalisation complex in mammalian brain systems (Haucke and De Camilli, 1999).

Specific interactions between SV2A, SYT1, stonin-2 and AP-2 at the synaptic terminal may aid the presentation of these SV cargos in the correct conformation needed for binding and clustering. This ensures maximum retrieval efficiency when

all members are present and potential functional redundancy when one member is absent or mutated. The phosphorylation of SV2A may play a key regulatory role in this process, as it may mediate SYT1's access to AP-2. Phosphorylated SV2A may bind to both the C2B domain of SYT1 as well as AP-2. This brings SYT1 and AP-2 to close proximity with each other and potentiates binding between AP-2 and the C2B domain of SYT1, facilitating the retrieval of SYT1 during SV endocytosis. Stonin-2 continues to interact with the C2A and C2B domains of SYT1 as well as AP-2 in a separate mechanistic pathway to assist further in SYT1 retrieval and endocytosis. Future SYT1-pHluorin fluorescence imaging experiments involving the knockdown of SV2A in stonin-2 deficient mice models and rescue with exogeneous Y46A SV2A, in comparison with WT SV2A rescue, may shed further light on whether the two mechanistic pathways are acting dependently or independently of each other. X-ray crystallographic experiments on the AP-2-SV2A-SYT1 complex may also shed further light on the proximity of SYT1 and AP-2 in space when both are bound to SV2A.

3.3.4 – The Y46A and T84A SV2A Mutations Affect the Same Mechanistic Pathway

As previously stated, the region within the μ2 subunit of AP-2 where SV2A interacts is distinct from the region that interacts with the SYT1 C2B domain (Haucke and De Camilli, 1999). SV2A may facilitate the retrieval of SYT1 by playing a role in mediating its access to AP-2. What happens to the retrieval of SYT1 if its interactions with both AP-2 and SV2A are ablated? It is reported here that genetic ablation of both the AP-2 and SYT1 binding motif within SV2A do not appear to show any additive SYT1 retrieval defects, compared to experiments when only one

binding motif is ablated. If SV2A merely mediated access of SYT1 to AP-2 in order to facilitate SYT1 retrieval during SV endocytosis, then it is not surprising that the ablation of both binding sites in SV2A do not present any additional mechanistic defects since both are an intrinsic part of the same retrieval pathway. The absence of additive defects also mean that the retrieval of SYT1 by stonin-2, which proceeds via a different retrieval pathway, is unaffected by the AP-2-SV2A-SYT1 interaction. It is entirely probable that SYT1 will randomly interact with AP-2 in the absence of SV2A. However, the results demonstrated here suggest that this probability remains unaffected by the binding of SV2A and AP-2 at the presynapse. It should be noted that the results observed in these experiments were compared to the baseline SYT1-pHluorin retrieval time course set by genetic depletion of SV2A by use of shRNA silencing. Since immunofluorescence studies have demonstrated that neuronal SV2A depletion was only around 50%, the T84A/Y46A double mutant could only exacerbate the SYT1 retrieval acceleration effect if it was dominant negative over the remaining expressed WT SV2A.

The presence of T84A/Y46A double mutant resulted in a reversal of the slight increase in SYT1 trafficking during exocytosis which was observed in the Y46A SV2A single mutant experiments, matching the levels of SYT1 externalisation seen in the T84A single mutant and WT SV2A experiments. This result was unexpected since both the T84A and Y46A SV2A mutations serve to disrupt SV2A interactions with SYT1 and AP-2 respectively, and was therefore predicted to disrupt SYT1 trafficking at least to the same extent as the Y46A single mutant. The results suggest that the SV2A-AP-2 interaction may be a factor in regulating SYT1 trafficking to the membrane surface during exocytosis under normal circumstances, however ablation

of the SV2A-SYT1 interaction may trigger a separate 'rescue mechanism' that re-normalises SYT1 trafficking during exocytosis. It is unlikely that this 'rescue mechanism' is the acceleration of SYT1 retrieval via a different mechanistic pathway (stonin-2), since the T84A/Y46A double mutant showed no exacerbation of SYT1 retrieval defects observed with the single mutants. This defect in SYT1 trafficking during exocytosis may be further investigated in future experiments by perfusion of bafilomycin onto transfected neurones to inhibit SV re-acidification prior to stimulation. Bafilomycin ablates the diminishment of pHluorin fluorescence caused by SV re-acidification during SV endocytosis, thus enabling full quantification of SYT1 externalisation as a ratio of the total SV pool during stimulation and may fully reveal the true extent of the T84A and Y46A SV2A mutations on SYT1 externalisation during exocytosis.

3.3.5 – Is Retrieval of SV2A Affected by Defective SYT1 Retrieval During SV Endocytosis?

If ablation of the AP-2 binding region in SV2A results in defective retrieval, surface expression and localisation of SYT1, then it is highly probable that defects in SYT1 binding to SV2A would affect SV2A in a similar manner if they are transported as a cargo complex during SV endocytosis. Mutation of the K326/328A residues on SYT1 has previously been shown to ablate binding of SYT1 to SV2A (Zhang et al., 2015) and results in defective SYT1 retrieval. Further experiments to probe the effect of K326/328A SYT1 on SV2A retrieval may provide greater insight to differentiating the endocytic mechanisms that drive the retrieval of SV2A and SYT1. It is currently unknown if: 1) ablation of SYT1 binding to SV2A leaves SV2A

stranded at the plasma membrane in a similar manner, thus triggering a parallel endocytic mode resulting in accelerated retrieval of SV2A or 2) ablation of SYT1 binding to SV2A results in retardation of SV2A retrieval as classically observed. A difference in retrieval behaviour between SV2A and SYT1 in the absence of the other may lead to further developments in elucidating the complex interactions underlying the transport of SV2A and SYT1 at the presynapse. It is also currently unknown if AP-2 binding to SYT1 would affect kinetics of SV2A retrieval, therefore experiments probing the retrieval, surface expression and localisation of SV2A in the presence of an ablation of the SYT1-AP-2 binding region may yet reveal more key interactions driving the transport of the SV2A-SYT1 complex.

Lastly, the effect of defective binding of stonin-2 to SYT1 on the retrieval of SV2A cannot be trivialised. Although it is likely that the pathway responsible for stonin-2-mediated retrieval of SYT1 is separate from SV2A/AP-2-mediated retrieval of SYT1, this has yet to be documented in the literature. Further experiments investigating the retrieval of SV2A in the presence of SYT1 that is defective in binding to stonin-2 may provide insight to previously undiscovered roles of stonin-2 in SV endocytosis. If retrieval of SYT1 by the stonin-2 pathway is indeed altered, then presence of Y46A SV2A in these experiments should result in additive defects in SV2A retrieval compared to WT SV2A.

3.3.6 – Technical Limitations of the Study

The use of pHluorins as a tool for determining the effects of Y46A on SYT1 trafficking must also be considered. Firstly, analysis of the data is based on the assumption that vesicle re-acidification takes place on a significantly faster timescale

than SV endocytosis during neuronal activity. This may not necessarily always be true since recent experiments have shown that SV re-acidification takes place with a time constant of ~15 s, which is three to four-fold slower than previously reported (Egashira et al., 2015). It is also unknown if the Y46A mutation has a direct effect on SV re-acidification, as the phenomenon observed may be a result of defect SV re-acidification kinetics rather than defective SYT1 retrieval during compensatory endocytosis. The use of an exogeneously expressed fusion protein to monitor presynaptic dynamics also relies on the assumption that the trafficking behaviour of the exogeneous cargo perfectly mimics that seen with the endogeneous cargo. It can be argued that fusion of a high molecular weight fluorophore such as GFP may significantly alter the trafficking behaviour of the cargo to an extent that it may not truly reflect the original behaviour. However, in these experiments all pHluorin investigations were compared against control experiments using GFP-fused WT SV2A, thus eliminating any small trafficking nuances that may have arisen from the presence of GFP. It is also noted that for an effect to be observed in the above experiments, the exogeneously-expressed mutant has to exert a dominant negative effect over the endogeneously-expressed WT protein. The presence of a phenotype with the Y46A SV2A mutant suggests that it is dominant negative over WT SV2A in these studies; however, the exact nature of the double mutant remains unclear.

4.0 –The Effects of an Epilepsy-Related SV2A Mutation on SYT1 Trafficking at the Presynapse

4.1 – Introduction to Epilepsy

Epilepsy is a group of common neurological disorders that are characterised by the onset of recurrent seizures in patients. The disorder affects up to 65 million people worldwide (1% of the world's population) with up to 80% of cases occurring in developing countries. During an epileptic seizure, it is hypothesised that neurones in the brain begin to fire in an excessive, synchronised manner compared to the normal state where neuronal firing patterns are non-synchronised (Jiruska et al., 2013).

The underlying causes of epilepsy are unknown in most cases as seizures occur spontaneously and they are not immediately caused by a pre-existing acute illness. In younger people, seizures are likely to be caused by underlying genetic disorders. Although some causes of juvenile epilepsies may be derived from single gene defects, the large majority of cases are a result of the interactions of multiple genes as well as environmental factors during brain development (Pandolfo, 2011). In older people, seizures are more likely to be caused by insults to the brain from incidents such as the development of brain tumours, strokes, head injuries or infections of the central nervous system. In accordance with the 2017 ILAE seizure classification guidelines, seizures are generally classified by the earliest prominent feature. Epileptic seizures can be classified into three main groups: i) focal onset seizures where the origin of the seizure is localised to a single region or hemisphere of the brain; ii) generalised onset seizures where the origins of the seizure are distributed generally throughout the whole brain and iii) unknown and unclassified onset seizures whereby there is inadequate information about the seizure or an inability to place it in other categories. After being classified into one of the three main groups, a seizure may be further classified into motor or non-motor onset sub-groups. Motor

onset seizures affect the motor activity of the body during seizure. These include tonic, clonic, myoclonic, atonic seizures and epileptic spasms. Non-motor onset seizures generally affect behaviour and include autonomic, cognitive, emotional, sensory seizures as well as behaviour arrest (Fisher et al., 2017).

4.1.1 – Implications of General Synaptic Dysfunction in Epilepsy

Although epileptogenesis usually initiates in the early stages of life, it has a neurodegenerative component that facilitates aberrant synaptic morphology and function and could result in cognitive failure. The underlying causes of epilepsy remain largely unknown to this day. Current evidence supports the hypothesis that an imbalance in the excitatory and inhibitory circuits facilitates the onset of the first seizure episodes, which in turn brings about cellular and molecular changes that may lower the threshold for subsequent sequential seizures. An increase in the release of excitatory amino acids has consistently been observed in the hippocampus during seizures in both humans and animals. Pilocarpine-induced status epilepticus in rat hippocampal cells increased the basal (spontaneous) glutamate outflow during the chronic period (Soukupova et al., 2015). Ultrastructural analysis of transmission electron micrographs of pilocarpine-treated rat hippocampal mossy fibre boutons revealed a significant increase in the number of release sites, active zone length, postsynaptic density area and number of vesicles in the readily releasable and recycling pools, all correlated with increased release probability in glutamatergic synapses (Upreti et al., 2012). These data support the theory that the excitatory presynaptic release machinery is persistently altered in structure and function by

status epilepticus, which could contribute to the development of the chronic epileptic state.

Impairment of inhibitory GABA-ergic synapses is another mechanism that is likely to contribute to development of the chronic epileptic state. Loss of hippocampal gamma aminobutyric acid-ergic (GABA-ergic) interneurones during epileptogenesis resulted in impairment of basal GABA outflow during the early course of temporal lobe epilepsy and the dysfunction persisted through to the late phases of the disease (Soukupová et al., 2014). This data suggests that the potentiation of glutamatergic signalling, together with impairment of extracellular GABA levels, can favour the onset of spontaneous recurrent seizures and the maintenance of an epileptic state in the hippocampus of epileptic rats. In support of this theory, alterations in the distribution and composition of AMPA receptors and NMDA receptors leading to increased excitatory tonus (Lopes et al., 2015) and reductions in the surface expression of specific subunits of GABA receptors during status epilepticus leading to reduced GABA-mediated synaptic inhibition (Goodkin et al., 2008) may further exacerbate the imbalance between excitatory and inhibitory activity leading to the onset of status epilepticus. However, if impaired GABA-ergic neurotransmission were to be involved in epileptogenesis, then one would expect synaptic boutons obtained from epileptic animal models to be smaller in volume, have fewer and smaller active zones, and contain fewer vesicles (including fewer docked vesicles). Interestingly, electron micrographs of synapses in the hippocampal basket cell to granule cell layer obtained from pilocarpine-induced epileptic rats revealed the opposite effect. Basket cell layer synaptic boutons contained over twice the average volume, active zone area and number of total vesicles (including docked vesicles and

with more vesicles closer to active zones) (Buckmaster et al., 2016). This result suggests that the neurotransmission failures at synapses of epileptic rats are not attributable to smaller boutons or fewer docked vesicles at inhibitory synapses. Instead, it may be the processes that follow vesicle docking (such as priming, Ca^{2+} entry into the synapse, Ca^{2+} coupling with exocytosis or SV endocytosis) that are responsible for epilepsy-related phenotypes.

Mutations in genes coding for ion channels have also provided evidence that are associated with syndromes implicated in human epilepsy. Two mutations that cause generalised epilepsy with febrile seizures, T875M and R1648H, have been identified in the SCN1A gene encoding the alpha subunit of the human voltage-gated sodium channel (Na(v)1.1). The T875M mutation led to enhanced slow inactivation of the channel, which decreased the ability of the neurone to fire action potentials at high frequency. Seizure activity may result from decreased firing of inhibitory neurones, which causes increased firing in excitatory postsynaptic neurones. The R1648H mutation accelerated recovery from channel inactivation, leading to neuronal hyperexcitability (Meisler et al., 2001). Point mutations in the human voltage-gated potassium channel (Kv1.1) gene have been shown to associate with episodic ataxia type 1 (EA1), which is a rare autosomal dominant disorder characterized by brief episodes of ataxia and partial epilepsy. Functional studies indicated mutant subunits in Kv1.1 exhibited a dominant negative effect on potassium channel function, possibly leading to impairment of neuronal repolarisation (Zuberi et al., 1999). Defects in ligand-gated neurotransmitter channels have also been implicated in human epilepsy. A mutation (R43Q) in the gene encoding for GABRG2, a GABA(A) receptor subunit, abolished *in vitro* sensitivity to diazepam, raising the

possibility that benzodiazepines may play an integral physiological role in preventing seizures (Wallace et al., 2001). GABA(A) receptors are ligand-gated chloride channels that mediate inhibitory synaptic transmission in the central nervous system. Reduced synaptic inhibition is a potential cause of epilepsy and many antiepileptic drugs, such as diazepam, are designed to target GABA. An association between a form of nocturnal epilepsy and a mutation (I279N) in CHRNA2, the gene encoding for the α2 subunit on nicotinic acetylcholine receptors (nAChR), was demonstrated and provided further support for the link between neuronal ion channel defects and epilepsy. The I279N mutation was shown to cause an increased sensitivity to acetylcholine, which leads to neuronal hyperexcitability (Aridon et al., 2006). The cause for epileptogenesis cannot be attributed to a specific defect in the neurotransmission pathway. Several lines of evidence (detailed in the following sub-chapter) have suggested that the defects in the SV recycling pathway at the presynapse might play an important role in the onset of certain types of epilepsy.

4.1.2 – Evidence of SV Recycling Defects in Epilepsy

In searching for persistent seizure-induced alterations in brain function that might be causally related to epilepsy, SV recycling and presynaptic neurotransmitter release has been relatively understudied. Several presynaptic proteins involved in the homeostatic regulation of neurotransmitter release have been linked to epilepsy, where excessive glutamate-induced synaptic activity results in neuronal toxicity. Ablation or alteration of these SV proteins in animal models leads to abnormal neurotransmission and behavioural phenotypes that are consistent with symptoms derived from epileptogenesis.

Synapsins I and II (SYN1 and SYN2) are neuronal phosphoproteins that can reversibly associate with SVs and tether them to the cytomatrix to maintain a reserve pool of vesicles (Shupliakov et al., 2011). SYN1 KO mice showed marked alteration in the way SVs are organised at the presynaptic terminal, leading to an increase in epileptic seizures invoked by electrical stimulation (Li et al., 1995). Genetic epidemiology studies have identified a nonsense mutation, W356x, in the human SYN1 gene that leads to mRNA decay and loss of protein function and underlies X-linked syndromic epilepsy (Giannandrea et al., 2013). Recent gene-gene interaction studies have also indicated that SYN2 A>G polymorphism is an important risk factor in the development of idiopathic generalised epilepsy in humans (Prasad et al., 2014). There have been several theories put forward to explain the connectivity between the molecular function of synapsins at the neuronal level and the onset of epilepsy. Synapsins are thought to play a role in the formation of synaptic connectivity during development, thus it is likely that mutations affecting their expression and function will result in significant imbalances in synaptic transmission, plasticity and development that could be potentially related to the epileptogenesis. In support of this, it has been shown that knockout of SYN1 in mice reduces the readily releasable pool at inhibitory synapses whilst increasing the pool at excitatory synapses (Baldelli et al., 2007).

Another SV protein that has been well documented to be involved in the onset of epilepsy is synaptosomal-associated protein 25 (SNAP-25). SNAP-25 is a member of the soluble NSF attachment protein receptor (SNARE) complex, along with syntaxin and synaptobrevin. SNARE complexes play a role in the docking, priming and fusion of SV vesicles at the synaptic terminal. This can occur through interactions with

other SV proteins such as synaptotagmin I (SYT1) and complexin, or through putative calcium-binding sites (see chapter 1). The first clues of SNAP-25's possible involvement in neuronal hyperexcitability was documented when Raber et.al showed that Coloboma (Cm/+) mice, a neurological mouse model of attention deficit hyperactivity disorder, has a 50% reduction in SNAP-25 mRNA and protein as well as impaired evoked neurotransmitter release (Raber et al., 1997). Studies in SNAP-25 heterozygous mice [SNAP-25(+/-)] mice showed that reduction of SNAP-25 protein levels associated with moderate hyperactivity. Electroencephalographic (EEG) recordings of the SNAP-25(+/-) mice revealed the occurrence of frequent spikes, suggesting a diffuse network hyperexcitability. The mice also displayed degeneration of the hilar neurones, which resulted in higher susceptibility to kainate-induced seizures. The EEG profile and defects in cognition could be improved with the use of anti-epileptic drugs such as carbamazepine and nimodipine (Corradini et al., 2014). Whole exome sequencing studies have also identified a novel SNAP-25 c.142G>T p.Phe48Val alteration which is implicated in generalised epilepsy and cognitive dysfunction (Rohena et al., 2013). The role of SNAP-25 in the pathology of epilepsy may involve alterations in synaptic formation and transmission, similar to that seen with synapsins. SNAP-25 is known to play a role in neurite extension (Osen-Sand et al., 1996), thus a reduction in SNAP-25 expression may consequently lead to a defect in overall brain connectivity and an epilepsy phenotype. SNAP-25 is expressed at much higher levels in excitatory synapses compared to inhibitory synapses (99:1 ratio) (Bragina et al., 2007), therefore neuronal hyperexcitability could also result from perturbations of the processes that govern the balance of excitatory and inhibitory synapses during developmental synaptic assembly. Other

studies have also indicated a role for SNAP-25 in the regulation of calcium at the neurone. It was shown that phosphorylated SNAP-25 inhibits voltage-gated calcium channels, therefore negatively modulating calcium dynamics and consequently leading to the onset of epileptic seizures (Condliffe et al., 2010). The presynaptic Ca^{2+} sensor SYT1 has also been implicated in epilepsy, as clinical studies have revealed an increased expression of SYT1 in temporal lobe tissue of patients with refractory epilepsy (Xiao et al., 2009).

Dynamin-associated mechanisms have been suggested as a possible target for novel antiepileptic drugs. Inhibition of dynamin I (DYN1) binding to syndapin with a peptide-based inhibitor produced an activity-dependent reduction in synaptic transmission. The peptide progressively inhibited synaptic transmission after a short delay, suggesting that this approach may lead to selective inhibition of sustained neuronal firing that occurs during a seizure, while allowing normal physiological neurotransmission (Anggono et al., 2006). Mice lacking in DYN1 displayed severe impairment of SV endocytosis during strong exogeneous stimulation but resumed efficiently when the stimulus was terminated, suggesting that DYN1 plays a key role in maintaining stable neurotransmission during high levels on neuronal activity (Ferguson et al., 2007). Synaptic dynamin-associated proteins (syndapin), which interact with dynamin and other SV proteins, may also participate in dynamin-associated mechanisms in epileptogenesis. Inhibition of syndapin I using syndapin antibodies resulted in strong impairment of inhibitory postsynaptic currents at high frequency stimulation (Andersson et al., 2008). Studies of protein expression in rat model of epilepsy as well as patients with temporal lobe epilepsy revealed an upregulation of DYN1. Inhibition of DYN1 using the DYN1 inhibitor, dynasore,

resulted in decreased frequency and severity of seizures (Li et al., 2015). Genetic studies have indicated that a missense *ftfl* (fitful) mutation in the DYN1a isoform results in recurrent seizures, severe ataxia and neurosensory deficits by altering developmental expression and self-assembly of DYN1 in mice (Boumil et al., 2010). There is also increasing evidence of epileptogenesis caused by DYN1 mutations in humans, as many clinical studies have now identified several *de novo* mutations in genes coding for DYN1 to be responsible for human epileptic encephalopathy (Consortium et al., 2014, Nakashima et al., 2016). These defects in dynamin I and syndapin I give evidence to severe impairment of neurotransmission during sustained high levels of neuronal activity, providing insight to a possible novel mechanism in the generation of seizures.

Genetic ablation of amphiphysin I led to severely reduced expression of amphiphysin II and defective assembly of endocytic protein complexes, resulting in a smaller functional SV recycling pool size, slower recycling kinetics or delayed vesicle priming. These cell biological defects potentially underlie the occurrence of rare spontaneous seizures observed in amphiphysin I knockout mice (Di Paolo et al., 2002). Synaptojanin I deficient mice progressively developed weakness, ataxia and displayed general convulsions until death within 2-3 weeks of birth. Reduced phosphoinositide activity led to a defect in vesicle uncoating and an accumulation of clathrin-coated SVs in the cytomatrix-rich area surrounding nerve terminals. Prolonged high frequency stimulation of hippocampal slices obtained from synaptojanin I deficient mice revealed enhanced synaptic depression followed by delayed recovery (Cremona et al., 1999). Studies on mice lacking the central region of the presynaptic active zone protein Bassoon demonstrated that the loss of Bassoon

led to inactivation of a significant fraction of glutamatergic synapses, resulting in reduction in normal synaptic transmission and spontaneous epileptic seizures (Altrock et al., 2003). Analysis of genome mutations in four unrelated individuals with early infantile epileptic encephalopathy revealed the existence of heterozygous missense mutations in the gene encoding for syntaxin binding protein 1 (STXBP1, also known as MUNC18-1). STXBP1 is an evolutionally conserved neuronal protein that is essential in SV fusion in several species, and functional studies indicated that the mutations in STXBP1 impaired binding to the SV protein syntaxin (Saitsu et al., 2008). Brain-derived neurotrophic factor (BDNF), a member of the neurotrophin family of growth factors that binds with high affinity to the receptor tyrosine protein kinase B (TrKB), may also be involved in epileptogenesis. In various animal seizure models, the seizures caused a prominent increase in the expression of BDNF in the brain, particularly in the hippocampus [see review: (Casillas-Espinosa et al., 2012)]. The acute administration of BDNF into the CA3 region of the hippocampus, the dentate gyrus and medial entorhinal cortex produces neuronal hyperexcitability (Messaoudi et al., 1998). BDNF has been suggested to regulate synaptic transmission by a variety of mechanisms including increasing excitatory NMDA currents (Xu et al., 2006) and attenuating inhibition on GABAergic postsynaptic cells by down-regulating chloride transport (Huang et al., 2012), thus possibly impacting on the very same mechanistic pathways implicated in the onset of epileptic seizures.

4.1.3 – SV2A and Epilepsy

Synaptic vesicle protein 2A (SV2A) is a SV glycoprotein which has been previously discussed to play a key role in SV trafficking and exocytosis. In 2004, SV2A was demonstrated to be the binding partner for the popular anti-epileptic drug levetiracetam (LEV) (Lynch et al., 2004). This discovery provided a platform for SV2A being a valid and novel target for further anti-epileptic drug discovery research and its role in epilepsy. In support of this, the correlation between LEV-SV2A binding affinity and anti-seizure potency was later confirmed in an audiogenic seizure model and extended to other models of epilepsy (Kaminski et al., 2008). Mice that harboured a 50 percent reduction in SV2A also displayed reduced anti-seizure activity when administered with LEV compared with wild-type animals (Kaminski et al., 2009).

Gorter et al. initially demonstrated that SV2A gene expression was downregulated in the endorhinal cortex of rats in which epilepsy was induced by sustained electrical stimulation (Gorter et al., 2006). Later studies showed that SV2A was also decreased in the hippocampus of chronic epileptic rats, resembling the decrease in SV2A that was observed in human patients with temporal lobe epilepsy (van Vliet et al., 2009). Hippocampal SV2A mRNA and protein expression were also found to be lower in phenytoin-resistant epileptic rats compared with normal anti-epileptic drug responding controls, suggesting a role for SV2A in the mechanism that underlies pharmacoresistant epilepsy (Wang et al., 2014). In support of this, previous findings have shown that SV2A expression was reduced by 30 to 50 percent in the anterior temporal neocortex of adult patients with temporal lobe epilepsy (Feng et al., 2009). Malformations that cause intractable epilepsy, such as focal cortical dysplasia and

tuberous sclerosis complex, also show significantly reduced SV2A expression in immunocytochemistry studies. Cortical tissue of patients with dysplasia displayed decreased SV2A immunoreactivity compared to tissue obtained from normal patients. This decrease was similarly observed in Western blot analyses of protein samples obtained from tissue from patients with both focal cortical dysplasia and tuberous sclerosis complex (Toering et al., 2009). These results suggest that decreased SV2A expression may contribute to the instability of neuronal networks and therefore to the progression of epilepsy. Recently, a homozygous mutation was discovered in the SV2A gene of a patient with intractable epilepsy, providing the first line of evidence that an SV2A mutation can cause epilepsy in humans. Exome sequencing identified a homozygous arginine to glutamine mutation in amino acid residue 383 (R383Q) in exon 5 of the SV2A gene. Both parents were carriers for the R383Q variant, suggesting that R383Q is a recessive mutation. No other candidate alterations in the exome were found that could otherwise explain the phenotype observed in the patient (Serajee and Huq, 2015). A missense leucine to glutamine mutation in amino acid residue 174 (L174Q) in rat models showed an increased susceptibility to induced seizures compared to control animals. Microdialysis studies also revealed that presence of the L174Q mutation preferentially reduced GABA release in the amygdala after depolarisation with elevated levels of K^+, indicating that dysfunction of SV2A leading to disruption of synaptic GABA release in the amygdala may play a crucial role in epileptogenesis (Tokudome et al., 2016).

It is tempting to speculate that epileptogenesis may be mediated by associated changes in the conformation and/or trafficking of SV2A that may occur after the first seizure episode. SV2A knockout mice via targeted gene disruption appear normal at

birth, but fail to grow normally and experience severe seizures before dying within three weeks of birth. Electrophysiological studies of hippocampal cells in the CA3 region revealed that loss of SV2A led to a reduction in action potential-dependent GABA-ergic neurotransmission, but action potential-independent neurotransmission was normal. Analysis of synapse structure suggested that the altered inhibitory neurotransmission was not caused by changes in synapse density or morphology(Crowder et al., 1999). Neurones lacking both SV2A and SV2B experienced sustained increases in Ca^{2+}-dependent synaptic transmission when two or more action potentials were triggered in succession. The increased synaptic transmission could be reversed by the calcium chelator ethylene glycol tetraacetic acetoxymethyl ester (EGTA-AM), which confirms the calcium dependence of the observed phenotype (Janz et al., 1999). This finding indicated that the absence of SV2 led to presynaptic Ca^{2+} accumulation during consecutive action potentials that led to abnormal increases in neurotransmitter release that may destabilise synaptic circuits and induce epilepsy.

4.1.4 – Aims and Objectives

SV2A is the binding site of the anti-epileptic drug, levetiracetam, and is currently the only known SV target for pharmacological treatment of epilepsy. There has been just a single identification of a pathogenic mutation in the gene coding for SV2A in humans to date. Exome sequencing has identified a homozygous arginine to glutamine mutation at residue 383 (R383Q) in the cytosolic loop of SV2A which leads to intractable epilepsy, involuntary movements, microcephaly, developmental and growth retardation in a five-year old female patient (Serajee and Huq, 2015). The R383Q change is not observed in known healthy cohorts, exome databases, or the Database of Single Nucleotide Polymorphisms, which supports the argument that there is a clear pathogenic role for the mutation. The mechanism by which the R383Q mutation affects SV2A normal function remains unclear. As it is currently known that SV2A and SYT1 are intrinsic trafficking partners, a random mutation in SV2A may lead to protein dysfunction and downstream effects of SYT1 recycling during compensatory endocytosis. I hypothesise that presence of the R383Q mutation disrupts the normal function of SV2A in neurones, eventually leading to a defect in SYT1 trafficking during SV recycling. This R383Q mutation may occur in a region that is critical to the maintenance of normal SV2A function, therefore resulting in a loss of protein-protein interactions with other known SV proteins. In this chapter, I aim to elucidate possible presynaptic mechanisms underlying the causes for the onset of epilepsy in patients carrying the R383Q SV2A mutation.

The primary objectives of the research in this chapter are:

1) To validate the knockdown of wild type SV2A by use of a small hairpin RNA (shRNA) sequence and subsequent rescue of SV2A expression with wild type (WT) or R383QA SV2A

2) To characterise the effect of R383Q SV2A on the surface expression of SYT1 at the plasma membrane and its localisation to presynaptic terminals

3) To characterise the effect of R383Q SV2A on the rate of SYT1 retrieval from the plasma membrane during compensatory endocytosis

4) To establish the SYT1 specificity of defects in SV recycling which are caused by R383Q SV2A

5) To compare and contrast between the mechanism of R383Q SV2A action of SYT1 trafficking at the presynapse and currently known mechanistic pathways which alter the SV2A-SYT1 interaction and result in defective SYT1 retrieval from the plasma membrane

6) To characterise the protein-protein interactions of R383Q SV2A in presence of mouse brain lysate and discriminate between any loss or gain of protein interaction which may lead to defective SYT1 recycling

4.2. – Results of Studies Using R383Q SV2A

Several lines of evidence implicate the SV2A gene in neuronal excitability and epilepsy. Homozygous SV2A mice appear normal at birth, but develop severe seizures and die within 3 weeks of birth (Crowder et al., 1999). The over-expression of SV2A in neurones was demonstrated to display a phenotype that was similar to that observed in neurones obtained from SV2A knockout mice (Nowack et al., 2011). Moreover, SV2A expression was significantly decreased in the hippocampus of patients diagnosed with temporal lobe epilepsy (van Vliet et al., 2009). The study conducted by Serajee et al. identified an arginine to glutamine mutation at residue 383 in SV2A (R383Q SV2A) in the cytosolic loop of the protein that led to the onset of intractable epilepsy, developmental and growth retardation. This was the first reported example of a pathogenic mutation in SV2A in humans that led to the onset of epilepsy. In this chapter, I aimed to characterise the effect of SV2A R383Q mutation on: 1) surface fraction and localisation of SYT1 and 2) rate of retrieval of SYT1 during SV endocytosis. I then proceeded to compare and evaluate the mechanism of R383Q SV2A action of SYT1 with other known mechanisms by which SYT1 trafficking dysfunction may be caused (e.g. mutation of the AP-2 binding motif, see chapter 3; mutation of the SV2A/SYT1 binding motif, see Zhang 2015). Finally, I characterised the protein-protein interactions of the SV2A cytosolic loop, which contained the R383Q SV2A mutation in an effort to discriminate between any loss (or gain) of protein interaction which may lead to defective SYT1 recycling.

Key research findings of this chapter:

- R383Q SV2A leads to the acceleration of SYT1 retrieval kinetics, increased surface expression and mislocalisation of SYT1 on the plasma membrane.
- The Y46A, R383Q and T84A SV2A mutations all perturb the same mechanistic pathway at the presynapse, suggesting a function for the R383Q SV2A mutation to affect SV2A-dependent retrieval of SYT1 by AP-2.
- Residue charge mutation at R383 affects SV2A interactions with actin, tubulin and V-ATPase, suggesting roles for these proteins in modulating SV2A/SYT1 retrieval.

4.2.1 – Expression of R383Q SV2A-mCer Successfully Rescues Defects in SV2A Expression Levels Caused By shRNA-mediated Knockdown

Initial experiments aimed to validate and quantify the effectiveness of the efficiency of exogeneously expressed R383Q SV2A-mCer vector in rescuing SV2A depletion in neurones caused by short hairpin RNA (shRNA)-mediated knockdown. Primary cultures of mice hippocampal cells were co-transfected with: 1) a SYT1-pHluorin plasmid also containing a shRNA sequence for SV2A (SV2A shRNA/SYT1-pHluorin) to simultaneously deplete SV2A levels and express SYT1-pHluorin in neurones; 2) plasmids containing either wild-type SV2A-mCer (WT SV2A) or R383Q SV2A-mCer (R383Q SV2A) to rescue SV2A expression after shRNA-mediated knockdown. Final SV2A expression levels in the cultures after transfection were detected by immunofluorescence (Figure 4.1 **A**).

The co-transfection of the SV2A shRNA plasmid with either wild-type (WT) or R383 SV2A plasmids resulted in a complete rescue of SV2A expression when compared to SV2A expression levels of non-transfected neurones in the same field of view [Ratio of SV2A expression in transfected neurones/untransfected neurones = 0.521 ± 0.039 (mCer), 1.062 ± 0.077 (WT SV2A), 1.028 ± 0.044 (R383Q SV2A); $p < 0.0001$ (WT vs mCer, R383Q vs mCer), one-way ANOVA, Bonferroni's post-hoc, $P < 0.0001$, $F = 29.1$] (Figure 4.1 **B**).

In agreement with previous results, these experiments show that depletion of SV2A expression in neurones was achieved by transfection with a previously described combined SV2A shRNA/SYT1-pHluorin plasmid and normal SV2A expression was subsequently rescued by co-transfection of the neurones with a plasmid that expressed either exogeneous WT SV2A or R383Q SV2A.

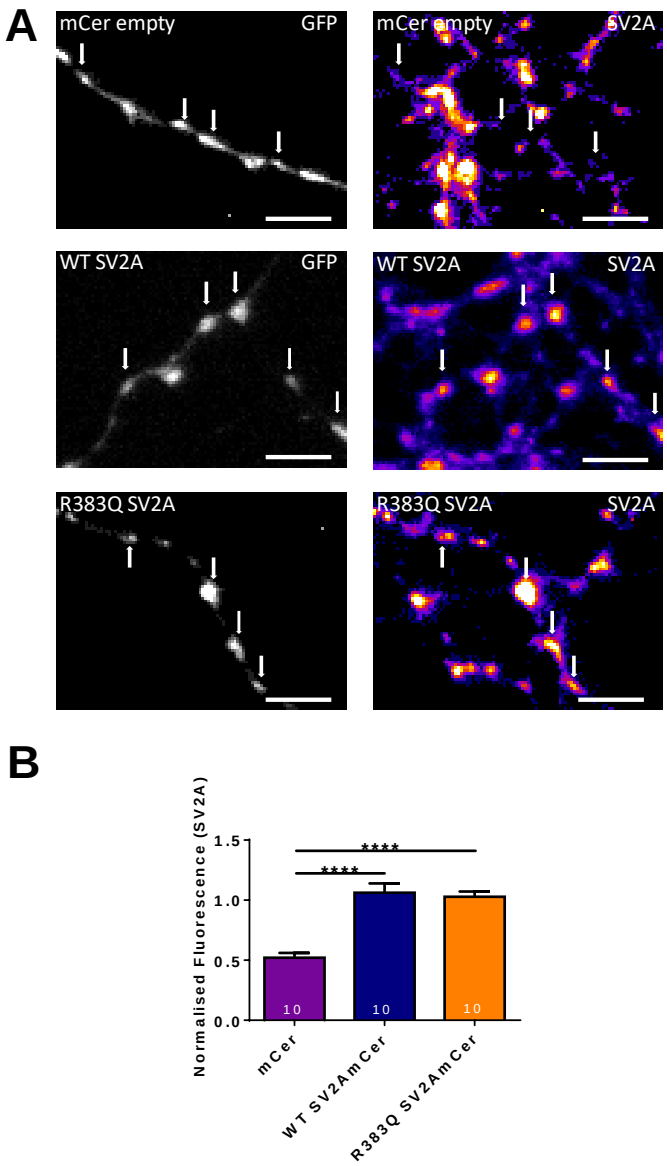

Figure 4.1: Expression of R383Q SV2A-mCer rescues deficits in SV2A Expression caused by shRNA-mediated knockdown: A) Images of cultures co-transfected with SV2A shRNA–Syt1–pHluorin vector and either empty rescue (mCer), wild-type (WT) SV2A or R383Q SV2A-mCer. Grayscale panels highlight transfected neurones (GFP), whereas false colour panels display exogeneous SV2A revealed by immunofluorescence staining. Arrows highlight nerve terminals. Scale bar = 10 µM. **B)** Bar graph shows levels of rescue of SV2A expression. The background-corrected SV2A immunofluorescence obtained from transfected neurones was normalised to the SV2A immunofluorescence obtained from non-transfected neurones within the same field of view [n=10 mCer empty, purple; n=10 WT SV2A-mCer, blue; n=10 R383Q SV2A-mCer, red; ****p<0.0001 (mCer vs WT, mCer vs R383Q); one-way ANOVA, Bonferroni's post-hoc, P<0.0001, F=29.1].

4.2.2 – R383Q SV2A Results in Increased but Delocalised Surface Expression of SYT1

The R383Q mutation in SV2A has only recently been documented to play a role in the onset of intractable epilepsy and developmental growth in humans (Serajee and Huq, 2015). As such, there has been no published literature of on the characterisation of the effects of this particular mutation on presynaptic activity and SV recycling. As previously described, SV2A is known to be the intrinsic trafficking partner for SYT1 at the presynapse. Therefore, any defect in SV2A function caused by a mutation may lead to downstream abnormalities in presynaptic activity because of defects in SYT1 trafficking. These specific defects in SV2A/SYT1 trafficking at the presynapse may provide unexplored insight into the mechanisms of certain forms of epileptogenesis.

In order to characterise a potential effect of the R383Q mutation in SV2A on presynaptic activity, I first proceeded to investigate the effect of the R383Q SV2A mutation on the surface expression and localisation of SYT1 to synaptic terminals. As in the above experiments, SV2A shRNA/SYT1-pHluorin was transfected into primary cultures to knockdown SV2A expression and co-express the SYT1-pHluorin reporter. Neuronal SV2A expression was rescued by co-transfection of either WT or R383Q SV2A-mCer plasmid (Figure 4.2 **A**).

In order to investigate surface expression of SYT1 after perturbation of SV2A levels, the fraction of surface-expressed SYT1-pHluorin in transfected neurones was compared to the total SYT1-pHluorin pool in the neurone. Surface fraction experiments revealed that knockdown of SV2A in neurones and rescue using an empty plasmid resulted in a significant increase of surface-expressed SYT1-pHluorin compared to control rescue experiments using WT SV2A, in consistency with

previously reported results. The knockdown of SV2A in neurones and rescue with R383Q SV2A plasmid also resulted in a significant increase in the percentage of surface-expressed SYT1-pHluorin when compared to control rescue experiments using WT SV2A [Surface expression of SYT1-pHluorin (% of total SYT1 pool) = 16.2 ± 4.8 (WT SV2A), 38.1 ± 4.5 (mCer), 50.8 ± 5.2 (R383Q SV2A); $p < 0.0001$ (R383Q vs WT), $p < 0.05$ (mCer vs WT), one-way ANOVA, Bonferroni's post-hoc, $P = 0.0006$, $F = 14.6$] (Figure 4.2 **B**). These results demonstrate that depletion of SV2A in neurones leads to increased expression of SYT1 at the plasma membrane surface. Rescue with R383Q SV2A fails to rescue the abnormality in SYT1 surface expression despite successful rescue of SV2A expression in the neurones. These observations suggest that like the Y46A mutation, the R383Q mutation also plays a crucial role in the internalisation of SYT1 from the plasma membrane.

In order to investigate the effect of R383Q SV2A on the localisation of SYT1 to synaptic terminals, an analysis of the coefficient of variation (CV) for SYT1-pHluorin fluorescence was performed. CV analysis of the expression of the total SYT1-pHluorin pool in a 50-µm length of neurite in SV2A knockdown cultures co-expressing a mCer empty plasmid revealed a significantly decreased coefficient of variation compared to control rescue experiments using WT SV2A. In SV2A knockdown cultures co-expressing the R383Q SV2A plasmid, CV analysis of SYT1-expression in a 50-µm length of neurite revealed similarly decreased CVs compared to control rescue experiments using WT SV2A [Mean CV = 42.1 ± 8.0 (WT SV2A), 22.0 ± 1.7 (mCer), 19.8 ± 2.3 (R383Q SV2A); $p < 0.05$ (mCer vs WT, R383Q vs WT), one-way ANOVA, Bonferroni's post-hoc, $P = 0.0136$, $F = 6.29$] (Figure 4.2 **C**).

These experiments demonstrate that R383Q mutation in SV2A leads to increased diffuseness of SYT1 expression across the neurite, suggesting a role for the R383 residue in the targeting SYT1 to presynaptic terminals during SV recycling. A similar phenotype is observed when the AP-2 binding motif in SV2A is mutated (Y46A), suggesting that the R383 residue in the cytosolic loop of SV2A may play a role in regulating the ability of SV2A to target SYT1 efficiently to synaptic terminals.

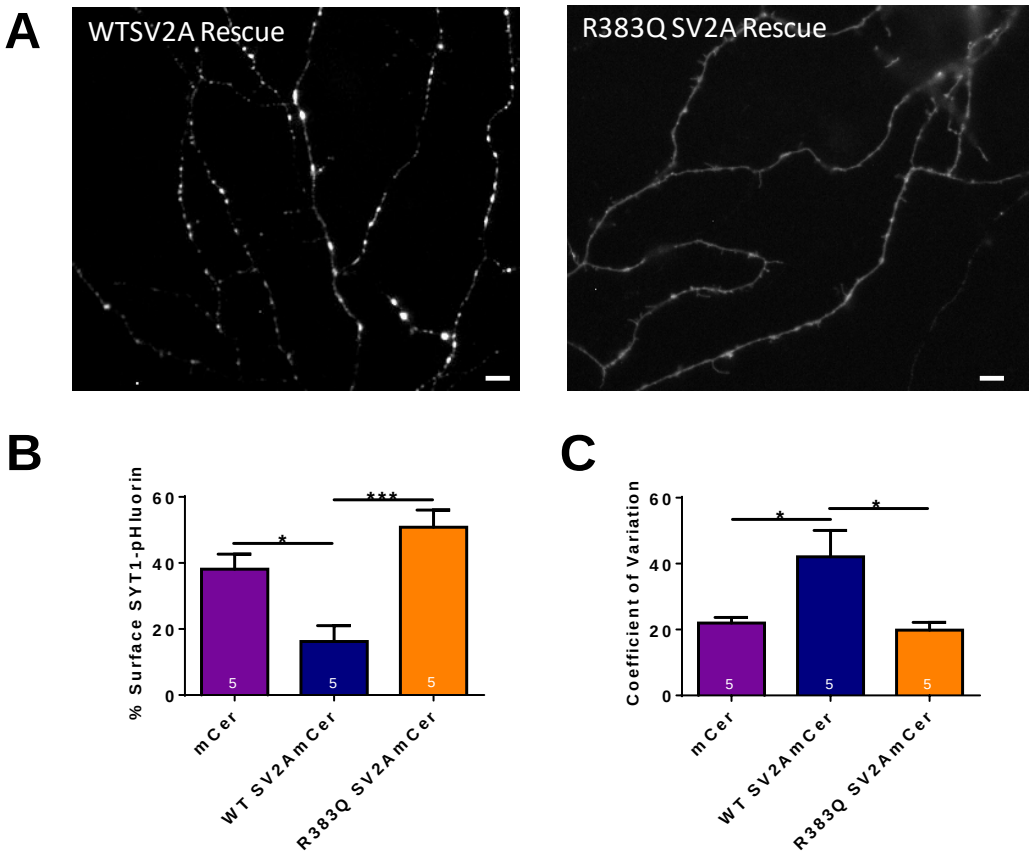

Figure 4.2: R383Q SV2A results in increased but delocalised surface expression of SYT1. A) Hippocampal neurones were co-transfected with an SV2A shRNA-SYT1-pHluorin plasmid and either wild-type (WT) or R383Q SV2A-mCer. Representative greyscale images show that rescue with R383Q SV2A-mCer resulted in less localisation to nerve terminals compared to WT SV2A-mCer rescue. Scale bar = 10 µM. **B)** Surface expression of SYT1–pHluorin after rescue with SV2A-mCer variants displayed as a percentage of total SYT1-pHluorin pool ± SEM [n=5 mCerN1 empty, purple; n=5 WT SV2A-mCer, blue; n=5 R383Q SV2A-mCer, orange; ***p<0.001 (R383Q vs WT); *p<0.05 (mCer vs WT); one-way ANOVA, Bonferroni's post-hoc, P=0.0006, F=14.6]. **C)** Bar graph displays the mean coefficient of variation of SYT1-pHluorin fluorescence along axons of neurones in alkaline buffer. Data are presented as ± SEM [n=5 mCerN1 empty, purple; n=5 WT SV2A-mCer, blue; n=5 R383Q SV2A-mCer, orange; *p<0.05 (R383Q vs WT, mCer vs WT); one-way ANOVA, Bonferroni's post-hoc, P=0.0136, F=6.29].

4.2.3 – R383Q SV2A Fails to Rescue the Acceleration of SYT1 Retrieval Caused by Knockdown of SV2A

The discovery that the R383Q mutation in SV2A led to increased diffuseness of SYT1 expression at the plasma membrane in neurones has presented novel insight into how the cytosolic loop of SV2A may play a key role in the regulation of normal SV2A function. In order to characterise further the role of SV2A R383 in regulating normal SYT1 trafficking, I proceeded to investigate the effect of the SV2A R383Q mutation on the rate of SYT1 retrieval and the proportion of externalised SYT1 (compared to the total available SYT1 pool) during compensatory SV endocytosis.

The shRNA-mediated knockdown of SV2A in neurones and rescue with an empty plasmid resulted in an acceleration of SYT1 retrieval compared with control rescue experiments using WT SV2A, consistent with previous results [$p < 0.05$ (mCer vs WT), two-way ANOVA of traces normalised to peak at stimulation]. Knockdown of SV2A and rescue with R383Q SV2A in neurones resulted in a failure to rescue SYT1 retrieval kinetics to WT levels, mimicking the SYT1 pHluorin recycling phenotype seen in SV2A-deficient neurones and in neurones where the AP-2 binding site was mutated [$p < 0.05$ (R383Q vs WT), two-way ANOVA of traces normalised to the peak at stimulation] (Figure 4.3 **A**). Knockdown of SV2A and rescue with the R383Q mutant resulted in a significantly increased proportion of SYT1 externalisation during stimulation [Max $\Delta F/F_0$ (as a fraction of the total pHluorin pool) = 0.347 ± 0.023 (WT SV2A), 0.395 ± 0.040 (mCer), 0.510 ± 0.061 (R383Q SV2A); $p < 0.05$ (R383Q vs WT), one-way ANOVA, Bonferroni's post-hoc, $P = 0.0316$, $F = 4.12$] (Figure 4.3 **B**). Quantification of the average time constant for retrieval (tau) of the evoked SYT1-pHluorin response previously revealed that the

rate of SYT1 retrieval during compensatory endocytosis is accelerated when SV2A levels are depleted in neurones. In agreement with the analysis of the average time traces in part A, the knockdown of SV2A in neurones and rescue using either empty vector or R383Q SV2A resulted in significantly decreased taus of SYT1-pHluorin retrieval compared to control rescue experiments using WT SV2A. [Tau (s) = 60.8 ± 4.4 (WT SV2A), 43.4 ± 3.1 (mCer), 43.4 ± 2.6 (R383Q SV2A); $p < 0.01$ (R383Q vs WT), $p < 0.05$ (mCer vs WT), one-way ANOVA, Bonferroni's post-hoc, $P = 0.0038$, $F = 7.45$] (Figure 4.3 **C**). The phenotype observed with the R383Q SV2A rescue experiments was similar to that observed when SV2A was depleted.

These experiments indicate that the R383Q mutation in SV2A results in the faster retrieval of SYT1 during endocytosis compared to WT SV2A. Interestingly, this dysfunction of SV2A is highly similar to previous observations when SV2A is depleted in neurones or when the AP-2 binding site in SV2A is mutated (Y46A) and will be discussed later. Unlike the Y46A SV2A mutation, the R383Q SV2A mutation significantly increased SYT1 trafficking to the membrane during exocytosis.

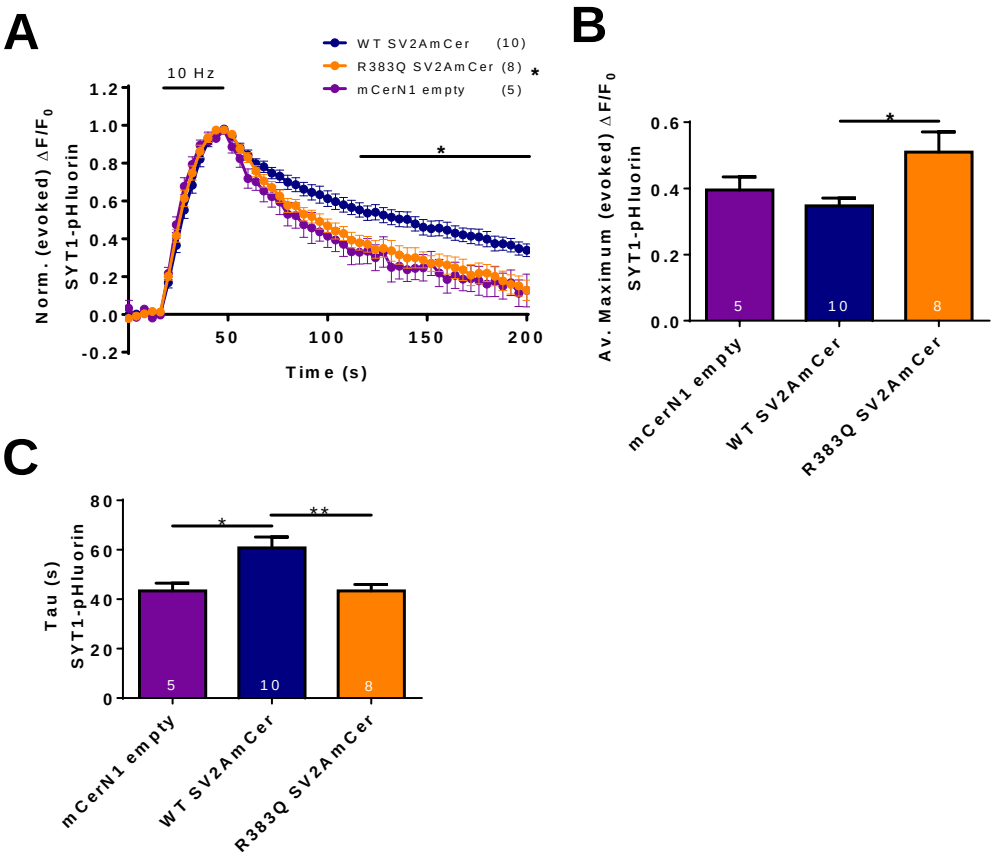

Figure 4.3: R383Q SV2A fails to rescue the acceleration of SYT1 retrieval caused by knockdown of SV2A. A) Hippocampal neurones were co-transfected with an SV2A shRNA-SYT1-pHluorin vector and either mCerulean (mCer) empty vector or SV2A-mCer variants. Cultures were stimulated using a train of 300 action potentials (Aps, 10 Hz, indicated by bar). After 200 seconds of recovery, the total recycling synaptic vesicle (SV) pool was revealed with a NH_4Cl pulse. Graph displays the mean $\Delta F/F_0$ time course for SYT1–pHluorin ± SEM normalized to the peak of stimulation [n=5 mCer empty, purple; n=10 wild-type (WT) SV2AmCer, blue; n=8 R383Q SV2AmCer, orange; *p<0.05 (Y46A vs WT), two-way ANOVA, Bonferroni's post-hoc (over times indicated by solid lines)]. **B)** Mean maximum evoked SYT1-pHluorin response ($\Delta F/F_0$) expressed as a fraction of the total SV pool [*p<0.05 (R383Q vs WT); one-way ANOVA, Bonferroni's posthoc, P=0.0316, F=4.12]. **C)** Graph shows quantification of the average time constant (Tau) ± SEM of the evoked SYT1-pH response [**p<0.01 (R383Q vs WT); *p<0.05 (mCer vs WT); one-way ANOVA, Bonferroni's post-hoc, P=0.0038, F=7.45].

4.2.4 – R383Q SV2A Does Not Affect SYP Retrieval or Surface Expression

Previous experiments have revealed that residue 383 in SV2A plays a role in regulating normal SV2A function. When residue 383 is mutated from arginine to glutamine, it results in defects in the localisation and trafficking of SYT1 at the synaptic terminal in a similar manner to that observed when SV2A is depleted in the neurone or when its own trafficking is disrupted (Y46A SV2A). However, this observed phenomenon could be a result of a general defect in global SV recycling caused by SV2A dysfunction rather than a specific effect on SYT1 trafficking. In order to discount the possibility of R383Q SV2A having a global effect on SV recycling, I investigated the effect of R383Q SV2A on the localisation of synaptophysin (SYP) and the rate of SYP retrieval from the plasma membrane. In these experiments, neuronal cultures were transfected with three constructs: 1) SV2A shRNA to knockdown SV2A expression in neurones; 2) synaptophysin-pHluorin (SYP-pHluorin) as a reporter for SYP expression and retrieval in neurones during compensatory endocytosis; 3) either WT or R383Q SV2A-mCer for the purposes of rescuing SV2A expression after knockdown.

The shRNA-mediated knockdown of SV2A in neurones and rescue using R383Q SV2A did not affect the rate of SYP-pHluorin retrieval compared to control rescue experiments using WT SV2A (ns, two-way ANOVA of traces normalised to peak at stimulation) (Figure 4.4 **A**). Knockdown of SV2A and rescue using either an empty vector or R383Q SV2A also did not have an effect on the amount of SYP-pHluorin externalisation during stimulation when compared to control rescue experiments with WT SV2A [Max $\Delta F/F_0$ (as a fraction of the total pHluorin pool) = 0.277 ± 0.024 (WT SV2A), 0.285 ± 0.028 (mCer), 0.320 ± 0.023 (R383Q SV2A); ns, one-way

ANOVA, P = 0.452, F = 0.841] (Figure 4.4 **B**). In agreement with the analysis of the average time traces, the quantification of the retrieval time constants for SYP-pHluorin in SV2A knockdown neurones rescued with R383Q SV2A revealed no significant effect compared to control rescue experiments using WT SV2A [Tau (s) = 43.0 ± 5.8 (WT SV2A), 41.7 ± 4.0 (mCer), 40.2 ± 3.2 (R383Q SV2A); ns, one-way ANOVA, P = 0.905, F = 0.101] (Figure 4.4 **C**). Surface fraction experiments revealed that knockdown of SV2A in neurones and rescue using an empty plasmid did not affect the expression of SYP-pHluorin compared to control rescue experiments using WT SV2A. Likewise, the rescue of SV2A expression using R383Q SV2A did not affect the surface expression of SYP-pHluorin [Surface expression of SYP-pHluorin (% of total SYP-pHluorin pool) = 22.7 ± 3.0 (WT SV2A), 23.9 ± 2.6 (mCer), 20.8 ± 0.9 (R383Q SV2A); ns, one-way ANOVA, P = 0.665, F = 0.422] (Figure 4.4 **D**).

This set of results provides evidence to support the hypothesis suggesting that the R383Q mutation in SV2A does not have an effect on the rate of SYP trafficking during endocytosis and exocytosis as well as the surface expression of SYP. Therefore, the findings from previous observations made using SYT1-pHluorin as a reporter can be attributed to a specific effect on the trafficking of SYT at the synaptic terminal and not a global effect on SV recycling.

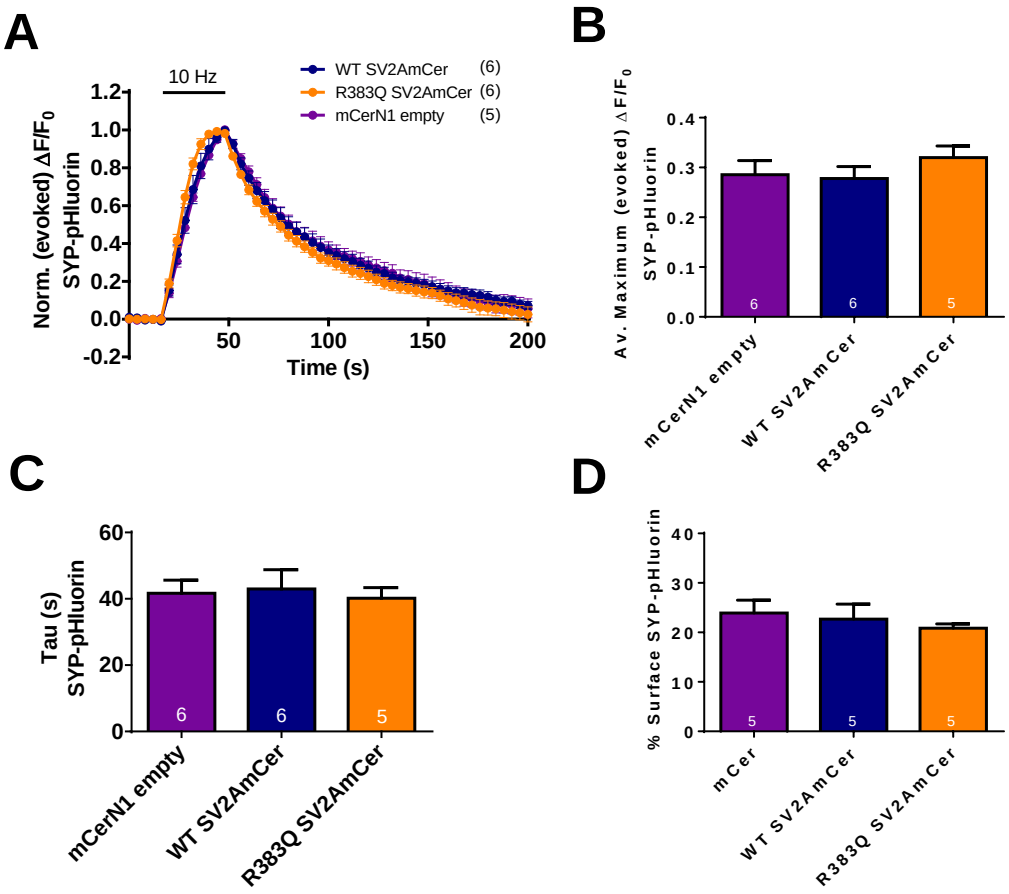

Figure 4.4: R383Q SV2A does not affect SYP retrieval or surface expression. A) Hippocampal neurones were co-transfected with SV2AshRNA, SYP-pHluorin and mCer or SV2AmCer variants. Cultures were stimulated using a train of 300 APs (10 Hz, indicated by bar) and the total recycling synaptic vesicle (SV) pool was revealed with a NH_4Cl pulse at the end of the experiment. Graph displays the mean $\Delta F/F_0$ time course for SYP–pHluorin ± SEM normalized to the peak of stimulation (n=6 mCerN1 empty, purple; n=6 wild type (WT) SV2A-mCer, blue; n=5 R383Q SV2A-mCer, orange; ns, two-way ANOVA). **B)** Mean maximum evoked response ($\Delta F/F_0$) of SYP-pHluorin during stimulation expressed as a fraction of the total SV pool (ns, one-way ANOVA, P=0.452, F=0.841). **C)** Graph shows quantification of the average time constant (Tau) ± SEM of the evoked SYP-pH response (ns, one-way ANOVA, P=0.905, F=0.101). **D)** Surface expression of SYP–pHluorin after rescue with SV2AmCer variants displayed as a percentage of total releasable pHluorin pool ± SEM (n=5 mCerN1 empty, purple; n=5 WT SV2A-mCer, blue; n=5 R383Q SV2A-mCer, orange; ns, one-way ANOVA, P=0.665, F=0.422).

4.2.5 – T84A/R383Q SV2A Does Not Exacerbate Defects in SYT1 Recycling

Mutation of the R383 residue in the cytosolic loop of SV2A has so far been shown to render SV2A incapable of localising SYT1 to synaptic terminals as well as incapable of retrieving SYT1 efficiently as its intrinsic trafficking partner during compensatory endocytosis. Similar loss-of function phenotypes were previously observed in similar experiments where the SV2A AP-2 binding motif was mutated (Y46A) and when the SV2A-SYT1 phosphorylation-dependent binding motif (T84A) was mutated (see chapter 3). These phenotypic defects are also believed to be dependent on the phosphorylation-mediated binding of SV2A to SYT1 at T84A as previously hypothesised, and therefore the combination of both T84A and R383Q SV2A mutations should not exacerbate the observed defects to SYT1 trafficking. Any exacerbation observed may be a direct indication of a separate SYT1 retrieval mechanism in action during endocytosis.

In order to shed further light on the SYT1-binding dependency of R383Q SV2A-induced defects in SYT1 trafficking, the T84A/R383Q SV2A double mutant was genetically engineered and used to rescue SV2A expression in SV2A knockdown neurones and the rate of SYT1 retrieval during endocytosis in these experiments was compared to results obtained from experiments using the individual single mutants to reveal any additive defects in SYT1 trafficking that may be present. The shRNA-mediated knockdown of SV2A and rescue using the T84A/R383Q SV2A double mutant resulted in a failure to rescue normal SYT1 recycling behaviour compared to control rescue experiments using WT SV2A. The observed phenotype was consistent with the findings obtained from rescue experiments using the single mutants only. Comparison of the average SYT1-pHluorin traces obtained from experiments using

T84A/R383Q SV2A double mutant to experiments using the corresponding single mutants did not reveal any additive defects in SYT1 recycling ($p < 0.05$ (T84A/R383Q vs WT), ns (T84/R383Q vs T84A or R383Q), two-way ANOVA of traces normalised to the peak at stimulation) (Figure 4.5 **A**). The proportion of SYT1 externalisation in rescue experiments using the T84A/R383Q SV2A double mutant was increased when compared to rescue experiments using either WT or T84A SV2A single mutant, but not to the extent of increase seen with the R383Q SV2A single mutant rescue experiments. [Max $\Delta F/F_0$ (as a fraction of the total pHluorin pool) = 0.270 ± 0.040 (WT SV2A), 0.292 ± 0.066 (T84 SV2A), 0.511 ± 0.056 (R383Q SV2A), 0.468 ± 0.060 (T84A/R383Q SV2A); $p < 0.05$ (R383Q vs WT), one-way ANOVA, Bonferroni's post-hoc, $P = 0.0126$, $F = 4.55$] (Figure 4.5 **B**). The quantification of retrieval time constants for SYT1-pHluorin in SV2A knockdown neurones rescued with T84A/R383Q SV2A revealed a significant decrease in retrieval time compared to control rescue experiments using WT SV2A. No added disruption to retrieval was observed when analysis of the T84A/R383Q double mutant time constants was compared to T84A and R383Q SV2A single mutants [Tau (s) = 59.3 ± 3.2 (WT SV2A), 39.2 ± 2.3 (T84A SV2A), 38.7 ± 3.3 (R383Q SV2A), 41.2 ± 2.1 (T84A/R383Q SV2A); $p < 0.05$ (T84A/R383Q vs WT), ns (T84A/R383Q vs T84A or R383Q), one-way ANOVA, Bonferroni's post-hoc, $P < 0.0001$, $F = 12.1$] (Figure 4.5 **C**).

These experiments indicate that mutation of both the R383 residue in SV2A and the SV2A/SYT1 binding motif results in faster retrieval of SYT1 during compensatory endocytosis. The presence of both mutations together in SV2A did not exacerbate the acceleration to SYT1 recycling and retrieval time constants compared to experiments

where only one mutation was present, suggesting that R383Q SV2A-induced defects were dependent on the SV2A-SYT1 interaction and that both mutations in SV2A are likely to disrupt targeting of SYT1 to presynaptic terminals via a similar mechanistic pathway. The proportion of SYT1 externalisation during exocytosis was slightly increased (but non-significant) when both the T84A and R383Q mutations are present in SV2A when compared to control rescue experiments using WT SV2A. These results indicate that ablation of SV2A binding to SYT1 disrupts normal SYT1 retrieval in a highly similar manner to that observed when binding to AP-2 is ablated, even though the binding motifs are located in different domains of the protein. This suggests an unknown interaction between the SV2A N-terminus domain and its cytosolic loop which has an overall effect on regulating SYT1 trafficking at the presynapse, which will be discussed further in later chapters.

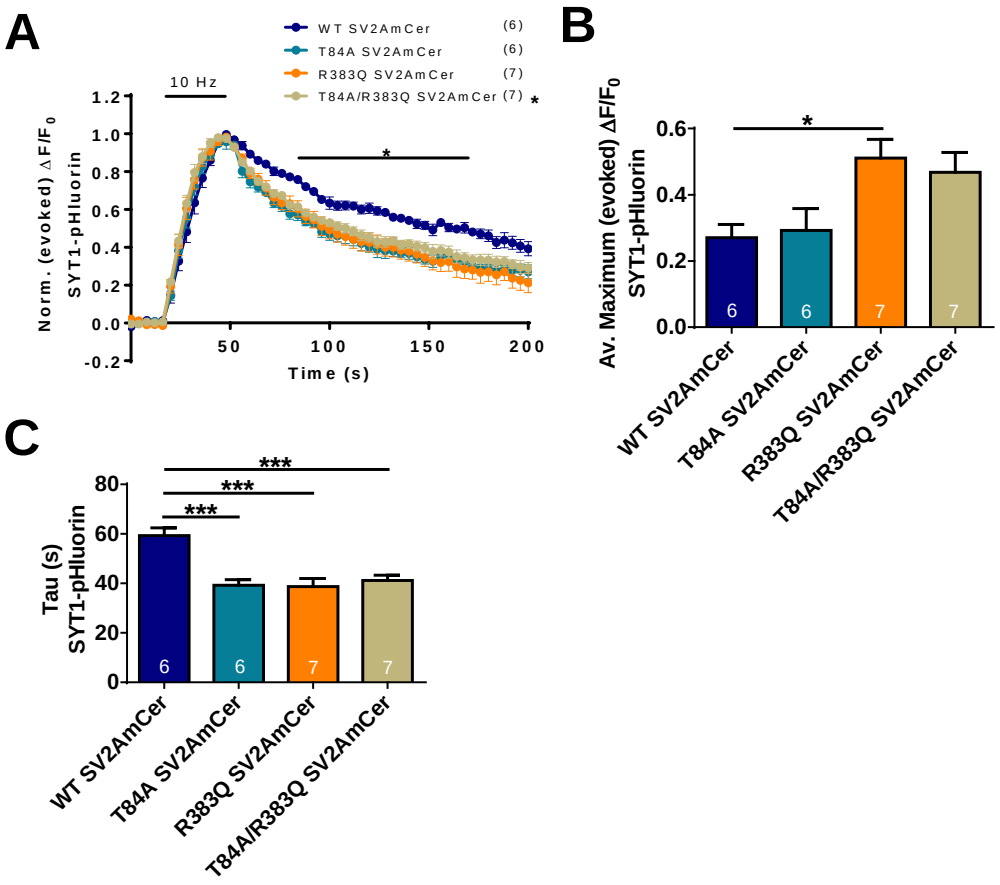

Figure 4.5: T84A/R383Q SV2A does not exacerbate defects in SYT1 recycling. A) Hippocampal neurones were co-transfected with SV2AshRNA-SYT1-pHluorin and mCer or SV2A-mCer variants. Cultures were stimulated using a train of 300 APs (10 Hz, indicated by bar) and the total releasable vesicle pool was revealed with a NH_4Cl pulse at the end of the experiment. Graph displays the mean $\Delta F/F_0$ time course for SYT1–pHluorin ± SEM normalized to the peak of stimulation [n=6 wild type (WT) SV2A-mCer, blue; n=6 T84A SV2A-mCer, cyan; n=7 R383Q SV2A-mCer, orange; n=7 T84A/R383Q SV2A-mCer, light brown]; *p<0.05 (T84A/R383Q vs WT), two-way ANOVA, Bonferroni's post-hoc (over times indicated by solid lines)]. **B)** Mean maximum evoked response ($\Delta F/F_0$) of SYT1-pHluorin during stimulation expressed as a fraction of the total releasable vesicle pool [*p<0.05 (R383Q vs WT); one-way ANOVA, Bonferroni's post-hoc, P=0.0126, F=4.55]. **C)** Graph shows quantification of the average time constant (Tau) ± SEM of the evoked SYT1-pH response [***p<0.001 (T84A/R383Q vs WT, T84A vs WT, R383Q vs WT); one-way ANOVA, Bonferroni's post-hoc, P<0.0001, F=12.1].

4.2.6 – T84A/R383Q SV2A Does Not Exacerbate Defects in SYT1 Surface Expression and Localisation

The presence of the T84A and R383Q double mutation in SV2A presented no significant additive effects on the time constant of SYT1 retrieval and its externalised proportion during evoked transmission. In order to ensure that this finding was not isolated to mechanisms specific to the retrieval of SYT1, I proceeded to investigate the effect of the T84A/R383Q SV2A double mutation on the fraction of surface-expressed SYT1 and its localisation to presynaptic terminals in neurones. As in previous experiments, SV2A shRNA/SYT1-pHluorin was transfected into primary cultures to knockdown SV2A expression and co-express the SYT1-pHluorin reporter. Neuronal SV2A expression was rescued by co-transfection of WT, T84A, R383Q and T84A/R383Q SV2A-mCer plasmids (Figure 4.6 **A**).

An investigation of the fraction of surface-expressed SYT1-pHluorin in SV2A knockdown neurones rescued with T84A/R383Q SV2A double mutant revealed a significant increase of surface fraction when compared to control rescue experiments using WT SV2A, consistent with previous results obtained from the single SV2A mutants. Comparison of results obtained from experiments using the T84A/R383Q double mutant to experiments using the corresponding single mutants revealed no additive defects in the fraction of SYT1 surface expression [Surface expression of SYT1-pHluorin (% of total SYT1-pHluorin pool) = 16.0 ± 0.9 (WT SV2A), 36.0 ± 3.5 (mCer), 32.1 ± 3.0 (T84A SV2A), 45.9 ± 2.2 (R383Q SV2A), 40.0 ± 5.2 (T84A/R383Q SV2A); $p < 0.01$ (T84A/R383Q SV2A vs WT), ns (T84A/R383Q SV2A vs T84A or R383Q SV2A), one-way ANOVA, Bonferroni's post-hoc, $P < 0.0001$, $F = 11.6$] (Figure 4.6 **B**). CV analysis of the expression of the total SYT1-

pHluorin pool in a 50-µm length of neurite in SV2A knockdown cultures co-expressing the T84A/R383Q SV2A double mutant revealed a significantly decreased coefficient compared to control rescue experiments using WT SV2A. Comparison of results obtained from experiments using the T84A/R383Q double mutant to experiments using the corresponding single mutants revealed no additive effects to the CV [Mean CV = 29.3 ± 3.0 (WT SV2A), 11.7 ± 0.9 (mCer), 16.2 ± 1.9 (T84A SV2A), 19.8 ± 2.3 (R383Q SV2A), 14.9 ± 0.5 (T84A/R383Q SV2A); $p < 0.001$ (T84A/R383Q SV2A vs WT), ns (T84A/R383Q SV2A vs T84A or R383Q SV2A), one-way ANOVA, Bonferroni's post-hoc, $P < 0.0001$, $F = 12.0$] (Figure 4.6 **C**).

These experiments demonstrate that the presence of both the T84A and R383Q mutations in SV2A lead to increased surfaced expression and increased diffuseness of SYT1 expression across the neurite, but these effects were not exacerbated compared to those observed in experiments with just a single SV2A mutation. These results are in agreement with the previous experiments demonstrating the lack of an exacerbated effect on the retrieval kinetics of SYT1 in the presence of the T84A/R383Q SV2A double mutant.

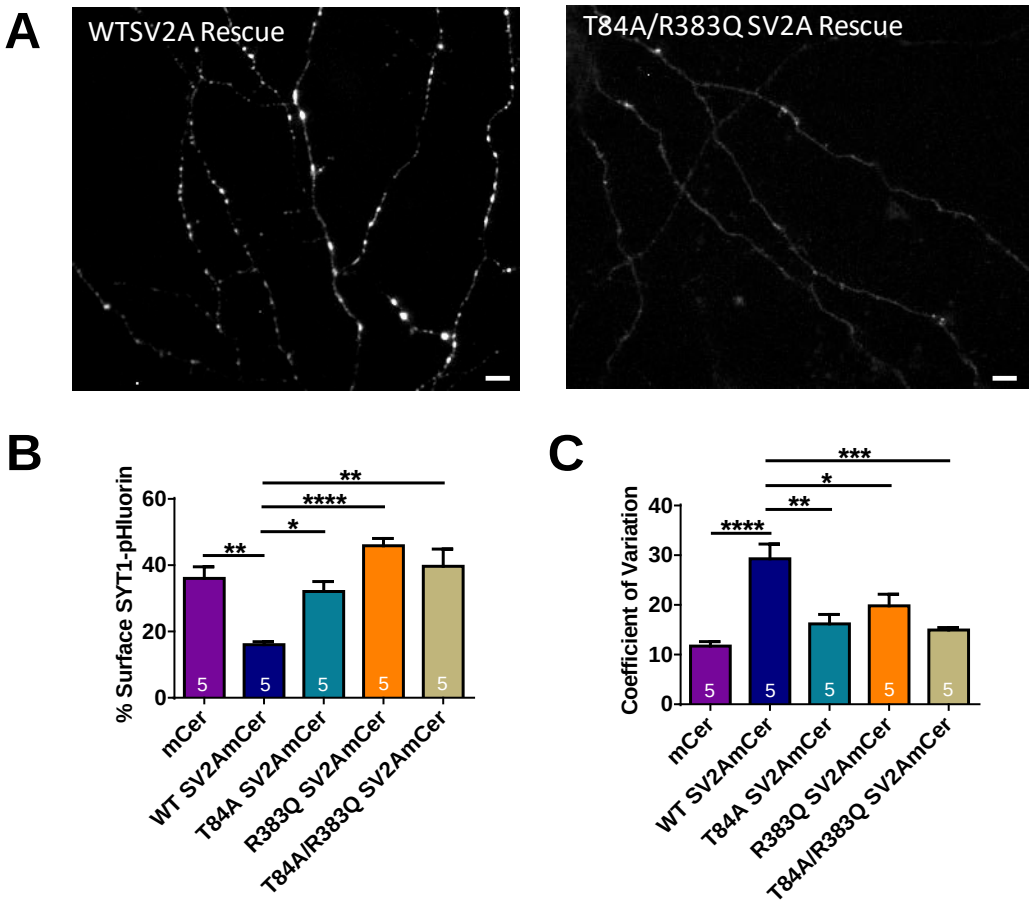

Figure 4.6: T84A/R383Q SV2A does not exacerbate defects to SYT1 surface expression and localisation. A) Hippocampal neurones were co-transfected with an SV2A shRNA-SYT1-pHluorin plasmid and either wild-type (WT) or SV2A-mCer variants. Representative greyscale images show that rescue with T84A/R383Q SV2A-mCer resulted in less localisation to nerve terminals compared to WT SV2A-mCer rescue. Scale bar = 10 µM. **B)** Surface expression of SYT1–pHluorin after rescue with SV2A-mCer variants displayed as a percentage of total SYT1-pHluorin pool ± SEM [n=5 mCerN1 empty, purple; n=5 WT SV2A-mCer, blue; n=5 T84A SV2A-mCer, cyan; n=5 R383Q SV2A-mCer, orange; n=5 T84A/R383Q SV2A-mCer, gold; ****p<0.0001 (R383Q vs WT); **p<0.01 (mCer vs WT, T84A/R383Q vs WT); *p<0.05 (T84A vs WT); one-way ANOVA, Bonferroni's post-hoc, P<0.0001, F=11.6]. **C)** Bar graph displays the mean coefficient of variation of SYT1-pHluorin fluorescence along axons of neurones in alkaline buffer. Data are presented as ± SEM (n=5 mCerN1 empty, purple; n=5 WT SV2A-mCer, blue; n=5 T84A SV2A-mCer, cyan; n=5 R383Q SV2A-mCer, orange; n=5 T84A/R383Q SV2A-mCer, gold; ****p<0.05 (mCer vs WT); ***p<0.001 (T84A/R383Q vs WT); **p<0.01 (T84A vs WT); *p<0.05 (mCer vs WT); one-way ANOVA, Bonferroni's post-hoc, P<0.0001, F=12.0).

4.2.7 – Y46A/R383Q SV2A Does Not Exacerbate Defects in SYT1 Recycling

Previous experiments have ascertained that the T84A/R383Q double mutation in SV2A resulted in no exacerbation of defects to the localisation of SYT1 to synaptic terminals as well as the rate of SYT1 retrieval from the plasma membrane during compensatory endocytosis. The next step was to probe the AP-2 binding dependency of the observed SYT1 trafficking defects due to R383Q SV2A. If this phenotype was dependent on AP-2 binding, then the presence of the Y46A mutation together with the R383Q mutation should not exacerbate any defects already observed in the experiments with only the single mutant.

In order to shed further light on the AP-2 binding dependency of R383Q SV2A-induced defects in SYT1 trafficking, the Y46A/R383Q SV2A double mutant was genetically engineered and used to rescue SV2A expression in SV2A knockdown neurones. The rate of SYT1 retrieval during endocytosis in these neurones was compared to the rates obtained from rescue using the individual single mutants to reveal any additive defects in SYT1 trafficking which may have been present due to the double mutation. The shRNA-mediated knockdown of SV2A and rescue using the Y46A/R383Q SV2A double mutant resulted in a failure to rescue normal SYT1 recycling behaviour compared to control rescue experiments using WT SV2A. The observed phenotype was consistent with the findings obtained from rescue experiments using the single mutants only. Comparison of the average SYT1-pHluorin traces obtained from experiments using the Y46A/R383Q SV2A double mutant to experiments using the corresponding single mutants did not reveal any additive defects in SYT1 recycling ($p < 0.05$ (Y46A/R383Q vs WT), ns (Y46A/R383Q vs Y46A or R383Q), two-way ANOVA of traces normalised to the

peak at stimulation) (Figure 4.7 **A**). The proportion of SYT1 externalisation in rescue experiments using the Y46A/R383Q SV2A double mutant was increased when compared to rescue experiments using the WT SV2A single mutant, but not to the extent of increase seen with the Y46A and R383Q SV2A single mutant rescue experiments. [Max $\Delta F/F_0$ (as a fraction of the total pHluorin pool) = 0.352 ± 0.028 (WT SV2A), 0.472 ± 0.041 (Y46A SV2A), 0.521 ± 0.036 (R383Q SV2A), 0.421 ± 0.038 (Y46A/R383Q SV2A); $p < 0.05$ (R383Q vs WT), one-way ANOVA, Bonferroni's post-hoc, P = 0.0207, F = 3.87] (Figure 4.7 **B**). The quantification of retrieval time constants for SYT1-pHluorin in SV2A knockdown neurones rescued with Y46A/R383Q SV2A revealed a significant decrease in retrieval time compared to control rescue experiments using WT SV2A. No additive disruption to SYT1 retrieval was observed when analysis of the Y46A/R383Q double mutant time constants was compared to Y46A and R383Q SV2A single mutants [Tau (s) = 70.6 ± 9.3 (WT SV2A), 47.7 ± 4.3 (Y46A SV2A), 45.4 ± 3.1 (R383Q SV2A), 45.1 ± 3.8 (Y46A/R383Q SV2A); $p < 0.05$ (Y46A/R383Q vs WT), ns (Y46A/R383Q vs Y46A or R383Q), one-way ANOVA, Bonferroni's post-hoc, P = 0.0075, F = 4.96] (Figure 4.7 **C**).

These experiments indicate that the presence of both Y46A and R383Q mutations in SV2A did not exacerbate the acceleration of SYT1 recycling and retrieval time constants compared to experiments where only a single mutation was present, suggesting that R383Q-induced defects in SYT1 trafficking are dependent on the AP-2-SV2A interaction. The proportion of SYT1 externalisation during exocytosis was increased (but non-significant) when both the Y46A and R383Q mutations are present in SV2A when compared to control rescue experiments using WT SV2A.

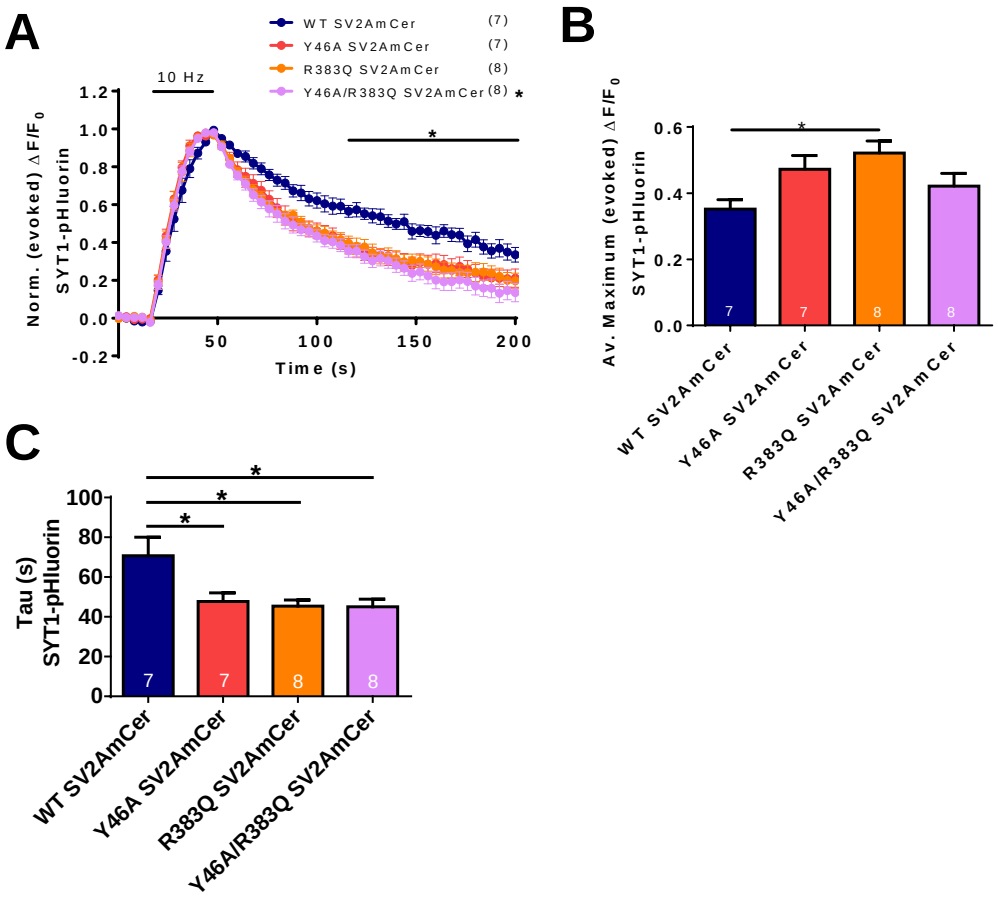

Figure 4.7: Y46A/R383Q SV2A does not exacerbate defects in SYT1 recycling. A) Hippocampal neurones were co-transfected with SV2AshRNA-SYT1-pHluorin and mCer or SV2A-mCer variants. Cultures were stimulated using a train of 300 APs (10 Hz, indicated by bar) and the total releasable vesicle pool was revealed with a NH_4Cl pulse at the end of the experiment. Graph displays the mean $\Delta F/F_0$ time course for SYT1–pHluorin ± SEM normalized to the peak of stimulation [n=7 wild type (WT) SV2A-mCer, blue; n=7 Y46A SV2A-mCer, red; n=8 R383Q SV2A-mCer, orange; n=8 Y46A/R383Q SV2A-mCer, pink; *p<0.05 (Y46A/R383Q vs WT), two-way ANOVA, Bonferroni's post-hoc (over times indicated by solid lines)]. **B)** Mean maximum evoked response ($\Delta F/F_0$) of SYT1-pHluorin during stimulation expressed as a fraction of the total releasable vesicle pool [*p<0.05 (R383Q vs WT); one-way ANOVA, Bonferroni's post-hoc, P=0.0207, F=3.87]. **C)** Graph shows quantification of the average time constant (Tau) ± SEM of the evoked SYT1-pH response [*p<0.05 (Y46A/R383Q vs WT, Y46A vs WT, R383Q vs WT); one-way ANOVA, Bonferroni's post-hoc, P=0.0075, F=4.96].

4.2.8 – Y46A/R383Q SV2A Does Not Exacerbate Defects to SYT1 Surface Expression and Localisation

The Y46A/R383Q double mutation in SV2A presented no significant additive defects on the time constant of SYT1 retrieval and its externalised proportion during evoked transmission compared with the respective SV2A single mutations. In order to ensure that this finding was not isolated to mechanisms specific to the retrieval of SYT1, I proceeded to investigate the effect of the Y46A/R383Q SV2A double mutation on the fraction of surface-expressed SYT1 and its localisation to presynaptic terminals in neurones. As in previous experiments, SV2A shRNA/SYT1-pHluorin was transfected into primary cultures to knockdown SV2A expression and co-express the SYT1-pHluorin reporter. Neuronal SV2A expression was rescued by co-transfection of WT, Y46A, R383Q and Y46A/R383Q SV2A-mCer plasmids (Figure 4.8 **A**).

An investigation of the fraction of surface-expressed SYT1-pHluorin in SV2A knockdown neurones rescued with Y46A/R383Q SV2A double mutant revealed a significant increase of surface fraction when compared to control rescue experiments using WT SV2A, consistent with previous results obtained from the single SV2A mutants. Comparison of results obtained from experiments rescued with the Y46A/R383Q double mutant to experiments rescued with the corresponding single mutants revealed no additive defects in the fraction of SYT1 surface expression [Surface expression of SYT1-pHluorin (% of total SYT1-pHluorin pool) = 16.0 ± 0.9 (WT SV2A), 36.0 ± 3.5 (mCer), 44.5 ± 3.3 (Y46A SV2A), 45.9 ± 2.2 (R383Q SV2A), 48.5 ± 3.6 (Y46A/R383Q SV2A); $p < 0.0001$ (Y46A/R383Q SV2A vs WT), ns (Y46A/R383Q SV2A vs Y46A or R383Q SV2A), one-way ANOVA,

Bonferroni's post-hoc, P < 0.0001, F = 20.1] (Figure 4.8 **B**). CV analysis of the expression of the total SYT1-pHluorin pool in a 50-µm length of neurite in SV2A knockdown cultures co-expressing the Y46A/R383Q SV2A double mutant revealed a significantly decreased coefficient compared to control rescue experiments using WT SV2A. Comparison of results from rescue experiments with the Y46A/R383Q double mutant to rescue experiments with the corresponding single mutants revealed no additive effects to the CV [Mean CV = 29.3 ± 3.0 (WT SV2A), 11.7 ± 0.9 (mCer), 14.8 ± 0.9 (Y46A SV2A), 19.8 ± 2.3 (R383Q SV2A), 14.6 ± 1.4 (Y46A/R383Q SV2A); p < 0.001 (Y46A/R383Q SV2A vs WT), ns (Y46A/R383Q SV2A vs Y46A or R383Q SV2A), one-way ANOVA, Bonferroni's post-hoc, P < 0.0001, F = 13.5] (Figure 4.8 **C**).

These experiments demonstrate that the presence of both the Y46A and R383Q mutations in SV2A lead to increased surfaced expression and increased diffuseness of SYT1 expression across the neurite, but with no additive effects compared to those observed in experiments with just a single SV2A mutation. These results are in agreement with the previous experiments demonstrating the lack of an exacerbated effect on the retrieval kinetics of SYT1 in the presence of the Y46A/R383Q SV2A double mutant.

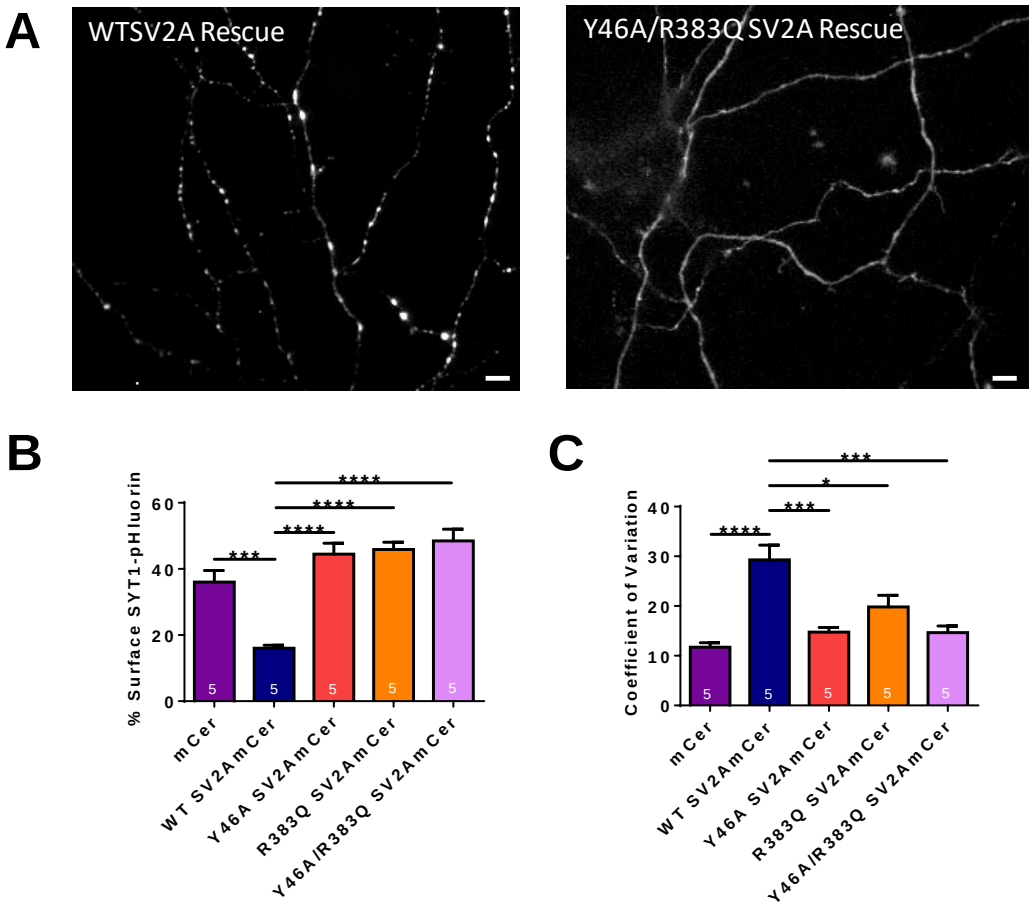

Figure 4.8: Y46A/R383Q SV2A does not result in additive defects to SYT1 surface expression and localisation. A) Hippocampal neurones were co-transfected with an SV2A shRNA-SYT1-pHluorin plasmid and either wild-type (WT) or SV2A-mCer variants. Representative greyscale images show that rescue with Y46A/R383Q SV2A-mCer resulted in less localisation to nerve terminals compared to WT SV2A-mCer rescue. Scale bar = 10 µM. **B)** Surface expression of SYT1–pHluorin after rescue with SV2A-mCer variants displayed as a percentage of total SYT1-pHluorin pool ± SEM [n=5 mCerN1 empty, purple; n=5 WT SV2A-mCer, blue; n=5 Y46A SV2A-mCer, red; n=5 R383Q SV2A-mCer, orange; n=5 Y46A/R383Q SV2A-mCer, light purple; ****p<0.0001 (Y46A vs WT, R383Q vs WT, Y46A/R383Q vs WT); ***p<0.001 (mCer vs WT); one-way ANOVA, Bonferroni's post-hoc, P<0.0001, F=20.1]. **C)** Bar graph displays the mean coefficient of variation of SYT1-pHluorin fluorescence along axons of neurones in alkaline buffer. Data are presented as ± SEM (n=5 mCerN1 empty, purple; n=5 WT SV2AmCer, blue; n=5 Y46A SV2A-mCer, red; n=5 R383Q SV2A-mCer, orange; n=5 Y46A/R383Q SV2A-mCer, light purple; ****p<0.05 (mCer vs WT); ***p<0.001 (Y46A vs WT, Y46A/R383Q vs WT); *p<0.05 (R383Q vs WT); one-way ANOVA, Bonferroni's post-hoc, P<0.0001, F=13.5).

4.2.9 – R383 Mutations in the SV2A Cytosolic Loop Results in Altered Interactions with Actin and V-ATPase V1B1. The SV2A Cytosolic Loop Does Not Interact with SYP, SYT1 or SV2A

Previous experiments investigating the effects on a point mutation in the cytosolic loop of SV2A (R383Q) have indicated that this mutation altered the normal SYT1 recycling phenotype. The R383Q mutation in SV2A resulted in defects in SYT1 expression and localisation to synaptic terminals, as well as an accelerated retrieval of SYT1 during compensatory endocytosis compared to normal WT SV2A controls. Although strong evidence was provided for this phenotypic result, the driving mechanism responsible for this change in phenotype remained unclear from prior results. It was predicted that the amino acid charges may have played a significant role in changing SV2A protein interactions, since the R383Q mutation results in a change from arginine (a polar positively charged amino acid residue) to glutamine (a polar neutral amino acid residue).

In order to investigate the effect of changing the amino acid charge at residue 383 on selective binding partners for the SV2A cytosolic loop (residues 356-447) in brain lysate, pull-down experiments were performed using recombinant GST fusion proteins containing the WT SV2A cytosolic loop (positively charged at residue 383), the R383Q SV2A cytosolic loop (neutral at residue 383) and the R383E (negatively charged at residue 383). GST bound binding partners were extracted from synaptosomes and separated using gel electrophoresis. The R383Q SV2A cytosolic loop displayed a highly similar protein interaction profile to WT SV2A, but with a few discernible differences. The associations of three proteins, with molecular masses of 53, 45 and 41 kilodaltons (kDa), were altered when the R383Q mutation

was introduced into the GST-fusion protein (Figure 4.9). Gel electrophoresis bands corresponding to these proteins were excised from the gel and sent for identification using ESI-QUAD-TOF mass spectrometry (data not shown). Mass spectrometry results identified the proteins as vesicular ATP-ase subunit V1B1 (V-ATPase V1B1, 53 kDa), β-III tubulin (45 kDa) and β-actin (41 kDa) and confirmed by western blotting (Figure 4.10 **A**). Further western blotting experiments provided no evidence of any interaction between the SV2A cytosolic loop and full-length SV2A, SYT1 or SYP (Figure 4.10 **B**). Quantification of protein association with various GST-SV2A fusion proteins show that the interaction with β-actin was increased ~3-5 fold when the R383Q mutation was present ($p < 0.001$, two-way ANOVA, Bonferroni's post-hoc), and reduced to ~ 0.4-0.5 fold when the R383E mutation was present ($p < 0.01$, two-way ANOVA, Bonferroni's post-hoc). Associations between β-III tubulin, V-ATPase V1B1 and V-ATPase V1E1 and the SV2A cytosolic loop were decreased, though not significantly, when the R383Q mutation was present. When the R383E SV2A mutation was present, a significant increase was observed in the binding of the SV2A loop to V-ATPase V1B1 ($p < 0.01$, two-way ANOVA, Bonferroni's post-hoc) (Figure 4.10 **C**).

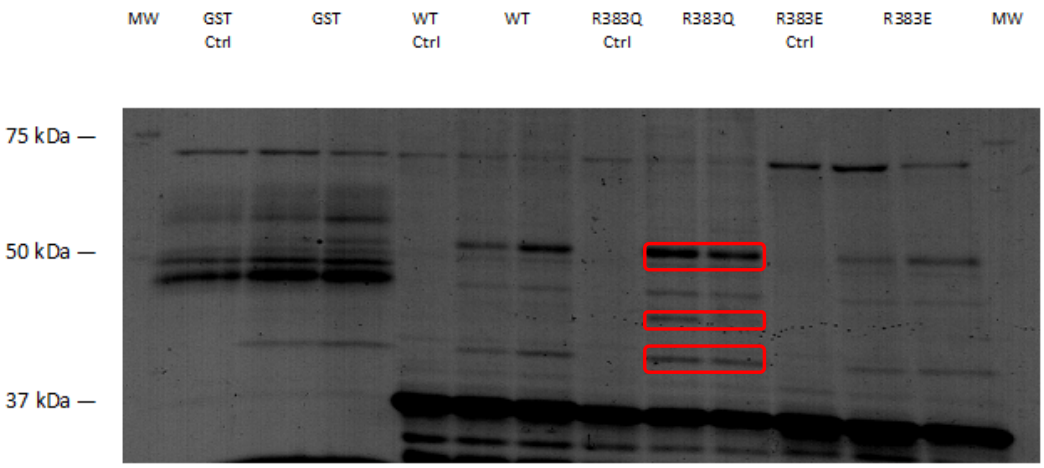

Figure 4.9: Mutation of R383 in the SV2A cytosolic loop results in altered interactions with SV proteins. Pulldown experiments using GST-SV2A cytosolic loop domains containing WT, R383Q and R383E SV2A from whole rat brain lysate. A synaptosome extract was used to isolate binding proteins for each GST-SV2A cytosolic loop domain in the order indicated. Results are shown in duplicate. Control pull-down experiments were performed with media in the absence of brain lysate. Bands at 53, 45 and 41 kDa (marked by red rectangles) were excised from the gel and identified by ESI-QUAD-TOF mass spectrometry. Results from mass spectrometry identified the bands as vesicular ATP-ase subunit V1B1, βIII-tubulin and β-actin respectively and band identities were confirmed by western blotting (Figure 4.10 A).

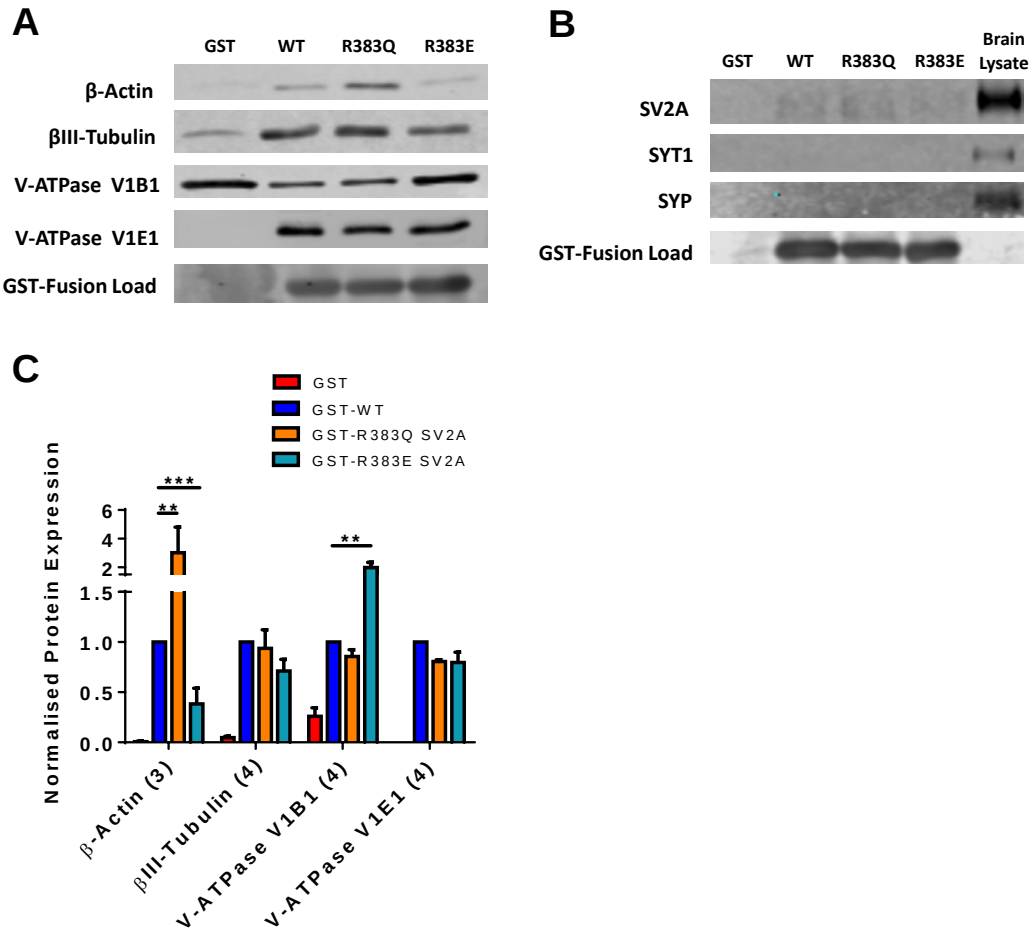

Figure 4.10: Mutation of R383 in the SV2A cytosolic loop results in altered interactions with actin and V-ATPase V1B1. The SV2A cytosolic loop does not interact with SYP, SYT1 or SV2A. A) Associated proteins from GST-SV2A pull-down experiments were extracted, separated using SDS gel electrophoresis and transferred to nitrocellulose membranes. Representative western blots for β-actin, βIII-tubulin, v-ATPase V1B1 and v-ATPase V1E1 are shown. **B)** Associated proteins from GST-SV2A pull-down experiments were extracted, separated using SDS gel electrophoresis and transferred to nitrocellulose membranes. Representative western blots for full-length SV2A, synaptotagmin I and synaptophysin are shown. **C)** Graph shows quantification of protein association with various GST-SV2A cytosolic loop fusion proteins, normalised to WT SV2A association. Interactions with β-actin were increased ~3-5 fold when the R383Q mutation was present, and reduced to ~ 0.4-0.5 fold when the R383E mutation was present. Association of β-III tubulin, V-ATPase V1B1 and V-ATPase V1E1 with the SV2A cytosolic loop was decreased, though not significantly, when the R383Q mutation was present. Data are presented as ± SEM [GST only, red; WT SV2A loop, blue; R383Q SV2A loop, orange; R383E SV2A loop, cyan; ***$p < 0.001$ (Actin – R383Q vs WT), **$p < 0.01$ (Actin – R383E vs WT, v-ATPase V1B1 – R383E vs WT); two-way ANOVA, Bonferroni's post-hoc].

4.3. – Discussion on the Presynaptic Effects of R383Q SV2A

Recent studies have shown that a homozygous arginine to glutamine mutation at residue 383 (R383Q) in the cytosolic loop of SV2A which leads to intractable epilepsy, involuntary movements, microcephaly, developmental and growth retardation in a five-year old female patient (Serajee and Huq, 2015). The molecular mechanism by which the R383Q mutation affects SV2A normal function remains unclear. SV2 is a key SV protein that has a role in the maintenance of both excitatory and inhibitory neurotransmission (Crowder et al., 1999) and plays a role in the trafficking of SYT1 as its intrinsic trafficking partner (see chapter 3). Therefore, the R383Q mutation in SV2A may represent an underlying factor in the onset of epilepsy symptoms through impairment of presynaptic function. This work aimed to characterise the effect of the R383Q SV2A mutation on SV and SYT1 recycling at the presynapse, as well as to determine the molecular mechanisms underlying any observations of synaptic malfunction.

4.3.1 – ShRNA-mediated Knockdown of SV2A Expression in Neurones Can Be Successfully Rescued by Use of Exogeneously Transfected R383Q SV2A DNA

Knockdown of endogeneous SV2A was achieved using a short hairpin DNA sequence and successfully reduced expression of SV2A to about 50% of its original level, consistent with the previous experimental results observed with the Y46A SV2A rescue. As previously discussed, this observation is slightly lower than in previously reported data (>75%) (Zhang et al., 2015) and discrepancies may have arisen from the selection of nerve terminals for analysis, which is a highly subjective

process and may inevitably lead to differences when reporting data. In comparison with internal controls, there was still significant reduction in average SV2A levels. As previously discussed, SV2A is known to have a relatively low copy number on SVs at the nerve terminal (around 2-12 per SV) compared to other intergral SV proteins, therefore it is also expected that a 50% reduction in expression levels in these experiments would exhibit a large effect on the sorting of SV2A and its related cargo. SV2A expression in these knockdown cells was then rescued by the transfection of exogenous DNA that codes for either full length WT SV2A or full length R383Q SV2A. The R383Q SV2A mutant was shown to rescue SV2A expression to similar levels to that seen when WT SV2A is used. Expression levels were similar to those observed in rescue experiments using Y46A SV2A. Therefore, any observable phenotype due to the use of these constructs is attributed to an effect resulting from the presence of the R383Q mutation and not due to an experimental failure to rescue SV2A expression in the cell.

4.3.2 – R383Q SV2A Leads to Acceleration of SYT1 Retrieval Kinetics and Increased Surface Expression and Mislocalisation of SYT1

The presence of R383Q SV2A in hippocampal neurones resulted in an acceleration of SYT1 retrieval during compensatory endocytosis, mimicking the phenotype observed when there is a deficiency of SV2A, or the presence of the Y46A mutation, at the synaptic terminal. This was not a general acceleration of endocytosis, as other SV cargos such as synaptophysin were not affected in a similar manner by the presence of the R383Q mutation. The presence of the R383Q SV2A mutation led to an increased fraction of SYT1 expression on the membrane surface as well as

defective localisation of SYT1 to synaptic terminals. This phenotype is highly similar to that previously observed with the Y46A mutation. Presence of the R383Q mutation also resulted in a significant increase of externalised SYT1 during SV exocytosis, suggesting that SV2A may have a role in the regulation of SV release through modulation of the Ca^{2+}-sensing function of SYT1. There are several pieces of evidence in support of this hypothesis: 1) SV2 has previously been shown to have an effect downstream of SV priming but upstream of the Ca^{2+} triggering of release (Chang and Südhof, 2009), possibly through enhancement of the responsiveness of SYT1 to Ca^{2+} influx; 2) SV2 plays a role in regulating the concentration of resting and evoked presynaptic Ca^{2+} levels, indicating a role in the regulation of exocytosis (Wan et al., 2010).

The acceleration of SYT1 retrieval caused by R383Q SV2A is an interesting phenomenon, since the R383Q mutation lies in the cytosolic loop region far away from the known SV2A-SYT1 binding region. Recent knockdown and rescue experiments within SV2A-depleted neurones have revealed rescue of SV2A expression with R383Q SV2A did not result in defects in SV2A retrieval during compensatory endocytosis compared to rescue with WT SV2A, suggesting that the R383 residue does not play a key role in the retrieval of SV2A during compensatory endocytosis. The presence of the R383Q mutation however did result in an increased fraction of SV2A expression on the membrane surface similar to the phenotype seen with SYT1, indicating that R383Q is involved in the correct localisation of SV2A to synaptic terminals (Dr. Callista Harper, personal communication, data not shown). These results suggest that the R383 residue in SV2A plays a key role in the localisation of both SV2A and SYT1 at the synaptic terminal as well as the retrieval

of SYT1 from the plasma membrane, but does not affect the trafficking of SV2A itself.

4.3.2.1 – How Might R383Q SV2A Mutation Affect SYT1 Retrieval?

The SV2A-SYT1 interaction is regulated by the phosphorylation of the T84 residue in SV2A by tau–tubulin protein kinases 1 and 2 (TTBK 1 and 2) (Zhang et al., 2015). The SYT1-binding pocket is located on residues 81-90 of SV2A in the N-terminus region, fairly close to the tyrosine-based AP-2 binding YSRF motif located on residues 46-49. The R383 residue lies in the cytosolic loop of SV2A, located between the sixth and seventh transmembrane region of the protein. This residue is distally located from the SV2A-SYT1 binding region and therefore the manner in which it may affect SYT1 trafficking is more complex. There are however, two possible explanations for the SYT1 trafficking phenotype observed in the presence of R383Q SV2A.

Firstly, SV2A is known to contain signature motifs that are linked to the major facilitator superfamily (MFS) of transporters. The MFS family of transporters contain nucleotide-binding sites and their transporter activity is regulated by ATP-binding in some cases e.g. ATP inhibition of glucose transport (Levine et al., 2002). Biochemical binding affinity studies have confirmed that SV2A does indeed have has a particular high binding affinity to adenine nucleotides, and further gene mapping studies have indicated that SV2A contains two nucleotide-binding sites in the cytoplasmic regions of the protein. The first site is located between residues 59-162 preceding the first transmembrane domain, while the second site is located at residues 382-439 preceding the seventh transmembrane domain (Yao and Bajjalieh,

2008). Interestingly, the R383 residue resides exactly in the adenine nucleotide-binding region preceding the seventh transmembrane domain. This suggests that adenine nucleotide binding to SV2A at the cytosolic loop region may play a crucial role in regulating the influence of SV2A on SYT1 trafficking during SV recycling, leading to the observed impairments in SYT1 surface expression, localisation and retrieval kinetics during compensatory endocytosis. In support of this, previous immunodetection studies have demonstrated that SV2 forms the core of the intra-vesicular matrix and is responsible for immobilisation and release of ATP (Reigada et al., 2003). It has been previously reported that maintenance of the SV cycle is the primary source of activity-driven metabolic demand at the presynapse, and that interruptions in presynaptic ATP synthesis and hydrolysis resulted in severe impairments in presynaptic function (Rangaraju et al., 2014). Interestingly, preliminary GST pulldown studies to probe the mechanism of R383Q SV2A action have indicated that presence of the R383Q mutation reduces the interaction of SV2A with the V1B1 sub-unit of the SV proton pump V-ATPase (Figure 4.10). It is noted however, that this study identified only severe impairments to SYT1 trafficking without affecting general SV function. Future protein-crosslinking experiments using photo-reactive ATP to probe the ATP-binding affinity of R383Q SV2A compared to WT SV2A may provide further insight into the degree modulation of ATP-SV2A binding afforded by the R383Q mutation.

Another possible reason which may explain how the R383Q mutation may regulate SYT1 trafficking is through altered protein interactions caused by a change in the amino acid charge. Arginine (R) is an amino acid with a positively charged side chain, whereas glutamine (Q) is an amino acid with a neutral side chain. This may

lead to partial misfolding of the protein in crucial areas, leading to altered intramolecular protein interactions. It is noted that both the R383 residue and the SYT1 binding domain of SV2A reside in the cytoplasmic regions of the protein. Changes in the interaction between the two cytoplasmic regions may therefore lead to an alteration of SYT1 binding affinity to N-terminus region of SV2A, leading to possible defects in the trafficking and function of SYT1. Preliminary GST pulldown studies with the SV2A cytoplasmic loop region containing mutations with differently charged amino acids at residue 383 (Q – neutral, E – negatively charged) have indicated significantly altered protein interactions with several structural and functional SV proteins. Unsurprisingly, the cytoplasmic region did not directly bind to SYT1. Future protein pulldown investigations between full-length R383Q/E SV2A and SYT1 and shed further light on the possibility that residue 383 may have a role in regulating binding of SV2A to SYT1.

4.3.3 – The R383Q and T84A SV2A Mutations Affect the Same Mechanistic Pathway

While the R383Q single mutation resulted in the acceleration of SYT1 retrieval and severe defects in its localisation and expression, the next experimental step looked to probe if the phenotype observed is dependent on SV2A binding to SYT1. It is reported here that ablation of the phosphorylation-dependent SV2A-SYT1 interaction together with R383Q SV2A resulted in no additive defects being observed in the surface expression, localisation and retrieval kinetics of SYT1 during compensatory endocytosis. This indicates that the defects in SYT1 retrieval observed with the R383Q mutation is dependent of SYT1-binding to SV2A and gives evidence

that both mutations therefore play a role in the same SYT1 retrieval mechanistic pathway. The affected pathway is likely to be the one involving the formation of a complex between AP-2-SV2A-SYT1 during compensatory endocytosis whereby SV2A, together with AP-2, plays a role in the correct sorting of SYT1 to SVs. The manner in which the R383Q mutation may play a role in regulating the mechanism in which AP-2 and SV2A retrieve SYT1 has already been discussed previously, however the absences of additive defects in the presence of both mutations also suggest that the retrieval of SYT1 by stonin-2, which operates via a different mechanistic pathway, remains unaffected by the presence of the R383Q mutation. As before, it should be noted that the lack of observed effects in experiments using the T84A/R383Q double mutant could also be attributed to the lack of a dominant negative effect over remaining expressed WT SV2A, since depletion of SV2A using shRNA does not result in 100% ablation of WT protein expression.

The presence of both T84A and R383Q mutations resulted in a slight reduction in the total amount of externalised SYT1 during SV exocytosis. However, the level observed with the double remain greatly elevated over the levels observed when only the single mutants were used, suggesting that increased SYT1 externalisation during exocytosis was most likely still present and that the T84A mutation did not largely affect the proposed role of SV2A in modulating of the Ca^{2+}-sensing function of SYT1.

4.3.4 – The R383Q/Y46A SV2A Double Mutation Does Not Exacerbate Defects in SYT1 Retrieval

Upon determination that the R383Q SV2A-induced defects in SYT1 trafficking was dependent upon binding of SV2A to SYT1, subsequent experiments proceeded to investigate the whether the R383Q SV2A-induced defects in SYT1 trafficking are dependent on binding of SV2A to AP-2. Previous experiments have demonstrated ablation of SV2A-AP-2 interaction by the Y46A mutation led to defects in the expression and localisation of SYT1 and accelerated retrieval during SV endocytosis. This phenotype is completely mirrored when the R383Q mutation is present in SV2A, indicating that both mutations exert an effect on the trafficking of SYT1 via the same mechanistic pathway. The presence of both Y46A and R383Q SV2A mutations resulted in no additive defects being observed in SYT1 expression, localisation and trafficking during SV recycling compared to the single mutant, suggesting that the effects of the R383Q SV2A as seen in previous experiments is dependent upon the binding of SV2A to AP-2. Taken together with the previous experimental results, this provides another layer of evidence to support the hypothesis that the R383Q mutation exerts an effect on the capability of SV2A to mediate formation of the AP-2-SV2A-SYT1 complex during SV cargo sorting, therefore resulting the observed SYT1 trafficking defects.

4.3.5 – Mutation at R383 Affects SV2A Interactions with Actin, Tubulin and V-ATPase

The discovery that use of the R383Q SV2A mutant resulted in defective SYT1 surface expression, localisation and trafficking similar to that observed with the

Y46A SV2A mutant presented an interesting point of debate, since the R383Q SV2A mutation resides in a sequential and structurally distinct region from the Y46A mutation. In order to probe the mechanisms underlying these defects, GST pulldown experiments were conducted to probe the protein interactions between the cytosolic loop region (between residues 356-447) of WT, R383Q and R383E SV2A and proteins present in rat brain lysate. The residue selection at 383 was important, since the R383Q mutation represented a change in the residue charge from positive to neutral. In these experiments, we also used the R383E SV2A mutation to investigate the effect of significant changes in protein charge on SV2A protein-protein interactions.

Preliminary GST pulldown/western blotting experiments demonstrate that the cytosolic loop of SV2A does not bind to full length SV2A or SYT1, providing evidence the cytosolic loop of SV2A does not directly affect SV2A-SYT1 binding by acting as a competitive binding partner for either protein during the formation of the AP-2-SV2A-SYT1 recycling complex. The experiments also show that interactions of the cytosolic loop of SV2A with β-actin were significantly increased ~3-5 fold when the R383Q mutation was present, and reduced to ~0.4-0.5 fold when the R383E mutation was present, suggesting a key role of the charge at residue 383 in mediating β-actin-SV2A interactions. The associations between β-III tubulin, V-ATPase V1B1 and V-ATPase V1E1 and the SV2A cytosolic loop were decreased, though not significantly, when the R383Q mutation was present. However, subsequent repeats of these experiments have since indicated significance differences in the changes in the interactions between β-III tubulin/V-ATPase V1B1 and the cytosolic loop of SV2A (Dr. Karen Smillie, personal communication, data not

shown). It is noted that the initial experiments that were conducted used a high loading of fusion protein in order to provide the best chance of identifying all potential binding partners, resulting in limitations in obtaining reliable protein quantification data. The repeat experiments used a reduced loading of GST-fusion protein and therefore provided a much more accurate result.

How do actin, tubulin and V-ATPase potentially alter presynaptic function and in particular the trafficking of SYT1? Actin filaments and tubulin-derived microtubules are major components of the neuronal cytoskeleton, which has a key role in ensuring the maintenance of neuronal polarity, morphology and integrity (Kapitein and Hoogenraad, 2011), cell migration (Katsuno et al., 2015), and molecular scaffolding of the exocytosis-endocytosis proteins to the SV release sites in the active zone (Haucke et al., 2011). Actin and myosin, together with syndapin and dynamin I, have been documented to play a part in the scission of SVs from the plasma membrane in SV endocytosis in chromaffin cells (Gormal et al., 2015). The exact mechanisms underpinning the link between the actin, SV2A and SYT1 function at the presynapse currently remains unclear, since SV2A is not known to be a major interaction partner for actin. ATP is bound to actin monomers and its hydrolysis is required for polymerisation of actin, thus it is probable that the observed binding of actin to the R383Q SV2A loop in this study may be a result of f-actin-ATP conjugates binding to the SV2A adenine nucleotide-binding site. Disruption of ATP binding to the SV2A loop due to the R383Q mutation would result in decreased binding to ATP and therefore actin, though it is unlikely that perturbation of this minor interaction would directly relate in large defects in SYT1 trafficking and may just be an artefact of the pulldown process. It is noted that there is increasing amounts of evidence for the role

of actin in the regulation of synaptic function in mammalian central synapses (Rust and Maritzen, 2015). In addition to its structural function, actin (together with n-cofilin) has been shown to play a role in the recruitment and positioning of SVs as well as regulation of SV exocytosis in mouse hippocampal synapses (Wolf et al., 2015). The activity-dependent assembly of actin filaments, facilitated by the active zone protein Piccolo, has been shown to be involved in the regulation of neurotransmitter release in mouse hippocampal synapses (Waites et al., 2011).

A role for tubulin in regulating presynaptic function is less evidenced. There are several lines of evidence implicating the microtubule stabilising and bundling protein MAP1 in synaptic function. Interference of the interaction between MAP1A/MAP1B and voltage-gated calcium channel 2.2 resulted in reduced calcium uptake into the presynapse and impaired uptake of the FM4-64 dye (Leenders et al., 2008, Gandini et al., 2014). Interestingly, immunohistochemistry experiments using hippocampal tissue in pentylenetetrazole-induced epileptic rats shown an increased expression of MAP1B (Popa-Wagner et al., 1997), providing evidence for a causal link between epileptogenesis and dysfunction of tubulin-binding proteins. Tau-tubulin protein kinases 1 and 2 (TTBK1/2), which primarily phosphorylate microtubule associated tau and tubulin, has been reported to play an integral role in mediating the phosphorylation-dependent binding of SV2A to SYT1 at the N-terminus (Zhang et al., 2015). However, it is noted that the previous studies did not identify any phosphorylation sites in the cytosolic loop of SV2A, thus TTBK is unlikely to be responsible for the binding of SV2A to tubulin in this case. The observed binding of the SV2A cytosolic loop with both actin and tubulin in this study suggests that the cytosolic loop of SV2A may interact with the neuronal cytoskeleton in an unknown

capacity. The neuronal cytoskeleton has been proposed to be confer directionality to the process of clearing the active zone of excess SV cargo, thus preventing a functional block of the of the previously used release site (Haucke et al., 2011), however it is unclear how this may affect the specific trafficking of SYT1 in the presence of all SV proteins. Future experiments to probe SYT1 trafficking in the presence of disruption of the neuronal cytoskeleton may serve to provide greater insight into this phenomenon.

Lastly, the interaction between the R383Q SV2A cytosolic loop and the V-ATPase V1 subunits presents evidence supporting the hypothesis that SV2A may be involved in normal ATP activity at the presynapse by interacting with presynaptic ATP at the adenine-binding site. V-ATPase is primarily responsible for SV re-acidification during endocytosis, although it has been shown to have a role in neurotransmitter release through direct interaction with the V-SNARE protein SYB2 (Di Giovanni et al., 2010). The cytosolic V1 units in V-ATPase contains the ATP catalytic site (Nelson et al., 2000), which suggests that the adenine-binding site of SV2A may play a role in mediating binding of ATP to V-ATPase for ATP hydrolysis. It is unclear whether the SV2A cytosolic loop simply acts as a carrier for ATP during SV endocytosis, or if it plays a more complex role in the regulation of SV re-acidification and thus neurotransmitter release. However, it is noted that R383Q SV2A rescue experiments using a SYP-pHluorin reporter showed no defects in SV recycling or SV re-acidification, suggesting that the latter explanation is unlikely. The manner in which the ATP-SV2A interaction may affect SYT1-trafficking again remains unclear. It is possible that that ATP-SV2A binding is coupled with the phosphorylation-dependent SV2A-SYT1 binding. Disruption of normal presynaptic

ATP activity caused by the R383Q mutation may lead to downstream effects in the local availability of inorganic phosphates for the phosphorylation of SV2A, thus leading to defective SYT1 binding. Future biochemical experiments probing the ATP-dependency of the SV2A-SYT1 binding, together with SYT1-pHluorin experiments using mOrange as a better reporter for SV re-acidification (Egashira et al., 2015), may provide further insight into the mechanisms in which V-ATPase, SV2A and SYT1 interact with each other to maintain normal presynaptic function.

4.3.6 – Technical Limitations of the Study

As previously discussed in chapter 3, the caveats for using pHluorins as a tool for determining the effects of R383Q on SYT1 trafficking must also be considered. Analysis of the data is based on the assumption that SV re-acidification takes place on a much faster timescale compared to SV endocytosis, and thus all data obtained can be directly related to the rate of SYT1 retrieval during compensatory endocytosis. It is also unknown if the R383Q mutation has a direct effect on SV re-acidification, since GST pulldown/western blot experiments have revealed that the cytosolic loop of R383Q SV2A has an altered interactions with the V1B1 and V1E1 subunits of the SV proton pump V-ATPase (see below). Similar to previous experiments, all of the above pHluorin investigations were compared against control experiments using GFP-fused WT SV2A, which should eliminate any intrinsic trafficking differences between exogeneous and endogeneously expressed protein. The presence of a phenotype with the R383Q SV2A mutant also suggests that it does exert a dominant negative effect over WT SV2A in these studies; however, the exact nature of the double mutants used remains unclear.

5.0 –The Effects of Levetiracetam on SYT1 Trafficking at the Presynapse

5.1. – Introduction to the Treatment of Seizures Associated with Epilepsy

The mainstay of epilepsy therapy is the use of anti-epileptic drugs (AEDs) which provide symptomatic treatment of spontaneously recurrent seizures that occur in epilepsy. In order to exhibit anti-epileptic properties, a drug must act on one or more target molecules in the brain. AED action can usually be categorised into three categories: 1) modulation of voltage-gated ion channels; 2) enhancement of synaptic inhibition and 3) inhibition of synaptic excitation (Rogawski and Löscher, 2004). Therefore, AEDs targets usually include ion channels, neurotransmitter transporters and neurotransmitter metabolic enzymes. The ultimate goal of AED interaction is to modify the burst firing properties of neurones and to reduce the synchronisation of localised neuronal sub-groups. For example, generalised absence seizures are believed to result from thalamocortical synchronisation (Gigout et al., 2013). In order to abort such seizures, it is necessary to interfere with the rhythm-generating mechanisms that underlie the synchronised activity. Voltage-gated ion channels (including sodium, calcium and potassium channels) allow neurones to fire action potentials and define the threshold of neuronal activity. In addition, voltage-gated ion channels regulate the response of the presynapse to action potentials and are crucial to neurotransmitter release. Consequently, they are key targets for AEDs that can inhibit epileptic bursting, synchronisation and spread of seizures after status epilepticus. Synaptic inhibition and excitation are mediated by neurotransmitter-regulated channels, which permit synchronisation of local synaptic activity. Therefore, AEDs that modify excitatory and inhibitory neurotransmission can also suppress burst firing of neurones and can have prominent effects on seizure spread (Rogawski and Löscher, 2004).

5.1.1 – Molecular Targets of Anti-Epileptic Drug Action

The first generation of anti-epileptic drugs (AED) used to treat generalised and partial seizures, such as phenytoin and sodium valproate, function through inhibition of voltage-gated sodium channel activity (Van den Berg et al., 1993, Kuo and Bean, 1994). Voltage-gated sodium channels in the brain can rapidly cycle through the resting, open and inactivated states, allowing neurones to fire high-frequency trains of action potentials (Bagal et al., 2015). Drugs that target sodium channels are able to block high-frequency repetitive burst firing, which is believed to occur during the spread of seizure activity, without affecting normal neural activity. This provides the basis for their ability to protect against seizures without causing a generalised impairment of brain function. Sodium channel inhibitors may also function via a channel inactivation mechanism. Phenytoin does not alter the conductance of the open state of sodium channels, but rather induces a non-conducting state in the channel that is akin to channel inactivation. Recovery from drug block of the channel therefore occurs more slowly than that which completely blocks the channel, therefore partly accounting for phenytoin's selective ability to block high-frequency firing (Kuo and Bean, 1994). Sodium channel inhibitors, however, produces severe side effects in patients. Although the spread of seizure activity was reduced in patients taking the medication, both phenytoin and valproate have been associated with detrimental effects of cognitive and behaviour (Aldenkamp et al., 1994, Meador et al., 2009).

Aside from voltage-gated sodium channels, AEDs can also target voltage-gated calcium channels. Voltage-gated calcium channels permit the flux of calcium ions when they are activated by membrane depolarisation. Calcium channels are broadly

grouped into two categories, high voltage-activated (HVA) and low voltage-activated (LVA) calcium channels. HVA calcium channels require strong membrane depolarisation to initiate gating activity and are responsible for the regulation of calcium entry and thus neurotransmitter release at the presynaptic terminal. Blocking HVA calcium channels inhibit neurotransmitter release, thus they are potentially good targets for AED action. Gabapentin, a drug originally synthesised to be a GABA receptor agonist, binds to the α2δ-1 and α2δ-2 auxiliary subunits of calcium channels with high affinity (Marais et al., 2001). The α2δ-binding affinities of gabapentin and its analogues such as pregabalin in rat cortical slices correlate with their antiepileptic potency, thus strongly implicating these subunits as a relevant target for AED action (Dooley et al., 2002). The mechanism by which gabapentin binding to α2δ-1 and α2δ-2 subunits of calcium channels produces anti-seizure effects are still not fully defined. Studies on dorsal root ganglion neurones have demonstrated that gabapentin produces small inhibitions in HVA calcium currents in a dose-dependent matter at clinically relevant concentrations (~10-100 μM) (Martin et al., 2002). Gabapentin has also been shown to inhibit potassium-evoked glutamate release in rat hippocampal slices (Dooley et al., 2000) and suppress excitatory postsynaptic currents in the dorsal horn of the rat spinal cord (Shimoyama et al., 2000). Taken together, these studies suggest that inhibition of HVA calcium currents by gabapentin may translate to a reduction in excitatory transmission.

Second and third generation AEDs have since been developed, many of which are demonstrated to be effective in improving symptoms of epilepsy thorough modulation of neurotransmitter release. The potentiation of inhibitory GABA-mediated neurotransmission represents a key mechanism for modern AED action.

Although inhibitory neurones that utilise GABA only represent a small fraction of neurones that are pivotal to epileptic activity such as the cortex, hippocampus and amygdala, these neuronal connections are vital in restraining the positive feedback which causes recurrently connected excitatory neurones to develop synchronised epileptiform bursts (Miles and Wong, 1987). GABA acts through fast chloride-permeable ionotropic $GABA_A$ receptors and through slower metabotropic G-protein-coupled $GABA_B$ receptors. Drugs that block $GABA_A$ receptors, such as bicuculline and pentylenetetrazole, reduce the efficacy of synaptic inhibition mediated by $GABA_A$ receptors and can lead to seizures. Conversely, the pharmacological enhancement of $GABA_A$ receptor-mediated inhibition can therefore be an effective anti-epileptic approach. Many modern AEDs influence $GABA_A$ receptor inhibition either by interacting with $GABA_A$ receptors or by modifying the activity of enzymes and transporters, which alters the dynamics of GABA release and recycling. Benzodiazepines and barbiturates act as positive allosteric modulators of $GABA_A$ receptors. Benzodiazepines potentiated $GABA_A$ receptor function, prolonged the duration of mini inhibitory postsynaptic currents (IPSCs) and increased tonic current amplitude in cultured neurones (Bai et al., 2001). The AED vigabatrin increases inhibitory GABA activity through inhibition of GABA transaminase, which is the enzyme responsible for breakdown of GABA. Administration of vigabatrin has led to large elevations in GABA levels in rat brain regions (Löscher and Hörstermann, 1994). The action of GABA at the synapse can also be terminated by rapid retrieval into presynaptic terminals and reuptake into the surrounding glia mediated by high affinity plasma membrane GABA transporters. The AED tiagabine is a potent and selective competitive inhibitor of the GABA transporter GAT1. Tiagabine bound

with high affinity to GAT1 and slowed the reuptake of synaptically released GABA, therefore prolonging inhibitory postsynaptic potentials in rat hippocampal slices (Jackson et al., 1999).

Ionotropic glutamate receptors mediate the bulk of fast excitatory neurotransmission in the central nervous system. Ionotropic glutamate receptors can be subdivided into three groups: 1) *N*-methyl-D-aspartate (NMDA) receptors; 2) α-amino-3-hydroxy-5-methyl-4-isoxazolepropionic acid (AMPA) receptors and 3) kainate receptors. Despite many efforts, clinical trials with selective NMDA/AMPA antagonists in the chronic treatment of epilepsy have been largely disappointing. However, there are a few examples of drugs that exhibit potential in their use for the treatment of status epilepticus. One of these drugs is topiramate, which has multiple modes of action that includes the blockade of kainate and AMPA receptors (Perucca, 1996). Topiramate is well established as an effective AED for partial-onset seizures, but it is associated with some significant adverse effects that include renal stones and word-finding difficulties (Aldenkamp et al., 2000).

5.1.2– Levetiracetam as a Treatment for Generalised Seizures in Epilepsy

Levetiracetam (LEV) [(*S*)-α-ethyl-2-oxo-1-pyrrolidineacetamide, also known as Keppra™] is an anti-convulsant medication manufactured by UCB Pharmaceuticals Ltd. Early pre-clinical development showed LEV to be an orally active, safe and broad-spectrum anti-convulsant agent that was effective against audiogenic seizures in mice (Gower et al., 1992). The use of LEV is associated with a minor side effect profile that included: rashes, itches, mood swings, irritability, lethargy, tiredness and

asthenia. However, it is generally well-tolerated in comparison to older AEDs such as phenytoin (Fuller et al., 2013).

Electrophysiological studies of cultured rat neocortical neurones showed that LEV did not exhibit any specific effects on neuronal voltage-gated Na^+ channels and voltage-gated Ca^{2+} channels (Zona et al., 2001). LEV also did not have an effect on inhibitory GABA-ergic transmission or the affinity of GABA or glutamatergic receptors for their respective neurotransmitter molecules (Klitgaard, 2001). These studies represent the most common modes of action for the vast majority of anti-epileptic drugs, with LEV seemingly excluded from any of these cases. A common idea that LEV may function via a mechanism that desynchronises excessive neuronal firing remains unsupported by evidence. There is currently a large research focus on the elucidation of molecular mechanisms of action that makes LEV a potent drug for the treatment of epilepsy.

5.1.3 – Mechanisms of Levetiracetam Action

Over the last decade, multiple studies have been conducted with the aim of obtaining further insight into LEV's mode of action. Although LEV does not affect inhibitory neurotransmission directly, it has been suggested to have several indirect effects at synaptic terminals. LEV-induced modifications of the enzymes involved in the synthesis and degradation of GABA, glutamic acid decarboxylase (GAD) and GABA aminotransferase in the striatum resulted in decreased spontaneous neural activity in discrete areas of the brain of anaesthetised rats (Löscher et al., 1996). Treatment of hippocampal neurones with LEV also produced a decrease in glutamate-mediated

excitatory transmission by preventing Zn^{2+}-induced presynaptic $GABA_A$ inhibition (Wakita et al., 2014). Addition of LEV also results in a significant reduction in the levels of the amino acid taurine, a low affinity agonist for $GABA_A$ receptors (Tong and Patsalos, 2001). These experiments have provided evidence that modulation of the inhibitory neuronal network could be a potential mechanism by which LEV operates.

The modulation of intracellular Ca^{2+} levels may also provide a possible candidate mechanism for LEV's antiepileptic activity. Ca^{2+} plays a large role in a multitude of neurological functions, in particular neuronal excitability and SV recycling (Sudhof, 2004). LEV has been reported to significantly depress neuronal high voltage activated Ca^{2+} current at clinically relevant conditions in rat hippocampal slices (Niespodziany et al., 2001), as well as inhibit voltage-dependent Ca^{2+} channels in superior cervical ganglion neurones through an intracellular pathway that is specific to a single enantiomer of the drug, leading to reduced neuronal excitability (Vogl et al., 2012). LEV has also been reported to inhibit the ryanodine and inositol 1,4,5-triphosphate receptors, both of which are implicated in the control of Ca^{2+} influx from extracellular space as well as output from intracellular Ca^{2+} stores (Fukuyama et al., 2012). LEV's effect on Ca^{2+} homeostasis could also limit epileptogenesis, since the inhibition of Ca^{2+} influx after an initial seizure have shown anti-epileptogenic effects (Nagarkatti et al., 2008).

5.1.4 – SV2A Mediates Entry of Levetiracetam into the Presynapse

The anticonvulsant properties of various SV2A ligands, including LEV, were initially demonstrated to correlate strongly with its in vitro binding affinity to SV2A in rat cerebral cortex (Noyer et al., 1995). Later studies incorporating photo-affinity labelling techniques on purified SVs from SV2A knockout mice brain membranes demonstrated no LEV binding, whereas experiments using wild type mice brain membranes exhibited a strong LEV binding affinity to purified SVs, suggesting SV2A is indeed the binding partner for LEV. No binding was observed to the related isoforms SV2B and SV2C in these experiments. The study also showed that a strong correlation existed between the binding affinity for a compound for SV2A and its protective effect against seizures (Lynch et al., 2004). Binding characteristics of LEV to SV2A was corroborated by further experiments using human brain samples and human recombinant SV2A expressed in Chinese hamster ovary cells (Gillard et al., 2006). Elucidation of the racetam binding site in SV2A remains highly debated, though it is becoming increasing clear that racetams are likely to function by binding onto multiple residues within SV2A rather than just a single residue. In an early biochemical study, Shi et al. identified three residues in the putative tenth transmembrane helix of SV2A (F658, G659 and V661) that altered binding of LEV and related racetam derivatives to SV2A when they are mutated (Shi et al., 2011). These residues aligned with critical functional residues with the major facilitator superfamily (MFS) protein lactose permease found in *E.Coli*. As SV2A is part of the MFS of transporter proteins, this suggests that LEV may play a role modulating key structural motifs within SV2A that may play critical role in the protection against seizures. More recently, a molecular dynamics simulation approach *in silico* has been

successful in building a complete model of SV2A protein with LEV, as well as other effective racetams, docked into the protein (Correa-Basurto et al., 2015). Although the simulations were performed on a relatively short timescale, the studies support the putative binding pocket previously observed by Shi et al. and identified five putative binding sites (T456, S665, W666, D670 and L689) with additional hydrophobic and hydrogen bond interactions that were important for racetam binding within the transmembrane hydrophilic core of SV2A.

With the knowledge that SV2A is a principal binding site for LEV, great efforts have been made recently to elucidate the effects of the drug at the presynapse. Incubation of rat hippocampal slices in 100 μM LEV for up to 3 hours resulted in a significant reversal of paired-pulse facilitation that is normally produced by repetitive stimulation. There was also a reduction of the rate of vesicle fusion, suggesting that LEV had an influence on the rate of neurotransmitter release (Yang et al., 2007). In other electrophysiological studies, rat hippocampal slices incubated in LEV for three hours revealed a dose-dependent decrease in excitatory postsynaptic currents (EPSCs) and a reduction of the readily releasable pool of vesicles. The same study also found that synaptic activity during LEV incubation significantly decreased the time at which the effect of LEV was observed, as well as its magnitude. Traditionally, studies on the mechanisms of LEV on neurones only reveal an effect after incubation times of at least 1 to 3 hours. Interestingly, either the use of 4-aminopyridine (4-AP) to increase spontaneous activity of neurones or induction of low frequency stimulation during LEV incubation (180 action potentials, 0.2 Hz) revealed an early LEV effect on EPSCs after an incubation period of only 30 minutes (Meehan et al., 2011). Further studies by the same research group also demonstrated

that LEV reduced IPSCs in a frequency-dependent manner, with the largest effect observed in later IPSCs in high-frequency stimulation trains in rat hippocampal slices. However, in contrast to their observations with EPSCs, a LEV effect was observed in IPSCs after only 30 minutes of LEV incubation compared to 3 hours of LEV incubation required to reveal an effect on EPSCs. Silencing of neuronal spontaneous activity by use of CNQX/APV ablated the early onset of the LEV effect on IPSCs (Meehan et al., 2012). These lines of evidence demonstrate a requirement for synaptic activity to reveal a LEV effect, perhaps as a means to mediate entry of the drug into the synaptic terminal. Differences in the level of spontaneous activity may also affect the probability of observing a LEV effect, since excitatory and inhibitory nerve terminals require significantly different LEV incubation times for an effect to be revealed.

LEV may also play a role in modulating synaptic protein levels that will have direct downstream effects on the SV recycling pathway. Overexpression of SV2A in autaptic hippocampal neurones increased the levels of synaptotagmin in tandem at the synapse and reduced EPSC amplitude. Treatment with 100 µM LEV for a period of 6 to 10 hours restored normal levels of SV2A and synaptotagmin as well as rescued normal neurotransmission, indicating that LEV may play a role in modulating SV2A protein interactions that may affect its expression and thus impact directly upon neurotransmission (Nowack et al., 2011).

5.1.5 – Levetiracetam in the Prevention of Epilepsy

A major goal of contemporary epilepsy research is the identification of therapies to prevent the development of recurrent seizures in individuals at risk. The first evidence that LEV may exhibit anti-epileptogenic properties came from a study on rats using the kindled model for epilepsy. Treatment of the rats with LEV suppressed the increase of seizure severity and duration in a dose-dependent manner. After termination of the treatment, the duration of the seizures remained significantly shorter than vehicle controls, which suggest that LEV did not simply have an anti-seizure effect but also exerted a true disease-modifying effect concomitantly (Löscher et al., 1998). In another study, chronic treatment with LEV in a dose-dependent manner counteracted the long-term effects of pilocarpine-induced status epilepticus in rats such as increased amplitude of neuronal spikes in the dentate gyrus and reduced paired-pulse inhibition in the CA1 region of the hippocampus, suggesting that LEV completely inhibits the development of hippocampal hyperexcitability following pilocarpine-induced status epilepticus (Margineanu et al., 2008). Treatment of rats with LEV also significantly decreased the mean duration of spontaneous seizures 58 days after treatment. LEV also prevented a status epilepticus-induced increase in the number of ectopic granule cells by suppressing neuronal proliferation in the dentate sub-granular zone and abnormal migration of nascent neurones from this zone (Sugaya et al., 2010). There is also evidence that suggests that LEV is able to exert long-term molecular effects at the synapse, which may be crucial in describing the mechanisms by which LEV may prevent the onset of epilepsy. The process of kindling is associated with an upregulation of hippocampal BDNF and neuropeptide Y mRNA levels and the downregulation of

neuropeptide Y1 and Y5-like receptors. Pre-treatment with LEV delayed the progression of kindling in rats by abolishing the kindling-induced rise in BDNF and neuropeptide Y mRNA and preventing a decrease in levels of neuropeptide Y1- and Y5-like receptors in the hippocampus (Husum et al., 2004). LEV treatment also prevented kindling-induced accumulation of SV2 as well as kindling-induced accumulation of 7S SNARE complexes in the ipsilateral hippocampus of rats (Matveeva et al., 2008).

5.1.6 – Aims and Objectives

It was previously reported that SV2A mediates the entry of LEV into vesicles via several putative racetam binding sites (T456, S665, W666, D670 and L689) but no evidence of a LEV effect on the trafficking and recycling of any SV proteins has been published to date. I hypothesise that LEV has a mode of action at the presynaptic terminal that involves modulation of the trafficking behaviour of SV proteins, in particular SV2A and its intrinsic trafficking partner SYT1. A perturbation of SYT1 recycling may lead to alterations in SV priming, docking and exocytosis behaviour, which may play a key role in the treatment of seizures associated with epilepsy. The aim of this study is to determine the effects of LEV on the trafficking behaviour of various common synaptic vesicle proteins in the vesicle recycling process.

The primary objectives of this project are:

1) To determine whether LEV exhibits any effect on SV recycling in mouse hippocampal neurones.

2) To determine the level of synaptic activity required to mediate LEV entry into nerve terminals in mouse hippocampal neurones.

3) To elucidate a possible mechanism for LEV action at the presynapse, by determining the effect of LEV on important SV proteins in the SV recycling pathway.

5.2. – Results of Studies on the Effect of Levetiracetam on SV and SYT1 Recycling

Prior studies on the effect of LEV at synaptic terminals have shown that synaptic activity is required to reveal a LEV effect. Incubation of the drug for an extended period of time (6 hrs or more) is usually required to reveal the effect of the drug on synaptic activity, however it has recently been demonstrated that the use of a low level loading stimulation, either with 4-aminopyridine or a low frequency electrical activity (180AP, 0.2 Hz), allowed a LEV-mediated effect to be observed within 30 min (Meehan et al., 2011). In inhibitory nerve terminals, defects in synaptic transmission were observed within 30 min of LEV application. This early LEV effect can be abolished with by use of the synaptic activity blockers CNQX/APV (Meehan et al., 2012). These lines of evidence suggest a need for synaptic activity as a loading mechanism for mediating LEV uptake into nerve terminals.

Key research findings of this chapter:

- Treatment of neurones with LEV under strong/mild synaptic stimulation does not affect recycling of SYP or VGLUT1.
- Treatment of neurones with LEV under strong/mild synaptic stimulation does not affect recycling of SYT1.
- Protocols designed to provide neurones with strong/mild synaptic stimulation were tested and verified for purpose to ensure reliability of results.

5.2.1 – Application of LEV in the Absence of Mild Synaptic Stimulation Does Not Affect SV Recycling

The requirement for synaptic activity to mediate LEV uptake into presynaptic nerve terminals was first investigated. Initial investigations were focused on whether a short incubation with LEV could affect SV recycling without prior neuronal activity to accumulate the drug. Synaptophysin-pHluorin (SYP-pHluorin) was used as a reporter for synaptic vesicle recycling (see Materials and Methods) in dissociated primary cultures of mouse hippocampal cells. Imaging of the SYP-pHluorin response was undertaken in the presence of the activity blockers CNQX/APV as per previous experiments (Figure 5.1 **A**). Incubation of cells in 100 and 300 µM LEV in the absence of a low-level stimulation to drive the loading of LEV into the synapses did not affect the rate of SYP-pHluorin retrieval (ns, two-way ANOVA of traces normalised to peak at evoked transmission) (Figure 5.1 **B**) or the total amount of SYP-pHluorin externalisation as a fraction of the total pHlurin pool during evoked transmission compared to controls [Max $\Delta F/F_0$ (as a fraction of the total pHluorin pool) = 0.323 ± 0.025 (No LEV), 0.338 ± 0.032 (100 µM LEV), 0.302 ± 0.033 (300 µM LEV); ns, one-way ANOVA, P = 0.705, F = 0.357] (Figure 5.1 **C**).

In order to ensure that the absence of an observed LEV effect was not due to a specific effect on SYP-pHluorin recycling, vesicle glutamate transporter 1-pHluorin (VGLUT1-pHluorin) was used in replicate experiments. Incubation of the cells with 100-300 µM LEV without a low-level loading stimulation did not have an effect on either the rate of VGLUT1-pHluorin retrieval (ns, two-way ANOVA of traces normalised to peak at evoked transmission) (Figure 5.1 **D**) or the total amount of externalised VGLUT1-pHluorin during evoked transmission [Max $\Delta F/F_0$ (as a

fraction of the total pHluorin pool) = 0.439 ± 0.037 (No LEV), 0.466 ± 0.046 (100 µM LEV), 0.415 ± 0.044 (300 µM LEV); ns, one-way ANOVA, P = 0.751, F = 0.294] (Figure 5.1 **E**). The lack of a LEV effect seen with either SYP-pHluorin or VGLUT1-pHluorin demonstrated that the absence of use of a loading stimulation resulted in a failure to reveal any effect of LEV at the presynapse, most likely due to the failure of uptake of the drug into the cell within a short space of time.

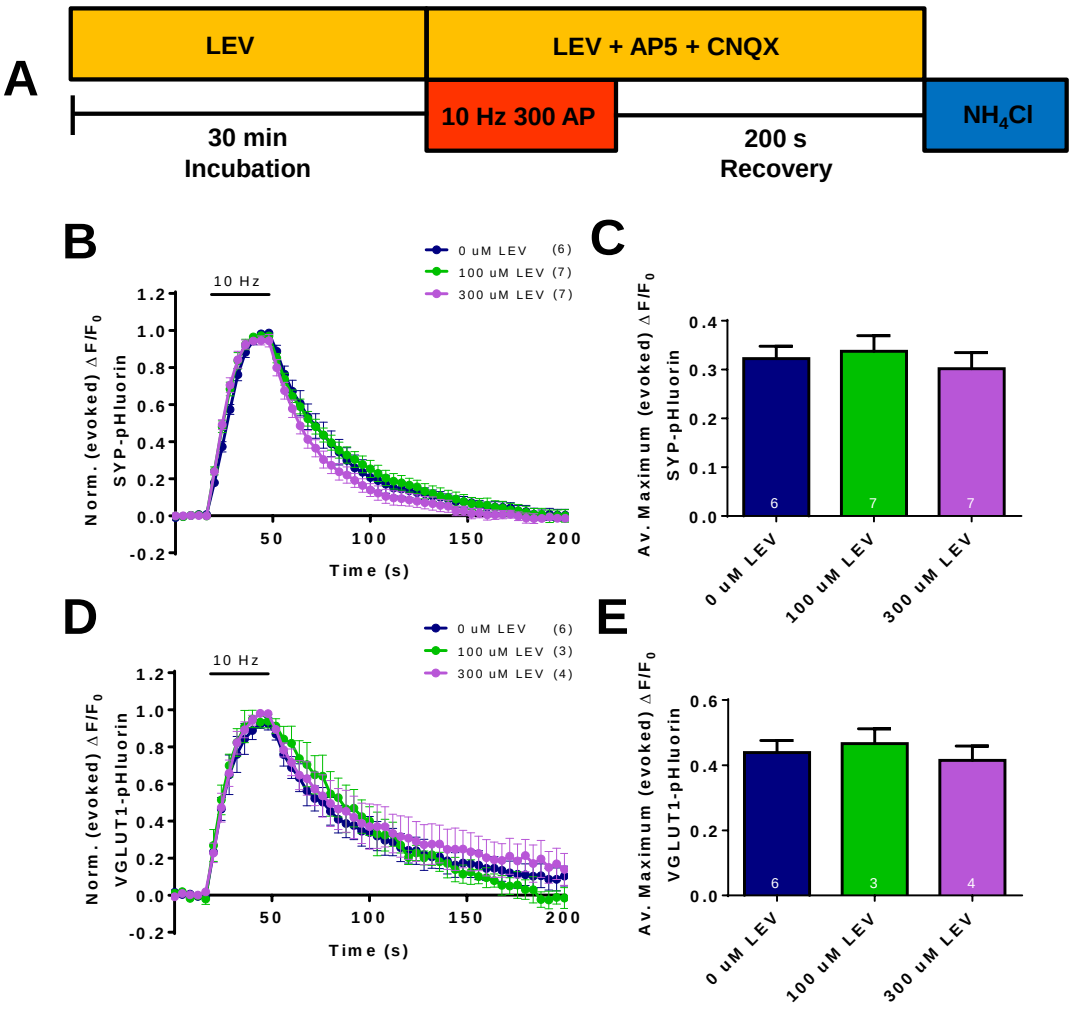

Figure 5.1: Application of levetiracetam in the absence of mild synaptic stimulation does not affect SV recycling. A) Experimental scheme. Hippocampal neurones were incubated with levetiracetam (LEV, 0, 100 or 300 µM) for 30 min prior to stimulation with a train of 300 action potentials (APs, 10Hz). After 200 seconds of recovery, the total recycling synaptic vesicle (SV) pool was revealed with an NH_4Cl buffer pulse. **B,C)** SYP-pHluorin-transfected neurones were incubated with LEV at the indicated concentrations and stimulated with a train of 300 APs (10 Hz, indicated by bar). **B)** Graph displays the mean $\Delta F/F_0$ time course for SYP–pHluorin ± SEM normalized to the peak of stimulation [n=6 0 µM LEV, blue; n=7 100 µM LEV, green; n=7 300 µM LEV, purple; ns, two-way ANOVA]. **C)** Mean maximum evoked SYP-pHluorin response ($\Delta F/F_0$ ± SEM) expressed as a fraction of the total SV pool (ns, one-way ANOVA, P=0.705, F=0.357). **D,E)** VGLUT1-pHluorin-transfected neurones were incubated with LEV at the indicated concentrations and stimulated with a train of 300 APs (10 Hz). **D)** Graph displays the mean $\Delta F/F_0$ time course for VGLUT1–pHluorin ± SEM normalized to the peak of stimulation [n=6 0 µM LEV, blue; n=3 100 µM LEV, green; n=4 300 µM LEV, purple; ns, two-way ANOVA]. **E)** Mean maximum evoked VGLUT1-pHluorin response ($\Delta F/F_0$ ± SEM) expressed as a fraction of the total SV pool (ns, one-way ANOVA, P=0.751, F=0.294).

5.2.2 – Application of LEV in the Presence of Intense Synaptic Stimulation Does Not Affect SV Recycling

The use of intense synaptic activity as a loading mechanism for LEV into synaptic terminals in order to reveal a LEV effect on SV recycling was next investigated. Exposure to high KCl concentrations maintains the cells in a membrane-depolarised state, mimicking cellular stress conditions experienced during high levels of synaptic activity. SYP-pHluorin transfected neurones were stimulated with an elevated KCl buffer (50 mM KCl added, with 50 mM NaCl removed to maintain osmolarity) containing 100 µM LEV. After depolarisation, the neurones were allowed to recover in standard imaging buffer containing 100 µM LEV before being challenged by a train of action potentials (300 APs, 10Hz) 30 minutes later (Figure 5.3 **A**). Application of 100 µM LEV in the presence of 50 mM KCl-induced synaptic activity did not affect either the subsequent rate of SYP-pHluorin trafficking (ns, two-way ANOVA of traces normalised to peak at evoked transmission) (Figure 5.3 **B**) or the total amount of SYP-pHluorin externalisation during evoked transmission compared to controls. The use of prior KCl in the absence of LEV as a positive control resulted in a reduction in post-stimulation SV recycling, indicating that resting synaptic activity was increased by the presence of KCl. [Max $\Delta F/F_0$ (as a fraction of the total pHluorin pool) = 0.385 ± 0.022 (No LEV), 0.371 ± 0.003 (100 µM LEV), 0.247 ± 0.019 (No LEV + KCl), 0.306 ± 0.035 (100 µM + KCl); $p < 0.01$ (0 µM LEV vs 50 mM KCl + 0 µM LEV), ns (No LEV + KCl vs 100 µM LEV + KCl), one-way ANOVA, Bonferroni's post-hoc, P = 0.0053, F = 8.57] (Figure 5.2 **C**).

In order to see whether the system could be altered by higher concentrations of the drug, the experiments were replicated using of a higher dose of 300 µM LEV (Figure

5.3 **A**). In agreement with previous results, the application of 300 µM LEV in the presence of 50 mM KCl-induced synaptic activity did not affect either the rate of SYP-pHluorin trafficking (ns, two-way ANOVA of traces normalised to peak at evoked transmission) (Figure 5.3 **B**) or the total amount of SYP-pHluorin externalisation during evoked transmission compared to controls [Max $\Delta F/F_0$ (as a fraction of the total pHluorin pool) = 0.456 ± 0.037 (No LEV), 0.394 ± 0.049 (300 µM LEV), 0.360 ± 0.035 (No LEV + KCl), 0.394 ± 0.037 (300 µM + KCl); ns, one-way ANOVA, P = 0.327, F = 1.24] (Figure 5.3 **C**).

In order to ensure that the lack of observed effect was not specific to SYP-pHluorin, the experiments were replicated with VGLUT1-pHluorin. In agreement with results obtained with SYP-pHluorin, application of 300 µM LEV in the presence of 50 mM KCl-induced synaptic activity did not affect either the rate of VGLUT1-pHluorin trafficking (ns, two-way ANOVA of traces normalised to peak at evoked transmission) (Figure 5.3 **D**) or the total amount of VGLUT1-pHluorin externalisation during evoked transmission compared to controls [Max $\Delta F/F_0$ (as a fraction of the total pHluorin pool) = 0.511 ± 0.036 (No LEV), 0.440 ± 0.019 (300 µM LEV), 0.442 ± 0.041 (No LEV + KCl), 0.385 ± 0.025 (300 µM + KCl); ns, one-way ANOVA, P = 0.101, F = 2.31] (Figure 5.3 **E**).

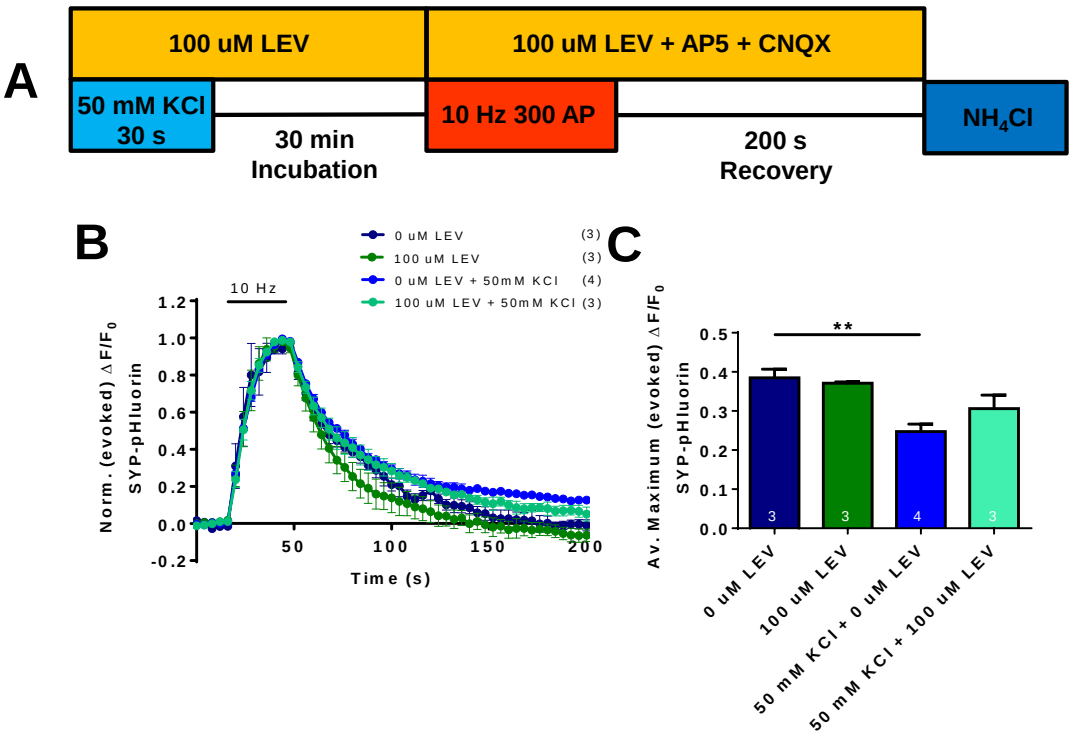

Figure 5.2: Application of 100 µM LEV in the presence of intense synaptic stimulation does not affect SV recycling. A) Experimental scheme. Hippocampal neurones were clamped in a membrane depolarised state with 50 mM KCl in the presence of levetiracetam (LEV, 100 µM) for 30 s and then incubated in LEV for 30 min prior to stimulation with a train of 300 action potentials (APs, 10Hz). After 200 seconds of recovery, the total recycling synaptic vesicle (SV) pool was revealed with a NH_4Cl buffer pulse. **B,C)** SYP-pHluorin-transfected neurones were incubated with LEV (100µM) after 50 mM KCl induced loading and stimulated with a train of 300 APs (10 Hz, indicated by bar). **B)** Graph displays the mean $\Delta F/F_0$ time course for SYP–pHluorin ± SEM normalized to the peak of stimulation [n=3 0 µM LEV, dark blue; n=3 100 µM LEV, dark green; n=4 50 mM KCl+ 100 µM LEV, blue; n=3 50 mM KCl + 100 uM LEV, cyan; ns, two-way ANOVA]. **C)** Mean maximum evoked SYP-pHluorin response ($\Delta F/F_0$) expressed as a fraction of the total SV pool [**p<0.01 (0 µM LEV vs 50 mM KCl + 0 µM LEV); one-way ANOVA, Bonferroni's post-hoc, P=0.0053, F=8.57].

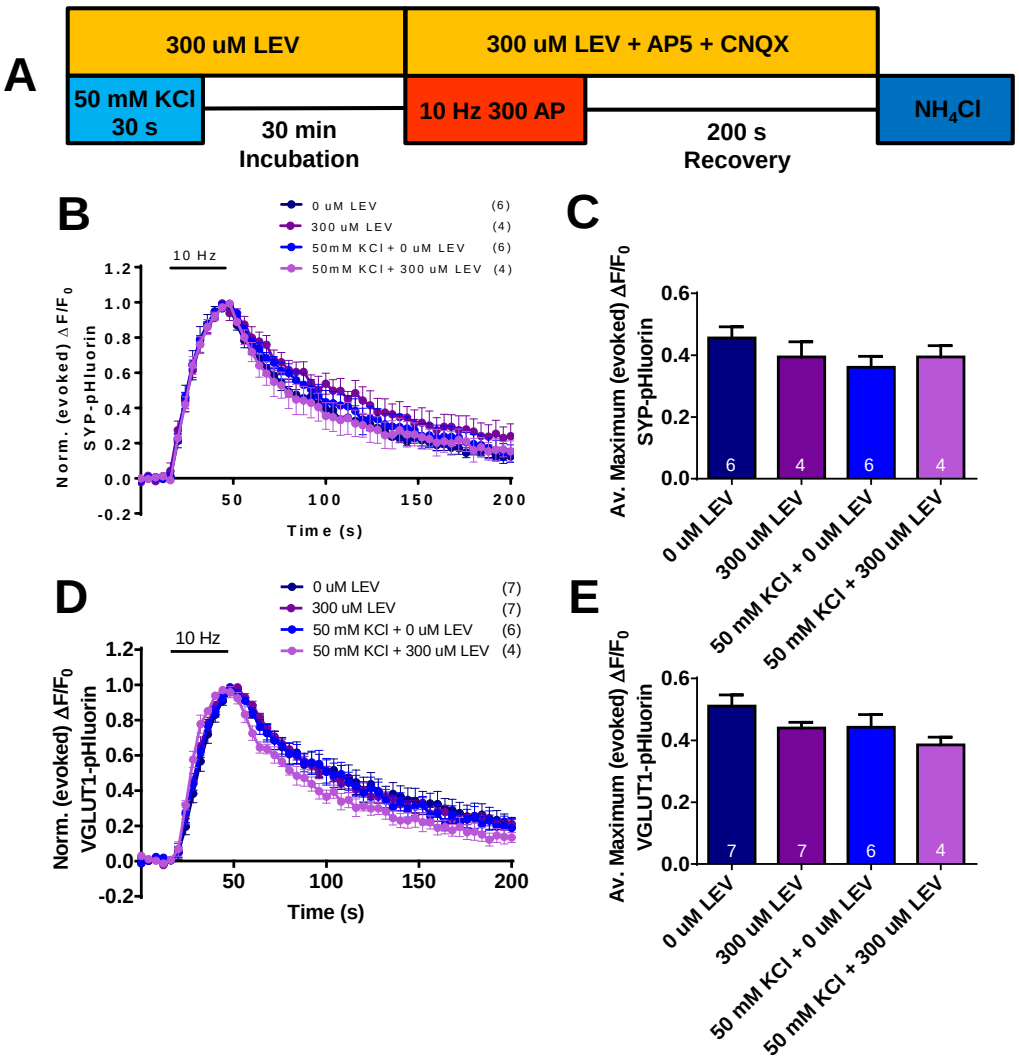

Figure 5.3: Application of 300 µM LEV in the presence intense synaptic stimulation does not affect SV recycling. A) Experimental scheme. Hippocampal neurones were clamped in a membrane depolarised state with 50 mM KCl in the presence of levetiracetam (LEV, 300 µM) and then incubated in LEV for 30 min prior to stimulation with a train of 300 action potentials (APs, 10Hz). After 200 seconds of recovery, the total recycling synaptic vesicle (SV) pool was revealed with a NH_4Cl buffer pulse. **B,C,D,E)** SYP-pHluorin-transfected (B,C) and VGLUT1-pHluorin-transfected (D,E) neurones were incubated with LEV (300 µM) after 50 mM KCl induced loading and stimulated with a train of 300 APs (10 Hz, indicated by bar). **B,D)** Graph displays the mean $\Delta F/F_0$ time course for SYP–pHluorin (B) ± SEM normalized to the peak of stimulation [n=6 0 µM LEV, dark blue; n=4 300 µM LEV, dark purple; n=6 50 mM KCl+300 µM LEV, blue; n=4 50 mM KCl+100 uM LEV, purple; ns, two-way ANOVA] and VGLUT1-pHluorin (D) ± SEM normalized to the peak of stimulation [n=7 0 µM LEV, dark blue; n=7 300 µM LEV, dark purple; n=6 50 mM KCl+300 µM LEV, blue; n=4 50 mM KCl+100 uM LEV, purple; ns, two-way ANOVA]. **C,E)** Mean maximum evoked SYP-pHluorin (C) and VGLUT1-pHluorin (E) response ($\Delta F/F_0$) expressed as a fraction of the total SV pool (ns, one-way ANOVA).

5.2.3 – Application of LEV in the Presence of Mild Synaptic Stimulation Does Not Affect SV Recycling

Previous work from Meehan demonstrated that a faster LEV effect was generated when mild synaptic activity was used to drive loading of the drug, and that use of intense synaptic stimulation resulted in a failure to reveal any drug effects. In light of previous results where the use of intense synaptic activity to drive LEV loading revealed no observed drug effect, LEV loading was next performed in the presence of mild synaptic activity. In initial attempts to utilise mild synaptic activity to mediate a LEV effect, 4-aminopyridine (4-AP) was used as a mild enhancer of non-evoked synaptic transmission by enhancing spontaneous neurotransmitter release in both excitatory and inhibitory synapses (Buckle and Haas, 1982). SYP-pHluorin transfected neurones were incubated with 100 µM LEV in the presence of 50 µM 4-AP before being challenged by a train of action potentials (300 AP, 10 Hz) (Figure 5.4 **A**). Application of LEV in the presence of 50 µM 4-AP did not significantly affect either the rate of SYP-pHluorin trafficking (ns, two-way ANOVA of traces normalised to peak at evoked transmission) (Figure 5.4 **B**) or the total amount of externalised SYP-pHluorin during evoked transmission compared to control [Max $\Delta F/F_0$ (as a fraction of the total pHluorin pool) = 0.321 ± 0.039 (No LEV + 4-AP), 0.406 ± 0.024 (100 µM LEV + 4-AP); ns, two-tailed t-test] (Figure 5.4 **C**).

In an effort to ensure that the lack of an observed LEV effect was not due to SYP-pHluorin specific interactions, VGLUT1-pHluorin was again used in replicate experiments. In agreement with results obtained using SYP-pHluorin, the use of 4-AP did not significantly affect either the rate of VGLUT1-pHluorin trafficking (ns, two-way ANOVA of traces normalised to peak at evoked transmission) (Figure 5.4

D) or the total amount of externalised VGLUT1-pHluorin during evoked transmission compared to control [Max $\Delta F/F_0$ (as a fraction of the total pHluorin pool) = 0.534 ± 0.054 (No LEV + 4-AP), 0.562 ± 0.044 (100 µM LEV + 4-AP); ns, two-tailed t-test] (Figure 5.4 **E**).

The lack of an observed LEV effect using 4-AP as a mild synaptic activity enhancer did not corroborate with previous results published by Meehan et al. (Meehan et al., 2011). In order to ensure that the LEV effect was not masked by any off-target effects due to the use of a second drug, the cells were subjected to weak electrical stimulation (180 AP, 0.2 Hz) as a means for generating mild synaptic activity required to mediate uptake of LEV into neurones. SYP-pHluorin transfected neurones were exposed to mild electrical stimulation (180 AP, 0.2 Hz) in the presence of 100 µM LEV before being challenged by a train of action potentials (300 AP, 10 Hz) (Figure 5.5 **A**). Application of LEV in the presence of mild electrical stimulation did not significantly affect either the rate of SYP-pHluorin trafficking (ns, two-way ANOVA of traces normalised to peak at evoked transmission) (Figure 5.5 **B**) or the total amount of externalised SYP-pHluorin during evoked transmission compared to controls [Max $\Delta F/F_0$ (as a fraction of the total pHluorin pool) = 0.442 ± 0.057 (No LEV + 4-AP), 0.391 ± 0.051 (100 µM LEV + 4-AP); ns, two-tailed t-test] (Figure 5.5 **C**). The lack of any observable LEV effect despite the change of loading method suggests that it is unlikely that an effect of LEV was masked due to off-target effects in the cell due to use of 4-AP.

These experiments indicate the presence of LEV at the presynapse did not have any effect on SV recycling despite a reduction in synaptic stimulation used to load the drug.

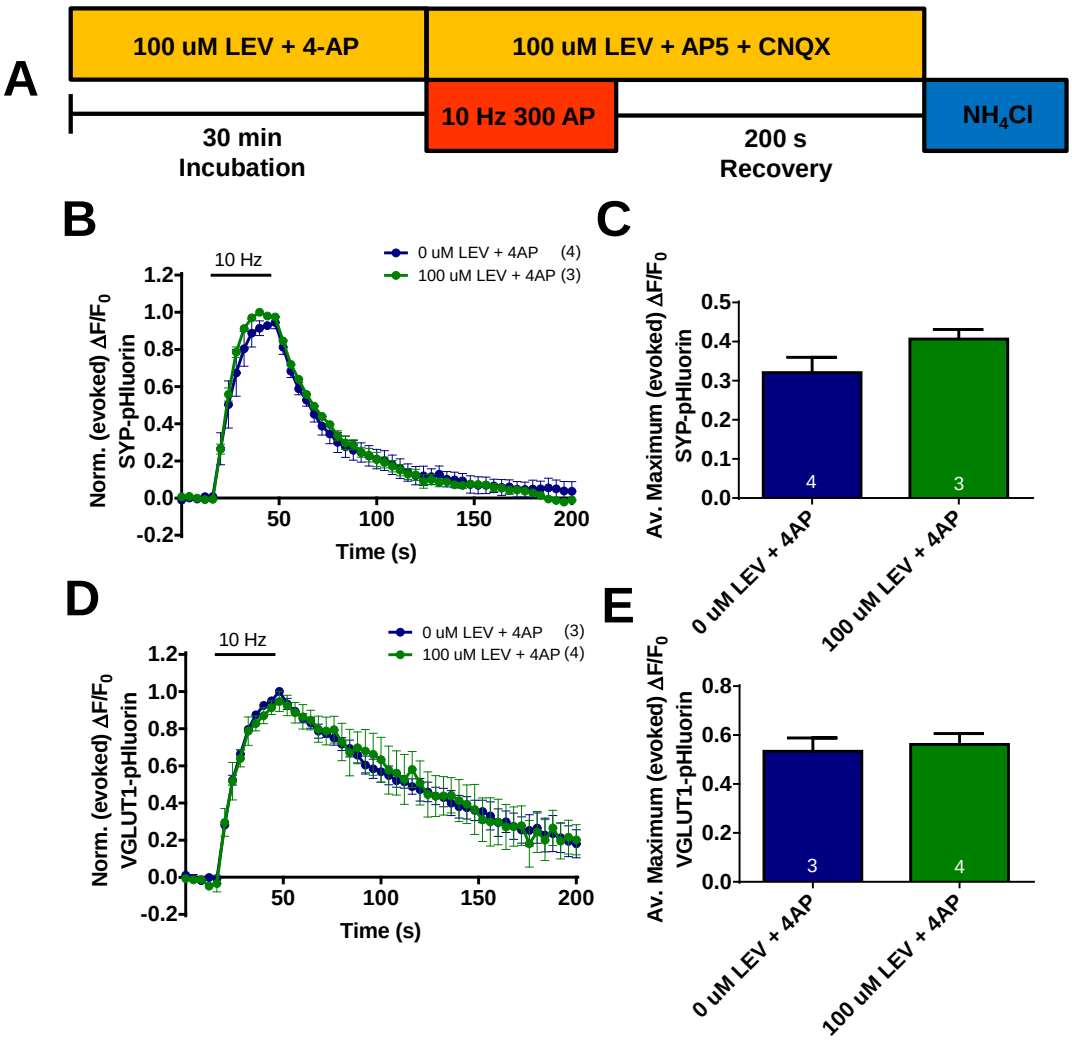

Figure 5.4: Application of 100 µM LEV in the presence of 4-AP induced activity does not affect SV recycling. A) Experimental scheme. Hippocampal neurones were incubated with levetiracetam (LEV, 100 µM) in the presence of 50 µM 4-AP for 30 min prior to stimulation with a train of 300 action potentials (APs, 10Hz). After 200 seconds of recovery, the total recycling synaptic vesicle (SV) pool was revealed with a NH_4Cl buffer pulse. **B,C)** SYP-pHluorin-transfected neurones were incubated with LEV (100 µM) in the presence of 50 µM 4-AP and stimulated with a train of 300 APs (10 Hz, indicated by bar). **B)** Graph displays the mean $\Delta F/F_0$ time course for SYP–pHluorin ± SEM normalized to the peak of stimulation [n=4 0 µM LEV, blue; n=3 100 µM LEV, green; ns, two-way ANOVA]. **C)** Mean maximum evoked SYP-pHluorin response ($\Delta F/F_0$) expressed as a fraction of the total SV pool (ns, two-tailed t-test). **D,E)** VGLUT1-pHluorin-transfected neurones were incubated with LEV (100 uM) in the presence of 4-AP and stimulated with a train of 300 APs (10 Hz). **D)** Graph displays the mean $\Delta F/F_0$ time course for VGLUT1–pHluorin ± SEM normalized to the peak of stimulation [n=3 0 µM LEV, blue; n=4 (100 µM LEV, green; ns, two-way ANOVA]. **E**) Mean maximum evoked VGLUT1-pHluorin response ($\Delta F/F_0$) expressed as a fraction of the total SV pool (ns, two-tailed t-test).

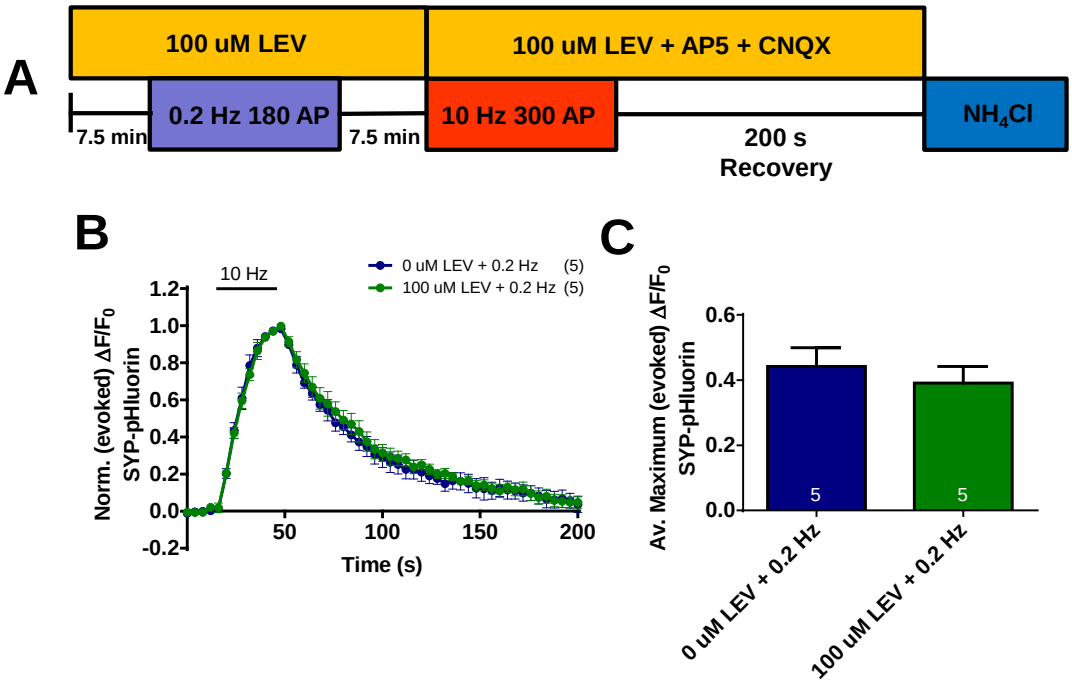

Figure 5.5: Application of 100 µM LEV in the presence of low-frequency electrical activity does not affect SV recycling. A) Experimental scheme. Hippocampal neurones were incubated with levetiracetam (LEV, 100 µM) in the presence of 180 AP (0.2Hz) prior to stimulation with a train of 300 action potentials (APs, 10Hz). After 200 seconds of recovery, the total recycling synaptic vesicle (SV) pool was revealed with a NH_4Cl buffer pulse. **B,C)** SYP-pHluorin-transfected neurones were incubated with LEV (100 µM) in the presence of 180 APs (0.2 Hz) and stimulated with a train of 300 APs (10 Hz, indicated by bar). **B)** Graph displays the mean $\Delta F/F_0$ time course for SYP–pHluorin ± SEM normalized to the peak of stimulation [n = 5 0 µM LEV, blue; n=5 100 µM LEV, green; ns, two-way ANOVA] **C)** Mean maximum evoked SYP-pHluorin response ($\Delta F/F_0$) expressed as a fraction of the total SV pool (ns, two-tailed t-test).

5.2.4 – Application of LEV in the Presence of Both Mild and Intense Synaptic Activity Does Not Affect SYT1 Trafficking

As SV2A is well documented to be the binding partner for both LEV and SYT1 (see chapter 3), there exists a potential mechanism for a presynaptic LEV effect that could be mediated through this SV2A-SYT1 interaction. Therefore, the hypothesis that LEV may specifically alter the trafficking of SYT1 through binding to SV2A was investigated. In order to investigate if LEV had an effect on SYT1-trafficking, SYT1-pHluorin transfected neurones were stimulated with an elevated KCl buffer containing 100 µM LEV. After depolarisation, the neurones were allowed to recover in normal buffer containing 100 µM LEV before being challenged by a train of action potentials (300 APs, 10Hz) (Figure 5.6 **A**). Application of LEV in the presence of 50 mM KCl-induced synaptic activity did not significantly affect either the rate of SYT1-pHluorin trafficking (ns, two-way ANOVA of traces normalised to peak at evoked transmission) (Figure 5.6 **B**) or the total amount of externalised SYT1-pHluorin during evoked transmission compared to controls [Max $\Delta F/F_0$ (as a fraction of the total pHluorin pool) = 0.331 ± 0.043 (100 µM LEV), 0.296 ± 0.015 (No LEV+ KCl), 0.270 ± 0.017 (100 µM LEV+KCl); ns, one-way ANOVA, P = 0.349, F = 1.19] (Figure 5.6 **C**).

In order to preclude the possibility that intense stimulation might be disrupting any weak LEV effect, previous experiments were replicated with the use of 4-AP as a mild enhancer of non-evoked synaptic activity. SYT1-pHluorin transfected neurones were incubated in 100 µM LEV, in the presence of 4-AP, before being challenged by a train of action potentials (300 AP, 10 Hz) (Figure 5.7 **A**). Application of LEV in the presence of 4-AP-induced synaptic activity did not significantly affect either the

rate of SYT1-pHluorin trafficking (ns, two-way ANOVA of traces normalised to peak at evoked transmission) (Figure 5.7 **B**) or the total amount of externalised SYT1-pHluorin during evoked transmission compared to controls [Max $\Delta F/F_0$ (as a fraction of the total pHluorin pool) = 0.410 ± 0.055 (100 µM LEV), 0.450 ± 0.039 (No LEV + KCl), 0.469 ± 0.015 (100 µM LEV+KCl); ns, one-way ANOVA, P = 0.469, F = 0.786] (Figure 5.7 **C**).

These experiments indicate that the use of LEV in the presence of either intense or mild synaptic stimulation did not alter the trafficking behaviour of SYT1 at the presynapse.

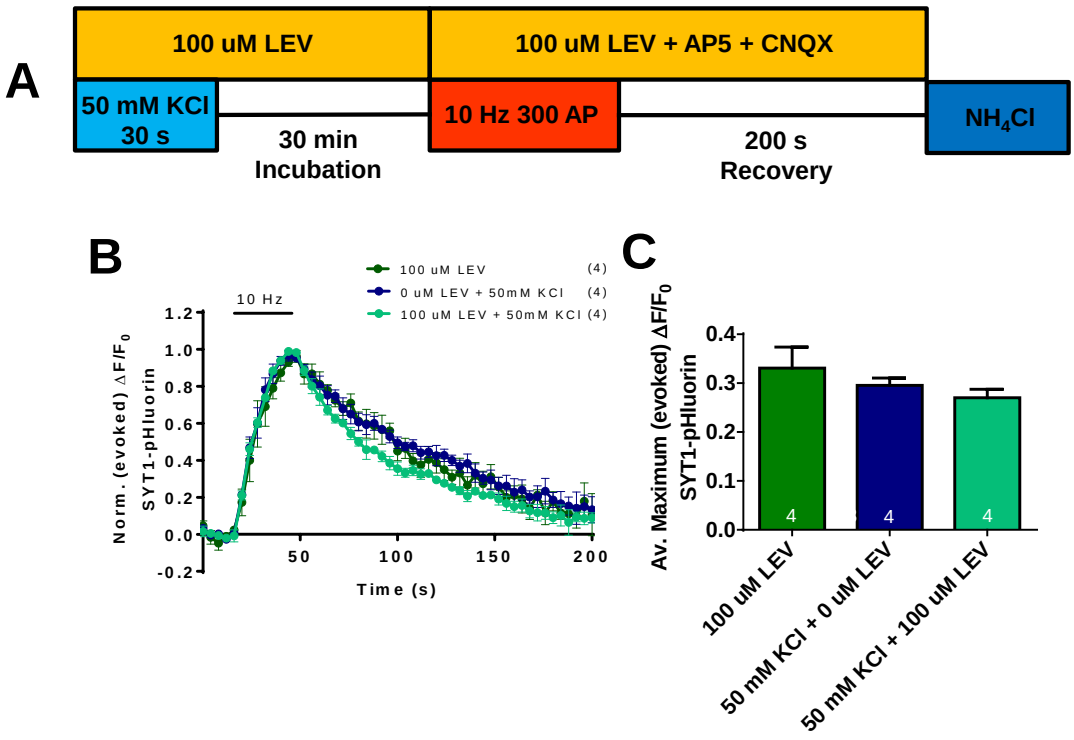

Figure 5.6: Application of 100 µM LEV in the presence of 50 mM KCl-induced activity does not affect SYT1 recycling. A) Experimental scheme. Hippocampal neurones were clamped in a membrane depolarised state with 50 mM KCl in the presence of levetiracetam (LEV, 100 µM) and then incubated in LEV for 30 min prior to stimulation with a train of 300 action potentials (APs, 10Hz). After 200 seconds of recovery, the total recycling synaptic vesicle (SV) pool was revealed with a NH_4Cl buffer pulse. **B,C)** SYT1-pHluorin-transfected neurones were incubated with LEV (100µM) after 50 mM KCl induced loading and stimulated with a train of 300 APs (10 Hz, indicated by bar). **B)** Graph displays the mean $\Delta F/F_0$ time course for SYT1–pHluorin ± SEM normalized to the peak of stimulation [n=4 100 µM LEV, green; n=4 0 µM LEV+50 mM KCl, blue; n=4 100 µM+50mM KCl, cyan; ns, two-way ANOVA]. **C)** Mean maximum evoked SYT1-pHluorin response ($\Delta F/F_0$) expressed as a fraction of the total SV pool (ns, one-way ANOVA, P=0.349, F=1.19).

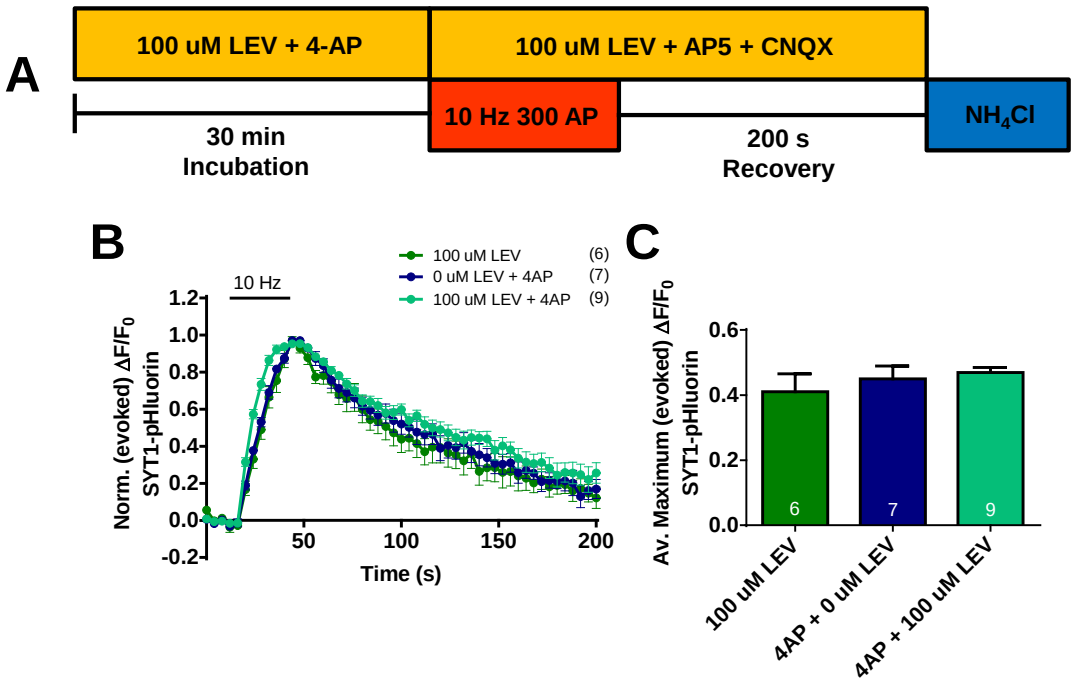

Figure 5.7: Application of 100 µM LEV in the presence of 4-AP-induced activity does not affect SYT1 recycling. A) Experimental scheme. Hippocampal neurones were incubated with levetiracetam (LEV, 100 µM) in the presence of 50 uM 4-AP for 30 min prior to stimulation with a train of 300 action potentials (APs, 10Hz). After 200 seconds of recovery, the total recycling synaptic vesicle (SV) pool was revealed with a NH_4Cl buffer pulse. **B,C)** SYT1-pHluorin-transfected neurones were incubated with LEV (100 uM) in the presence of 4AP and stimulated with a train of 300 APs (10 Hz). **B)** Graph displays the mean $\Delta F/F_0$ time course for SYT1–pHluorin ± SEM normalized to the peak of stimulation [n=6 100 µM LEV, green; n=7 0 µM LEV+50mM KCl, blue; n=9 100 µM LEV+50mM KCl, cyan; ns, two-way ANOVA]. **C)** Mean maximum evoked SYT1-pHluorin response ($\Delta F/F_0$) expressed as a fraction of the total SV pool (ns, one-way ANOVA, P=0.469, F=0.786).

5.2.5 – Verification of Effects of KCl and 4-AP on Synaptic Activity

The lack of any LEV effect observed with the previous experiments did not corroborate with published data indicating a mechanism of LEV action at the presynapse (Nowack et al., 2011, Meehan et al., 2011, Meehan et al., 2012). To ensure that this lack of effect was not due to a failure in the protocols to stimulate synaptic activity, the effect of 50 mM KCl and 50 µM 4-AP on synaptic Ca^{2+} responses was visualised by use of the fluorescent calcium reporter Fluo-3 AM. To verify the protocol for stimulating intense synaptic activity, hippocampal neurones that were loaded with Fluo-3 AM were stimulated with an elevated KCl buffer (50 mM). The cells were allowed to recover before being challenged by a train of action potentials (300 AP, 10 Hz) to act as a positive control for the experiment (Figure 5.8 **A**). Application of elevated KCl buffer to the neurones led to a significant transient increase in the level of intracellular free calcium to nearly two-fold the level observed under electrical stimulation ($p < 0.05$, two-way ANOVA of traces normalised to peak of calcium response at evoked transmission) (Figure 5.8 **C**).

To verify the protocol for stimulating mild synaptic activity, hippocampal neurones loaded with Fluo-3 AM were stimulated with 50 µM 4-AP. The cells were allowed to recover before being challenged by a train of action potentials (300 AP, 10 Hz) (Figure 5.8 **B**). Application of 50 µM 4-AP to the neurones led to significant long lasting increase in levels of intracellular free calcium of about 0.2 fold the level observed under electrical stimulation ($p < 0.05$, two-way ANOVA of traces normalised to peak of calcium activity at evoked transmission) (Figure 5.8 **D**).

These experiments verified that the protocols alteredpresynaptic activity as predicted and that the lack an experimental LEV effectwas not due to protocol failures.

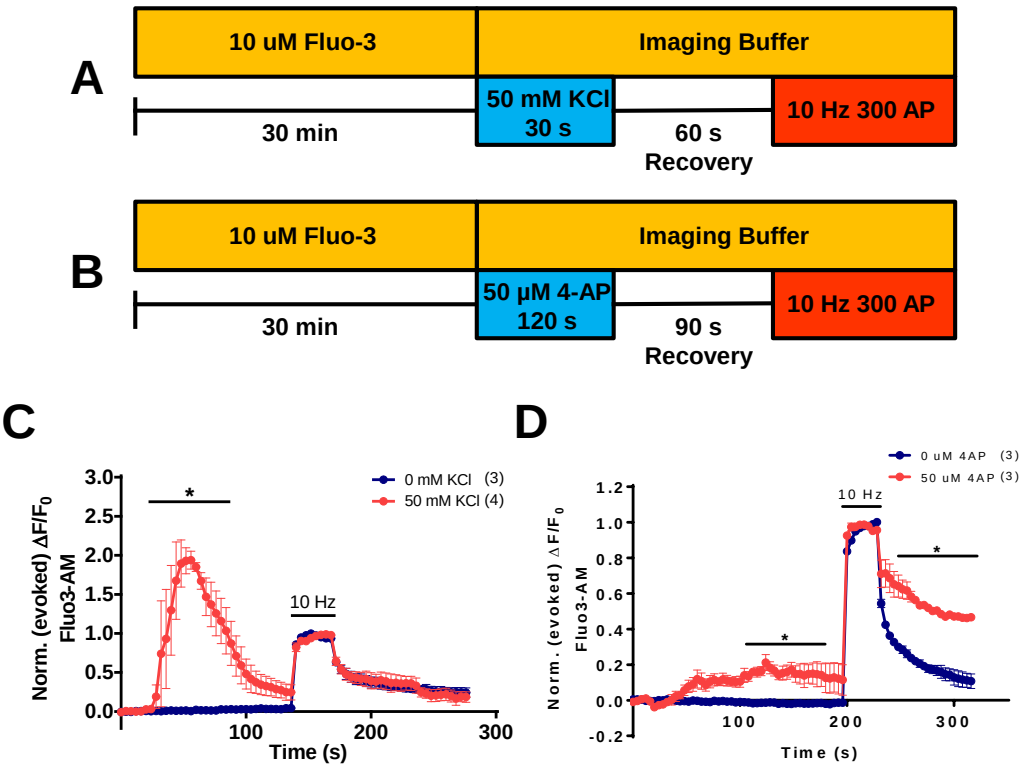

Figure 5.8: Verification of the effects of KCl and 4-AP on synaptic activity. A) Experimental scheme. Hippocampal neurones were incubated with 10 µM Fluo-3 AM for 30 min prior to a 30 s stimulation with 50 mM KCl. The neurones were allowed to recover being challenged with a train of 300 action potentials (APs, 10Hz). **B)** Experimental scheme. Hippocampal neurones were incubated with 10 µM Fluo-3 AM for 30 min prior to a 120 s stimulation with 50 µM 4-AP. The neurones were allowed to recover being challenged with a train of 300 action potentials (APs, 10Hz). **C)** Neurones were incubated in 50 mM KCl for 30 s before being stimulated with a train of 300 action potentials (AP, 10 Hz). Graph displays the mean $\Delta F/F_0$ time course for Fluo-3 AM ± SEM normalized to the peak of electrical stimulation [n=3 0 mM KCl, blue; n=4 50 mM KCl, pink; *p<0.05, two-way ANOVA, Bonferroni's post-hoc (over times indicated by the solid lines)]. **D)** Neurones were incubated in 50 µM 4-AP for 120 s before being stimulated with a train of 300 action potentials (AP, 10 Hz). Graph displays the mean $\Delta F/F_0$ time course for Fluo-3 AM ± SEM normalized to the peak of electrical stimulation [n=3 0 µM 4-AP, blue; n=3 50 µM 4-AP, pink; *p<0.05, two-way ANOVA, Bonferroni's post-hoc (over times indicated by the solid lines)].

5.3. – Discussion on the Effects of LEV on SV and SYT1 Recycling

The exact mechanism by which LEV functions in the treatment of generalised seizures remains unknown, even though it is one of the most popular anti-epileptic drugs available on the market. The SV protein SV2A was has been shown to mediate LEV entry into the neurone via SV recycling at the presynapse (Lynch et al., 2004). Several electrophysiological studies (previously described in chapter 5.1) have demonstrated that LEV has a mechanism of action at the post-synapse (Yang et al., 2007, Meehan et al., 2011, Meehan et al., 2012). Immunohistochemistry experiments have also indicated possible modulation of key SV protein levels at the presynapse (Nowack et al., 2011), however studies that investigate the real-time trafficking of key SV proteins during synaptic activity, under the influence of LEV action, has not been documented.

5.3.1 – Treatment of Neurones with LEV under Mild/Strong Synaptic Simulation Does Not Affect Recycling of SYP or VGLUT1

Previous experiments have demonstrated that long incubation times of greater than 3 hrs are required to evoke a LEV effect on mammalian hippocampal tissue slices (Meehan et al., 2011). In agreement with this finding, it has been also shown that incubation with LEV for up to 6-10 hours is necessary for revealing a LEV effect on regulating SYT1 and SV2A expression levels at the presynapse in primary hippocampal cell cultures (Nowack et al., 2011). In my initial experiments, it was observed that the acute application of 100-300 µM LEV onto hippocampal cell

cultures revealed no effect on the recycling of key SV proteins synaptophysin (SYP) and VGLUT1. This is in agreement with previously published literature.

An early LEV effect was achieved in hippocampal slices by increasing synaptic activity upon application of the drug by use of 4-aminopyridine [4-AP, a potassium channel blocker that is known to increase spontaneous ESPC frequency and amplitude (Buckle and Haas, 1982)] as well as low-frequency electrical stimulation (0.2 Hz). These actions presumably increase the rate of internalisation of LEV molecules into the neurone, resulting in accelerated action. Interestingly, the same study revealed that the use of higher intensity stimulation (10 Hz compared to 0.2 Hz) abolished any observed LEV effects in hippocampal slices (Meehan et al., 2011). A possible explanation for this observation is that LEV is still taken up by SVs, but is immediately released again due to the higher intensity of stimulation, thus negating the uptake overall. In my experiments, the use of a high KCl solution (50 mM) to clamp neurones in a membrane-depolarised state during incubation with LEV resulted in no observable drug effect on the recycling of SYP and VGLUT1. This result indicates that clamping the membrane potential in a depolarised state does not promote a LEV effect on the general SV recycling, which is in agreement with previously published data. Another possible reason for the lack of a LEV effect under elevated KCl conditions is the uptake of LEV by ADBE into bulk endosomes, since ADBE is the dominant mode of endocytosis under these conditions (Clayton et al., 2008).

Interestingly, the use of 4-AP to increase spontaneous neuronal network activity during incubation of the neurones with LEV resulted in no significant effect on general SV recycling. Stimulation of the cells using low frequency electrical

stimulation (0.2 Hz) during incubation of neurones with LEV also revealed no significant LEV effect on general SV recycling. This is in contrast to previous observations by Meehan et.al where LEV was shown to have a modulating effect on synaptic activity in hippocampal slices. The lack of an observed drug effect cannot be attributed to a fault in the protocol for the generation of synaptic activity during LEV incubation, as control experiments showed that the use of 50 mM KCl and 75 µM 4-AP in solution resulted in an observable increase in baseline neuronal activity, using intracellular free calcium as a reporter. There are several possible explanations for these observations: Firstly, although LEV has previously been documented to enter the synapse via binding to SV2A in SVs, there has been no clear evidence that the drug has a mode of action that alters SV recycling. If SV2A does play a part in the immobilisation and liberation of neurotransmitter as previously been suggested (Reigada et al., 2003), then LEV could alter the efficiency of neurotransmitter refilling in SVs. If SVs do not refill themselves efficiently, this may have an effect on the release probability of SVs. In support of this, recent optogenetic studies have suggested that incompletely filled SVs exhibit a lower release probability compared to full SVs (Rost et al., 2015). If this mode of action is true, it could be revealed by investigating on the effect of LEV on the frequency of spontaneous EPSCs in cell electrophysiological studies. Secondly, LEV may act specifically on inhibitory neurones with minimal effect on excitatory neurones. As hippocampal cell cultures contain a higher proportion of excitatory neurones, any potential LEV effect mediated by inhibitory neurones may be masked. Studies using SV2A L174Q missense mutant animals have demonstrated that dysfunction of SV2A preferentially disrupts action potential-induced GABA, but not glutamate, release in the limbic

regions of the brain (e.g. hippocampus) and greatly facilitates kindling epileptogenesis (Tokudome et al., 2016). This evidence suggests that the SV2A-GABAergic system may play a crucial role in modulating epileptogenesis. If LEV has a mode of action at inhibitory neurones, future experiments to investigate SV recycling in inhibitory neurones by use of fluorescent anti-VGAT C antibodies to label cellular VGAT *in vivo* (Martens et al., 2008) may prove fruitful. Lastly, the previous experiments by Meehan demonstrated that the LEV effect was only observable when the concentrations of LEV used were significantly higher (300 µM) than the known clinically relevant concentrations used in treatment of epilepsy in humans [70-140 µM, (Leppik, 2002)]. When a lower LEV concentration was used in the key experiments of this study (100 µM), no significant LEV effect was observed. While it is clear that incubation of mammalian tissue with high concentrations of LEV revealed a drug effect on synaptic transmission within a shortened timeframe, more work needs to be done to affirm that this effect can be observed when LEV is used at clinically relevant doses.

5.3.2 – Treatment of Neurones with LEV under Mild/Strong Synaptic Stimulation Does Not Affect Recycling of SYT1

As SV2A has been previously shown to be an intrinsic trafficking partner for SYT1 (chapter 3) as well as a binding partner for LEV, it is possible that LEV may have a role in modulating the recycling of SYT1, which is a key SV protein involved in the docking and fusion of vesicles at the presynapse. In experiments designed to probe the effect of LEV on SYT1 recycling, the use of 4-AP to increase spontaneous neuronal network activity during incubation of the neurones with LEV resulted in no

significant observed effect on SYT1 recycling. This is consistent with the results discussed above where LEV displayed no effect on general SV recycling. There are several explanations for the observed results. Firstly, it is possible that synaptic activity is a key factor in determining the onset of LEV's anti-epileptic action *in vivo.* Previous pharmacokinetic research has indicated that concentration levels of LEV in cerebrospinal fluid reaches its peak within a few hours after initial oral administration, yet the onset of LEV's anti-convulsant effect can take up to two days after treatment initiation (Stefan et al., 2006). This delayed onset of drug action could be explained by the requirement of synaptic activity to "load" LEV into presynaptic terminals, most likely by binding of LEV to SV2A and internalisation during SV recycling. Secondly, LEV may have a function in altering protein synthesis or protein degradation at the presynapse. This phenomenon would not have been observed using the assays used in this study. Future experiments probing the effect of LEV on protein translation and transport from the soma as well as the effect of LEV on classical endocytosis and protein ubiquitination in central synapses may shed further light on these hypotheses.

5.3.3 – Implications of SV2A in Promoting a LEV Effect at the Presynapse

If LEV exhibits no effect on general SV recycling or specific SYT1 recycling at the presynapse, then the role that SV2A plays in mediating LEV entry into the synaptic terminal must be further discussed. SV2A contains several putative LEV binding sites, thus there is a high possibility that SV2A may simply act as a carrier for the drug into the synapse and that LEV has a mode of action that is largely disconnected from SV recycling. The question remains: Is the LEV effect on synapses dependent

on the normal SV2A function? There is evidence to show that LEV has the ability to rescue deficits in SV2A and SYT1 expression and presynaptic localisation when SV2A is overexpressed, however no literature has been published which documents the effect of LEV on neurones where SV2A expression is ablated or SV2A function has been altered. Further immunofluorescence studies using LEV in SV2A knockdown cell cultures may provide further insight to the effects of LEV at the presynapse. If LEV does indeed rescue the expression of SV2A in an SV2A knockdown neurone, then it can be ascertained that the drug has a modulating effect on SV2A expression levels in neurones. Mechanisms of SV2A action can then be probed through further immunofluorescence loss-of-function experiments where SV2A knockdown is subsequently rescued using either SV2A mutants that exhibit defects in SV protein trafficking (e.g. Y46A, T84A), or SV2A mutants where the LEV-binding site (W666) is mutated and ablated.

Another question that remains unanswered is whether LEV has an effect on the recycling behaviour of SV2A itself. If SV2A is the intrinsic trafficking partner for SYT1 at the presynapse, then it follows that SYT1 recycling will be closely coupled to SV2A recycling. Since these results demonstrate that LEV has no observable effect on SYT1 recycling, it can be predicted that the drug would also exert no observable effects on the recycling of SV2A. Future live-cell, epifluorescence experiments in the presence of LEV using SV2A-pHluorin as a tool for observing SV2A trafficking will provide the platform for answering this key question.

It is also possible that LEV has a mode of action on SV2A at inhibitory synapses rather than excitatory synapses. Traditional hippocampal culture preparations consist of predominantly excitatory synapses, with only around 6% of the total number of

cultured synapses being inhibitory (Benson et al., 1994). As a result, any presynaptic LEV effect at inhibitory synapses may not be revealed by the techniques used in this study. Further studies of a potential LEV effect on SV2A function in inhibitory synapse-enriched hippocampal cell cultures is required to provide a full picture. In conclusion, live-cell epifluorescence studies after 30-minute incubation with LEV have shown that there is no drug effect on the general SV and SYT1 recycling.

6.0 – Final Discussion

6.1 – Final Discussion of Studies

The sorting and retrieval of SV cargo from the presynaptic plasma membrane is a highly complex process with specific monomeric adaptor proteins such as AP-2 playing a key role (Kelly and Owen, 2011). There is, however, evidence which indicates that certain SV proteins, such as SYP and SYB2, are intrinsically coupled and recycled as a complex during compensatory endocytosis (Gordon et al., 2011). The investigations in this thesis have provided evidence of a similar trafficking relationship between SV2A and SYT1 at the presynapse, and there is further evidence to indicate that defects in the trafficking of the SV2A/SYT1 complex caused by a point mutation may serve as an underlying mechanism for the cause of generalised epilepsy in humans.

6.2 – SV2A and SYT1 are Intrinsic Trafficking Partners at the Presynapse

The retrieval of SV2A during SV endocytosis is predominantly governed by the adaptor protein AP-2, whilst SYT1 is retrieved by the monomeric adaptor stonin-2 (which itself binds to AP-2) during SV endocytosis. The experiments in this study have shown that the trafficking of SYT1 is greatly dependent on SV2A binding to both AP-2 and SYT1, since the defects in AP-2 SV2A binding led to increased surface expression, mislocalisation and accelerated retrieval of SYT1 during compensatory endocytosis. In agreement with this, the loss of stonin-2 at the synaptic terminal also results in increased surface expression and accelerated retrieval of SYT1 (Kononenko et al., 2013). These data suggest that the trafficking of SYT1 at the presynapse is tightly regulated by not just one specific adaptor protein, but

instead a synergistic effort between several key proteins. It is proposed that SYT1 trafficking at the presynapse is dependent on two key factors: 1) the phosphorylation-mediated binding of SYT1 to SV2A at residues at the C2B domain and 2) the binding of SYT1 to stonin-2 at the C2A domain. Since both stonin-2 and SV2A cargo are directed and sorted by AP-2 during SV endocytosis, it is likely that AP-2 indirectly influences the endocytic sorting of SYT1 through its interactions with both SV2A and stonin-2. It is proposed that two different complexes are formed during SV CME that internalises SYT1 via two different mechanisms: 1) an AP-2-SV2A-SYT1 complex which is dependent on the phosphorylation-mediated SV2A-SYT1 interaction and 2) an AP-2-stonin-2-SYT1 complex which is independent of phosphorylation. Disruption of either pathway is therefore insufficient to cause total ablation of SYT1 trafficking, as the other sorting pathway is altered to maintain sufficient SYT1 retrieval for normal neurotransmission. In agreement with this, the Y46A SV2A mutation did not affect the retrieval of SYP in this study and the loss of stonin-2 also revealed no effect on endocytic sorting of SYP in earlier mentioned studies. In both cases, SYT1 retrieval is accelerated when their respective pathways were disrupted as opposed to retardation of retrieval normally observed when endocytic sorting mechanisms are disrupted. The lack of normal function in either SV2A or stonin-2 may trigger a cellular rescue mechanism by which SYT1 is retrieved by faster, clathrin-independent endocytic pathway such as ADBE or ultrafast endocytosis. On the bulk endosome that is formed, SV cargo sorting is predominantly mediated by AP-1 and AP-3, rather than AP-2, and thus a steady supply of SYT1 is maintained for presynaptic function. In support of this, electron micrographs and immunofluorescence experiments of stonin-2 deficient mice

hippocampal tissue has revealed profound decrease in the number and size of endosomal structures and a significant up-regulation of AP-1 at the synaptic boutons (Kononenko et al., 2013).

6.3 – The Epilepsy-related R383Q SV2A Mutation Perturbs the AP-2-SV2A-SYT1 CME Pathway

The initial discovery of the homozygous R383Q mutation in SV2A leading to intractable epilepsy and involuntary movements in a five-year old South East Asian girl presented the first indication that SV2A dysfunction may play an underlying role in the onset of epileptogenesis (Serajee and Huq, 2015). Building on from earlier work, pHluorin imaging studies in this thesis has demonstrated that genetic knockdown and rescue of SV2A with a R383Q mutant variant led to an increased surface expression and mislocalisation of SYT1 at the synaptic terminal, an increased ratio of externalised SYT1 during SV exocytosis and an acceleration of its retrieval during SV endocytosis. This observed phenotype mimics those seen with the Y46A SV2A mutant as well as earlier data obtained from stonin-2 knockdown experiments, suggesting that the presence of the R383Q mutation in SV2A perturbs the abovementioned AP-2-SV2A-SYT1 retrieval pathway during CME.

How the does R383Q mutation affect this CME pathway? One possibility that has already been discussed is that the R383 residue lies within known adenine-nucleotide binding sites of SV2A, suggesting that molecules such as ATP, ADP and AMP which are involved in cellular energy transfer may be transient binding partners for SV2A at the presynapse. This is supported by observations that R383Q/E mutant

variants of the SV2A cytosolic loop resulted in altered protein interactions with certain subunits of V-ATPase. There is very currently little evidence to support the role of SV2A as a transporter protein in synaptic terminals, despite its highly conserved sequence homology with the MFS transporter family of proteins, thus it is unlikely that SV2A is solely responsible for the transport of ATP at the presynapse. The potential binding of adenine nucleotides to SV2A may however be critical for the retrieval of SYT1 during SV endocytosis, since the SV2A-SYT1 interaction is dependent upon the availability of inorganic phosphate carriers (such as ATP) for the phosphorylation of the T84A residue by TTBK 1/2 (Zhang et al., 2015). Disruption of the adenine nucleotide-binding site due to the R383Q mutation may therefore lead to defects in the phosphorylation of SV2A at T84 resulting in defective SYT1 binding and therefore trafficking at the presynapse. In support of this, it has been previously documented that SV2A forms the core for an intra-vesicular matrix that is responsible for the immobilisation and release of ATP, thus regulating the availability of freely diffusible ATP (Reigada et al., 2003). The alteration of SV2A interaction with the cellular cytoskeleton may also be crucial to the localisation of SYT1 to synaptic terminals, since this study has shown that presence of the R383Q/E mutation leads to altered interactions with actin and tubulin, which are key cytoskeletal proteins. It is possible that the change in residue charge at 383 leads to localised protein misfolding, which may act to disrupt the ability of SV2A to bind to actin and tubulin thus leading to the mislocalisation of SV2A. This theory is supported by recent unpublished SV2A-pHluorin studies revealing a significant increase in the surface expression of R383Q SV2A compared to WT SV2A (Dr. Callista Harper, Edinburgh, data not shown).

6.4 – There is a Lack of Evidence to Support a Mechanism for LEV Function via Modulation of the AP-2-SV2A-SYT1 CME Pathway

SV2A is known to be a binding partner for the popular anti-epileptic drug, LEV, at the presynaptic terminal (Lynch et al., 2004), however it has not been determined whether SV2A dysfunction has an integral role in the onset of epilepsy-related symptoms or if it acts simply as a transporter of the drug into the presynapse. It was initially hypothesised that the drug may have a mode of action at the AP-2-SV2A-SYT1 CME pathway that is mediated by SV2A binding. The treatment of hippocampal cultures with LEV did not reveal any SV2A-mediated drug effects on the trafficking of SYT1 or SV recycling at the presynapse, suggesting that LEV does not have a mode of action mediated by the trafficking of the AP-2-SV2A-SYT1 complex. This finding is in contrast with previously described work showing that LEV rescues normal levels of SV2A and SYT1 at the presynapse in SV2A knockout (Nowack et al., 2011), however this is likely explained by the differences in the incubation times and model systems used. Considering all evidence, it is most likely that entry of LEV into the synapse is mediated by SV2A binding and may have a significant effect on the expression and localisation of both SV2A and SYT1, however, it does not have a profound drug effect on the mechanisms involved in CME of SV2A and SYT1.

6.5 – Model of SV2A-Mediated SYT1 Trafficking at the Presynaptic Terminal

The trafficking of SV2A at the presynaptic terminal is mediated by binding to the adaptor protein AP-2 at residue Y46. SV2A itself binds to SYT1 and this interaction is mediated by phosphorylation of residue T84. It is proposed that these specific

interactions between SV2A, SYT1, stonin-2 and AP-2 at the synaptic terminal may aid the presentation of these SV cargos in the correct conformation needed for binding and clustering. This ensures maximum retrieval efficiency when all members are present and potential functional redundancy when one member is absent or mutated. The phosphorylation of SV2A may play a key regulatory role in this process, as it may mediate SYT1's access to AP-2. Phosphorylated SV2A may bind to both the C2B domain of SYT1 as well as AP-2. This brings SYT1 and AP-2 to close proximity with each other and potentiates binding between AP-2 and the C2B domain of SYT1, facilitating the retrieval of SYT1 and SV endocytosis. Stonin-2 continues to interact with the C2A and C2B domains of SYT1 as well as AP-2 in a separate mechanistic pathway to assist in SYT1 retrieval and endocytosis. The normal trafficking of SYT1 is dependent upon the fidelity of this process, and any perturbations to key interactions in the formation of this complex result in defective SYT1 expression and localisation at the plasma membrane and an acceleration of its retrieval during SV endocytosis. Disruption of the formation of the complex may be achieved either through ablation of any binding interactions between the three proteins (Y46, T84), or through disruption of key adenine-nucleotide binding motifs (R383) in SV2A. It is proposed that either arrestment of ATP binding at these sites in SV2A, or the misfolding of SV2A caused by the R383Q mutation, results in an inability of the protein to bind properly to SYT1. This causes downstream defects in SYT1 trafficking at the presynaptic terminal and may present an underlying mechanism in the onset of certain seizure phenotypes in humans. In support of this, previous clinical studies have demonstrated altered SYT1 expression in the temporal lobe tissue of patients with refractory epilepsy (Xiao et al., 2009).

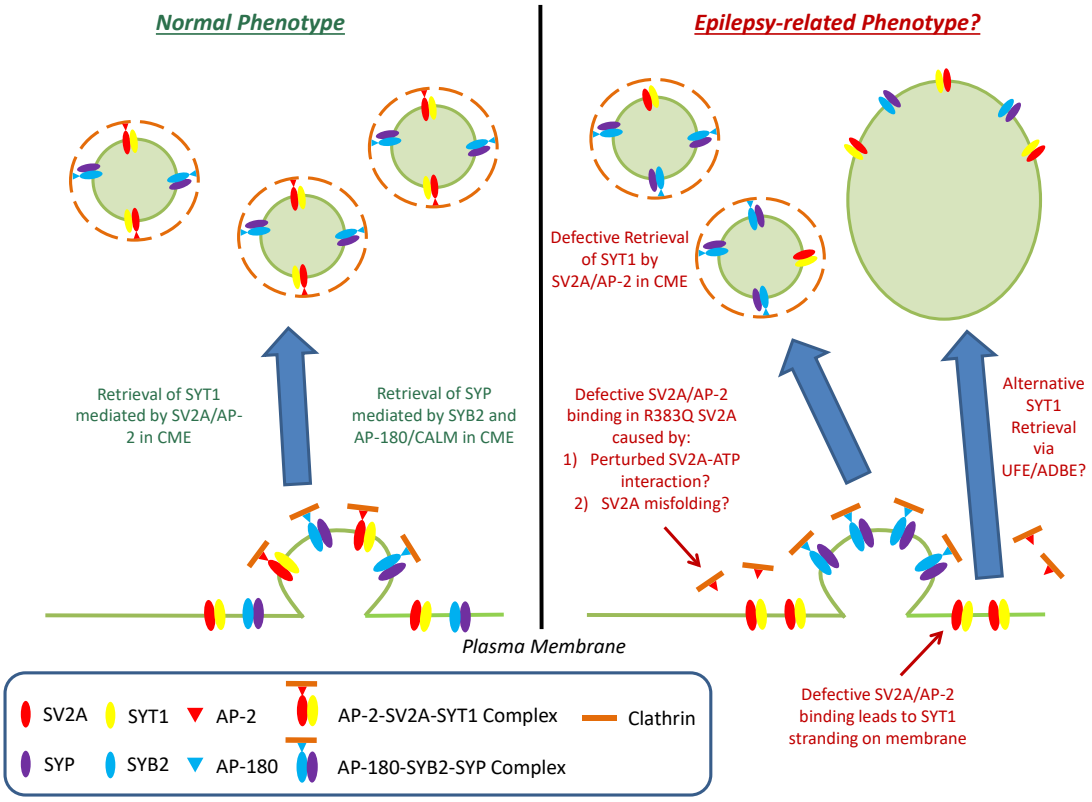

Figure 6.5: Model of SV2A-mediated SYT1 trafficking at the presynaptic terminal. The trafficking of SYT1 at the presynaptic terminal is partially mediated by formation of the AP-2-SV2A-SYT1 complex. Disruption of the formation of this complex via ablation of the AP-2-SV2A interaction (Y46A) or SV2A-SYT1 interaction (T84A) leads to aberrant localisation and expression of SYT1 at the plasma membrane and an acceleration of its retrieval during SV endocytosis. This acceleration may be explained by either an increased retrieval by other adaptor proteins such as stonin-2, or the retrieval of SYT1 by a faster alternative mechanism such as UFE/ADBE. The epilepsy-related R383Q SV2A mutation may perturb SYT1 retrieval through disruption of key adenine-nucleotide binding sites in SV2A, causing arrestment of ATP binding to SV2A that result in an inability of SV2A to bind properly to SYT1. SV2A protein misfolding caused by the R383Q mutation may also play a role in the disrupting normal SV2A-SYT1 interactions.

6.6 – Future Work

There are a number of future studies that could be attempted in order to expand and clarify the mechanisms by which SV2A mediates the trafficking of SYT1 at the presynaptic terminal.

6.6.1 – Retrieval of SYT1 by a Parallel Endocytic Mechanism When CME Pathway is Perturbed

It has been proposed earlier that the acceleration of SYT1 retrieval due to defective SV2A binding may have due to the activation of a mode of endocytosis that operates on a faster timescale compared to CME. This mode of endocytosis may be ADBE or ultrafast endocytosis. Labelling of SYT1 during immunoelectron microscopy of hippocampal neurones after stimulation in the presence of Y46A SV2A or defective SYT1-binding stonin-2 may shed light on a possible increased accumulation of SYT1 on bulk endosomal structures compared to WT SV2A, thus providing evidence of ADBE as an alternative retrieval mechanism for SYT1 when CME is perturbed. In addition, a modified approach of the 'flash-and-freeze' cryo-electron microscopy technique (Watanabe et al., 2013b) to include SYT1 immunolabelling used on hippocampal tissue from Y46A SV2A or a stonin-2 knockout mice models may provide evidence of a role for ultrafast endocytosis in the retrieval of SYT1 when CME is perturbed.

6.6.2 – The Dependency of SV2A-SYT1 Complex Formation on the Presence of ATP

It has been proposed in this thesis that the R383Q mutation alters the AP-2-SV2A-SYT1 complex. The R383 mutation lies within the adenine nucleotide binding region of SV2A, suggesting that ATP binding may play a key role in the maintenance of the AP-2-SV2A-SYT1 complex. Further SV2A/SYT1 affinity studies in the absence and presence of ATP may provide further insight on this hypothesis. In addition, biochemical experiments probing the capability of TTBK 1/2 to phosphorylate SV2A (Zhang et al., 2015) in the presence of the R383Q mutation would provide further support for the requirement of local presence of ATP for the formation of the SV2A-SYT1 complex. If it were true that ATP is essential for the formation of the complex, then it would be interesting to determine the outcome when the second ATP binding site (residues 59-162) in SV2A is disrupted or ablated. Since this binding site is in far closer proximity to the SV2A-SYT1 binding site compared to the R383 site, it would be useful to probe if the two adenine-binding sites are have an equal influence on SV2A-SYT1 binding or if one site is dominant over the other. Experiments comparing the effect of double ablation of both binding sites compares to just a single ablation may provide further insight to the ablation of either adenine-binding site affects the same SYT1 retrieval pathway, or if the adenine-binding sites perform different roles for SV2A in SV recycling. Finally, it would be interesting to probe if the R383Q SV2A mutation activates parallel endocytic modes to aid in the retrieval of SYT1. Similar to experiments described above, SYT1-labelled immunoelectron microscopy or ‘flash-and-freeze’ experiments may reveal ADBE or ultrafast endocytosis as the primary mode of SYT1 retrieval when CME is perturbed.

6.6.3 – Probing the Involvement of the Neuronal Cytoskeleton on SYT1 Trafficking

The discovery that the SV2A cytosolic loop interacts with actin and tubulin in pulldown experiments suggests that interaction between SV2A and the neuronal cytoskeleton may be a key step in the retrieval of SYT1 during SV endocytosis. It is possible that the neuronal cytoskeleton is involved in the siphoning of SYT1 and other SV cargo away from the active zone in preparation for its retrieval, thus clearing the release sites in preparation for the next round of SV fusion. A possible method to investigate this phenomenon would be the use of super-resolution imaging techniques such as stimulated emission depletion (STED) or photo-activated localization (PALM) microscopy that allows cell imaging at a resolution great enough to differentiate between the active and periactive zone. Quantification of the travelling distance between SYT1 and the active zone (using an active zone marker such as GFP-Piccolo) after stimulation in fixed hippocampal culture samples transfected with either WT SV2A or R383Q SV2A may provide further insight into the role of SV2A in the clearing of release site blockage at the active zone. Similar techniques probing the diffusional spread and confinement of exocytosed SV proteins using STED microscopy have been previously described (Gimber et al., 2015).

6.6.4 – A Possible Mode of LEV Action on SV Recycling in Inhibitory Neurones

The lack of an observed LEV effect on SV recycling in this study may be attributable to a prevalent effect on inhibitory neurotransmission rather than excitatory. The viral transduction of the cells with an inhibitory synaptic marker such as GFP-fused (or its

coloured variants) versions of the vesicular GABA transporter (VGAT) or glutamate decarboxylase 1 (GAD1) in the presence of a GABA-ergic neurone-specific promoter (Rasmussen et al., 2007) may provide a means of identifying inhibitory synapses in prepared cultures of hippocampal neurones. SYT1-pHluorin imaging of these synapses will then provide further insight on a possible mode of LEV action on the inhibitory synaptic pathway.

7.0 – References

References

ADAMS, D. J., ARTHUR, C. P. & STOWELL, M. H. 2015. Architecture of the Synaptophysin/Synaptobrevin Complex: Structural Evidence for an Entropic Clustering Function at the Synapse. *Sci Rep,* 5**,** 13659.

ALABI, A. A. & TSIEN, R. W. 2012. Synaptic vesicle pools and dynamics. *Cold Spring Harb Perspect Biol,* 4**,** a013680.

ALDENKAMP, A. P., ALPHERTS, W. C., DIEPMAN, L., VAN 'T SLOT, B., OVERWEG, J. & VERMEULEN, J. 1994. Cognitive side-effects of phenytoin compared with carbamazepine in patients with localization-related epilepsy. *Epilepsy Res,* 19**,** 37-43.

ALDENKAMP, A. P., BAKER, G., MULDER, O. G., CHADWICK, D., COOPER, P., DOELMAN, J., DUNCAN, R., GASSMANN-MAYER, C., DE HAAN, G. J., HUGHSON, C., HULSMAN, J., OVERWEG, J., PLEDGER, G., RENTMEESTER, T. W., RIAZ, H. & WROE, S. 2000. A multicenter, randomized clinical study to evaluate the effect on cognitive function of topiramate compared with valproate as add-on therapy to carbamazepine in patients with partial-onset seizures. *Epilepsia,* 41**,** 1167-78.

ALTROCK, W. D., TOM DIECK, S., SOKOLOV, M., MEYER, A. C., SIGLER, A., BRAKEBUSCH, C., FÄSSLER, R., RICHTER, K., BOECKERS, T. M., POTSCHKA, H., BRANDT, C., LÖSCHER, W., GRIMBERG, D., DRESBACH, T., HEMPELMANN, A., HASSAN, H., BALSCHUN, D., FREY, J. U., BRANDSTÄTTER, J. H., GARNER, C. C., ROSENMUND, C. & GUNDELFINGER, E. D. 2003. Functional inactivation of a fraction of excitatory synapses in mice deficient for the active zone protein bassoon. *Neuron,* 37**,** 787-800.

ANDERSSON, F., JAKOBSSON, J., LÖW, P., SHUPLIAKOV, O. & BRODIN, L. 2008. Perturbation of syndapin/PACSIN impairs synaptic vesicle recycling evoked by intense stimulation. *J Neurosci,* 28**,** 3925-33.

ANGGONO, V., SMILLIE, K. J., GRAHAM, M. E., VALOVA, V. A., COUSIN, M. A. & ROBINSON, P. J. 2006. Syndapin I is the phosphorylation-regulated dynamin I partner in synaptic vesicle endocytosis. *Nature Neuroscience,* 9**,** 752-760.

ARIDON, P., MARINI, C., DI RESTA, C., BRILLI, E., DE FUSCO, M., POLITI, F., PARRINI, E., MANFREDI, I., PISANO, T., PRUNA, D., CURIA, G., CIANCHETTI, C., PASQUALETTI, M., BECCHETTI, A., GUERRINI, R. & CASARI, G. 2006. Increased sensitivity of the neuronal nicotinic receptor alpha 2 subunit causes familial epilepsy with nocturnal wandering and ictal fear. *Am J Hum Genet,* 79**,** 342-50.

ATLURI, P. P. & REGEHR, W. G. 1998. Delayed release of neurotransmitter from cerebellar granule cells. *J Neurosci,* 18**,** 8214-27.

ATLURI, P. P. & RYAN, T. A. 2006. The kinetics of synaptic vesicle reacidification at hippocampal nerve terminals. *J Neurosci,* 26**,** 2313-20.

AUGUSTIN, I., ROSENMUND, C., SÜDHOF, T. C. & BROSE, N. 1999. Munc13-1 is essential for fusion competence of glutamatergic synaptic vesicles. *Nature,* 400**,** 457-61.

BAGAL, S. K., MARRON, B. E., OWEN, R. M., STORER, R. I. & SWAIN, N. A. 2015. Voltage gated sodium channels as drug discovery targets. *Channels (Austin),* 9**,** 360-6.

BAI, D., ZHU, G., PENNEFATHER, P., JACKSON, M. F., MACDONALD, J. F. & ORSER, B. A. 2001. Distinct functional and pharmacological properties of tonic and quantal inhibitory postsynaptic currents mediated by gamma-aminobutyric acid(A) receptors in hippocampal neurons. *Mol Pharmacol,* 59**,** 814-24.

BAI, J., TUCKER, W. C. & CHAPMAN, E. R. 2004. PIP2 increases the speed of response of synaptotagmin and steers its membrane-penetration activity toward the plasma membrane. *Nat Struct Mol Biol,* 11**,** 36-44.

BAJJALIEH, S. M., FRANTZ, G. D., WEIMANN, J. M., MCCONNELL, S. K. & SCHELLER, R. H. 1994. DIFFERENTIAL EXPRESSION OF SYNAPTIC VESICLE PROTEIN-2 (SV2) ISOFORMS. *Journal of Neuroscience,* 14**,** 5223-5235.

BAJJALIEH, S. M., PETERSON, K., LINIAL, M. & SCHELLER, R. H. 1993. Brain contains two forms of synaptic vesicle protein 2. *Proc Natl Acad Sci U S A,* 90**,** 2150-4.

BALAJI, J. & RYAN, T. A. 2007. Single-vesicle imaging reveals that synaptic vesicle exocytosis and endocytosis are coupled by a single stochastic mode. *Proc Natl Acad Sci U S A,* 104**,** 20576-81.

BALDELLI, P., FASSIO, A., VALTORTA, F. & BENFENATI, F. 2007. Lack of synapsin I reduces the readily releasable pool of synaptic vesicles at central inhibitory synapses. *J Neurosci,* 27**,** 13520-31.

BAO, H., DANIELS, R. W., MACLEOD, G. T., CHARLTON, M. P., ATWOOD, H. L. & ZHANG, B. 2005. AP180 maintains the distribution of synaptic and vesicle proteins in the nerve terminal and indirectly regulates the efficacy of Ca2+-triggered exocytosis. *J Neurophysiol,* 94**,** 1888-903.

BAROUCH, W., PRASAD, K., GREENE, L. & EISENBERG, E. 1997. Auxilin-induced interaction of the molecular chaperone Hsc70 with clathrin baskets. *Biochemistry,* 36**,** 4303-8.

BELLOCCHIO, E. E., REIMER, R. J., FREMEAU, R. T. & EDWARDS, R. H. 2000. Uptake of glutamate into synaptic vesicles by an inorganic phosphate transporter. *Science,* 289**,** 957-60.

BENSON, D. L., WATKINS, F. H., STEWARD, O. & BANKER, G. 1994. Characterization of GABAergic neurons in hippocampal cell cultures. *J Neurocytol,* 23**,** 279-95.

BEST, A. R. & REGEHR, W. G. 2009. Inhibitory regulation of electrically coupled neurons in the inferior olive is mediated by asynchronous release of GABA. *Neuron,* 62**,** 555-65.

BETZ, W. J., MAO, F. & SMITH, C. B. 1996. Imaging exocytosis and endocytosis. *Curr Opin Neurobiol,* 6**,** 365-71.

BHALLA, A., CHICKA, M. C., TUCKER, W. C. & CHAPMAN, E. R. 2006. Ca(2+)-synaptotagmin directly regulates t-SNARE function during reconstituted membrane fusion. *Nat Struct Mol Biol,* 13**,** 323-30.

BORDEN, C. R., STEVENS, C. F., SULLIVAN, J. M. & ZHU, Y. 2005. Synaptotagmin mutants Y311N and K326/327A alter the calcium dependence of neurotransmission. *Mol Cell Neurosci,* 29**,** 462-70.

BOUMIL, R. M., LETTS, V. A., ROBERTS, M. C., LENZ, C., MAHAFFEY, C. L., ZHANG, Z. W., MOSER, T. & FRANKEL, W. N. 2010. A missense mutation in a highly conserved alternate exon of dynamin-1 causes epilepsy in fitful mice. *PLoS Genet,* 6.

BOURNE, H. R. 1988. Do GTPases direct membrane traffic in secretion? *Cell,* 53**,** 669-71.

BRAGINA, L., CANDIRACCI, C., BARBARESI, P., GIOVEDÌ, S., BENFENATI, F. & CONTI, F. 2007. Heterogeneity of glutamatergic and GABAergic release machinery in cerebral cortex. *Neuroscience,* 146**,** 1829-40.

BREWER, K. D., BACAJ, T., CAVALLI, A., CAMILLONI, C., SWARBRICK, J. D., LIU, J., ZHOU, A., ZHOU, P., BARLOW, N., XU, J., SEVEN, A. B., PRINSLOW, E. A., VOLETI, R., HÄUSSINGER, D., BONVIN, A. M., TOMCHICK, D. R., VENDRUSCOLO, M., GRAHAM, B., SÜDHOF, T. C. & RIZO, J. 2015. Dynamic binding mode of a Synaptotagmin-1-SNARE complex in solution. *Nat Struct Mol Biol,* 22**,** 555-64.

BRODSKY, F. M., CHEN, C. Y., KNUEHL, C., TOWLER, M. C. & WAKEHAM, D. E. 2001. Biological basket weaving: formation and function of clathrin-coated vesicles. *Annu Rev Cell Dev Biol,* 17**,** 517-68.

BROSE, N., PETRENKO, A. G., SÜDHOF, T. C. & JAHN, R. 1992. Synaptotagmin: a calcium sensor on the synaptic vesicle surface. *Science,* 256**,** 1021-5.

BUCKLE, P. J. & HAAS, H. L. 1982. Enhancement of synaptic transmission by 4-aminopyridine in hippocampal slices of the rat. *J Physiol,* 326**,** 109-22.

BUCKMASTER, P. S., YAMAWAKI, R. & THIND, K. 2016. More Docked Vesicles and Larger Active Zones at Basket Cell-to-Granule Cell Synapses in a Rat Model of Temporal Lobe Epilepsy. *J Neurosci,* 36**,** 3295-308.

BURKHARDT, P., HATTENDORF, D. A., WEIS, W. I. & FASSHAUER, D. 2008. Munc18a controls SNARE assembly through its interaction with the syntaxin N-peptide. *EMBO J,* 27**,** 923-33.

BURNETTE, W. N. 1981. "Western blotting": electrophoretic transfer of proteins from sodium dodecyl sulfate--polyacrylamide gels to unmodified nitrocellulose and radiographic detection with antibody and radioiodinated protein A. *Anal Biochem,* 112**,** 195-203.

CALAKOS, N. & SCHELLER, R. H. 1994. Vesicle-associated membrane protein and synaptophysin are associated on the synaptic vesicle. *J Biol Chem,* 269**,** 24534-7.

CASAL, E., FEDERICI, L., ZHANG, W., FERNANDEZ-RECIO, J., PRIEGO, E. M., MIGUEL, R. N., DUHADAWAY, J. B., PRENDERGAST, G. C., LUISI, B. F. & LAUE, E. D. 2006. The crystal structure of the BAR domain from human Bin1/amphiphysin II and its implications for molecular recognition. *Biochemistry,* 45**,** 12917-28.

CASILLAS-ESPINOSA, P. M., POWELL, K. L. & O'BRIEN, T. J. 2012. Regulators of synaptic transmission: roles in the pathogenesis and treatment of epilepsy. *Epilepsia,* 53 Suppl 9**,** 41-58.

CESTRA, G., CASTAGNOLI, L., DENTE, L., MINENKOVA, O., PETRELLI, A., MIGONE, N., HOFFMÜLLER, U., SCHNEIDER-MERGENER, J. & CESARENI, G. 1999. The SH3 domains of endophilin and amphiphysin bind to the proline-rich region of synaptojanin 1 at distinct sites that display an unconventional binding specificity. *J Biol Chem,* 274**,** 32001-7.

CHANG, W.-P. & SUEDHOF, T. C. 2009. SV2 Renders Primed Synaptic Vesicles Competent for Ca2+-Induced Exocytosis. *Journal of Neuroscience,* 29**,** 883-897.

CHANG, W. P. & SÜDHOF, T. C. 2009. SV2 renders primed synaptic vesicles competent for Ca2+ -induced exocytosis. *J Neurosci,* 29**,** 883-97.

CHAPMAN, E. R. 2008. How does synaptotagmin trigger neurotransmitter release? *Annu Rev Biochem,* 77**,** 615-41.

CHAPMAN, E. R., AN, S., EDWARDSON, J. M. & JAHN, R. 1996. A novel function for the second C2 domain of synaptotagmin. Ca2+-triggered dimerization. *J Biol Chem,* 271**,** 5844-9.

CHAPMAN, E. R., HANSON, P. I., AN, S. & JAHN, R. 1995. Ca2+ regulates the interaction between synaptotagmin and syntaxin 1. *J Biol Chem,* 270**,** 23667-71.

CHEUNG, G. & COUSIN, M. A. 2012. Adaptor protein complexes 1 and 3 are essential for generation of synaptic vesicles from activity-dependent bulk endosomes. *J Neurosci,* 32**,** 6014-23.

CHEUNG, G. & COUSIN, M. A. 2013. Synaptic Vesicle Generation from Activity-Dependent Bulk Endosomes Requires Calcium and Calcineurin. *Journal of Neuroscience,* 33**,** 3370-3379.

CHEUNG, G., JUPP, O. J. & COUSIN, M. A. 2010. Activity-Dependent Bulk Endocytosis and Clathrin-Dependent Endocytosis Replenish Specific Synaptic Vesicle Pools in Central Nerve Terminals. *Journal of Neuroscience,* 30**,** 8151-8161.

CLAYTON, E. L., ANGGONO, V., SMILLIE, K. J., CHAU, N., ROBINSON, P. J. & COUSIN, M. A. 2009. The Phospho-Dependent Dynamin-Syndapin Interaction Triggers Activity-Dependent Bulk Endocytosis of Synaptic Vesicles. *Journal of Neuroscience,* 29**,** 7706-7717.

CLAYTON, E. L., EVANS, G. J. O. & COUSIN, M. A. 2008. Bulk synaptic vesicle endocytosis is rapidly triggered during strong stimulation. *Journal of Neuroscience,* 28**,** 6627-6632.

CLAYTON, E. L., SUE, N., SMILLIE, K. J., O'LEARY, T., BACHE, N., CHEUNG, G., COLE, A. R., WYLLIE, D. J., SUTHERLAND, C., ROBINSON, P. J. & COUSIN, M. A. 2010. Dynamin I phosphorylation by GSK3 controls activity-dependent bulk endocytosis of synaptic vesicles. *Nature Neuroscience,* 13**,** 845-U85.

COCUCCI, E., AGUET, F., BOULANT, S. & KIRCHHAUSEN, T. 2012. The first five seconds in the life of a clathrin-coated pit. *Cell,* 150**,** 495-507.

CONDLIFFE, S. B., CORRADINI, I., POZZI, D., VERDERIO, C. & MATTEOLI, M. 2010. Endogenous SNAP-25 regulates native voltage-gated calcium channels in glutamatergic neurons. *J Biol Chem,* 285**,** 24968-76.

CONSORTIUM, E.-R., PROJECT, E. P. G. & CONSORTIUM, E. K. 2014. De novo mutations in synaptic transmission genes including DNM1 cause epileptic encephalopathies. *Am J Hum Genet,* 95**,** 360-70.

CORRADINI, I., DONZELLI, A., ANTONUCCI, F., WELZL, H., LOOS, M., MARTUCCI, R., DE ASTIS, S., PATTINI, L., INVERARDI, F., WOLFER, D., CALEO, M., BOZZI, Y., VERDERIO, C., FRASSONI, C., BRAIDA, D., CLERICI, M., LIPP, H. P., SALA, M. & MATTEOLI, M. 2014. Epileptiform activity and cognitive deficits in SNAP-25(+/-) mice are normalized by antiepileptic drugs. *Cereb Cortex,* 24**,** 364-76.

CORREA-BASURTO, J., CUEVAS-HERNÁNDEZ, R. I., PHILLIPS-FARFÁN, B. V., MARTÍNEZ-ARCHUNDIA, M., ROMO-MANCILLAS, A., RAMÍREZ-SALINAS, G. L., PÉREZ-GONZÁLEZ, Ó., TRUJILLO-FERRARA, J. & MENDOZA-TORREBLANCA, J. G. 2015. Identification of the antiepileptic racetam binding site in the synaptic vesicle protein 2A by molecular dynamics and docking simulations. *Front Cell Neurosci,* 9**,** 125.

COUSIN, M. A. 2015. Synaptic Vesicle Endocytosis and Endosomal Recycling in Central Nerve Terminals: Discrete Trafficking Routes? *Neuroscientist,* 21**,** 413-23.

COUSIN, M. A. & ROBINSON, P. J. 1999. Mechanisms of synaptic vesicle recycling illuminated by fluorescent dyes. *J Neurochem,* 73**,** 2227-39.

CREMONA, O., DI PAOLO, G., WENK, M. R., LÜTHI, A., KIM, W. T., TAKEI, K., DANIELL, L., NEMOTO, Y., SHEARS, S. B., FLAVELL, R. A., MCCORMICK, D. A. & DE CAMILLI, P. 1999. Essential role of phosphoinositide metabolism in synaptic vesicle recycling. *Cell,* 99**,** 179-88.

CROWDER, K. M., GUNTHER, J. M., JONES, T. A., HALE, B. D., ZHANG, H. Z., PETERSON, M. R., SCHELLER, R. H., CHAVKIN, C. & BAJJALIEH, S. M. 1999. Abnormal neurotransmission in mice lacking synaptic vesicle protein 2A (SV2A). *Proceedings of the National Academy of Sciences of the United States of America,* 96**,** 15268-15273.

CUSTER, K. L., AUSTIN, N. S., SULLIVAN, J. M. & BAJJALIEH, S. M. 2006. Synaptic vesicle protein 2 enhances release probability at quiescent synapses. *J Neurosci,* 26**,** 1303-13.

DARCY, K. J., STARAS, K., COLLINSON, L. M. & GODA, Y. 2006. Constitutive sharing of recycling synaptic vesicles between presynaptic boutons. *Nat Neurosci,* 9**,** 315-21.

DAVID, C., SOLIMENA, M. & DE CAMILLI, P. 1994. Autoimmunity in stiff-Man syndrome with breast cancer is targeted to the C-terminal region of human amphiphysin, a protein similar to the yeast proteins, Rvs167 and Rvs161. *FEBS Lett,* 351**,** 73-9.

DAVIS, A. F., BAI, J., FASSHAUER, D., WOLOWICK, M. J., LEWIS, J. L. & CHAPMAN, E. R. 1999. Kinetics of synaptotagmin responses to Ca2+ and assembly with the core SNARE complex onto membranes. *Neuron,* 24**,** 363-76.

DE LANGE, R. P. J., DE ROOS, A. D. G. & BORST, J. G. G. 2003. Two modes of vesicle recycling in the rat calyx of Held. *Journal of Neuroscience,* 23**,** 10164-10173.

DELVENDAHL, I., VYLETA, N. P., VON GERSDORFF, H. & HALLERMANN, S. 2016. Fast, Temperature-Sensitive and Clathrin-Independent Endocytosis at Central Synapses. *Neuron,* 90**,** 492-8.

DENKER, A., KRÖHNERT, K., BÜCKERS, J., NEHER, E. & RIZZOLI, S. O. 2011. The reserve pool of synaptic vesicles acts as a buffer for proteins involved in synaptic vesicle recycling. *Proc Natl Acad Sci U S A,* 108**,** 17183-8.

DI GIOVANNI, J., BOUDKKAZI, S., MOCHIDA, S., BIALOWAS, A., SAMARI, N., LÉVÊQUE, C., YOUSSOUF, F., BRECHET, A., IBORRA, C., MAULET, Y., MOUTOT, N., DEBANNE, D., SEAGAR, M. & EL FAR, O. 2010. V-ATPase membrane sector associates with synaptobrevin to modulate neurotransmitter release. *Neuron,* 67**,** 268-79.

DI PAOLO, G., SANKARANARAYANAN, S., WENK, M. R., DANIELL, L., PERUCCO, E., CALDARONE, B. J., FLAVELL, R., PICCIOTTO, M. R., RYAN, T. A., CREMONA, O. & DE CAMILLI, P. 2002. Decreased synaptic vesicle recycling efficiency and cognitive deficits in amphiphysin 1 knockout mice. *Neuron,* 33**,** 789-804.

DIRIL, M. K., WIENISCH, M., JUNG, N., KLINGAUF, J. & HAUCKE, V. 2006. Stonin 2 is an AP-2-dependent endocytic sorting adaptor for synaptotagmin internalization and recycling. *Dev Cell,* 10**,** 233-44.

DOBRUNZ, L. E. & STEVENS, C. F. 1997. Heterogeneity of release probability, facilitation, and depletion at central synapses. *Neuron,* 18**,** 995-1008.

DODGE, F. A. & RAHAMIMOFF, R. 1967. Co-operative action a calcium ions in transmitter release at the neuromuscular junction. *J Physiol,* 193**,** 419-32.

DOOLEY, D. J., DONOVAN, C. M., MEDER, W. P. & WHETZEL, S. Z. 2002. Preferential action of gabapentin and pregabalin at P/Q-type voltage-sensitive

calcium channels: inhibition of K+-evoked [3H]-norepinephrine release from rat neocortical slices. *Synapse,* 45**,** 171-90.

DOOLEY, D. J., DONOVAN, C. M. & PUGSLEY, T. A. 2000. Stimulus-dependent modulation of [(3)H]norepinephrine release from rat neocortical slices by gabapentin and pregabalin. *J Pharmacol Exp Ther,* 295**,** 1086-93.

DRAKE, M. T., ZHU, Y. & KORNFELD, S. 2000. The assembly of AP-3 adaptor complex-containing clathrin-coated vesicles on synthetic liposomes. *Mol Biol Cell,* 11**,** 3723-36.

DULUBOVA, I., SUGITA, S., HILL, S., HOSAKA, M., FERNANDEZ, I., SÜDHOF, T. C. & RIZO, J. 1999. A conformational switch in syntaxin during exocytosis: role of munc18. *EMBO J,* 18**,** 4372-82.

EDELMANN, L., HANSON, P. I., CHAPMAN, E. R. & JAHN, R. 1995. Synaptobrevin binding to synaptophysin: a potential mechanism for controlling the exocytotic fusion machine. *EMBO J,* 14**,** 224-31.

EGASHIRA, Y., TAKASE, M. & TAKAMORI, S. 2015. Monitoring of vacuolar-type H+ ATPase-mediated proton influx into synaptic vesicles. *J Neurosci,* 35**,** 3701-10.

ENCARNAÇÃO, M., ESPADA, L., ESCREVENTE, C., MATEUS, D., RAMALHO, J., MICHELET, X., SANTARINO, I., HSU, V. W., BRENNER, M. B., BARRAL, D. C. & VIEIRA, O. V. 2016. A Rab3a-dependent complex essential for lysosome positioning and plasma membrane repair. *J Cell Biol,* 213**,** 631-40.

EVANS, G. J. O. & COUSIN, M. A. 2007. Activity-dependent control of slow synaptic vesicle endocytosis by cyclin-dependent kinase 5. *Journal of Neuroscience,* 27**,** 401-411.

FATT, P. & KATZ, B. 1950. Some observations on biological noise. *Nature,* 166**,** 597-8.

FATT, P. & KATZ, B. 1952. Spontaneous subthreshold activity at motor nerve endings. *J Physiol,* 117**,** 109-28.

FAÚNDEZ, V., HORNG, J. T. & KELLY, R. B. 1998. A function for the AP3 coat complex in synaptic vesicle formation from endosomes. *Cell,* 93**,** 423-32.

FENG, G., XIAO, F., LU, Y., HUANG, Z., YUAN, J., XIAO, Z., XI, Z. & WANG, X. 2009. Down-regulation synaptic vesicle protein 2A in the anterior temporal neocortex of patients with intractable epilepsy. *J Mol Neurosci,* 39**,** 354-9.

FERGUSON, S. M., BRASNJO, G., HAYASHI, M., WÖLFEL, M., COLLESI, C., GIOVEDI, S., RAIMONDI, A., GONG, L. W., ARIEL, P., PARADISE, S., O'TOOLE, E., FLAVELL, R., CREMONA, O., MIESENBÖCK, G., RYAN, T. A. & DE CAMILLI, P. 2007. A selective activity-dependent requirement for dynamin 1 in synaptic vesicle endocytosis. *Science,* 316**,** 570-4.

FERNANDEZ-ALFONSO, T. & RYAN, T. A. 2008. A heterogeneous "resting" pool of synaptic vesicles that is dynamically interchanged across boutons in mammalian CNS synapses. *Brain Cell Biol,* 36**,** 87-100.

FERNÁNDEZ-ALFONSO, T., KWAN, R. & RYAN, T. A. 2006. Synaptic vesicles interchange their membrane proteins with a large surface reservoir during recycling. *Neuron,* 51**,** 179-86.

FISHER, R. S., CROSS, J. H., FRENCH, J. A., HIGURASHI, N., HIRSCH, E., JANSEN, F. E., LAGAE, L., MOSHÉ, S. L., PELTOLA, J., ROULET PEREZ, E., SCHEFFER, I. E. & ZUBERI, S. M. 2017. Operational classification of seizure types by the International League Against Epilepsy: Position Paper of the ILAE Commission for Classification and Terminology. *Epilepsia,* 58**,** 522-530.

FORD, M. G., MILLS, I. G., PETER, B. J., VALLIS, Y., PRAEFCKE, G. J., EVANS, P. R. & MCMAHON, H. T. 2002. Curvature of clathrin-coated pits driven by epsin. *Nature,* 419**,** 361-6.

FOSS, S. M., LI, H., SANTOS, M. S., EDWARDS, R. H. & VOGLMAIER, S. M. 2013. Multiple dileucine-like motifs direct VGLUT1 trafficking. *J Neurosci,* 33**,** 10647-60.

FOTIN, A., CHENG, Y., GRIGORIEFF, N., WALZ, T., HARRISON, S. C. & KIRCHHAUSEN, T. 2004. Structure of an auxilin-bound clathrin coat and its implications for the mechanism of uncoating. *Nature,* 432**,** 649-53.

FREDJ, N. B. & BURRONE, J. 2009. A resting pool of vesicles is responsible for spontaneous vesicle fusion at the synapse. *Nat Neurosci,* 12**,** 751-8.

FROST, A., UNGER, V. M. & DE CAMILLI, P. 2009. The BAR domain superfamily: membrane-molding macromolecules. *Cell,* 137**,** 191-6.

FUKUYAMA, K., TANAHASHI, S., NAKAGAWA, M., YAMAMURA, S., MOTOMURA, E., SHIROYAMA, T., TANII, H. & OKADA, M. 2012. Levetiracetam inhibits neurotransmitter release associated with CICR. *Neurosci Lett,* 518**,** 69-74.

FULLER, K. L., WANG, Y. Y., COOK, M. J., MURPHY, M. A. & D'SOUZA, W. J. 2013. Tolerability, safety, and side effects of levetiracetam versus phenytoin in intravenous and total prophylactic regimen among craniotomy patients: a prospective randomized study. *Epilepsia,* 54**,** 45-57.

GAFFANEY, J. D., DUNNING, F. M., WANG, Z., HUI, E. & CHAPMAN, E. R. 2008. Synaptotagmin C2B domain regulates Ca2+-triggered fusion in vitro: critical residues revealed by scanning alanine mutagenesis. *J Biol Chem,* 283**,** 31763-75.

GANDINI, M. A., SANDOVAL, A., ZAMPONI, G. W. & FELIX, R. 2014. The MAP1B-LC1/UBE2L3 complex catalyzes degradation of cell surface CaV2.2 channels. *Channels (Austin),* 8**,** 452-7.

GEPPERT, M., GODA, Y., HAMMER, R. E., LI, C., ROSAHL, T. W., STEVENS, C. F. & SÜDHOF, T. C. 1994. Synaptotagmin I: a major Ca2+ sensor for transmitter release at a central synapse. *Cell,* 79**,** 717-27.

GIANNANDREA, M., GUARNIERI, F. C., GEHRING, N. H., MONZANI, E., BENFENATI, F., KULOZIK, A. E. & VALTORTA, F. 2013. Nonsense-mediated mRNA decay and loss-of-function of the protein underlie the X-

linked epilepsy associated with the W356× mutation in synapsin I. *PLoS One,* 8**,** e67724.

GIGOUT, S., LOUVEL, J., RINALDI, D., MARTIN, B. & PUMAIN, R. 2013. Thalamocortical relationships and network synchronization in a new genetic model "in mirror" for absence epilepsy. *Brain Res,* 1525**,** 39-52.

GILLARD, M., CHATELAIN, P. & FUKS, B. 2006. Binding characteristics of levetiracetam to synaptic vesicle protein 2A (SV2A) in human brain and in CHO cells expressing the human recombinant protein. *Eur J Pharmacol,* 536**,** 102-8.

GIMBER, N., TADEUS, G., MARITZEN, T., SCHMORANZER, J. & HAUCKE, V. 2015. Diffusional spread and confinement of newly exocytosed synaptic vesicle proteins. *Nat Commun,* 6**,** 8392.

GODA, Y. & STEVENS, C. F. 1994. Two components of transmitter release at a central synapse. *Proc Natl Acad Sci U S A,* 91**,** 12942-6.

GOODKIN, H. P., JOSHI, S., MTCHEDLISHVILI, Z., BRAR, J. & KAPUR, J. 2008. Subunit-specific trafficking of GABA(A) receptors during status epilepticus. *J Neurosci,* 28**,** 2527-38.

GORDON, S. L. & COUSIN, M. A. 2013. X-Linked Intellectual Disability-Associated Mutations in Synaptophysin Disrupt Synaptobrevin II Retrieval. *Journal of Neuroscience,* 33**,** 13695-13700.

GORDON, S. L. & COUSIN, M. A. 2016. The iTRAPs: Guardians of Synaptic Vesicle Cargo Retrieval During Endocytosis. *Front Synaptic Neurosci,* 8**,** 1.

GORDON, S. L., LEUBE, R. E. & COUSIN, M. A. 2011. Synaptophysin Is Required for Synaptobrevin Retrieval during Synaptic Vesicle Endocytosis. *Journal of Neuroscience,* 31**,** 14032-14036.

GORMAL, R. S., NGUYEN, T. H., MARTIN, S., PAPADOPULOS, A. & MEUNIER, F. A. 2015. An acto-myosin II constricting ring initiates the fission of activity-dependent bulk endosomes in neurosecretory cells. *J Neurosci,* 35**,** 1380-9.

GORTER, J. A., VAN VLIET, E. A., ARONICA, E., BREIT, T., RAUWERDA, H., LOPES DA SILVA, F. H. & WADMAN, W. J. 2006. Potential new antiepileptogenic targets indicated by microarray analysis in a rat model for temporal lobe epilepsy. *J Neurosci,* 26**,** 11083-110.

GOWER, A. J., NOYER, M., VERLOES, R., GOBERT, J. & WÜLFERT, E. 1992. ucb L059, a novel anti-convulsant drug: pharmacological profile in animals. *Eur J Pharmacol,* 222**,** 193-203.

GRANSETH, B. & LAGNADO, L. 2008. The role of endocytosis in regulating the strength of hippocampal synapses. *J Physiol,* 586**,** 5969-82.

GRANSETH, B., ODERMATT, B., ROYLE, S. J. & LAGNADO, L. 2006. Clathrin-mediated endocytosis is the dominant mechanism of vesicle retrieval at hippocampal synapses. *Neuron,* 51**,** 773-86.

GRASS, I., THIEL, S., HÖNING, S. & HAUCKE, V. 2004. Recognition of a basic AP-2 binding motif within the C2B domain of synaptotagmin is dependent on multimerization. *J Biol Chem,* 279**,** 54872-80.

HANSON, P. I., ROTH, R., MORISAKI, H., JAHN, R. & HEUSER, J. E. 1997. Structure and conformational changes in NSF and its membrane receptor complexes visualized by quick-freeze/deep-etch electron microscopy. *Cell,* 90**,** 523-35.

HARATA, N., RYAN, T. A., SMITH, S. J., BUCHANAN, J. & TSIEN, R. W. 2001. Visualizing recycling synaptic vesicles in hippocampal neurons by FM 1-43 photoconversion. *Proc Natl Acad Sci U S A,* 98**,** 12748-53.

HAUCKE, V. & DE CAMILLI, P. 1999. AP-2 recruitment to synaptotagmin stimulated by tyrosine-based endocytic motifs. *Science,* 285**,** 1268-71.

HAUCKE, V., NEHER, E. & SIGRIST, S. J. 2011. Protein scaffolds in the coupling of synaptic exocytosis and endocytosis. *Nat Rev Neurosci,* 12**,** 127-38.

HAUCKE, V., WENK, M. R., CHAPMAN, E. R., FARSAD, K. & DE CAMILLI, P. 2000. Dual interaction of synaptotagmin with mu2- and alpha-adaptin facilitates clathrin-coated pit nucleation. *EMBO J,* 19**,** 6011-9.

HEERSSEN, H., FETTER, R. D. & DAVIS, G. W. 2008. Clathrin dependence of synaptic-vesicle formation at the Drosophila neuromuscular junction. *Curr Biol,* 18**,** 401-9.

HENNE, W. M., BOUCROT, E., MEINECKE, M., EVERGREN, E., VALLIS, Y., MITTAL, R. & MCMAHON, H. T. 2010. FCHo proteins are nucleators of clathrin-mediated endocytosis. *Science,* 328**,** 1281-4.

HENNE, W. M., KENT, H. M., FORD, M. G., HEGDE, B. G., DAUMKE, O., BUTLER, P. J., MITTAL, R., LANGEN, R., EVANS, P. R. & MCMAHON, H. T. 2007. Structure and analysis of FCHo2 F-BAR domain: a dimerizing and membrane recruitment module that effects membrane curvature. *Structure,* 15**,** 839-52.

HERZOG, E., NADRIGNY, F., SILM, K., BIESEMANN, C., HELLING, I., BERSOT, T., STEFFENS, H., SCHWARTZMANN, R., NÄGERL, U. V., EL MESTIKAWY, S., RHEE, J., KIRCHHOFF, F. & BROSE, N. 2011. In vivo imaging of intersynaptic vesicle exchange using VGLUT1 Venus knock-in mice. *J Neurosci,* 31**,** 15544-59.

HEUSER, J. E. & REESE, T. S. 1973. Evidence for recycling of synaptic vesicle membrane during transmitter release at the frog neuromuscular junction. *J Cell Biol,* 57**,** 315-44.

HOLT, M., COOKE, A., WU, M. M. & LAGNADO, L. 2003. Bulk membrane retrieval in the synaptic terminal of retinal bipolar cells. *J Neurosci,* 23**,** 1329-39.

HOLYOAKE, J. & SANSOM, M. S. 2007. Conformational change in an MFS protein: MD simulations of LacY. *Structure,* 15**,** 873-84.

HUANG, Y., KO, H., CHEUNG, Z. H., YUNG, K. K., YAO, T., WANG, J. J., MOROZOV, A., KE, Y., IP, N. Y. & YUNG, W. H. 2012. Dual actions of

brain-derived neurotrophic factor on GABAergic transmission in cerebellar Purkinje neurons. *Exp Neurol,* 233**,** 791-8.

HUSUM, H., BOLWIG, T. G., SÁNCHEZ, C., MATHÉ, A. A. & HANSEN, S. L. 2004. Levetiracetam prevents changes in levels of brain-derived neurotrophic factor and neuropeptide Y mRNA and of Y1- and Y5-like receptors in the hippocampus of rats undergoing amygdala kindling: implications for antiepileptogenic and mood-stabilizing properties. *Epilepsy Behav,* 5**,** 204-15.

HÖNING, S., RICOTTA, D., KRAUSS, M., SPÄTE, K., SPOLAORE, B., MOTLEY, A., ROBINSON, M., ROBINSON, C., HAUCKE, V. & OWEN, D. J. 2005. Phosphatidylinositol-(4,5)-bisphosphate regulates sorting signal recognition by the clathrin-associated adaptor complex AP2. *Mol Cell,* 18**,** 519-31.

IEZZI, M., THEANDER, S., JANZ, R., LOZE, C. & WOLLHEIM, C. B. 2005. SV2A and SV2C are not vesicular Ca2+ transporters but control glucose-evoked granule recruitment. *J Cell Sci,* 118**,** 5647-60.

IKEDA, K. & BEKKERS, J. M. 2009. Counting the number of releasable synaptic vesicles in a presynaptic terminal. *Proc Natl Acad Sci U S A,* 106**,** 2945-50.

JACKSON, M. F., ESPLIN, B. & CAPEK, R. 1999. Activity-dependent enhancement of hyperpolarizing and depolarizing gamma-aminobutyric acid (GABA) synaptic responses following inhibition of GABA uptake by tiagabine. *Epilepsy Res,* 37**,** 25-36.

JAKOBSSON, J., GAD, H., ANDERSSON, F., LÖW, P., SHUPLIAKOV, O. & BRODIN, L. 2008. Role of epsin 1 in synaptic vesicle endocytosis. *Proc Natl Acad Sci U S A,* 105**,** 6445-50.

JANZ, R., GODA, Y., GEPPERT, M., MISSLER, M. & SÜDHOF, T. C. 1999. SV2A and SV2B function as redundant Ca2+ regulators in neurotransmitter release. *Neuron,* 24**,** 1003-16.

JANZ, R. & SÜDHOF, T. C. 1999. SV2C is a synaptic vesicle protein with an unusually restricted localization: anatomy of a synaptic vesicle protein family. *Neuroscience,* 94**,** 1279-90.

JIRUSKA, P., DE CURTIS, M., JEFFERYS, J. G., SCHEVON, C. A., SCHIFF, S. J. & SCHINDLER, K. 2013. Synchronization and desynchronization in epilepsy: controversies and hypotheses. *J Physiol,* 591**,** 787-97.

JOCKUSCH, W. J., PRAEFCKE, G. J., MCMAHON, H. T. & LAGNADO, L. 2005. Clathrin-dependent and clathrin-independent retrieval of synaptic vesicles in retinal bipolar cells. *Neuron,* 46**,** 869-78.

JUNG, N., WIENISCH, M., GU, M., RAND, J. B., MÜLLER, S. L., KRAUSE, G., JORGENSEN, E. M., KLINGAUF, J. & HAUCKE, V. 2007. Molecular basis of synaptic vesicle cargo recognition by the endocytic sorting adaptor stonin 2. *J Cell Biol,* 179**,** 1497-510.

JUNG, S., MARITZEN, T., WICHMANN, C., JING, Z., NEEF, A., REVELO, N. H., AL-MOYED, H., MEESE, S., WOJCIK, S. M., PANOU, I., BULUT, H., SCHU, P., FICNER, R., REISINGER, E., RIZZOLI, S. O., NEEF, J.,

STRENZKE, N., HAUCKE, V. & MOSER, T. 2015. Disruption of adaptor protein 2μ (AP-2μ) in cochlear hair cells impairs vesicle reloading of synaptic release sites and hearing. *EMBO J,* 34**,** 2686-702.

KAEMPF, N., KOCHLAMAZASHVILI, G., PUCHKOV, D., MARITZEN, T., BAJJALIEH, S. M., KONONENKO, N. L. & HAUCKE, V. 2015. Overlapping functions of stonin 2 and SV2 in sorting of the calcium sensor synaptotagmin 1 to synaptic vesicles. *Proc Natl Acad Sci U S A,* 112**,** 7297-302.

KAESER, P. S. & REGEHR, W. G. 2014. Molecular mechanisms for synchronous, asynchronous, and spontaneous neurotransmitter release. *Annu Rev Physiol,* 76**,** 333-63.

KAMINSKI, R. M., GILLARD, M., LECLERCQ, K., HANON, E., LORENT, G., DASSESSE, D., MATAGNE, A. & KLITGAARD, H. 2009. Proepileptic phenotype of SV2A-deficient mice is associated with reduced anticonvulsant efficacy of levetiracetam. *Epilepsia,* 50**,** 1729-40.

KAMINSKI, R. M., MATAGNE, A., LECLERCQ, K., GILLARD, M., MICHEL, P., KENDA, B., TALAGA, P. & KLITGAARD, H. 2008. SV2A protein is a broad-spectrum anticonvulsant target: Functional correlation between protein binding and seizure protection in models of both partial and generalized epilepsy. *Neuropharmacology,* 54**,** 715-720.

KANDEL, E. R., BARRES, B. A. & HUDSPETH, A. J. 2012. *Principles of Neural Science,* New York, McGraw-Hill.

KANDEL, E. R. & HUDSPETH, A. J. 2012. *Principals of Neural Science,* New York, McGraw-Hill.

KAPITEIN, L. C. & HOOGENRAAD, C. C. 2011. Which way to go? Cytoskeletal organization and polarized transport in neurons. *Mol Cell Neurosci,* 46**,** 9-20.

KASPROWICZ, J., KUENEN, S., MISKIEWICZ, K., HABETS, R. L., SMITZ, L. & VERSTREKEN, P. 2008. Inactivation of clathrin heavy chain inhibits synaptic recycling but allows bulk membrane uptake. *J Cell Biol,* 182**,** 1007-16.

KASPROWICZ, J., KUENEN, S., SWERTS, J., MISKIEWICZ, K. & VERSTREKEN, P. 2014. Dynamin photoinactivation blocks Clathrin and α-adaptin recruitment and induces bulk membrane retrieval. *J Cell Biol,* 204**,** 1141-56.

KATSUNO, H., TORIYAMA, M., HOSOKAWA, Y., MIZUNO, K., IKEDA, K., SAKUMURA, Y. & INAGAKI, N. 2015. Actin Migration Driven by Directional Assembly and Disassembly of Membrane-Anchored Actin Filaments. *Cell Rep,* 12**,** 648-60.

KELLY, B. T. & OWEN, D. J. 2011. Endocytic sorting of transmembrane protein cargo. *Curr Opin Cell Biol,* 23**,** 404-12.

KIM, S. H. & RYAN, T. A. 2009. Synaptic vesicle recycling at CNS snapses without AP-2. *J Neurosci,* 29**,** 3865-74.

KLITGAARD, H. 2001. Levetiracetam: the preclinical profile of a new class of antiepileptic drugs? *Epilepsia,* 42 Suppl 4**,** 13-8.

KOCH, D., SPIWOKS-BECKER, I., SABANOV, V., SINNING, A., DUGLADZE, T., STELLMACHER, A., AHUJA, R., GRIMM, J., SCHÜLER, S., MÜLLER, A., ANGENSTEIN, F., AHMED, T., DIESLER, A., MOSER, M., TOM DIECK, S., SPESSERT, R., BOECKERS, T. M., FÄSSLER, R., HÜBNER, C. A., BALSCHUN, D., GLOVELI, T., KESSELS, M. M. & QUALMANN, B. 2011. Proper synaptic vesicle formation and neuronal network activity critically rely on syndapin I. *EMBO J,* 30**,** 4955-69.

KONONENKO, N. L., DIRIL, M. K., PUCHKOV, D., KINTSCHER, M., KOO, S. J., PFUHL, G., WINTER, Y., WIENISCH, M., KLINGAUF, J., BREUSTEDT, J., SCHMITZ, D., MARITZEN, T. & HAUCKE, V. 2013. Compromised fidelity of endocytic synaptic vesicle protein sorting in the absence of stonin 2. *Proc Natl Acad Sci U S A,* 110**,** E526-35.

KONONENKO, N. L., PUCHKOV, D., CLASSEN, G. A., WALTER, A. M., PECHSTEIN, A., SAWADE, L., KAEMPF, N., TRIMBUCH, T., LORENZ, D., ROSENMUND, C., MARITZEN, T. & HAUCKE, V. 2014. Clathrin/AP-2 mediate synaptic vesicle reformation from endosome-like vacuoles but are not essential for membrane retrieval at central synapses. *Neuron,* 82**,** 981-8.

KOO, S. J., KOCHLAMAZASHVILI, G., ROST, B., PUCHKOV, D., GIMBER, N., LEHMANN, M., TADEUS, G., SCHMORANZER, J., ROSENMUND, C., HAUCKE, V. & MARITZEN, T. 2015. Vesicular Synaptobrevin/VAMP2 Levels Guarded by AP180 Control Efficient Neurotransmission. *Neuron,* 88**,** 330-44.

KOO, S. J., MARKOVIC, S., PUCHKOV, D., MAHRENHOLZ, C. C., BECEREN-BRAUN, F., MARITZEN, T., DERNEDDE, J., VOLKMER, R., OSCHKINAT, H. & HAUCKE, V. 2011. SNARE motif-mediated sorting of synaptobrevin by the endocytic adaptors clathrin assembly lymphoid myeloid leukemia (CALM) and AP180 at synapses. *Proc Natl Acad Sci U S A,* 108**,** 13540-5.

KUO, C. C. & BEAN, B. P. 1994. Slow binding of phenytoin to inactivated sodium channels in rat hippocampal neurons. *Mol Pharmacol,* 46**,** 716-25.

KWON, S. E. & CHAPMAN, E. R. 2012. Glycosylation is dispensable for sorting of synaptotagmin 1 but is critical for targeting of SV2 and synaptophysin to recycling synaptic vesicles. *J Biol Chem,* 287**,** 35658-68.

LEENDERS, A. G., LIN, L., HUANG, L. D., GERWIN, C., LU, P. H. & SHENG, Z. H. 2008. The role of MAP1A light chain 2 in synaptic surface retention of Cav2.2 channels in hippocampal neurons. *J Neurosci,* 28**,** 11333-46.

LEENDERS, A. G. M., SCHOLTEN, G., DE LANGE, R. P. J., DA SILVA, F. H. L. & GHIJSEN, W. 2002. Sequential changes in synaptic vesicle pools and endosome-like organelles during depolarization near the active zone of central nerve terminals. *Neuroscience,* 109**,** 195-206.

LEPPIK, I. E. 2002. Three new drugs for epilepsy: levetiracetam, oxcarbazepine, and zonisamide. *J Child Neurol,* 17 Suppl 1**,** S53-7.

LEVEQUE, C., HOSHINO, T., DAVID, P., SHOJI-KASAI, Y., LEYS, K., OMORI, A., LANG, B., EL FAR, O., SATO, K. & MARTIN-MOUTOT, N. 1992. The synaptic vesicle protein synaptotagmin associates with calcium channels and is a putative Lambert-Eaton myasthenic syndrome antigen. *Proc Natl Acad Sci U S A,* 89**,** 3625-9.

LEVINE, K. B., CLOHERTY, E. K., HAMILL, S. & CARRUTHERS, A. 2002. Molecular determinants of sugar transport regulation by ATP. *Biochemistry,* 41**,** 12629-38.

LI, L., CHIN, L. S., SHUPLIAKOV, O., BRODIN, L., SIHRA, T. S., HVALBY, O., JENSEN, V., ZHENG, D., MCNAMARA, J. O. & GREENGARD, P. 1995. Impairment of synaptic vesicle clustering and of synaptic transmission, and increased seizure propensity, in synapsin I-deficient mice. *Proc Natl Acad Sci U S A,* 92**,** 9235-9.

LI, Y. Y., CHEN, X. N., FAN, X. X., ZHANG, Y. J., GU, J., FU, X. W., WANG, Z. H., WANG, X. F. & XIAO, Z. 2015. Upregulated dynamin 1 in an acute seizure model and in epileptic patients. *Synapse,* 69**,** 67-77.

LI, Z., BURRONE, J., TYLER, W. J., HARTMAN, K. N., ALBEANU, D. F. & MURTHY, V. N. 2005. Synaptic vesicle recycling studied in transgenic mice expressing synaptopHluorin. *Proc Natl Acad Sci U S A,* 102**,** 6131-6.

LIGUZ-LECZNAR, M. & SKANGIEL-KRAMSKA, J. 2007. Vesicular glutamate transporters (VGLUTs): the three musketeers of glutamatergic system. *Acta Neurobiol Exp (Wars),* 67**,** 207-18.

LITTLETON, J. T., STERN, M., PERIN, M. & BELLEN, H. J. 1994. Calcium dependence of neurotransmitter release and rate of spontaneous vesicle fusions are altered in Drosophila synaptotagmin mutants. *Proc Natl Acad Sci U S A,* 91**,** 10888-92.

LOPES, M. W., LOPES, S. C., COSTA, A. P., GONÇALVES, F. M., RIEGER, D. K., PERES, T. V., EYNG, H., PREDIGER, R. D., DIAZ, A. P., NUNES, J. C., WALZ, R. & LEAL, R. B. 2015. Region-specific alterations of AMPA receptor phosphorylation and signaling pathways in the pilocarpine model of epilepsy. *Neurochem Int,* 87**,** 22-33.

LU, B., KIESSLING, V., TAMM, L. K. & CAFISO, D. S. 2014. The juxtamembrane linker of full-length synaptotagmin 1 controls oligomerization and calcium-dependent membrane binding. *J Biol Chem,* 289**,** 22161-71.

LU, J., MACHIUS, M., DULUBOVA, I., DAI, H., SÜDHOF, T. C., TOMCHICK, D. R. & RIZO, J. 2006. Structural basis for a Munc13-1 homodimer to Munc13-1/RIM heterodimer switch. *PLoS Biol,* 4**,** e192.

LU, T. & TRUSSELL, L. O. 2000. Inhibitory transmission mediated by asynchronous transmitter release. *Neuron,* 26**,** 683-94.

LYLES, V., ZHAO, Y. & MARTIN, K. C. 2006. Synapse formation and mRNA localization in cultured Aplysia neurons. *Neuron,* 49**,** 349-56.

LYNCH, B. A., LAMBENG, N., NOCKA, K., KENSEL-HAMMES, P., BAJJALIEH, S. M., MATAGNE, A. & FUKS, B. 2004. The synaptic vesicle

protein SV2A is the binding site for the antiepileptic drug levetiracetam. *Proc Natl Acad Sci U S A,* 101**,** 9861-6.

LYNCH, B. A., MATAGNE, A., BRÄNNSTRÖM, A., VON EULER, A., JANSSON, M., HAUZENBERGER, E. & SÖDERHÄLL, J. A. 2008. Visualization of SV2A conformations in situ by the use of Protein Tomography. *Biochem Biophys Res Commun,* 375**,** 491-5.

LÖSCHER, W., HÖNACK, D. & BLOMS-FUNKE, P. 1996. The novel antiepileptic drug levetiracetam (ucb L059) induces alterations in GABA metabolism and turnover in discrete areas of rat brain and reduces neuronal activity in substantia nigra pars reticulata. *Brain Res,* 735**,** 208-16.

LÖSCHER, W., HÖNACK, D. & RUNDFELDT, C. 1998. Antiepileptogenic effects of the novel anticonvulsant levetiracetam (ucb L059) in the kindling model of temporal lobe epilepsy. *J Pharmacol Exp Ther,* 284**,** 474-9.

LÖSCHER, W. & HÖRSTERMANN, D. 1994. Differential effects of vigabatrin, gamma-acetylenic GABA, aminooxyacetic acid, and valproate on levels of various amino acids in rat brain regions and plasma. *Naunyn Schmiedebergs Arch Pharmacol,* 349**,** 270-8.

MA, C., LI, W., XU, Y. & RIZO, J. 2011. Munc13 mediates the transition from the closed syntaxin-Munc18 complex to the SNARE complex. *Nat Struct Mol Biol,* 18**,** 542-9.

MADEO, M., KOVÁCS, A. D. & PEARCE, D. A. 2014. The human synaptic vesicle protein, SV2A, functions as a galactose transporter in Saccharomyces cerevisiae. *J Biol Chem,* 289**,** 33066-71.

MANI, M., LEE, S. Y., LUCAST, L., CREMONA, O., DI PAOLO, G., DE CAMILLI, P. & RYAN, T. A. 2007. The dual phosphatase activity of synaptojanin1 is required for both efficient synaptic vesicle endocytosis and reavailability at nerve terminals. *Neuron,* 56**,** 1004-18.

MANSEAU, F., MARINELLI, S., MÉNDEZ, P., SCHWALLER, B., PRINCE, D. A., HUGUENARD, J. R. & BACCI, A. 2010. Desynchronization of neocortical networks by asynchronous release of GABA at autaptic and synaptic contacts from fast-spiking interneurons. *PLoS Biol,* 8.

MARAIS, E., KLUGBAUER, N. & HOFMANN, F. 2001. Calcium channel alpha(2)delta subunits-structure and Gabapentin binding. *Mol Pharmacol,* 59**,** 1243-8.

MARGINEANU, D. G., MATAGNE, A., KAMINSKI, R. M. & KLITGAARD, H. 2008. Effects of chronic treatment with levetiracetam on hippocampal field responses after pilocarpine-induced status epilepticus in rats. *Brain Res Bull,* 77**,** 282-5.

MARRA, V., BURDEN, J. J., THORPE, J. R., SMITH, I. T., SMITH, S. L., HÄUSSER, M., BRANCO, T. & STARAS, K. 2012. A preferentially segregated recycling vesicle pool of limited size supports neurotransmission in native central synapses. *Neuron,* 76**,** 579-89.

MARTENS, H., WESTON, M. C., BOULLAND, J. L., GRØNBORG, M., GROSCHE, J., KACZA, J., HOFFMANN, A., MATTEOLI, M., TAKAMORI, S., HARKANY, T., CHAUDHRY, F. A., ROSENMUND, C., ERCK, C., JAHN, R. & HÄRTIG, W. 2008. Unique luminal localization of VGAT-C terminus allows for selective labeling of active cortical GABAergic synapses. *J Neurosci,* 28**,** 13125-31.

MARTIN, D. J., MCCLELLAND, D., HERD, M. B., SUTTON, K. G., HALL, M. D., LEE, K., PINNOCK, R. D. & SCOTT, R. H. 2002. Gabapentin-mediated inhibition of voltage-activated Ca2+ channel currents in cultured sensory neurones is dependent on culture conditions and channel subunit expression. *Neuropharmacology,* 42**,** 353-66.

MARXEN, M., VOLKNANDT, W. & ZIMMERMANN, H. 1999. Endocytic vacuoles formed following a short pulse of K+ -stimulation contain a plethora of presynaptic membrane proteins. *Neuroscience,* 94**,** 985-96.

MATVEEVA, E. A., VANAMAN, T. C., WHITEHEART, S. W. & SLEVIN, J. T. 2008. Levetiracetam prevents kindling-induced asymmetric accumulation of hippocampal 7S SNARE complexes. *Epilepsia,* 49**,** 1749-58.

MAXIMOV, A., LAO, Y., LI, H., CHEN, X., RIZO, J., SØRENSEN, J. B. & SÜDHOF, T. C. 2008. Genetic analysis of synaptotagmin-7 function in synaptic vesicle exocytosis. *Proc Natl Acad Sci U S A,* 105**,** 3986-91.

MAYCOX, P. R., LINK, E., REETZ, A., MORRIS, S. A. & JAHN, R. 1992. Clathrin-coated vesicles in nervous tissue are involved primarily in synaptic vesicle recycling. *J Cell Biol,* 118**,** 1379-88.

MCADAM, R. L., VARGA, K. T., JIANG, Z., YOUNG, F. B., BLANDFORD, V., MCPHERSON, P. S., GONG, L. W. & SOSSIN, W. S. 2015. The juxtamembrane region of synaptotagmin 1 interacts with dynamin 1 and regulates vesicle fission during compensatory endocytosis in endocrine cells. *J Cell Sci,* 128**,** 2229-35.

MCKINNEY, R. A., CAPOGNA, M., DÜRR, R., GÄHWILER, B. H. & THOMPSON, S. M. 1999. Miniature synaptic events maintain dendritic spines via AMPA receptor activation. *Nat Neurosci,* 2**,** 44-9.

MCMAHON, H. T. & BOUCROT, E. 2011. Molecular mechanism and physiological functions of clathrin-mediated endocytosis. *Nat Rev Mol Cell Biol,* 12**,** 517-33.

MCNIVEN, M. A., KIM, L., KRUEGER, E. W., ORTH, J. D., CAO, H. & WONG, T. W. 2000. Regulated interactions between dynamin and the actin-binding protein cortactin modulate cell shape. *J Cell Biol,* 151**,** 187-98.

MEADOR, K. J., BAKER, G. A., BROWNING, N., CLAYTON-SMITH, J., COMBS-CANTRELL, D. T., COHEN, M., KALAYJIAN, L. A., KANNER, A., LIPORACE, J. D., PENNELL, P. B., PRIVITERA, M., LORING, D. W. & GROUP, N. S. 2009. Cognitive function at 3 years of age after fetal exposure to antiepileptic drugs. *N Engl J Med,* 360**,** 1597-605.

MEARS, J. A., RAY, P. & HINSHAW, J. E. 2007. A corkscrew model for dynamin constriction. *Structure,* 15**,** 1190-202.

MEEHAN, A. L., YANG, X., MCADAMS, B. D., YUAN, L. & ROTHMAN, S. M. 2011. A new mechanism for antiepileptic drug action: vesicular entry may mediate the effects of levetiracetam. *J Neurophysiol,* 106**,** 1227-39.

MEEHAN, A. L., YANG, X., YUAN, L. L. & ROTHMAN, S. M. 2012. Levetiracetam has an activity-dependent effect on inhibitory transmission. *Epilepsia,* 53**,** 469-76.

MEISLER, M. H., KEARNEY, J., OTTMAN, R. & ESCAYG, A. 2001. Identification of epilepsy genes in human and mouse. *Annu Rev Genet,* 35**,** 567-88.

MENDOZA-TORREBLANCA, J. G., VANOYE-CARLO, A., PHILLIPS-FARFÁN, B. V., CARMONA-APARICIO, L. & GÓMEZ-LIRA, G. 2013. Synaptic vesicle protein 2A: basic facts and role in synaptic function. *Eur J Neurosci,* 38**,** 3529-39.

MESSAOUDI, E., BÂRDSEN, K., SREBRO, B. & BRAMHAM, C. R. 1998. Acute intrahippocampal infusion of BDNF induces lasting potentiation of synaptic transmission in the rat dentate gyrus. *J Neurophysiol,* 79**,** 496-9.

MIESENBÖCK, G., DE ANGELIS, D. A. & ROTHMAN, J. E. 1998. Visualizing secretion and synaptic transmission with pH-sensitive green fluorescent proteins. *Nature,* 394**,** 192-5.

MILES, R. & WONG, R. K. 1987. Inhibitory control of local excitatory circuits in the guinea-pig hippocampus. *J Physiol,* 388**,** 611-29.

MILOSEVIC, I., GIOVEDI, S., LOU, X., RAIMONDI, A., COLLESI, C., SHEN, H., PARADISE, S., O'TOOLE, E., FERGUSON, S., CREMONA, O. & DE CAMILLI, P. 2011. Recruitment of endophilin to clathrin-coated pit necks is required for efficient vesicle uncoating after fission. *Neuron,* 72**,** 587-601.

MINTA, A., KAO, J. P. & TSIEN, R. Y. 1989. Fluorescent indicators for cytosolic calcium based on rhodamine and fluorescein chromophores. *J Biol Chem,* 264**,** 8171-8.

MURTHY, V. N. & STEVENS, C. F. 1999. Reversal of synaptic vesicle docking at central synapses. *Nat Neurosci,* 2**,** 503-7.

NAGARKATTI, N., DESHPANDE, L. S. & DELORENZO, R. J. 2008. Levetiracetam inhibits both ryanodine and IP3 receptor activated calcium induced calcium release in hippocampal neurons in culture. *Neurosci Lett,* 436**,** 289-93.

NAKASHIMA, M., KOUGA, T., LOURENÇO, C. M., SHIINA, M., GOTO, T., TSURUSAKI, Y., MIYATAKE, S., MIYAKE, N., SAITSU, H., OGATA, K., OSAKA, H. & MATSUMOTO, N. 2016. De novo DNM1 mutations in two cases of epileptic encephalopathy. *Epilepsia,* 57**,** e18-23.

NEHER, E. 2010. What is Rate-Limiting during Sustained Synaptic Activity: Vesicle Supply or the Availability of Release Sites. *Front Synaptic Neurosci,* 2**,** 144.

NEHER, E. & MARTY, A. 1982. DISCRETE CHANGES OF CELL-MEMBRANE CAPACITANCE OBSERVED UNDER CONDITIONS OF ENHANCED SECRETION IN BOVINE ADRENAL CHROMAFFIN CELLS. *Proceedings of the National Academy of Sciences of the United States of America-Biological Sciences,* 79**,** 6712-6716.

NELSON, N. & HARVEY, W. R. 1999. Vacuolar and plasma membrane proton-adenosinetriphosphatases. *Physiol Rev,* 79**,** 361-85.

NELSON, N., PERZOV, N., COHEN, A., HAGAI, K., PADLER, V. & NELSON, H. 2000. The cellular biology of proton-motive force generation by V-ATPases. *J Exp Biol,* 203**,** 89-95.

NICHOLSON-FISH, J. C., KOKOTOS, A. C., GILLINGWATER, T. H., SMILLIE, K. J. & COUSIN, M. A. 2015. VAMP4 Is an Essential Cargo Molecule for Activity-Dependent Bulk Endocytosis. *Neuron,* 88**,** 973-84.

NIESPODZIANY, I., KLITGAARD, H. & MARGINEANU, D. G. 2001. Levetiracetam inhibits the high-voltage-activated Ca(2+) current in pyramidal neurones of rat hippocampal slices. *Neurosci Lett,* 306**,** 5-8.

NISHIZUKA, Y. 1988. The molecular heterogeneity of protein kinase C and its implications for cellular regulation. *Nature,* 334**,** 661-5.

NONET, M. L., GRUNDAHL, K., MEYER, B. J. & RAND, J. B. 1993. Synaptic function is impaired but not eliminated in C. elegans mutants lacking synaptotagmin. *Cell,* 73**,** 1291-305.

NONET, M. L., HOLGADO, A. M., BREWER, F., SERPE, C. J., NORBECK, B. A., HOLLERAN, J., WEI, L., HARTWIEG, E., JORGENSEN, E. M. & ALFONSO, A. 1999. UNC-11, a Caenorhabditis elegans AP180 homologue, regulates the size and protein composition of synaptic vesicles. *Mol Biol Cell,* 10**,** 2343-60.

NOWACK, A., MALARKEY, E. B., YAO, J., BLECKERT, A., HILL, J. & BAJJALIEH, S. M. 2011. Levetiracetam reverses synaptic deficits produced by overexpression of SV2A. *PLoS One,* 6**,** e29560.

NOYER, M., GILLARD, M., MATAGNE, A., HÉNICHART, J. P. & WÜLFERT, E. 1995. The novel antiepileptic drug levetiracetam (ucb L059) appears to act via a specific binding site in CNS membranes. *Eur J Pharmacol,* 286**,** 137-46.

ORENBUCH, A., SHALEV, L., MARRA, V., SINAI, I., LAVY, Y., KAHN, J., BURDEN, J. J., STARAS, K. & GITLER, D. 2012. Synapsin selectively controls the mobility of resting pool vesicles at hippocampal terminals. *J Neurosci,* 32**,** 3969-80.

OSEN-SAND, A., STAPLE, J. K., NALDI, E., SCHIAVO, G., ROSSETTO, O., PETITPIERRE, S., MALGAROLI, A., MONTECUCCO, C. & CATSICAS, S. 1996. Common and distinct fusion proteins in axonal growth and transmitter release. *J Comp Neurol,* 367**,** 222-34.

PAN, P. Y., MARRS, J. & RYAN, T. A. 2015. Vesicular glutamate transporter 1 orchestrates recruitment of other synaptic vesicle cargo proteins during synaptic vesicle recycling. *J Biol Chem,* 290**,** 22593-601.

PANDOLFO, M. 2011. Genetics of Epilepsy. *Seminars in Neurology,* 31**,** 506-518.

PARK, Y., SEO, J. B., FRAIND, A., PÉREZ-LARA, A., YAVUZ, H., HAN, K., JUNG, S. R., KATTAN, I., WALLA, P. J., CHOI, M., CAFISO, D. S., KOH, D. S. & JAHN, R. 2015. Synaptotagmin-1 binds to PIP(2)-containing membrane but not to SNAREs at physiological ionic strength. *Nat Struct Mol Biol,* 22**,** 815-23.

PEARSE, B. M. 1976. Clathrin: a unique protein associated with intracellular transfer of membrane by coated vesicles. *Proc Natl Acad Sci U S A,* 73**,** 1255-9.

PENNUTO, M., BONANOMI, D., BENFENATI, F. & VALTORTA, F. 2003. Synaptophysin I controls the targeting of VAMP2/synaptobrevin II to synaptic vesicles. *Mol Biol Cell,* 14**,** 4909-19.

PERERA, R. M., ZONCU, R., LUCAST, L., DE CAMILLI, P. & TOOMRE, D. 2006. Two synaptojanin 1 isoforms are recruited to clathrin-coated pits at different stages. *Proc Natl Acad Sci U S A,* 103**,** 19332-7.

PERUCCA, E. 1996. Pharmacokinetic profile of topiramate in comparison with other new antiepileptic drugs. *Epilepsia,* 37 Suppl 2**,** S8-S13.

PETER, B. J., KENT, H. M., MILLS, I. G., VALLIS, Y., BUTLER, P. J., EVANS, P. R. & MCMAHON, H. T. 2004. BAR domains as sensors of membrane curvature: the amphiphysin BAR structure. *Science,* 303**,** 495-9.

POPA-WAGNER, A., FISCHER, B., SCHMOLL, H., PLATT, D. & KESSLER, C. 1997. Increased expression of microtubule-associated protein 1B in the hippocampus, subiculum, and perforant path of rats treated with a high dose of pentylenetetrazole. *Exp Neurol,* 148**,** 73-82.

POSKANZER, K. E., FETTER, R. D. & DAVIS, G. W. 2006. Discrete residues in the c(2)b domain of synaptotagmin I independently specify endocytic rate and synaptic vesicle size. *Neuron,* 50**,** 49-62.

PRASAD, D. K., SHAHEEN, U., SATYANARAYANA, U., PRABHA, T. S., JYOTHY, A. & MUNSHI, A. 2014. Association of GABRA6 1519 T>C (rs3219151) and Synapsin II (rs37733634) gene polymorphisms with the development of idiopathic generalized epilepsy. *Epilepsy Res,* 108**,** 1267-73.

PRASAD, K., HEUSER, J., EISENBERG, E. & GREENE, L. 1994. Complex formation between clathrin and uncoating ATPase. *J Biol Chem,* 269**,** 6931-9.

PYLE, R. A., SCHIVELL, A. E., HIDAKA, H. & BAJJALIEH, S. M. 2000. Phosphorylation of synaptic vesicle protein 2 modulates binding to synaptotagmin. *Journal of Biological Chemistry,* 275**,** 17195-17200.

QIAN, S. & HUANG, H. W. 2012. A novel phase of compressed bilayers that models the prestalk transition state of membrane fusion. *Biophys J,* 102**,** 48-55.

QUALMANN, B., KOCH, D. & KESSELS, M. M. 2011. Let's go bananas: revisiting the endocytic BAR code. *EMBO J,* 30**,** 3501-15.

RABER, J., MEHTA, P. P., KREIFELDT, M., PARSONS, L. H., WEISS, F., BLOOM, F. E. & WILSON, M. C. 1997. Coloboma hyperactive mutant mice exhibit regional and transmitter-specific deficits in neurotransmission. *J Neurochem,* 68**,** 176-86.

RAIMONDI, A., FERGUSON, S. M., LOU, X., ARMBRUSTER, M., PARADISE, S., GIOVEDI, S., MESSA, M., KONO, N., TAKASAKI, J., CAPPELLO, V., O'TOOLE, E., RYAN, T. A. & DE CAMILLI, P. 2011. Overlapping role of dynamin isoforms in synaptic vesicle endocytosis. *Neuron,* 70**,** 1100-14.

RAINGO, J., KHVOTCHEV, M., LIU, P., DARIOS, F., LI, Y. C., RAMIREZ, D. M., ADACHI, M., LEMIEUX, P., TOTH, K., DAVLETOV, B. & KAVALALI, E. T. 2012. VAMP4 directs synaptic vesicles to a pool that selectively maintains asynchronous neurotransmission. *Nat Neurosci,* 15**,** 738-45.

RAJAPPA, R., GAUTHIER-KEMPER, A., BÖNING, D., HÜVE, J. & KLINGAUF, J. 2016. Synaptophysin 1 Clears Synaptobrevin 2 from the Presynaptic Active Zone to Prevent Short-Term Depression. *Cell Rep,* 14**,** 1369-81.

RANGARAJU, V., CALLOWAY, N. & RYAN, T. A. 2014. Activity-driven local ATP synthesis is required for synaptic function. *Cell,* 156**,** 825-35.

RAO, Y., RUECKERT, C., SAENGER, W. & HAUCKE, V. 2012. The early steps of endocytosis: From cargo selection to membrane deformation. *European Journal of Cell Biology,* 91**,** 226-233.

RASMUSSEN, M., KONG, L., ZHANG, G. R., LIU, M., WANG, X., SZABO, G., CURTHOYS, N. P. & GELLER, A. I. 2007. Glutamatergic or GABAergic neuron-specific, long-term expression in neocortical neurons from helper virus-free HSV-1 vectors containing the phosphate-activated glutaminase, vesicular glutamate transporter-1, or glutamic acid decarboxylase promoter. *Brain Res,* 1144**,** 19-32.

REIGADA, D., DÍEZ-PÉREZ, I., GOROSTIZA, P., VERDAGUER, A., GÓMEZ DE ARANDA, I., PINEDA, O., VILARRASA, J., MARSAL, J., BLASI, J., ALEU, J. & SOLSONA, C. 2003. Control of neurotransmitter release by an internal gel matrix in synaptic vesicles. *Proc Natl Acad Sci U S A,* 100**,** 3485-90.

ROGAWSKI, M. A. & LÖSCHER, W. 2004. The neurobiology of antiepileptic drugs. *Nat Rev Neurosci,* 5**,** 553-64.

ROHENA, L., NEIDICH, J., TRUITT CHO, M., GONZALEZ, K. D., TANG, S., DEVINSKY, O. & CHUNG, W. K. 2013. Mutation in SNAP25 as a novel genetic cause of epilepsy and intellectual disability. *Rare Dis,* 1**,** e26314.

ROST, B. R., SCHNEIDER, F., GRAUEL, M. K., WOZNY, C., BENTZ, C., BLESSING, A., ROSENMUND, T., JENTSCH, T. J., SCHMITZ, D., HEGEMANN, P. & ROSENMUND, C. 2015. Optogenetic acidification of synaptic vesicles and lysosomes. *Nat Neurosci,* 18**,** 1845-1852.

ROTHNIE, A., CLARKE, A. R., KUZMIC, P., CAMERON, A. & SMITH, C. J. 2011. A sequential mechanism for clathrin cage disassembly by 70-kDa heat-shock cognate protein (Hsc70) and auxilin. *Proc Natl Acad Sci U S A,* 108**,** 6927-32.

ROUX, A., UYHAZI, K., FROST, A. & DE CAMILLI, P. 2006. GTP-dependent twisting of dynamin implicates constriction and tension in membrane fission. *Nature,* 441**,** 528-31.

ROYLE, S. J., QURESHI, O. S., BOBANOVIĆ, L. K., EVANS, P. R., OWEN, D. J. & MURRELL-LAGNADO, R. D. 2005. Non-canonical YXXGPhi endocytic motifs: recognition by AP2 and preferential utilization in P2X4 receptors. *J Cell Sci,* 118**,** 3073-80.

RUST, M. B. & MARITZEN, T. 2015. Relevance of presynaptic actin dynamics for synapse function and mouse behavior. *Exp Cell Res,* 335**,** 165-71.

RYAN, T. A. 2001. Presynaptic imaging techniques. *Curr Opin Neurobiol,* 11**,** 544-9.

SAITSU, H., KATO, M., MIZUGUCHI, T., HAMADA, K., OSAKA, H., TOHYAMA, J., URUNO, K., KUMADA, S., NISHIYAMA, K., NISHIMURA, A., OKADA, I., YOSHIMURA, Y., HIRAI, S., KUMADA, T., HAYASAKA, K., FUKUDA, A., OGATA, K. & MATSUMOTO, N. 2008. De novo mutations in the gene encoding STXBP1 (MUNC18-1) cause early infantile epileptic encephalopathy. *Nat Genet,* 40**,** 782-8.

SAKABA, T. & NEHER, E. 2001. Calmodulin mediates rapid recruitment of fast-releasing synaptic vesicles at a calyx-type synapse. *Neuron,* 32**,** 1119-31.

SANKARANARAYANAN, S. & RYAN, T. A. 2000. Real-time measurements of vesicle-SNARE recycling in synapses of the central nervous system. *Nat Cell Biol,* 2**,** 197-204.

SARA, Y., VIRMANI, T., DEÁK, F., LIU, X. & KAVALALI, E. T. 2005. An isolated pool of vesicles recycles at rest and drives spontaneous neurotransmission. *Neuron,* 45**,** 563-73.

SCHENCK, S., WOJCIK, S. M., BROSE, N. & TAKAMORI, S. 2009. A chloride conductance in VGLUT1 underlies maximal glutamate loading into synaptic vesicles. *Nat Neurosci,* 12**,** 156-62.

SCHIAVO, G., GU, Q. M., PRESTWICH, G. D., SÖLLNER, T. H. & ROTHMAN, J. E. 1996. Calcium-dependent switching of the specificity of phosphoinositide binding to synaptotagmin. *Proc Natl Acad Sci U S A,* 93**,** 13327-32.

SCHIVELL, A. E., BATCHELOR, R. H. & BAJJALIEH, S. M. 1996. Isoform-specific, calcium-regulated interaction of the synaptic vesicle proteins SV2 and synaptotagmin. *J Biol Chem,* 271**,** 27770-5.

SCHIVELL, A. E., MOCHIDA, S., KENSEL-HAMMES, P., CUSTER, K. L. & BAJJALIEH, S. M. 2005. SV2A and SV2C contain a unique synaptotagmin-binding site. *Mol Cell Neurosci,* 29**,** 56-64.

SCOTT, D. & ROY, S. 2012. α-Synuclein inhibits intersynaptic vesicle mobility and maintains recycling-pool homeostasis. *J Neurosci,* 32**,** 10129-35.

SERAJEE, F. J. & HUQ, A. M. 2015. Homozygous Mutation in Synaptic Vesicle Glycoprotein 2A Gene Results in Intractable Epilepsy, Involuntary Movements, Microcephaly, and Developmental and Growth Retardation. *Pediatr Neurol,* 52**,** 642-6.e1.

SHI, J., ANDERSON, D., LYNCH, B. A., CASTAIGNE, J. G., FOERCH, P. & LEBON, F. 2011. Combining modelling and mutagenesis studies of synaptic vesicle protein 2A to identify a series of residues involved in racetam binding. *Biochem Soc Trans,* 39**,** 1341-7.

SHIMADA, A., NIWA, H., TSUJITA, K., SUETSUGU, S., NITTA, K., HANAWA-SUETSUGU, K., AKASAKA, R., NISHINO, Y., TOYAMA, M., CHEN, L., LIU, Z. J., WANG, B. C., YAMAMOTO, M., TERADA, T., MIYAZAWA, A., TANAKA, A., SUGANO, S., SHIROUZU, M., NAGAYAMA, K., TAKENAWA, T. & YOKOYAMA, S. 2007. Curved EFC/F-BAR-domain dimers are joined end to end into a filament for membrane invagination in endocytosis. *Cell,* 129**,** 761-72.

SHIMOYAMA, M., SHIMOYAMA, N. & HORI, Y. 2000. Gabapentin affects glutamatergic excitatory neurotransmission in the rat dorsal horn. *Pain,* 85**,** 405-14.

SHUPLIAKOV, O., HAUCKE, V. & PECHSTEIN, A. 2011. How synapsin I may cluster synaptic vesicles. *Semin Cell Dev Biol,* 22**,** 393-9.

SIEGELBAUM, S. A. & KANDEL, E. R. 2012. *Principles of Neural Science,* New York, McGraw-Hill.

SMITH, D. B. & JOHNSON, K. S. 1988. Single-step purification of polypeptides expressed in Escherichia coli as fusions with glutathione S-transferase. *Gene,* 67**,** 31-40.

SOUKUPOVA, M., BINASCHI, A., FALCICCHIA, C., PALMA, E., RONCON, P., ZUCCHINI, S. & SIMONATO, M. 2015. Increased extracellular levels of glutamate in the hippocampus of chronically epileptic rats. *Neuroscience,* 301**,** 246-53.

SOUKUPOVÁ, M., BINASCHI, A., FALCICCHIA, C., ZUCCHINI, S., RONCON, P., PALMA, E., MAGRI, E., GRANDI, E. & SIMONATO, M. 2014. Impairment of GABA release in the hippocampus at the time of the first spontaneous seizure in the pilocarpine model of temporal lobe epilepsy. *Exp Neurol,* 257**,** 39-49.

SOYKAN, T., KAEMPF, N., SAKABA, T., VOLLWEITER, D., GOERDELER, F., PUCHKOV, D., KONONENKO, N. L. & HAUCKE, V. 2017. Synaptic Vesicle Endocytosis Occurs on Multiple Timescales and Is Mediated by Formin-Dependent Actin Assembly. *Neuron,* 93**,** 854-866.e4.

STARAS, K. & BRANCO, T. 2010. Sharing vesicles between central presynaptic terminals: implications for synaptic function. *Front Synaptic Neurosci,* 2**,** 20.

STARAS, K., BRANCO, T., BURDEN, J. J., POZO, K., DARCY, K., MARRA, V., RATNAYAKA, A. & GODA, Y. 2010. A vesicle superpool spans multiple presynaptic terminals in hippocampal neurons. *Neuron,* 66**,** 37-44.

STEFAN, H., WANG-TILZ, Y., PAULI, E., DENNHÖFER, S., GENOW, A., KERLING, F., LORBER, B., FRAUNBERGER, B., HALBONI, P., KOEBNICK, C., GEFELLER, O. & TILZ, C. 2006. Onset of action of levetiracetam: a RCT trial using therapeutic intensive seizure analysis (TISA). *Epilepsia,* 47**,** 516-22.

STEVENS, C. F. & TSUJIMOTO, T. 1995. Estimates for the pool size of releasable quanta at a single central synapse and for the time required to refill the pool. *Proc Natl Acad Sci U S A,* 92**,** 846-9.

STEVENS, C. F. & WESSELING, J. F. 1998. Activity-dependent modulation of the rate at which synaptic vesicles become available to undergo exocytosis. *Neuron,* 21**,** 415-24.

STEVENS, C. F. & WILLIAMS, J. H. 2007. Discharge of the readily releasable pool with action potentials at hippocampal synapses. *J Neurophysiol,* 98**,** 3221-9.

STOWELL, M. H., MARKS, B., WIGGE, P. & MCMAHON, H. T. 1999. Nucleotide-dependent conformational changes in dynamin: evidence for a mechanochemical molecular spring. *Nat Cell Biol,* 1**,** 27-32.

SUDHOF, T. C. 2004. The synaptic vesicle cycle. *Annual Review of Neuroscience,* 27**,** 509-547.

SUGAYA, Y., JINDE, S., KATO, N. & MARU, E. 2010. Levetiracetam inhibits kindling-induced synaptic potentiation in the dentate gyrus of freely moving rats. *Neurosci Res,* 66**,** 228-31.

SUNDBORGER, A., SODERBLOM, C., VORONTSOVA, O., EVERGREN, E., HINSHAW, J. E. & SHUPLIAKOV, O. 2011. An endophilin-dynamin complex promotes budding of clathrin-coated vesicles during synaptic vesicle recycling. *J Cell Sci,* 124**,** 133-43.

SUTTON, M. A., ITO, H. T., CRESSY, P., KEMPF, C., WOO, J. C. & SCHUMAN, E. M. 2006. Miniature neurotransmission stabilizes synaptic function via tonic suppression of local dendritic protein synthesis. *Cell,* 125**,** 785-99.

SUZUKI, R., TOSHIMA, J. Y. & TOSHIMA, J. 2012. Regulation of clathrin coat assembly by Eps15 homology domain-mediated interactions during endocytosis. *Mol Biol Cell,* 23**,** 687-700.

SWEITZER, S. M. & HINSHAW, J. E. 1998. Dynamin undergoes a GTP-dependent conformational change causing vesiculation. *Cell,* 93**,** 1021-9.

SÖLLNER, T., BENNETT, M. K., WHITEHEART, S. W., SCHELLER, R. H. & ROTHMAN, J. E. 1993. A protein assembly-disassembly pathway in vitro that may correspond to sequential steps of synaptic vesicle docking, activation, and fusion. *Cell,* 75**,** 409-18.

SÜDHOF, T. C. & RIZO, J. 2011. Synaptic vesicle exocytosis. *Cold Spring Harb Perspect Biol,* 3.

SÜDHOF, T. C. & ROTHMAN, J. E. 2009. Membrane fusion: grappling with SNARE and SM proteins. *Science,* 323**,** 474-7.

TAKAMORI, S., HOLT, M., STENIUS, K., LEMKE, E. A., GRØNBORG, M., RIEDEL, D., URLAUB, H., SCHENCK, S., BRÜGGER, B., RINGLER, P., MÜLLER, S. A., RAMMNER, B., GRÄTER, F., HUB, J. S., DE GROOT, B. L., MIESKES, G., MORIYAMA, Y., KLINGAUF, J., GRUBMÜLLER, H., HEUSER, J., WIELAND, F. & JAHN, R. 2006. Molecular anatomy of a trafficking organelle. *Cell,* 127**,** 831-46.

TAKAMORI, S., RHEE, J. S., ROSENMUND, C. & JAHN, R. 2000. Identification of a vesicular glutamate transporter that defines a glutamatergic phenotype in neurons. *Nature,* 407**,** 189-94.

TANG, X., XIE, C., WANG, Y. & WANG, X. 2017. Localization of Rab3A-binding site on C2A domain of synaptotagmin I to reveal its regulatory mechanism. *Int J Biol Macromol,* 96**,** 736-742.

TENG, H., LIN, M. Y. & WILKINSON, R. S. 2007. Macroendocytosis and endosome processing in snake motor boutons. *J Physiol,* 582**,** 243-62.

THOMAS, L. & BETZ, H. 1990. Synaptophysin binds to physophilin, a putative synaptic plasma membrane protein. *J Cell Biol,* 111**,** 2041-52.

TOERING, S. T., BOER, K., DE GROOT, M., TROOST, D., HEIMANS, J. J., SPLIET, W. G., VAN RIJEN, P. C., JANSEN, F. E., GORTER, J. A., REIJNEVELD, J. C. & ARONICA, E. 2009. Expression patterns of synaptic vesicle protein 2A in focal cortical dysplasia and TSC-cortical tubers. *Epilepsia,* 50**,** 1409-18.

TOKUDOME, K., OKUMURA, T., TERADA, R., SHIMIZU, S., KUNISAWA, N., MASHIMO, T., SERIKAWA, T., SASA, M. & OHNO, Y. 2016. A Missense Mutation of the Gene Encoding Synaptic Vesicle Glycoprotein 2A (SV2A) Confers Seizure Susceptibility by Disrupting Amygdalar Synaptic GABA Release. *Front Pharmacol,* 7**,** 210.

TONG, X. & PATSALOS, P. N. 2001. A microdialysis study of the novel antiepileptic drug levetiracetam: extracellular pharmacokinetics and effect on taurine in rat brain. *Br J Pharmacol,* 133**,** 867-74.

UNGEWICKELL, E., UNGEWICKELL, H., HOLSTEIN, S. E., LINDNER, R., PRASAD, K., BAROUCH, W., MARTIN, B., GREENE, L. E. & EISENBERG, E. 1995. Role of auxilin in uncoating clathrin-coated vesicles. *Nature,* 378**,** 632-5.

UPRETI, C., OTERO, R., PARTIDA, C., SKINNER, F., THAKKER, R., PACHECO, L. F., ZHOU, Z. Y., MAGLAKELIDZE, G., VELÍŠKOVÁ, J., VELÍŠEK, L., ROMANOVICZ, D., JONES, T., STANTON, P. K. & GARRIDO-SANABRIA, E. R. 2012. Altered neurotransmitter release, vesicle recycling and presynaptic structure in the pilocarpine model of temporal lobe epilepsy. *Brain,* 135**,** 869-85.

VAN DEN BERG, R. J., KOK, P. & VOSKUYL, R. A. 1993. Valproate and sodium currents in cultured hippocampal neurons. *Exp Brain Res,* 93**,** 279-87.

VAN VLIET, E. A., ARONICA, E., REDEKER, S., BOER, K. & GORTER, J. A. 2009. Decreased expression of synaptic vesicle protein 2A, the binding site for levetiracetam, during epileptogenesis and chronic epilepsy. *Epilepsia,* 50**,** 422-433.

VOGL, C., MOCHIDA, S., WOLFF, C., WHALLEY, B. J. & STEPHENS, G. J. 2012. The synaptic vesicle glycoprotein 2A ligand levetiracetam inhibits presynaptic Ca2+ channels through an intracellular pathway. *Mol Pharmacol,* 82**,** 199-208.

VOGLMAIER, S. M., KAM, K., YANG, H., FORTIN, D. L., HUA, Z., NICOLL, R. A. & EDWARDS, R. H. 2006. Distinct endocytic pathways control the rate and extent of synaptic vesicle protein recycling. *Neuron,* 51**,** 71-84.

WAITES, C. L., LEAL-ORTIZ, S. A., ANDLAUER, T. F., SIGRIST, S. J. & GARNER, C. C. 2011. Piccolo regulates the dynamic assembly of presynaptic F-actin. *J Neurosci,* 31**,** 14250-63.

WAKITA, M., KOTANI, N., KOGURE, K. & AKAIKE, N. 2014. Inhibition of excitatory synaptic transmission in hippocampal neurons by levetiracetam involves Zn^{2+}-dependent GABA type A receptor-mediated presynaptic modulation. *J Pharmacol Exp Ther,* 348**,** 246-59.

WALLACE, R. H., MARINI, C., PETROU, S., HARKIN, L. A., BOWSER, D. N., PANCHAL, R. G., WILLIAMS, D. A., SUTHERLAND, G. R., MULLEY, J. C., SCHEFFER, I. E. & BERKOVIC, S. F. 2001. Mutant GABA(A) receptor gamma2-subunit in childhood absence epilepsy and febrile seizures. *Nat Genet,* 28**,** 49-52.

WAN, Q. F., ZHOU, Z. Y., THAKUR, P., VILA, A., SHERRY, D. M., JANZ, R. & HEIDELBERGER, R. 2010. SV2 acts via presynaptic calcium to regulate neurotransmitter release. *Neuron,* 66**,** 884-95.

WANG, C. T., GRISHANIN, R., EARLES, C. A., CHANG, P. Y., MARTIN, T. F., CHAPMAN, E. R. & JACKSON, M. B. 2001. Synaptotagmin modulation of fusion pore kinetics in regulated exocytosis of dense-core vesicles. *Science,* 294**,** 1111-5.

WANG, L., SHI, J., WU, G., ZHOU, F. & HONG, Z. 2014. Hippocampal low-frequency stimulation increased SV2A expression and inhibited the seizure degree in pharmacoresistant amygdala-kindling epileptic rats. *Epilepsy Res,* 108**,** 1483-91.

WANG, Q., NAVARRO, M. V., PENG, G., MOLINELLI, E., GOH, S. L., JUDSON, B. L., RAJASHANKAR, K. R. & SONDERMANN, H. 2009. Molecular mechanism of membrane constriction and tubulation mediated by the F-BAR protein Pacsin/Syndapin. *Proc Natl Acad Sci U S A,* 106**,** 12700-5.

WASHBOURNE, P., SCHIAVO, G. & MONTECUCCO, C. 1995. Vesicle-associated membrane protein-2 (synaptobrevin-2) forms a complex with synaptophysin. *Biochem J,* 305 (Pt 3)**,** 721-4.

WATANABE, S., LIU, Q., DAVIS, M. W., HOLLOPETER, G., THOMAS, N., JORGENSEN, N. B. & JORGENSEN, E. M. 2013a. Ultrafast endocytosis at Caenorhabditis elegans neuromuscular junctions. *Elife,* 2**,** e00723.

WATANABE, S., ROST, B. R., CAMACHO-PÉREZ, M., DAVIS, M. W., SÖHL-KIELCZYNSKI, B., ROSENMUND, C. & JORGENSEN, E. M. 2013b. Ultrafast endocytosis at mouse hippocampal synapses. *Nature,* 504**,** 242-247.

WATANABE, S., TRIMBUCH, T., CAMACHO-PÉREZ, M., ROST, B. R., BROKOWSKI, B., SÖHL-KIELCZYNSKI, B., FELIES, A., DAVIS, M. W., ROSENMUND, C. & JORGENSEN, E. M. 2014. Clathrin regenerates synaptic vesicles from endosomes. *Nature,* 515**,** 228-33.

WIENISCH, M. & KLINGAUF, J. 2006. Vesicular proteins exocytosed and subsequently retrieved by compensatory endocytosis are nonidentical. *Nat Neurosci,* 9**,** 1019-27.

WILHELM, B. G., GROEMER, T. W. & RIZZOLI, S. O. 2010. The same synaptic vesicles drive active and spontaneous release. *Nat Neurosci,* 13**,** 1454-6.

WILHELM, B. G., MANDAD, S., TRUCKENBRODT, S., KRÖHNERT, K., SCHÄFER, C., RAMMNER, B., KOO, S. J., CLAßEN, G. A., KRAUSS, M., HAUCKE, V., URLAUB, H. & RIZZOLI, S. O. 2014. Composition of isolated synaptic boutons reveals the amounts of vesicle trafficking proteins. *Science,* 344**,** 1023-8.

WILLOX, A. K. & ROYLE, S. J. 2012. Stonin 2 is a major adaptor protein for clathrin-mediated synaptic vesicle retrieval. *Curr Biol,* 22**,** 1435-9.

WOLF, M., ZIMMERMANN, A. M., GÖRLICH, A., GURNIAK, C. B., SASSOÈ-POGNETTO, M., FRIAUF, E., WITKE, W. & RUST, M. B. 2015. ADF/Cofilin Controls Synaptic Actin Dynamics and Regulates Synaptic Vesicle Mobilization and Exocytosis. *Cereb Cortex,* 25**,** 2863-75.

WU, X. S., ZHANG, Z., ZHAO, W. D., WANG, D., LUO, F. & WU, L. G. 2014. Calcineurin is universally involved in vesicle endocytosis at neuronal and nonneuronal secretory cells. *Cell Rep,* 7**,** 982-8.

XIAO, Z., GONG, Y., WANG, X. F., XIAO, F., XI, Z. Q., LU, Y. & SUN, H. B. 2009. Altered expression of synaptotagmin I in temporal lobe tissue of patients with refractory epilepsy. *J Mol Neurosci,* 38**,** 193-200.

XU, F., PLUMMER, M. R., LEN, G. W., NAKAZAWA, T., YAMAMOTO, T., BLACK, I. B. & WU, K. 2006. Brain-derived neurotrophic factor rapidly increases NMDA receptor channel activity through Fyn-mediated phosphorylation. *Brain Res,* 1121**,** 22-34.

XU, T. & BAJJALIEH, S. M. 2001. SV2 modulates the size of the readily releasable pool of secretory vesicles. *Nat Cell Biol,* 3**,** 691-8.

XUE, M., CRAIG, T. K., XU, J., CHAO, H. T., RIZO, J. & ROSENMUND, C. 2010. Binding of the complexin N terminus to the SNARE complex potentiates synaptic-vesicle fusogenicity. *Nat Struct Mol Biol,* 17**,** 568-75.

YANG, X., KAESER-WOO, Y. J., PANG, Z. P., XU, W. & SÜDHOF, T. C. 2010. Complexin clamps asynchronous release by blocking a secondary Ca(2+) sensor via its accessory α helix. *Neuron,* 68**,** 907-20.

YANG, X. F., WEISENFELD, A. & ROTHMAN, S. M. 2007. Prolonged exposure to levetiracetam reveals a presynaptic effect on neurotransmission. *Epilepsia,* 48**,** 1861-9.

YAO, J. & BAJJALIEH, S. M. 2008. Synaptic vesicle protein 2 binds adenine nucleotides. *J Biol Chem,* 283**,** 20628-34.

YAO, J., GAFFANEY, J. D., KWON, S. E. & CHAPMAN, E. R. 2011. Doc2 is a Ca2+ sensor required for asynchronous neurotransmitter release. *Cell,* 147**,** 666-77.

YAO, J., NOWACK, A., KENSEL-HAMMES, P., GARDNER, R. G. & BAJJALIEH, S. M. 2010. Cotrafficking of SV2 and Synaptotagmin at the Synapse. *Journal of Neuroscience,* 30**,** 5569-5578.

YIM, Y. I., SUN, T., WU, L. G., RAIMONDI, A., DE CAMILLI, P., EISENBERG, E. & GREENE, L. E. 2010. Endocytosis and clathrin-uncoating defects at synapses of auxilin knockout mice. *Proc Natl Acad Sci U S A,* 107**,** 4412-7.

YOSHIHARA, M. & LITTLETON, J. T. 2002. Synaptotagmin I functions as a calcium sensor to synchronize neurotransmitter release. *Neuron,* 36**,** 897-908.

ZHANG, N., GORDON, S. L., FRITSCH, M. J., ESOOF, N., CAMPBELL, D. G., GOURLAY, R., VELUPILLAI, S., MACARTNEY, T., PEGGIE, M., VAN AALTEN, D. M., COUSIN, M. A. & ALESSI, D. R. 2015. Phosphorylation of synaptic vesicle protein 2A at Thr84 by casein kinase 1 family kinases controls the specific retrieval of synaptotagmin-1. *J Neurosci,* 35**,** 2492-507.

ZHOU, Q., LAI, Y., BACAJ, T., ZHAO, M., LYUBIMOV, A. Y., UERVIROJNANGKOORN, M., ZELDIN, O. B., BREWSTER, A. S., SAUTER, N. K., COHEN, A. E., SOLTIS, S. M., ALONSO-MORI, R., CHOLLET, M., LEMKE, H. T., PFUETZNER, R. A., CHOI, U. B., WEIS, W. I., DIAO, J., SÜDHOF, T. C. & BRUNGER, A. T. 2015. Architecture of the synaptotagmin-SNARE machinery for neuronal exocytosis. *Nature,* 525**,** 62-7.

ZONA, C., NIESPODZIANY, I., MARCHETTI, C., KLITGAARD, H., BERNARDI, G. & MARGINEANU, D. G. 2001. Levetiracetam does not modulate neuronal voltage-gated Na+ and T-type Ca2+ currents. *Seizure,* 10**,** 279-86.

ZUBERI, S. M., EUNSON, L. H., SPAUSCHUS, A., DE SILVA, R., TOLMIE, J., WOOD, N. W., MCWILLIAM, R. C., STEPHENSON, J. B., STEPHENSON, J. P., KULLMANN, D. M. & HANNA, M. G. 1999. A novel mutation in the human voltage-gated potassium channel gene (Kv1.1) associates with episodic ataxia type 1 and sometimes with partial epilepsy. *Brain,* 122 (Pt 5)**,** 817-25.